



**HAL**  
open science

# Intensification of ATRP polymer syntheses by microreaction technologies

Dambarudhar Parida

► **To cite this version:**

Dambarudhar Parida. Intensification of ATRP polymer syntheses by microreaction technologies. Material chemistry. Université de Strasbourg, 2014. English. NNT : 2014STRAE011 . tel-01124285

**HAL Id: tel-01124285**

**<https://theses.hal.science/tel-01124285>**

Submitted on 6 Mar 2015

**HAL** is a multi-disciplinary open access archive for the deposit and dissemination of scientific research documents, whether they are published or not. The documents may come from teaching and research institutions in France or abroad, or from public or private research centers.

L'archive ouverte pluridisciplinaire **HAL**, est destinée au dépôt et à la diffusion de documents scientifiques de niveau recherche, publiés ou non, émanant des établissements d'enseignement et de recherche français ou étrangers, des laboratoires publics ou privés.



**Thèse présentée pour obtenir le grade de Docteur de l'Université de Strasbourg**

Discipline : *Chimie des matériaux*  
Spécialité : *Génie des procédés de polymérisation*  
Ecole doctorale : *Physique et Chimie – Physique*

Présentée par:  
**Dambarudhar PARIDA**

---

**Intensification of ATRP polymer syntheses by microreaction technologies**

---

Soutenue publiquement le 13 février 2014

Directeur de Thèse :	C. A. SERRA	Professeur, Université de Strasbourg
Rapporteur Externe :	T. F. L. MCKENNA	Directeur de Recherche, CNRS - CPE Lyon
Rapporteur Externe :	A. RENKEN	Professeur, EPFL Lausanne
Examineur Interne :	J.-F. LUTZ	Directeur de Recherche, CNRS - ICS Strasbourg

## Acknowledgements

Since we started working as a team and exchanging ideas, we are moving at much greater pace than ever before. Sometimes, we travel far in search of ideas or to share our ideas and it is happening for centuries. Following such a route, I came to Strasbourg to sharpen my knowledge and skill. This simple looking route was never easy without a team. They worked like a support, when I was weak and they helped me to grow stronger. Their guidance helped me in my research endeavour. Along with human factors there was a need for financial support to carryout research for which ANR grant n° 09-CP2D-DIP<sup>2</sup> is greatly appreciated. I would like to thank Dr. T. F. L. Mckenna, Prof. A. Renken, Dr. J.-F Lutz for accepting to become a member of jury.

Prof. C.A. Serra at ECPM, University of Strasbourg, thank you for being amazing guide/Guru and giving me an opportunity to explore the field of microfluidic and controlled radical polymerization. You have been a continuous source of inspiration and motivation for me. Ever since I arrived at Strasbourg, You have supported me not only in research but also emotionally through the ups and downs to finish the thesis, especially towards the end. Every time I came with a proposal, always I got the answer “You have my green light”. Thank you for moral support and freedom I needed to move on. Special thanks to Isabelle for her support and encouragement.

Dr Florence. Bally, Université de Haute Alsace, Thank you for introducing me to micro and CORSEMP. You always welcomed my queries and shared your experiences which helped me to overcome small yet significant obstacles. Truly, it was a great experience working with you. I would like to thank Dr. Yannick Hoarau and Dhiraj K. Garg for their observations and reasoning made while working together which helped me to answer some important questions. Dhiraj, working with you was really fun and exciting.

Since the day I started working in the lab, many times I found difficult barriers. But, you were there, who helped me to cross those barriers. Thank you Christoph for your help during building and modifying the microreaction setup. Christophe Sutter, thank you for putting life to the setup by sensors and softwares. Dr. Sebastien, I will never forget your help and advices for running the CORSEMP smoothly. I can say, I was with three Musketeers from 2011 to 2014. I was able to focus on my research because both of you were there. Thank you Cheng for your ultrafast procurement of consumables and GPC trouble shooting. Catherine, I appreciate your effort which kept me away from lot of paper work (written in french). Hassle

free travel to different conferences was possible because of your effort. Merci Cheng and Catherine for your continuous support.

Dozens of people taught me and helped me in many ways at ICPEES. Dr. Anne was always ready to listen and discuss the problems. You helped me in many ways to think from a different perspective. Dr. Nicolas, your tracer was really helpful; you were like a ray of hope during that time. I cannot imagine determining residence time distribution without the tracer. Prof. Muller, Dr. Rigoberto and Dr. M. Bouquey shared their experiences and expertise with me for rheological analysis of samples. It helped me to have a look inside the microreactors. Discussion with Dr. Rigoberto on world religion was also very interesting. Special acknowledgement for Prof. Muller, Dr. Nicolas, Dr. Anne, Dr. Rigoberto and Dr. M. Bouquey.

In the lab there were many amazing people around me who taught many things in many ways. Mumu is a great friend ever since she came to our lab and has been supportive in every way. Yu Wei, a nice co-worker who likes to talk and solve different problems of the lab. It was interesting to discuss Chinese philosophy and lifestyle with him. Salima, a smiling, helpful and talented friend. Thank you for bringing Bollywood to Strasbourg. FX; Alexandar, Dr. Mathieu, Dr. Patricia, Dr. Korine, Ibrahim, Lucas...thank you for all your support for all these years.

People in the office R1 H2 B1 are not mentioned yet, because they deserve their own part. I learned a lot from them. They were always there to help me in every possible and impossible ways. They were always ready to listen and discuss on various topics and issues, be it polymer or politics. Our discussions on polymers, helped me to shape my experiments in a significant way. I will remember 4:00 pm as the time for Technologic or Philosophy or Cricket. I really appreciate their efforts for tolerating me in the office and teaching me French. Thank you Dr. TGV for gâteau au chocolat (Monday Special), Alice for gâteau aux pommes (Though you made it Twice) and Ikhran for biscuits. Marie, you came late to the office but soon you became a good friend. Stephanie, Alice, Ikhran, Marie, Mumu...you people registered my stay at Strasbourg in the unforgettable part of my memory. Even hundred pages are not sufficient to describe what you did for me.

My parents, uncles and aunts, Nana, Bhauja, Manu, Mita, Dhiren and Sirohi sir, I cannot imagine coming so far in life without your endless encouragement and support. Special acknowledgements and thanks to everyone for everything you did for me.

*FRENCH SUMMARY*

---

## Résumé de Thèse

### Intensification de la synthèse de polymères par ATRP au moyen de technologies de microréaction

#### 1. Introduction

Contrairement à tout autre composé chimique, les macromolécules synthétiques ont des caractéristiques (masse molaire moyenne, distribution des longueurs de chaîne) qui sont fortement dépendantes des paramètres du procédé de synthèse. L'augmentation de la viscosité, qui peut atteindre jusqu'à 7 décades pour les procédés en masse et en solution concentrée, s'accompagne d'une diminution des transferts de matière et de chaleur. Cette situation conduit généralement à l'élargissement de la distribution des longueurs de chaînes, une masse molaire différente de celle souhaitée et peut également entraîner l'emballement thermique du réacteur. Cependant, un mélange rapide des réactifs en entrée de réacteur et en son sein est souvent conseillé pour résoudre ces problèmes.

Tant du point de vue du mélange que de l'évacuation des calories libérées par la réaction, les micromélangeurs et microréacteurs peuvent être une option pour surmonter les limitations diffusionnelles. En effet, la très faible dimension caractéristique (10 à quelques centaines de micromètres) de ces systèmes microfluidiques leur confère un avantage certain par rapport à leurs homologues en verre de laboratoire et leurs versions industrielles. A cette échelle, il a été constaté que les microsystèmes peuvent améliorer considérablement les transferts de masse et de chaleur. Comparés à d'autres produits chimiques, la synthèse de polymères dans les systèmes microfluidiques est relativement nouvelle et peut largement bénéficier des caractéristiques précitées de ces microsystèmes (cf. chapitre 1).

D'un point de vue chimique, les techniques de polymérisation radicalaire contrôlée ont été conçues pour accroître le contrôle sur les caractéristiques macromoléculaires (longueur de la chaîne, distribution des masses molaires et architecture) comparativement à la technique classique de polymérisation radicalaire. Toutefois, en raison de limites inhérentes à leur mise en œuvre, leurs potentiels ne peuvent pas être utilisés pleinement. Elles sont en effet intrinsèquement lentes ce qui diminue leur productivité horaire et rend leur procédés de synthèse coûteux. Parmi ces techniques, la polymérisation radicalaire par transferts d'atomes (ATRP) est la plus employée. Ainsi la polymérisation par ATRP de polymères à base de

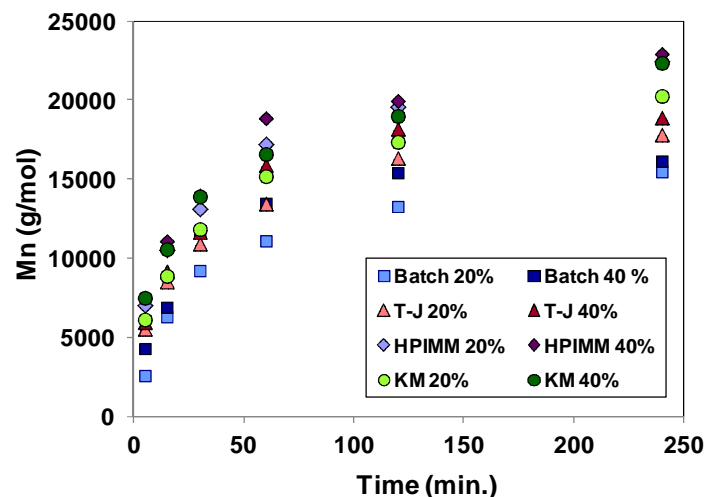
méthacrylate de 2-(diméthylamino)éthyle (DMAEMA) servira de cas d'étude tout au long de ce travail de thèse. L'objectif de cette dernière étant d'intensifier la production de (co)polymères linéaires et branchés au moyen de systèmes microfluidiques et des paramètres de procédés.

## 2. Effet d'un prémélange sur la polymérisation en microréacteur hélicoïdal

Afin d'étudier l'effet de différents principes de micromélange sur les caractéristiques de copolymères statistiques, plusieurs types de micromélangeurs (à bilaminaion, jonction en T ; à jet d'impact, KM Mixer ; à multilamination interdigitale, HPIMM) ont été considérés pour la copolymérisation par ATRP du DMAEMA et du méthacrylate de benzyle (BzMA) de compositions différentes (20 et 40 mol.% BzMA) dans un microréacteur hélicoïdal (CT, schéma 1.a) de diamètre interne 876  $\mu\text{m}$  (Figure 1). D'après les résultats obtenus, l'impact du prémélange est évident puisque, toute chose égale par ailleurs, les copolymères ont des propriétés différentes en fonction du type de micromélangeurs employé. La jonction en T a conduit à la conversion en monomère la plus faible alors que le micromélangeur à multilamination a donné les conversions les élevées (+ 30% par rapport à un réacteur discontinu) tout en assurant des masse molaires plus élevées et une distribution des longueurs de chaînes plus étroite. Les détails sont expliqués dans le chapitre 3.



**Schéma 1.** Dessin d'un microréacteur hélicoïdal (CT, a) et à inversion de flux (CFI, b)

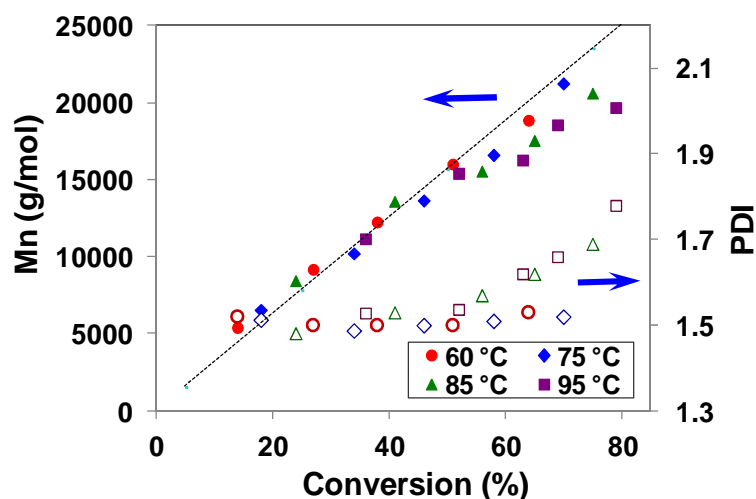


**Figure 1.** Evolution de la masse molaire moyenne en nombre des copolymères synthétisés pour différents temps de séjour, micromélangeurs et compositions molaire en BzMA.

### 3. Accélération de la cinétique ATRP en microréacteur hélicoïdal

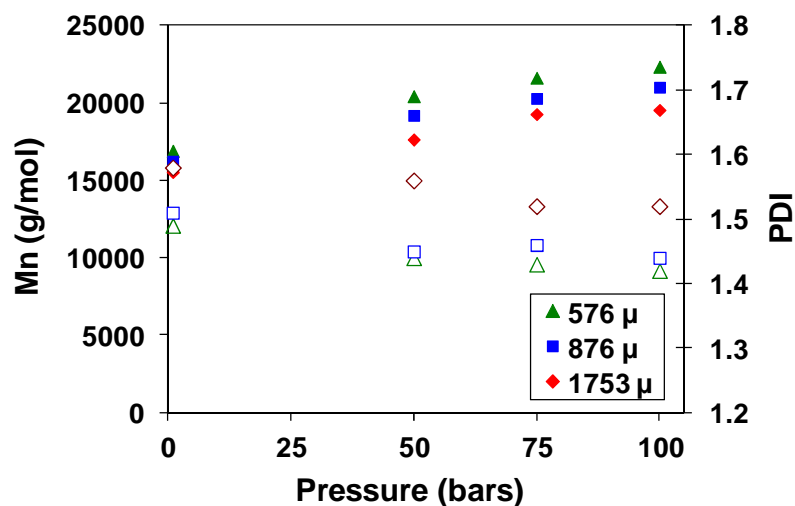
La cinétique de synthèse du DMAEMA par ATRP a été étudiée dans un microréacteur hélicoïdal (CT, diamètre interne de 876  $\mu\text{m}$ ) à des températures différentes. La vitesse de polymérisation augmente de manière significative avec la température comme le montre la Figure 2. Les masses molaires du polymère obtenues sont très proches des valeurs théoriques à 60°C et 75°C, indiquant des caractéristiques contrôlées de la polymérisation. Cependant, la différence entre la masse molaire théorique et réelle commence à apparaître à des températures de polymérisation supérieures à 85°C et après 30 minutes de temps de séjour. Cela est notamment reflété par l'indice de polymolécularité (PDI, un paramètre rendant compte de la largesse de la distribution des masses molaires) qui augmente significativement à hautes températures (> 85°C) pour les temps de séjour supérieurs à 30 minutes indiquant ainsi une réaction incontrôlée. Cependant, pour des masses molaires proches de 15000 g / mole, des températures plus élevées se révèlent être une alternative intéressante car elles permettent de réduire le temps de polymérisation de façon significative (15 minutes à 95°C au lieu de 1 heure à 60°C) et d'ainsi augmenter d'un facteur 4 la productivité horaire du procédé de synthèse.





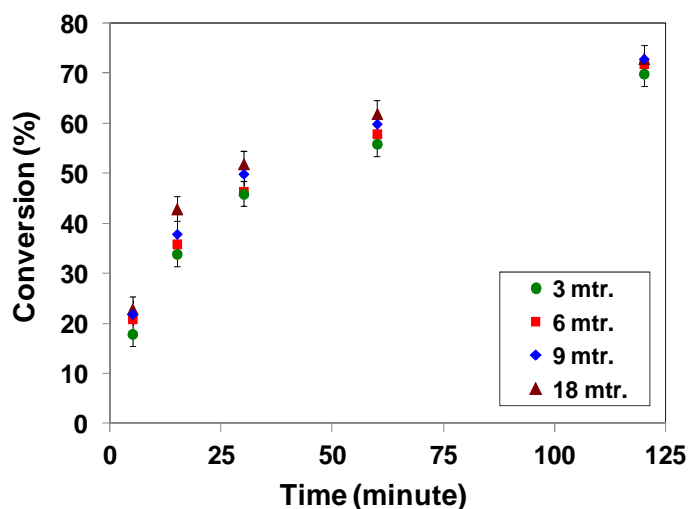
**Figure 2.** Evolution de la masse molaire moyenne en nombre (symboles pleins) et du PDI (symboles vides) avec la conversion du monomère pour différentes températures de polymérisation.

La pression à laquelle se déroule la polymérisation du DMAEMA en microréacteur hélicoïdal (CT, diamètre interne de 876  $\mu\text{m}$ ) a un effet notable sur les propriétés du polymère synthétisé. En effet, une augmentation de la conversion (+15 %) et de la masse molaire (+ 5000 g / mole) a été observée avec une augmentation de pression de près de 100 bars (figure 3). Par ailleurs, la courbe de variation de la masse molaire moyenne en fonction de la conversion du monomère suit de près l'évolution théorique indiquant ainsi que la réaction reste contrôlée. Cette augmentation significative de la conversion peut être attribuée en partie à une augmentation de la constante de vitesse de propagation avec la pression. De plus, l'augmentation de la densité de la solution à polymériser avec la pression peut être un autre facteur de la conversion accrue obtenue en microréacteur. En outre, on observe une diminution du PDI avec la pression (figure 3) qui peut être expliquée par une diminution du taux de terminaison sous pressions élevées. La polymérisation a également été conduite dans des microréacteurs hélicoïdaux de diamètres internes différents (576, 876 et 1753  $\mu\text{m}$ ). Il a été observé que des vitesses de propagation plus élevées à hautes pressions en conjonction avec des diffusions moléculaires plus rapides dans des microréacteurs de faible dimension induit une cinétique de réaction plus rapide. Fait intéressant, cette étude a également montré que des pressions modérées permettent d'accélérer la polymérisation de manière significative dans des microréacteurs en comparaison des pressions beaucoup plus importantes requises pour des réacteurs « macrofluidiques » discontinus.



**Figure 3.** Effet de la pression sur la masse molaire moyenne en nombre (symboles pleins) et le PDI (symboles vide) pour différents diamètres de microéacteur.

Partant du principe qu'une conformation allongée d'une chaîne polymère en croissance permet d'accroître la réactivité du site réactif en opposition à la conformation thermodynamique en pelote, tout moyen de promouvoir une telle déformation devrait engendrer une augmentation de la vitesse de réaction ainsi que du contrôle de la polymérisation. Cela fut démontré expérimentalement en faisant varier le taux de cisaillement à la paroi interne de microréacteurs hélicoïdaux par l'entremise de la longueur des réacteurs et du temps de séjour. Ainsi, ce taux fut varié entre  $3,81 \text{ s}^{-1}$  pour un réacteur de 3 m de long / 2 heures de temps de séjour et  $547,7 \text{ s}^{-1}$  pour un réacteur de 18 m de long / 5 minutes de temps de séjour. Il a été observé que quel que soit le temps de séjour, plus le taux de cisaillement est élevé (c.-à-d. plus le réacteur est long), plus le taux de conversion du monomère augmente (jusqu'à + 10 points de conversion, figure 4). Il en est de même pour la masse molaire moyenne en nombre (+ 2000 g/mol). Cependant ces gains diminuent lorsque le temps de séjour augmente ; ainsi passé 1 heure de réaction quand les chaînes en croissance ont atteint une certaine longueur, les quatre réacteurs, quelle que soit leur longueur, ont donné des conversions et masse molaires quasi similaires. Par ailleurs, il est intéressant de noter qu'aucune différence significative n'a été observée entre les PDI des échantillons polymérisés à différents taux de cisaillement.

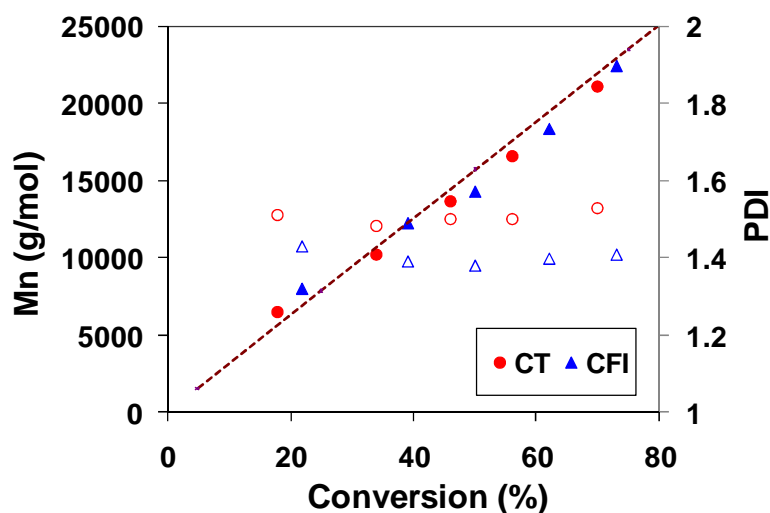


**Figure 4.** Effet de la longueur du microréacteur et du temps de séjour sur la conversion du DMAEMA.

Toutes ces observations sont détaillées dans le chapitre 4.

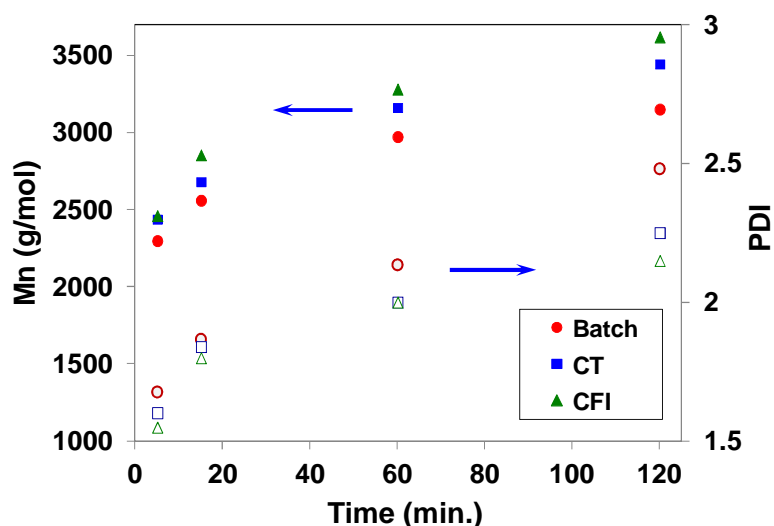
#### 4. Influence de la géométrie du microréacteur

L'augmentation de la viscosité au cours d'une polymérisation limite la diffusion des espèces ce qui résulte en un mauvais contrôle de la réaction et donc des propriétés des macromolécules synthétisées. Pour surmonter ces limitations et réduire la distribution des temps de séjour, également responsable d'une perte de contrôle sur les propriétés des macromolécules, une simple technique d'inversion de flux a été considérée et mise en œuvre dans nos microréacteurs hélicoïdaux en inversant le flux à intervalle régulier par le cou dage à 90°C des serpentins (CFI, schéma 1.b) . Cette technique est une alternative beaucoup plus simple et moins onéreuse par rapport aux réacteurs à microstructures internes rapportés dans la littérature. Lors de la polymérisation du DMAEMA, une augmentation marginale (~ 3-5%) dans la conversion a été observée pour le cas du microréacteur CFI par rapport au microréacteur hélicoïdal (CT). En raison de la présence de coudes à 90°, les changements de direction ramènent les chaînes en croissance proches de la paroi vers le centre du réacteur et vice-versa. La comparaison des caractéristiques des polymères synthétisés en CT et CFI (figure 5) montre que la masse molaire moyenne en nombre est plus élevée de 2000 g/mole pour le réacteur à inversion de flux. D'autre part une réduction significative du PDI est également observée.



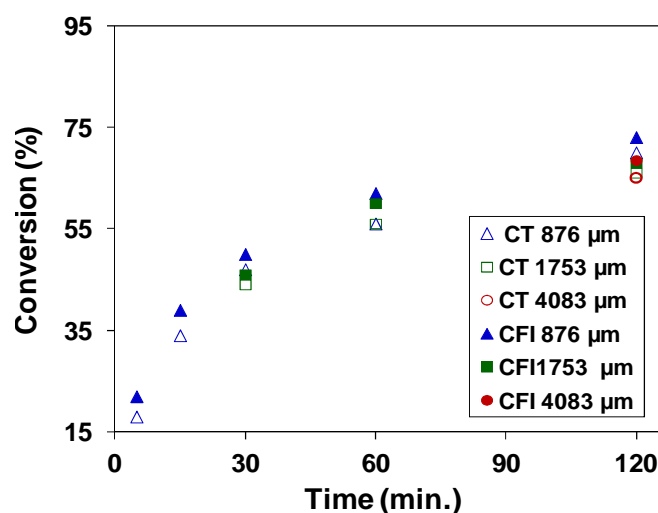
**Figure 5.** Evolution de la masse molaire moyenne en nombre (symboles pleins) et du PDI (symboles vides) avec la conversion du monomère pour différents microréacteurs tubulaire.

Le bénéfice de la technique d'inversion de flux est encore plus marqué lorsqu'on étudie la synthèse d'un polymère branché. Il a ainsi été observé, lors de l'incorporation dans le mélange réactif initial d'un inimère (molécule capable d'agir comme un monomère et un amorceur), que la masse molaire obtenue augmentait et que le PDI diminuait très significativement (figure 6). Par ailleurs, le taux de branchement, déterminé par chromatographie d'exclusion stérique, était sensiblement plus élevé dans le cas de l'emploi du CFI que pour le CT ou bien le réacteur discontinu et cela pour des taux d'inimère allant jusqu'à 10% en mole.



**Figure 6.** Evolution de la masse molaire moyenne en nombre (symboles pleins) et du PDI (symboles vides) avec le temps pour différents réacteurs.

Afin d'améliorer la productivité horaire du procédé de synthèse du PDMAEMA par ATRP dans un réacteur tubulaire, de plus grands diamètres internes ont été testés (1753 et 4084 mm) à temps de passage constants. L'augmentation du diamètre engendra certes une augmentation de la quantité horaire de polymère synthétisé mais s'accompagna d'une diminution marginale de la conversion du monomère (figure 7) et surtout d'une augmentation importante du PDI. Pour limiter cet effet néfaste, nous avons eu recours à la technique d'inversion ; et pour bénéficier au mieux du mélange interne promu par cette technique, nous avons également augmenté la longueur du réacteur. Ainsi ces plus « gros » CFI ont engendré non seulement un accroissement du taux de conversion du monomère (figure 7) et de la masse molaire mais surtout une forte réduction du PDI et cela au prix d'une augmentation quasi négligeable de la perte de charge, c'est-à-dire de l'énergie requise.



**Figure 7.** Evolution de la conversion du monomère en fonction du temps pour différents types de réacteurs et diamètres et une longueur de 3m.

Le chapitre 5 explique toutes ces observations dans le détail.

## 5. Conclusion

La mise en œuvre de synthèses de (co)polymères par la technique ATRP dans des systèmes microfluidiques a permis de mettre en évidence les aspects suivants :

- le prémélange est une étape importante lors de la copolymérisation en microréacteurs et affecte grandement les caractéristiques du copolymère synthétisé. Une mauvaise sélection du micromélangeur peut conduire à une polymérisation incontrôlée. La cinétique de réaction est plus rapide en microréacteurs que celle observée dans un réacteur discontinu.

- 
- les paramètres du procédé comme la température ou la pression peuvent accélérer de manière significative la réaction de polymérisation. Une fenêtre étroite existe pour laquelle l'augmentation de température présente un effet bénéfique. Une augmentation modérée de la pression (100 bars) engendre un contrôle accru sur la polymérisation. L'effet du cisaillement lors de la polymérisation s'est révélé être dépendant de la longueur de chaîne. L'augmentation de la longueur de chaîne a tendance à réduire l'effet bénéfique du cisaillement. Ainsi l'augmentation du cisaillement d'un facteur 6 a peu d'effet sur la conversion du monomère au bout de 2 heures de temps de polymérisation mais l'effet est plus prononcé pour de faibles masses molaires (temps de séjour inférieurs à 1 heure).
  - une très nette amélioration du contrôle de la polymérisation a été observée avec un changement de la géométrie du microréacteur tubulaire. L'introduction d'inversions de flux à intervalles réguliers le long du microréacteur a ainsi permis de réduire sensiblement le PDI. La polymérisation en CFI a également montré une augmentation significative de l'efficacité de branchement qui est un indicateur de l'amélioration de l'architecture branchée. Enfin l'emploi de CFI de plus grand diamètres a validé la possibilité d'augmenter la productivité horaire au détriment cependant d'une petite perte de contrôle sur les caractéristiques macromoléculaires, toutefois moins importante que dans le cas des CT.

En conclusion, cette thèse a démontré que des technologies simples de microréaction comme la combinaison de l'emploi de micromélangeur et la technique d'inversion de flux dans des microréacteurs tubulaires, permet d'accélérer de manière significative la synthèse par ATRP de (co)polymères ; à cela s'ajoute la possibilité d'accroître le contrôle de leurs caractéristiques.

---

*ABBREVIATIONS AND NOTATIONS*

---

## Abbreviations

<b><sup>1</sup>H NMR</b>	Proton nuclear magnetic resonance
<b>ATRP</b>	Atom Transfer Radical Polymerization
<b>BIEM</b>	2-(2-bromoisobutyryloxy)ethyl methacrylate
<b>BzMA</b>	Benzyl methacrylate
<b>CFI</b>	Coil flow inverter
<b>CORSEMP</b>	Continuous online rapid size-exclusion monitoring of polymerization
<b>CRP</b>	Controlled radical polymerization
<b>CT</b>	Coiled tube
<b>CuBr</b>	Copper (I) bromide
<b>DCM</b>	Dichloromethane
<b>DMAEMA</b>	2-(Dimethylamino) ethyl methacrylate
<b>DMF</b>	Dimethylformamide
<b>DP</b>	Degree of polymerization
<b>EBIB</b>	Ethyl 2-bromoisobutyrate
<b>FRP</b>	Free radical polymerization
<b>GPC</b>	Gel Permeation Chromatography
<b>HEMA</b>	2-hydroxyethyl methacrylate
<b>HMTETA</b>	1,1,4,7,10,10-hexamethyltriethylenetetramine
<b>HPIMM</b>	High Pressure Interdigital Multilamination Micromixer,
<b>HPLC</b>	High performance liquid chromatography
<b>KM</b>	Impact jet micromixer
<b>MALS</b>	Multi angle light scattering
<b>NMP</b>	Nitroxide mediated polymerization
<b>PDI</b>	Polydispersity index
<b>PDMAEMA</b>	Poly(2-(dimethylamino) ethyl methacrylate)
<b>PMMA</b>	Poly(methyl methacrylate)
<b>RAFT</b>	Reversible Addition-Fragmentation chain Transfer polymerization



<b>RI</b>	Refractive index
<b>RTD</b>	Residence time distribution
<b>SCVCP</b>	Self condensing vinyl copolymerization
<b>SI-ATRP</b>	Surface Initiated Atom Transfer Radical Polymerization
<b>TEA</b>	Triethylamine
<b>THF</b>	Tetrahydrofuran

## Notations

<b>C</b>	Polymer concentration (g/L)
<b>C*</b>	Overlap concentration (g/L)
<b>K<sub>ATRP</sub></b>	Equilibrium constant (-)
<b>k<sub>p</sub></b>	Propagation constant (mol/L/s)
<b>k<sub>t</sub></b>	Termination constant (mol/L/s)
<b>L</b>	Tubular reactor length (m)
<b>M<sub>n</sub></b>	Number-average molecular weight (g/mol)
<b>M<sub>w</sub></b>	Weight-average molecular weight (g/mol)
<b>M<sub>w</sub> MALS</b>	Weight-average molecular weight as seen by multi angle light scattering detector (g/mol)
<b>M<sub>w</sub> RI</b>	Weight-average molecular weight as seen by refractive index detector (g/mol)
<b>n</b>	Flow index of power-law fluids (-)
<b>Q</b>	Volume flow rate (m <sup>3</sup> /s)
<b>R</b>	Tubular reactor radius (m)
<b>η</b>	Polymer solution viscosity (Pa.s)
<b>η<sub>0</sub></b>	Solvent viscosity (Pa.s)
<b>η<sub>sp</sub></b>	Specific viscosity (-)
<b>[η]</b>	Intrinsic viscosity (L/g)
<b><math>\dot{\gamma}_w</math></b>	Shear rate at the wall (1/s)

---

*TABLE OF CONTENT*

---

<b>1. INTRODUCTION</b>	2
<b>2. BACKGROUND LITERATURE</b>	
<i>Preface</i>	6
<b>2.1 Aspects of controlled radical polymerization (CRP)</b>	7
2.1.1 General overview	7
2.1.2 Special considerations for ATRP	8
2.1.3 Intensification of CRP in batch reactors	9
2.1.3.1. Acceleration of NMP	9
2.1.3.2. Acceleration of RAFT	10
2.1.3.3 Acceleration of ATRP	12
2.1.4 Summary	14
<b>2.2 Microreaction technology</b>	14
2.2.1 Microreactors	16
2.2.1.1 Different types	16
2.2.1.2 Special features	19
2.2.2 Microdevices for polymer synthesis	23
2.2.2.1 Microreactor setup	23
2.2.2.2 Micromixers	25
2.2.3 Benefits of microdevices for polymers and copolymers synthesis	31
2.2.3.1 Polymers with controlled macromolecular characteristics	32
2.2.3.2 Polymers with controlled chemical composition	40
2.2.3.3 Polymers with controlled architecture	45
2.2.3.4 New operating windows	49
2.2.4 Online monitoring	55
2.2.5 Summary	55
<b>2.3 Conclusion</b>	56
<b>References</b>	57
<b>3. MATERIALS AND METHODS</b>	
<i>Preface</i>	68
<b>3.1 Materials</b>	69
3.1.1 Main reagents and chemicals	69
3.1.2 Synthesis of 2-(2-bromoisobutyryloxy)ethyl methacrylate	69
<b>3.2 ATRP in batch reactor</b>	70
3.2.1 Linear homo polymerization	70
3.2.2 Linear statistical copolymer synthesis	70

---

3.2.3 Branched PDMAEMA synthesis	71
<b>3.3 ATRP in microreactor</b>	<b>72</b>
3.3.1 Microreactor setup and instrumentation	72
3.3.2 Primary components	73
3.3.2.1 Reservoirs and nitrogen supply	73
3.3.2.2 Pumps	74
3.3.2.3 Oven	74
3.3.2.4 Feed tubes	74
3.3.2.5 Microreactor	74
3.3.3 Secondary components	76
3.3.3.1 Micromixers	76
3.3.3.2 Back pressure regulator (BPR)	77
3.3.4 Auxiliary components	78
3.3.5 General procedure of microreaction	79
3.3.6 High pressure reaction	81
3.3.7 Reaction under high shear rate	82
<b>3.4 Characterizations</b>	<b>83</b>
3.4.1 Precipitation of polymer	83
3.4.2 <sup>1</sup> H NMR analysis	83
3.4.2.1 Conversion calculation during homopolymerization	84
3.4.2.2 Conversion calculation during copolymerization of DMAEMA & BzMA	84
3.4.2.3 Conversion calculation during branched polymerization	85
3.4.3 Gel permeation chromatography	87
3.4.3.1 Determination of steady state of continuous polymerization microreactor	88
3.4.3.2 Branching efficiency	89
3.4.4 Rheological behavior of polymerizing solution	90
3.4.4.1 General procedure	90
3.4.4.1 Intrinsic viscosity and different rheological parameters	90
3.4.5 Pressure drop determination	91
<b>References</b>	<b>92</b>

---

## **4. EFFECT OF PREMIXING AND OPERATING PARAMETERS ON REACTION RATE**

*Preface* 94

### **4.1 Intensifying the ATRP synthesis of statistical copolymers by continuous micromixing flow techniques**

4.1.1 Introduction	96
4.1.2 Materials and methods	97
4.1.3 Results and discussion	97
4.1.4 Summary	103
4.1.5 Supporting Information	104

**References** 106

### **4.2 Atom Transfer Radical Polymerization in continuous-microflow: effect of process parameters**

4.2.1 Introduction	109
4.2.2 Materials and methods	110
4.2.3 Results and discussion	110
4.2.3.1 <i>Effect of temperature on polymerization in microreactor</i>	110
4.2.3.2 <i>Effect of pressure</i>	111
4.2.3.3 <i>Effect of shear rate on polymerization</i>	114
4.2.4 Summary	117
4.2.5 Supporting Information	119

**References** 123

## **5. COIL FLOW INVERSION AS A ROUTE TO CONTROL POLYMERIZATION IN MICROREACTORS**

*Preface* 127

### **5.1 Effect of coil flow inversion on macromolecular characteristics**

5.1.1 Introduction	129
5.1.2 Materials and methods	130
5.1.3 Results and discussions	130
5.1.3.1 <i>Linear polymer synthesis</i>	130
5.1.3.2 <i>Branched polymer synthesis</i>	131
5.1.4 Summary	137
5.1.5 Supporting Information	138

**References** 141

---

## **5.2. Flow inversion: an effective mean to scale-up controlled radical polymerization in tubular microreactors**

5.2.1 Introduction	144
5.2.2 Materials and methods	145
5.2.3 Results and discussion	146
5.2.3.1 <i>Effect of reactor geometry</i>	146
5.2.3.2 <i>Effect of reactor diameter</i>	147
5.2.3.3 <i>Effect of reactor length</i>	149
5.2.3.4 <i>Process parameters</i>	150
5.2.4 Summary	152
5.2.5 Supporting Information	153
<b>References</b>	158
<b>6. CONCLUSION AND PERSPECTIVES</b>	160

---

*CHAPTER 1*  
*INTRODUCTION*

## ***Introduction***

Nowadays polymers and polymeric materials are used for unconventional applications because of their functional properties (e.g. electronics, solar cells, biomedical ...) conversely to conventional applications which rely on bulk properties (e.g. automotive parts, textile ...). Such high end applications demand for well controlled characteristics of macromolecules. Minor changes in these characteristics can influence the final properties.<sup>1-3</sup> Poly(2-(dimethylamino)ethyl methacrylate) (PDMAEMA) is one of such functional polymers. pH and thermo responsive nature of PDMAEMA makes it a preferred candidate for a variety of demanding applications like drug and non-viral gene deliveries among others.<sup>4-11</sup> To extract maximum benefit of such polymer, high control on its macromolecular characteristics is a prerequisite.

Controlled radical polymerization (CRP) techniques are among the most effective chemical-based methods to control macromolecular characteristics of a polymer; unlike the established free radical polymerization technique which suffers from termination reactions resulting in a broad molecular weight distribution. Among all the CRP techniques, Atom Transfer Radical Polymerization (ATRP) is the most widely used technique from an academic and industrial research point of view.<sup>12</sup> However due to its inherent kinetic scheme, which exhibits an equilibrium reaction between dormant and propagating species, ATRP suffers from low productivity resulting from a slow kinetics.

On the other hand, any polymerization reaction is affected by the process conditions especially in case of concentrated solutions. Besides, polymers are known to be process products. Therefore the process conditions should be well adapted to avoid any detrimental effect on the chemical control of the macromolecular characteristics. New process considerations referred as microreaction technology has emerged during the last decade which can at the same time intensify polymerization processes while maintaining or improving the control over polymer characteristics.

In this context, the PhD work aims at intensifying ATRP processes for the production of DMAEMA-based polymers by relying on microreaction technology tools (microreactor, micromixers) and process parameters (reactor geometry, temperature, pressure...).

In following chapter, different chemical- and process-based methods to accelerate CRP reactions will be reviewed. The benefit of microreaction technology will be also reviewed in light of polymer synthesis. Compared to other fields of chemical reactions, polymer synthesis



in microfluidic systems is relatively new and lot of benefits can be achieved from characteristics features of microdevices.

Chapter 3 details materials and methods used during this work. Among other, the polymerization system composition and procedures followed during experiments in batch reactor will be presented. Microreaction setup used for polymer continuous-flow synthesis will be illustrated in details along with operating parameters. Microreactors with different dimensions and geometries will be described. Procedures for high pressure and high shear reaction will be explained. Finally the characterization section will highlight all the different methods and techniques used to characterize reactors and determine macromolecular characteristics.

Chapter 4 will present the effect of different micromixing principles on the characteristics of statistical DMAEMA-based copolymer. Bilaminaion (T-Junction), impact jet (KM Mixer) and interdigital multilamination (HPIMM) micromixers were considered for the ATRP copolymerization of 2-(dimethylamino)ethyl methacrylate (DMAEMA) with benzyl methacrylate (BzMA). Polymers of two different compositions of BzMA (20 mol.% and 40 mol.% BzMA) were synthesized in coiled tubular (CT) microreactor. In the second section of this chapter, ATRP polymerization of DMAEMA in CT reactors under different operating conditions (temperature, pressure and shear rate) is discussed. It gives a clear idea how such polymerization reaction can be accelerated. This section also highlights the effect of CT reactors diameter.

Chapter 5 addresses the issue of increased viscosity during polymerization in microreactor and its detrimental effect on the control of macromolecular characteristics as observed in chapter 4. To overcome such limitations and reduce residence time distribution in tubular microreactor, a simple flow inversion technique was considered which is known as coil flow inverter (CFI). It is a much simpler and cheaper alternative compared to patterned reactors reported in literature. Thus stainless steel microreactors having 90° bends at equal interval were used for polymerization. In the first section, the synthesis of linear and branched PDMAEMA in different reactors (batch, CT and CFI) will be presented and results thoroughly explained. The second section tries the tackle down the problem of microreactor low throughput and will present different strategies in order to increase polymer productivity without sacrificing the benefits of microreaction. Hence CT and CFI of larger diameters (1753 and 4084  $\mu\text{m}$ ) and different lengths (3 and 6 m) were considered.

---

Finally chapter 6 will highlight the overall outcome of this work. Experience and knowledge gained during this thesis should be quite helpful for future work. Thus suggestions and recommendations are to be given to proceed further.

*This PhD work is part of a larger project named DIP<sup>2</sup>, funded by the French Research Agency (ANR grant n ° 09-CP2D-DIP<sup>2</sup>), which aim was to intensify a CRP process for the production of architecture-controlled polymers. It comprised an experimental work (this thesis) as well as a numerical work for the geometry optimization of CFI reactors.*

## References

- (1) Ramkissoon-Ganorkar, C.; Liu, F.; Baudys, M.; Kim, S. W. *Journal of biomaterials science. Polymer edition* **1999**, *10*, 1149.
- (2) Rathfon, J. M.; Tew, G. N. *Polymer* **2008**, *49*, 1761.
- (3) Xu Zheng, Z. T.; Xie, X.; Zeng, F. *Polymer Journal* **1998**, *30*, 5.
- (4) Mao, J.; Ji, X.; Bo, S. *Macromolecular Chemistry and Physics* **2011**, *212*, 744.
- (5) Pietrasik, J.; Sumerlin, B. S.; Lee, R. Y.; Matyjaszewski, K. *Macromolecular Chemistry and Physics* **2007**, **208**, 30.
- (6) Yuan, W.; Guo, W.; Zou, H.; Ren, J. *Polymer Chemistry* **2013**, *4*, 3934.
- (7) Jiang, X.; Lok, M. C.; Hennink, W. E. *Bioconjugate Chemistry* **2007**, *18*, 2077.
- (8) Lin, S.; Du, F.; Wang, Y.; Ji, S.; Liang, D.; Yu, L.; Li, Z. *Biomacromolecules* **2007**, *9*, 109.
- (9) Park, T. G.; Jeong, J. H.; Kim, S. W. *Advanced Drug Delivery Reviews* **2006**, *58*, 467.
- (10) Yancheva, E.; Paneva, D.; Maximova, V.; Mespouille, L.; Dubois, P.; Manolova, N.; Rashkov, I. *Biomacromolecules* **2007**, *8*, 976.
- (11) Vigliotta, G.; Mella, M.; Rega, D.; Izzo, L. *Biomacromolecules* **2012**, *13*, 833.
- (12) Matyjaszewski, K.; Spanswick, J. *Materials Today* **2005**, *8*, 26.

---

# CHAPTER 2

## BACKGROUND LITERATURE

<i>Preface</i>	6
<b>2.1 Aspects of Controlled Radical Polymerization (CRP)</b>	7
2.1.1 General overview	7
2.1.2 Special considerations for ATRP	8
2.1.3 Intensification of CRP in batch reactors	9
2.1.3.1. <i>Acceleration of NMP</i>	9
2.1.3.2. <i>Acceleration of RAFT</i>	10
2.1.2.3 <i>Acceleration of ATRP</i>	12
2.1.4 Summary	14
<b>2.2 Microreaction technology</b>	14
2.2.1 Microreactors	16
2.2.1.1 <i>Different types</i>	16
2.2.1.2 <i>Special features</i>	19
2.2.2 Microdevices for polymer synthesis	23
2.2.2.1 <i>Microreactor setup</i>	23
2.2.2.2 <i>Micromixers</i>	25
2.2.3 Benefits of microdevices for polymers and copolymers synthesis	31
2.2.3.1 <i>Polymers with controlled macromolecular characteristics</i>	32
2.2.3.2 <i>Polymers with controlled chemical composition</i>	40
2.2.3.3 <i>Polymers with controlled architecture</i>	45
2.2.3.4 <i>New operating windows</i>	49
2.2.4 Online monitoring	55
2.2.5 Summary	55
<b>2.3 Conclusion</b>	56
<b>References</b>	57

## ***Preface***

Controlled radical polymerizations (CRP) find wide acceptance due to their efficient control over polymerization and macromolecular characteristics. However, slow rate of reaction is a major challenge for CRP. Acceleration of CRP without losing control over polymerization will be beneficial from industrial perspective. Several methods to achieve faster kinetics of CRP in batch reactor are reported in literature. Overview of such strategies to accelerate different CRP like NMP, RAFT and ATRP are briefly discussed in the first part of this chapter.

On the other hand, microreaction technology is by now largely considered for process intensification in fine chemical and pharmaceutical synthesis. In the field of polymer reaction engineering, microreaction is just a decade old and genuine fear of increased viscosity and low throughput are few hurdles which force researchers and industries to undermine its potential. Nevertheless some applications of microfluidics can be found in the field of polymer synthesis but quite few concern the rate enhancement of CRP. To have a clear understanding about this budding technique and its impact in the field of polymer reaction engineering a detailed discussion is needed. Therefore polymerization micro-chemical plants for the synthesis of polymers and copolymers composed of microdevices are described and commented in the second part of this chapter. Due to their unique characteristics, microdevices allow rapid heat removal and mixing. This contributes to improve the control over the polymerization by reducing or eliminating mass transfer limitations and hot spot formation. This chapter also highlights how fast mixing and heat management allow obtaining macromolecules with better controlled characteristics (molecular weights and narrower molecular weight distributions), compositions and architectures.

*This chapter is partially adapted from the following online review:*

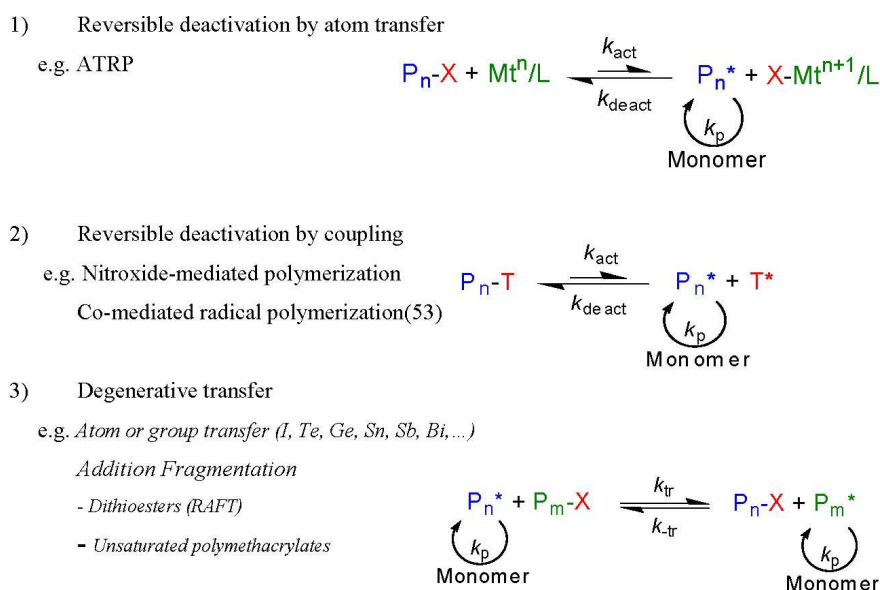
- C. A. Serra, D. Parida, F. Bally, D.K. Garg, Y. Hoarau, and V. Hessel, "Micro-Chemical Plants" in «*Encyclopedia of Polymer Science and Technology* »; Wiley-VCH, Weinheim (Germany), DOI: 10.1002/0471440264.pst612.

## 2.1. Aspects of Controlled Radical Polymerization (CRP)

### 2.1.1 General overview

Simple reaction conditions, faster kinetics and ability to polymerize a wide range of vinyl monomers makes Free Radical Polymerization (FRP) a robust and economical process to synthesize commodity polymers.<sup>1</sup> However, unavoidable termination and transfer reactions due to high reactivity of transient species result in broad molecular weight distributions. Poor control over molecular weight distribution, composition and architecture limits application of FRP in the field where above mentioned polymer characteristics are of prime importance.

To overcome limitations of FRP some techniques were developed in last few decades and known as controlled radical polymerization (CRP). CRP allows synthesizing polymer with controlled characteristics and architecture for high end applications. Among all the CRP techniques developed Nitroxide Mediated Polymerization (NMP),<sup>4-6</sup> Reversible Addition-Fragmentation chain Transfer polymerization (RAFT)<sup>7-9</sup> and Atom Transfer Radical Polymerization (ATRP)<sup>10,11</sup> are most widely used and reported.



**Scheme 2.1.** General scheme of NMP, RAFT and ATRP.<sup>12</sup>

CRP achieves greater control over reaction by increasing the lifetime of a growing chain. Such philosophy relies on dynamic equilibrium between low concentrations of growing chain and capped dormant chains which can neither propagate nor terminate.<sup>12,13</sup> This dynamic equilibrium is self regulating and also known as persistent radical effect (PRE). The PRE is a special feature in CRP system in which the propagating chain ( $P_n^*$ ) are capped by a

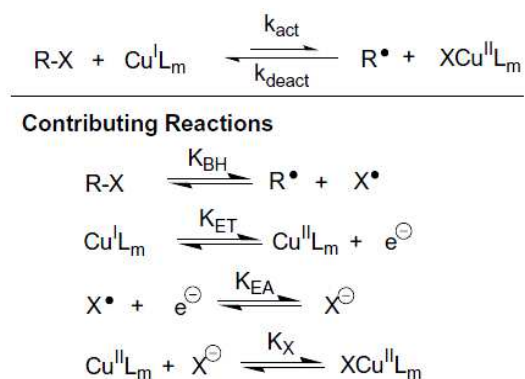
deactivating species (X) as shown in scheme 1. These new dormant species are stable and can be reactivated easily with the help of heat, light or catalyst. After reactivation, the newly formed radical can propagate like in normal FRP. In case of radical–radical termination, concentration of deactivating species (X) increases in the system. Detailed mechanisms of different CRP techniques are extensively discussed in the literature.<sup>2,11-13</sup>

Controlled characteristics of CRP enable to synthesize gradient, block, star copolymers and polymers with controlled graft densities.<sup>14-16</sup> From adaptability and tolerance point of view CRP systems are superior to conventional FRP. They are more tolerant towards different solvent systems<sup>17-20</sup> and functionality of monomers.<sup>21-23</sup> These features of CRP draw lot of attention not only from academia, but also from industries.

### 2.1.2. Special considerations for ATRP

ATRP was devised by two independent groups in mid 90s.<sup>8,9</sup> Since then many modifications and developments have taken place and by the years ATRP is emerging as a powerful technique for the synthesis of polymers with controlled molecular weight, low polydispersity, controlled chain end functionality, morphology and composition. The ATRP method relies on the reversible homolytic cleavage of an alkyl halide initiator molecule in the presence of transition metal salt complexed with a suitable bi- or tridentate ligand acting together as catalyst. After cleavage the monomer starts to be incorporated in growing chains.

Considering the wide acceptance and its relevance to the thesis, ATRP is discussed in brief.<sup>12</sup> The mechanism involved to control the polymerization is the atom transfer between growing chains and catalyst. Like other CRP, dynamic equilibrium of ATRP is of prime importance to get a controlled polymer characteristics.



**Scheme 2.2.** Reactions responsible for equilibrium in ATRP, where RX represents alkyl halide and L a ligand.

Equilibrium in ATRP ( $K_{ATRP}$ ) is mainly governed by 4 set of reversible reactions shown in scheme 2.2.<sup>24</sup> These reactions are (i) homolysis of alkyl halide bond ( $K_{BH}$ ), (ii) oxidation of metal complex (indicated as  $K_{ET}$ , the equilibrium constant for electron transfer), (iii) reduction of halogen to halide ions ( $K_{EA}$ , equilibrium constant for electron affinity) and (iv) association of halide ion with metal complex ( $K_X$ ).

ATRP allows producing functional polymers quite easily. Two methods are commonly used. Post functionalization method relies on the modification of the chain end. Indeed carbon-halogen chain end present in an active macromolecule can form hydroxyl, allyl, azido and ammonium or phosphonium end groups by nucleophilic substitution.<sup>25-27</sup> Preparation of polymer having amino end groups is also reported in literature. It is achieved by the substitution of the halogen end groups with azides followed by the conversion of the azide groups to phosphoranimine end groups and finally hydrolyzed to form amino groups.<sup>24-27</sup> The second method of preparing polymer having different functionalities employs initiator with functional groups.

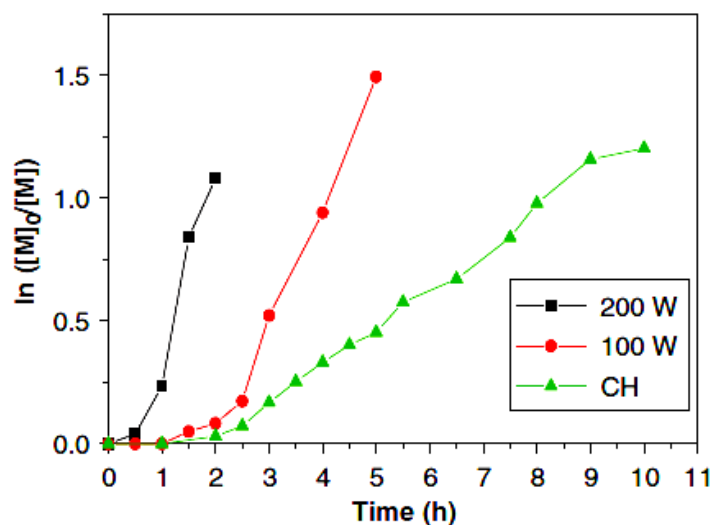
### 2.1.3. Intensification of CRP in batch reactors

Slow reaction rate of CRP, originating from the equilibrium reaction, is one of the major challenges on its way towards wide acceptability in commercial applications. To extract maximum benefits of CRP, polymerization rate needs to be enhanced without sacrificing its controlled nature. Acceleration can be achieved by changing chemical system and by process conditions. Such methods to accelerate CRP are discussed in brief in the following section.

#### 2.1.3.1. Acceleration of NMP

In literature very limited information is available on methods to accelerate NMP. One of such method is by using microwave heating instead of conventional heating.<sup>28-30</sup> Li *et al.* demonstrated the accelerating effect of microwave during bulk NMP of styrene.<sup>31</sup> A much higher polymerization rate was observed during polymerization of styrene under microwave as shown in Figure 1. Rate was also found to increase with power of microwave at a particular polymerization temperature. Under microwave, equilibrium reaction was found to establish rapidly (Figure 2.1). In microwave polymerization system, molecules of monomer and polymer rotate and oscillate rapidly. Microwave is also responsible for polarization and deformation of molecules, which may be responsible for the enhanced reactivity of the system. In another development, Rigolini *et al.* reported the use of microwave in pulsed

power mode and dynamic mode.<sup>28</sup> They observed a significant acceleration in NMP rate in pulsed power mode compared to dynamic mode.



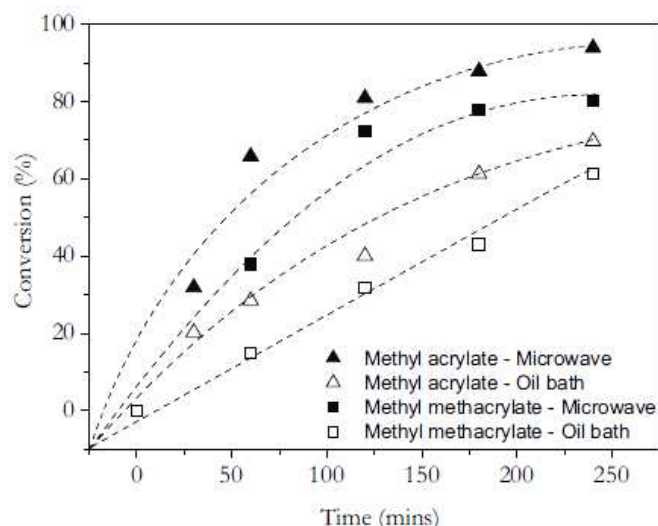
**Figure 2.1.** Kinetic plots of  $\ln([M]_0/[M])$  vs. reaction time for bulk polymerization of styrene under microwave (100 and 200 W) and conventional heating (CH) at 125 °C.<sup>30</sup>

Accelerator molecules like photo-acid generators were also used to enhance the rate of NMP reaction. One such example is the use of (4-*tert*-butylphenyl) diphenylsulfonium triflate (*t*BuS) as an accelerator molecule during Nitroxide Mediated photo polymerization of methacrylic acid. This photo-NMP was carried out using azoinitiators and 2,2,6,6-tetramethylpiperidine-1-oxyl (TEMPO) as the mediator. Larger accelerator/mediator ratios resulted in increased polymerization rates both in bulk and solution.<sup>31</sup> Molecular weight distribution was found to decrease with increase in accelerator/mediator ratio and solvent content in the system.

### 2.1.3.2. Acceleration of RAFT

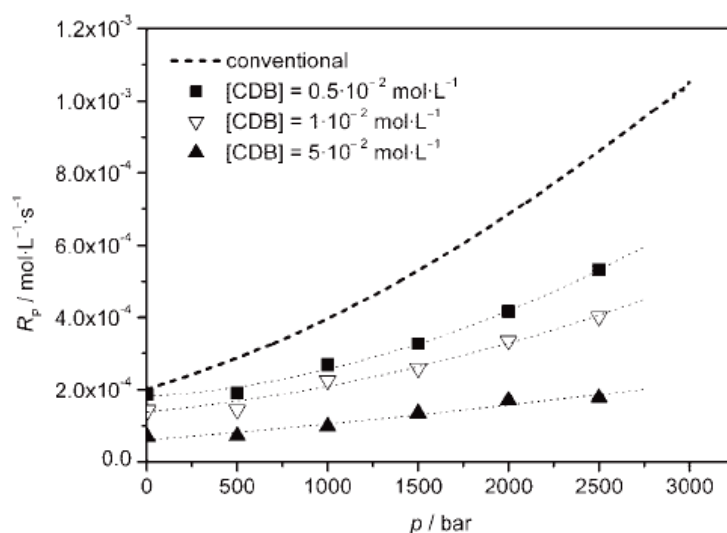
As in case of NMP, polymerization rate of RAFT also increased significantly under microwave irradiation as shown in Figure 2.2.<sup>32-37</sup> Zhu *et al.* reported a 5.4 times faster polymerization rate in microwave assisted RAFT compared to conventional heating and polydispersity index (PDI) remained within 1.25. It indicates polymerization was accelerated without sacrificing controlled nature of RAFT.<sup>32</sup>





**Figure 2.2.** Relative conversion of monomers with time in different heating systems.<sup>33</sup>

Pressure is another parameter which was found to have a significant impact on polymerization kinetics of RAFT polymerization.<sup>38-40</sup> Initially high pressure RAFT polymerization was used to polymerize methyl ethacrylate which is a monomer difficult to polymerize at ambient pressure because of steric hindrance of  $\alpha$ -ethyl substituent.<sup>38</sup> Another example was reported by Arita *et al.* who observed a rapid increase in styrene polymerization rate (by a factor of 3) going from ambient pressure to 2500 bars as shown in Figure 2.3.<sup>39</sup> Interestingly reduced molecular weight distribution was observed in case of high pressure polymerization indicating better control over polymerization.

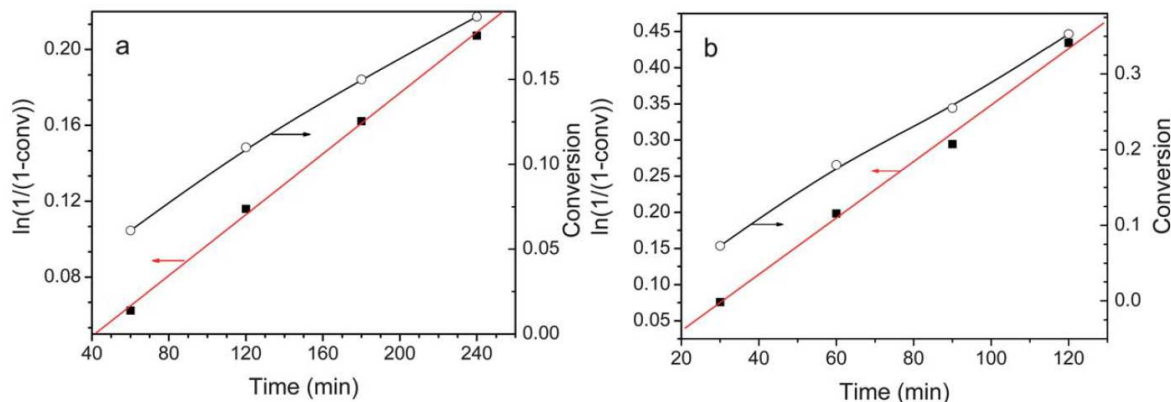


**Figure 2.3.** Effect of pressure on rate of polymerization of styrene at different cumyl dithiobenzoate (CDB) concentrations.<sup>39</sup>

### 2.1.2.3 Acceleration of ATRP

Like other two CRP techniques discussed above, there are also different methods reported to accelerate ATRP. One such method relies on use of alcohol/water (95/5 vol. %) as solvent and mixed transition metal catalyst ( $\text{Fe(0)/CuBr}_2 = 1/0.1$ ). It was found that within few hours (16 h instead of days) 98 % conversion was reached at 30 °C polymerization temperature. This method has the advantage of cheaper solvent and significant reduction of toxic copper from the polymerization system.<sup>40</sup>

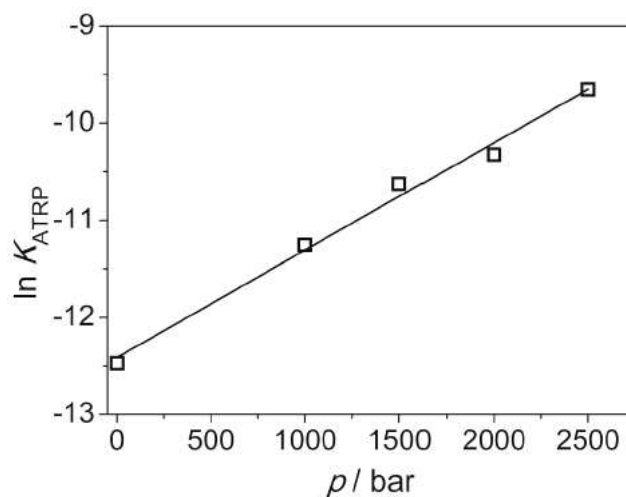
Another way to accelerate ATRP in case of silica nanoparticles surface initiated process was reported by Liu *et al.*<sup>41</sup> Usually surface initiated ATRP (SI-ATRP) polymerization rate is much slower than volume polymerization rate due to geometric constraints of high density polymer chains on the surface. High surface density of chains leads to irreversible termination and slows down the polymerization rate. To reduce termination, Liu *et al.* used self polymerized polystyrene chains during SI-ATRP of styrene. They observed acceleration of SI-ATRP as a faster kinetics was obtained with increase in polystyrene content (Figure 2.4). However, such strategy had no effect on polymerization rate during volume polymerization of styrene.



**Figure 2.4.** SI-ATRP of styrene on silica nano particles using 0.5% polystyrene (a) and 1% polystyrene in polymerization system.<sup>41</sup>

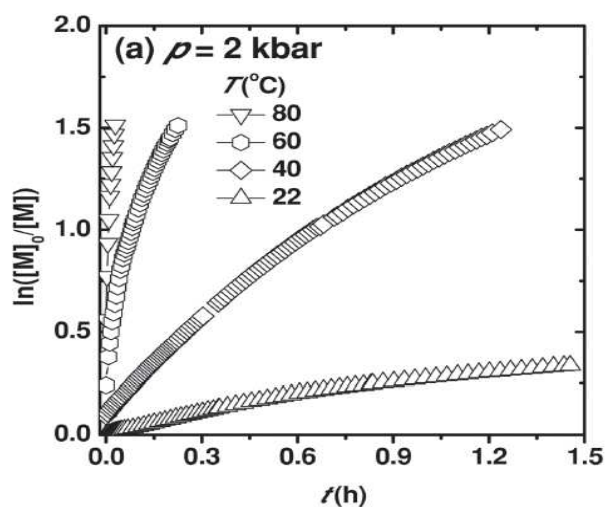
Unlike two other CRP techniques (NMP and RAFT) high pressure route to accelerate ATRP was more explored.<sup>42-47</sup> High pressure enhances propagation (higher  $k_p$ ) and reduces termination (lower  $k_t$ ) rates. As a result polymerization rate increases significantly and reduced termination leads to controlled macromolecular characteristics. This feature of high pressure polymerization is also helpful to synthesize high and ultra high molecular weight polymers.<sup>42-45</sup> Matyjaszewski and co-workers reported increase in rate of polymerization of

methyl methacrylate under high pressure (up to 2500 bars) in acetonitrile. Equilibrium constant ( $K_{\text{ATRP}}$ ) at ambient pressure was  $3.8 \times 10^{-6}$  and increases by one order of magnitude with an increase in the pressure up to 2500 bars (Figure 2.5).<sup>46</sup> Propagation kinetic constant ( $k_p$ ) also increased by nearly one order of magnitude with pressure. Overall consequence was an increase in polymerization rate by two orders of magnitude from atmospheric pressure to 2500 bars.



**Figure 2.5.** Pressure dependence of  $K_{\text{ATRP}}$  for ATRP of MMA at 25 °C.<sup>46</sup>

High pressure polymerization also allows carrying out polymerization at elevated temperature without increasing termination.<sup>49</sup> It accelerates the polymerization further without affecting the characteristics of ATRP as shown in Figure 2.6. Interestingly it was found that very low level of Cu catalyst ( $\sim 100$  ppm) is required in case of high pressures.



**Figure 2.6.** Plot of  $\ln([M]_0/[M])$  vs time for ATRP of n-butyl acrylate at different temperatures under 2000 bars pressure.<sup>49</sup>

### 2.1.4 Summary

Two distinctive strategies can be worked out in batch reactors to accelerate CRP, namely chemical- and process-based methods. The former is likely to be strongly dependent of the polymerization system like in the above mentioned SI-ATRP and thus should be adapted for each new case. The latter is composed of microwave- and pressure-assisted polymerization processes. However failure to accelerate polymerization of non-polar monomers like styrene is a serious limitation of the microwave method.<sup>34</sup> High pressure was found to be beneficial in all CRP techniques from kinetics point of view. However polymerization at such high pressure (few thousands bars) is always troublesome and requires specialized equipments. This makes the process very expensive and unsafe. Nevertheless for these two methods, controlled nature of the CRP was not altered.

On the other hand, there is a new technique available which has the ability to accelerate polymerization rate and improve the control over macromolecular characteristics. This technique refers to microreaction technology. Features, abilities and advantages of this new technique in the field of polymer synthesis are discussed in the following section.

## 2.2 Microreaction technology

Roots of present microdevices dates back to 1970s when Stephan Terry designed what is now considered as the first microfluidic device.<sup>50</sup> However, this work remained unnoticed till the concept of  $\mu$ TAS (miniaturized Total Analysis System) was developed.<sup>51</sup> Thus microfluidics emerged as a new multidisciplinary field aiming at the precise manipulation of fluids in sub-millimeter scale devices also referred as microdevices. Since then these microfluidic devices have evolved with much greater pace in different domains. At present they cover a broad spectrum of applications starting from analytics, life science, clinical diagnostics and pharmaceuticals to synthetic chemistry. The design and use of microreactors, micromixers and micro heat exchangers, three special classes of microdevices, to carry out and control chemical reactions at small scale led to the development of a new scientific and technical discipline named Micro Reaction Technology (MRT).<sup>52,53</sup> Just recently, microseparators (extraction, distillation, crystallization) and enzymatic microreactors added as new development lines.<sup>54-56</sup> Compared to other fields of chemical reactions, polymer synthesis in microfluidic systems is relatively new and can benefit a lot from MRT. Indeed polymerization reactions have unique features. Unlike any other chemical compound, synthetic macromolecules have characteristics (average molecular weight, chain length distribution)

---

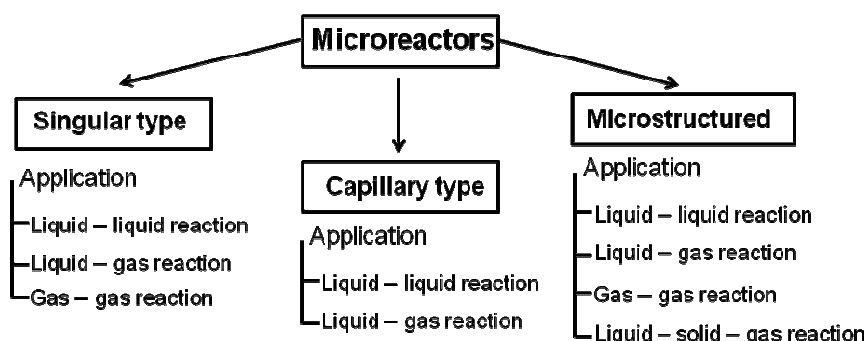
which are greatly affected by the process parameters which in turn influence their properties (e.g. mechanical, thermal, and processing). Viscosity increase is considered as one of the foremost important parameters.<sup>57</sup> This increase, which can reach up to 7 decades for bulk and highly concentrated solution processes, is followed by a respective decrease of the reactants molecular diffusion coefficients and the reduction of mass and thermal transports.<sup>57,58</sup> As an overall consequence, the polymerization rate may locally increase. This is the gel or Trommsdorff effect. This uncontrolled acceleration of the polymerization reaction rate leads to the broadening of the chain lengths distribution and the polydispersity (PDI) increases. Another frequent problem encountered with polymerization processes is the removal of the heat released by the reaction. For exothermic polymerization reactions, insufficient thermal transport towards the cooling system (e.g. double jacket or immersed serpentine) may lead to thermal runaways. The consequences on polymer properties are usually twofold. First of all, a significant broadening of the chain lengths distribution can be observed. Secondly, beside non-reproducible results, the number-average chain length may significantly vary (several orders of magnitude) from the expected value. Mixing is also an extremely important issue in homogeneous polymerization processes. Low quality mixing between on one hand, the monomer phase, and on the other hand, the solvent and initiator phase, will generate large local concentration gradients, often termed segregation.<sup>55</sup> Since the propagation reaction is usually very fast zones of high monomer concentrations will produce high molecular weight polymers and release a lot of energy. Thus, a hot spot is formed which can lead to degradation of the polymer and/or the monomer.

Attribute which gives microdevices an edge over conventional glass wares or industrial equipments is their smaller dimension, ranging from few micrometers to several hundreds of microns; the first more for functional short-path elements such as mixing nozzles, the latter for the subsequent reaction channels. At such scale, it was found that microdevices can significantly improve mass and heat transfers.<sup>59-78</sup> By slight expansion of the dimensions, e.g. in the milli range, and with some compromises of performance (smart scaling-out), a path to industrial production of polymers is opened, at least in the lower range of specialties of a few 10-100 t/a. Therefore Micro Reaction Technology in combination with Polymer Reaction Engineering has unleashed new opportunities to get polymers and copolymers with better controlled characteristics.<sup>79,80</sup>

## 2.2.1 Microreactors

### 2.2.1.1 Different types

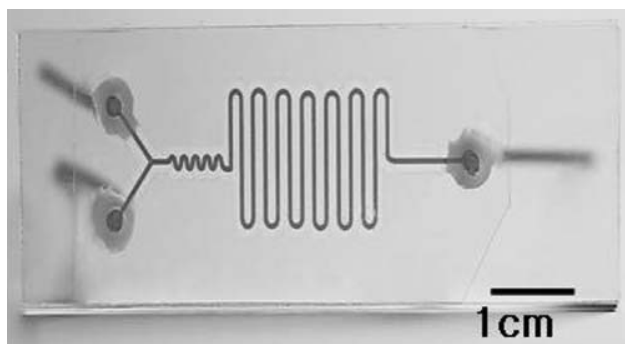
A microreactor (or several) constitutes the heart of any micro-chemical plant and its selection depends on the type of reaction to be performed and operating conditions (e.g. temperature, pressure). Microreactors can be broadly classified into three different categories as shown in scheme 2.3.



**Scheme 2.3.** Different types of microreactors and their areas of application.

#### 2.2.1.1.1 Singular type

Singular type microreactors are made typically by advanced clean-room technologies (Si microfabrication being most dominant) or with increasing acceptance by much simplified PDMS manufacture. They comprise microchannels embedded into a flat surface of credit-card size whose width or depth range typically from few tens of microns up to 500  $\mu\text{m}$  (see Figure 2.7). The singular type of microreactors possesses the highest surface to volume ratio among all microreactor types, respectively the smallest channels. It can be constructed from different materials but silicon, glass, poly(dimethyl siloxane) (PDMS) and poly(methyl methacrylate) (PMMA) are mainly employed. Silicon and glass are most popular as material for construction because of their inertness to most of the reagents and solvents. Their transparency nature is also an added advantage which allows visual inspection or detection during reaction. Although both glass and silicon are suitable for many applications, silicon is usually preferred when rapid heat or cool cycles are requested which is a consequence of its excellent thermal conductivity. Singular type microreactors are normally suitable for low pressure application due to the limited mechanical strengths of most interconnects between cover plate and microstructure plate. Thus, industrial applications of singular type microreactors are very limited.



**Figure 2.7.** Image of a singular type microreactor.<sup>81</sup>

#### 2.2.1.1.2 Capillary type

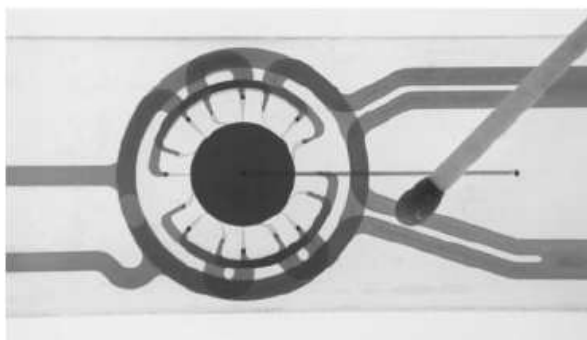
Capillary type microreactors are tubes of internal diameter less than one millimeter and length ranging from millimeters to few meters e.g., those commonly used for HPLC applications. Poly(tetrafluoroethylene) (PTFE), poly(ether ether ketone) (PEEK) and stainless steel are the most common materials for this type of microreactors allowing to carry out chemical reactions under a wide range of pressures from few bars up to several hundreds. This kind of microreactors do not have inbuilt mixers as in case of the singular type and microstructured reactors. The idea is that premixing can be done without initiating reaction and rising (substantially) temperature sets the reaction starting point. This indeed works out well for many known homogeneous and heterogeneous liquid-liquid reactions. Microfluidic reactors made from tubing are relatively cheap and long reactor lengths can be easily achieved. This enables chemical reactions to be conducted with few seconds of residence time to several hours to achieve high conversion; yet in the latter case it is obtained at expense of reducing the flow rate. The throughput of capillary microreactors is higher as compared to singular type microreactors mainly to a higher internal volume. Thus, flow rates of up to hundreds of milliliters per hour are commonly employed. However, careful selection of the reactor material should be made depending upon the reaction conditions like pressure, oxygen sensitivity or resistance to solvent etc. For example polymeric capillaries are not suitable for high pressure reactions. Depending on the thickness of the wall of capillary, oxygen can diffuse through it. It can be detrimental to oxygen sensitive reactions like RAFT polymerization.<sup>80</sup>

A relatively new concept is the tube-in-tube microreactor which has a porous membrane permeable for gases, but not for liquids. Thus, a gas can flow in the outer core and move through a membrane which is the inner tube into the reaction flow. Dangerous gases such as

ozone are easily fed into a liquid medium in this way. Naturally, a (released) gas can be immediately removed in the same manner.<sup>83</sup>

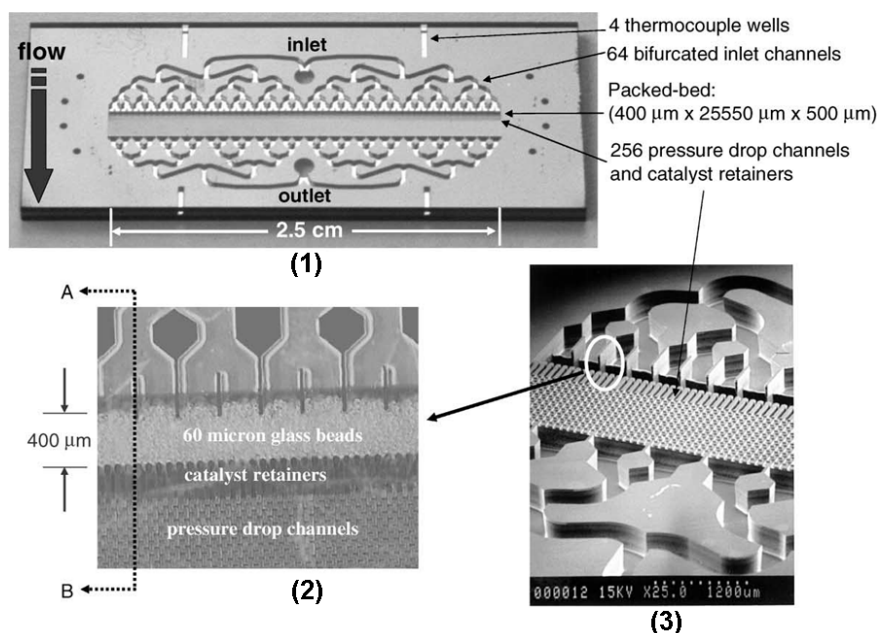
#### 2.2.1.1.3 Microstructured

Complex geometries on microscale can be realised by this type of microreactors through flexible interconnection and integration of highly specialised mixers, reactors, and other process functions along a flow process line. These geometries are designed to provide additional functions (e.g. mixing, separation, delay loop) to the microdevice beside the locus of a chemical reaction. Thus, these microreactors can be equipped with upstream micromixing zones of even embedded mixing elements in the reaction microchannels. Figure 2.8a shows an example of a microstructured reactor, named cyclone mixer, designed for the production of foams and gas-liquid dispersions in general. It has 11 microstructured stacks each containing 3 groups of nozzles for supplying reagents. The gas and liquid injection nozzles are 30  $\mu\text{m}$  and 50  $\mu\text{m}$  wide respectively. Inside the reaction area, the gas bubbles form a cyclone-like pattern within the liquid which deform and coalesce in smaller microchannels. This pattern is very advantageous when efficient contact between a slurry catalyst and a gas phase is necessary in liquid-gas reactions. The mixer can also perform liquid-liquid reactions efficiently.<sup>84</sup> Microstructured reactors as shown in Figure 2.8b were designed for gas-liquid reactions and the microstructures were designed to act like a catalyst retainer.<sup>85</sup> Numerous examples of such microreactors have reported in the literature performing different functions like catalytic reaction or separation.<sup>77,86-88</sup> These microstructured reactors are efficient in handling most kind of reactions. However they are not preferred for polymerization reactions because of their inability to handle viscous solutions. Moreover, this type of microreactors is expensive and may require long fabrication time.



(a)





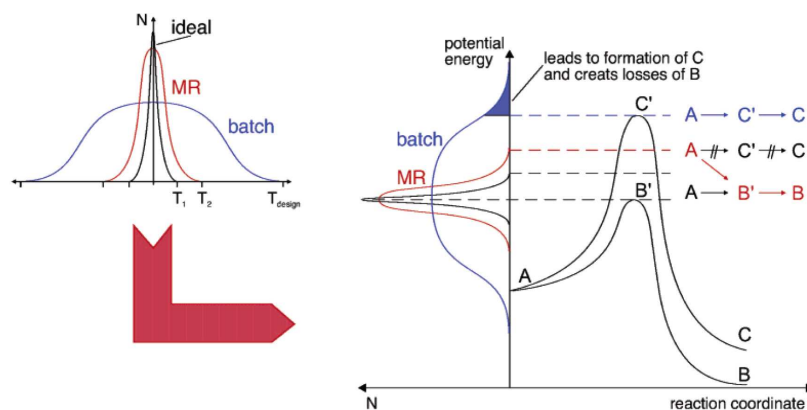
(b)

**Figure 2.8.** (a) Glass cyclone mixer<sup>78</sup>, (b) a microstructured reactor (1) bifurcating the reactant to 64 inlets which pass over a catalyst bed, (2) picture showing microreactor packed with 60  $\mu\text{m}$  glass beads, (3) SEM image of the microreactor.<sup>85</sup>

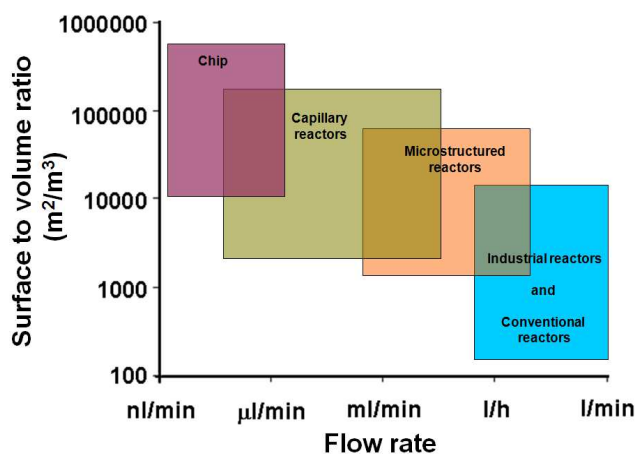
### 2.2.1.2 Special features

#### 2.2.1.2.1 Efficient thermal management

Heating and cooling are important parameters in controlling the course of any reaction. Uncontrolled heating can lead to multiple reaction pathways and ultimately to either a very slow or explosive reaction. Batch reactors and macroscale reactors often have a very broad temperature profile which leads to undesired side reactions. Figure 3 gives an idea how different side products are formed in a batch reactor because of its broad temperature profile.<sup>89</sup> In case of microreactors (MR), reaction is much more controlled because of its narrow temperature profile (Figure 2.9). High surface to volume ratios in the range of 10,000 to 500,000  $\text{m}^2/\text{m}^3$  make microreactors an efficient candidate for thermal management during the reaction (Figure 2.10).<sup>90</sup> Modern microreactors can have a heat transfer coefficient as high as  $\sim 25,000 \text{ W}/\text{m}^2\text{K}$  which is quite large as compared to commonly used heat exchangers and thus allow avoiding any hot spot formation. Therefore microreactors are suitable for highly exothermic reactions like the free radical (or anionic) polymerizations of acrylate-based monomers or anionic polymerizations.



**Figure 2.9.** Typical temperature profile for different reactors and formation of by products.<sup>89</sup>



**Figure 2.10.** Surface to volume ratio of different microdevices and conventional reactors.<sup>90</sup>

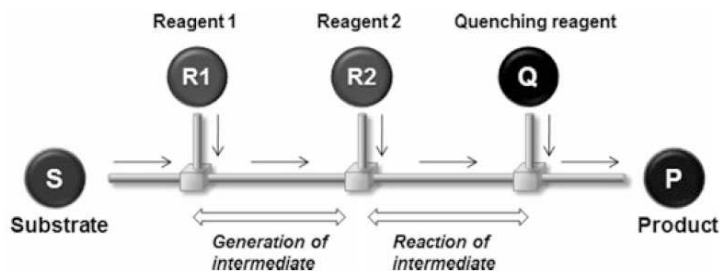
### 2.2.1.2.2 Enhanced mixing

Mixing is of prime importance in any kind of fast reaction and is usually achieved by stirring. Turbulence, convection and diffusion are the three physical processes responsible for mixing. In convection, transportation of materials takes place to different reactor's regions in bulk quantity and recirculation (e.g. chaotic advection, Dean flow) can be observed. With increase in size of reactor, transportation time also increases significantly. When rotation of the stirrer is sufficiently high, at least for low-viscous fluids such as the typical organic solvents, the fluid no longer is in laminar regime, turbulence is generated leading to the formation of eddies. Within eddies the mixing is mainly achieved by mass diffusion. However, before diffusion can take place, eddies "defragmentate" via Lyapunov stretching. The Smaller eddies, the faster is the mixing. Thus, mixing within an eddy can be achieved within few seconds depending on the size of the eddy. However, high viscosity (likely the case for bulk

and semi diluted polymerization reactors) and design considerations impose limitation on turbulent mixing at macroscale. Unlike macroreactors, mixing in microreactors is only governed by diffusion. Typical mixing times achieved are usually in the range of few milliseconds; even by order of magnitude faster is doable. Therefore, microreactors are suitable for mass-limited reactions which are often encountered in the synthesis of polymers due to the viscosity increase during the course of the reaction.

#### *2.2.1.2.3 Residence time control*

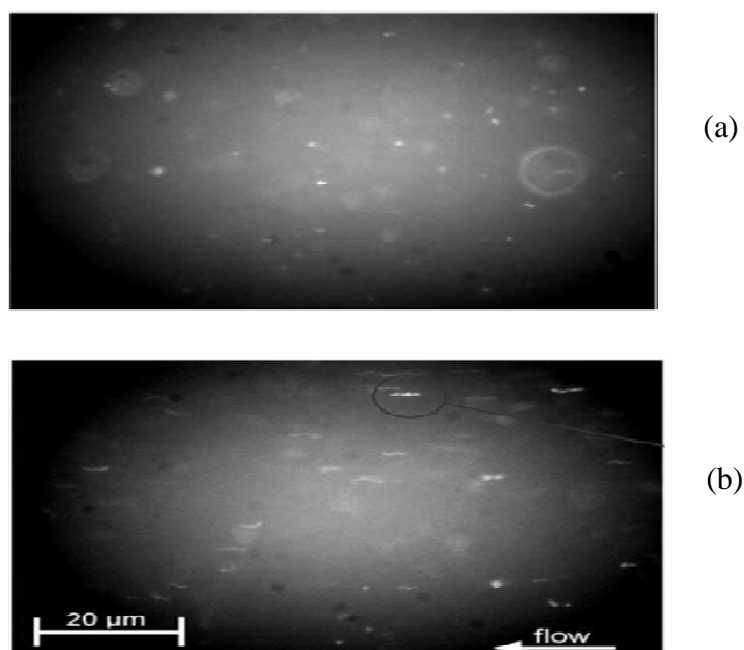
The average hydrodynamic time, the ratio of reactor volume over flow rate, during which the solution remains inside a reactor is known as the mean residence time or space time. However, due to the presence of possible dead volume, channelling in porous beds or simply due to the laminar parabolic velocity profile in cylindrical tubes, all molecules entering in a reactor can have broad residence time distribution unlike the ideal plug flow reactor. By proper setting of dimensions and flow, however, a near plug-flow profile can be achieved with the aid of axial dispersion which can also be actively promoted by virtue of internal convective-flow elements. This can be achieved by as simple structures as given by a zig-zag channel. Microreactors are usually operated in continuous-flow, thus their space time can be adjusted easily by changing the flow rate or the reactor length, increasing by decreasing the former and increasing the latter. Thus, the mean residence times can be obtained favourably from few seconds to several ten minutes, in rare cases even to milliseconds or hours allowing running both very fast and reasonably slow reactions. Operated in the very fast mode, it helps to control reactions involving unstable short-lived reactive intermediates. Chemical reactions that are very difficult or infeasible to carry out in macroreactors can be achieved in microreactors, by transporting the reactive species to the desired reaction sites before it decomposes (Figure 2.11).<sup>91</sup> Therefore, microreactors are suitable for kinetic studies, including and most relevant for this chapter living polymerization techniques (ionic and controlled radical polymerizations) for rapid production of (co)polymers with different molecular weights.



**Figure 2.11.** Principle for generation and reaction of unstable short-lived reactive intermediates based on residence time control in a flow microreactor.<sup>91</sup>

#### 2.2.1.2.4 Conformation of macromolecules

Extensional flow field generated in micro dimension due to laminar flow can make macromolecules aligned. Yamashita and coworkers have observed elongated conformation of DNA strands along the direction of flow within a microfluidic setup as shown by the optical micrograph in Figure 2.12b compared to a coiled conformation observed during non flowing condition as shown in Figure 2.12a.<sup>92</sup> It is believed that aligned conformation of macromolecules makes active sites more accessible for reaction by reducing the steric hindrance. However, this feature was not well explored even if a possible application may involve the synthesis of functional polymers with dendritic structure.



**Figure 2.12.** Optical micrographs showing coiled DNA strands at rest (a), stretched DNA strands due to flow in microchannels (b).<sup>92</sup>

#### *2.2.1.2.5 Modularity and versatility*

This feature concerns the possible arrangement of multiple microreactor units in series or in parallel by standardized interconnects, placements, or dimensions. This might be quite helpful for combinatorial synthesis approach or simply for throughput increase. Indeed, for the latter case, it enables to retain the same characteristics that are achieved on a single unit without need for up scaling, this is known as the numbering-up approach. Moreover arrangement in series gives the flexibility of multi-stage operations allowing to easily varying the product quantity and diversification. Therefore, the modularity and versatility of microreactors can be advantageously used for the production of libraries of copolymers with different compositions.

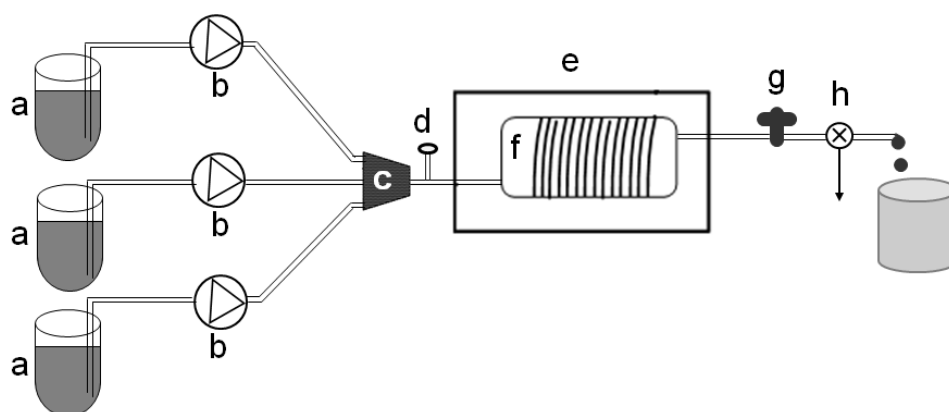
### **2.2.2 Microdevices for polymer synthesis**

#### ***2.2.2.1 Microreactor setup***

The microreactor setup for a given polymerization reaction resembles more or less the same constitutional elements. A typical setup showing the different components of a polymerization microreactor is given in Figure 2.13. All these components can be grouped into three categories like primary, secondary and auxiliary components. Reservoir, supply pumps, microreactors are primary components of any setup. As shown in the Figure, different reservoirs are used to store monomer, solvent and initiator separately. A minimum of 2 reservoirs is required to feed the microreactor as it is advisable not to mix initiator and monomer in order to avoid unwanted polymerization during storage. However, under some circumstances (e.g. low polymerization rate at room or chilled temperature) initiator can be mixed with the monomer. Enough care must be taken to avoid premature reaction before the microreactor. Concerning the reaction, a main issue is to optimize the lengths of supply tubings or microchannels, to suppress dead volumes, and to keep temperature low enough to quench the polymerization. Before entering the microreactor, sub-streams from the different reservoirs pass usually through a secondary component consisting in a micromixer which ensures an intimate mixing between all reagents. In case of poorly mixed situation, the reaction takes place at substreams' interface and can generate large concentration gradients. This situation can also lead to different reaction pathways. To avoid such kind of inconvenience, micromixers play a vital role which makes them an integral part of any microreactor setup. Small dimensions of microreactors allow placing them inside an oven, oil or water bath or equipping them with heating collars to attain desired temperature of polymerization. Components like back pressure regulators, flow controller, pressure gauges

---

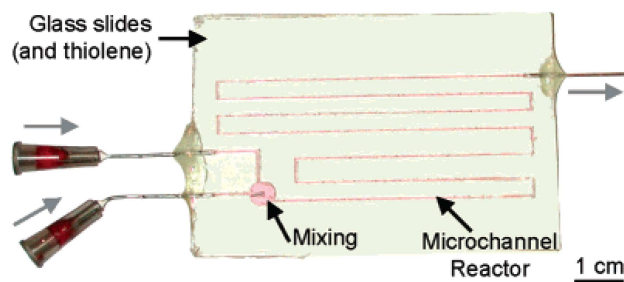
and temperature probes can also be classified as secondary components. Back pressure regulators are used at the exit of the microreactor to control the pressure during polymerization and maintain uniform reaction condition. They also allow conducting the reaction above the boiling point of reactants as the pressure inside the reactor can be maintained above atmospheric pressure. Auxiliary components like two-way valves, three-way valves are quite helpful to change the composition of reactions, remove waste during cleaning of the microdevice. Sometimes non invasive online monitoring systems (optic or spectroscopic methods) can be used to monitor the reaction and this kind of equipments falls in the category of auxiliary components. It is worth mentioning that a microreactor setup is a modular device. Thus another microreactor can be attached downstream to the first one such as the inlet stream of the first microreactor serves as one feed line of the second. This is quite helpful during synthesis of block copolymers for instance.



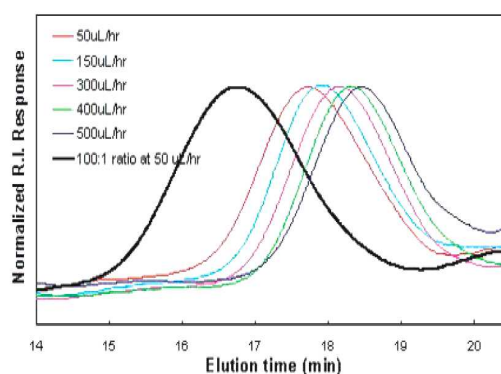
**Figure 2.13.** A typical microreaction setup for polymerization showing: Reservoirs (a), HPLC Pumps (b), Micromixer (c), Pressure sensor (d), Oven (e), Tubular microreactor (f), Back pressure regulator (g), Three-way valve (h).

One of the earliest and simplest example of polymerization in microreactors was reported by Beers and coworkers.<sup>93</sup> Using the inherent small dimensions/volumes and the corresponding ease and fastness of changing experimental parameters in microdevices they synthesized polymer libraries. The polymerization was carried out using only primary components. They demonstrated the successful polymerization of 2-hydroxypropyl methacrylate (HPMA) by Atom Transfer Radical Polymerization technique (ATRP). Polymerization was carried out in a microchannel-based reactor ( $500\mu\text{m} \times 600\mu\text{m}$ ) having two inlets and an active mixing chamber as shown in Figure 2.14a. Mixing chamber housed a small magnetic stir bar for mixing. As shown in Figure 2.14b, just by varying either the flow rate or the relative

concentrations of reactants (stoichiometry), polymer libraries, with polymers presenting controlled molecular masses, could be rapidly generated.



(a)



(b)

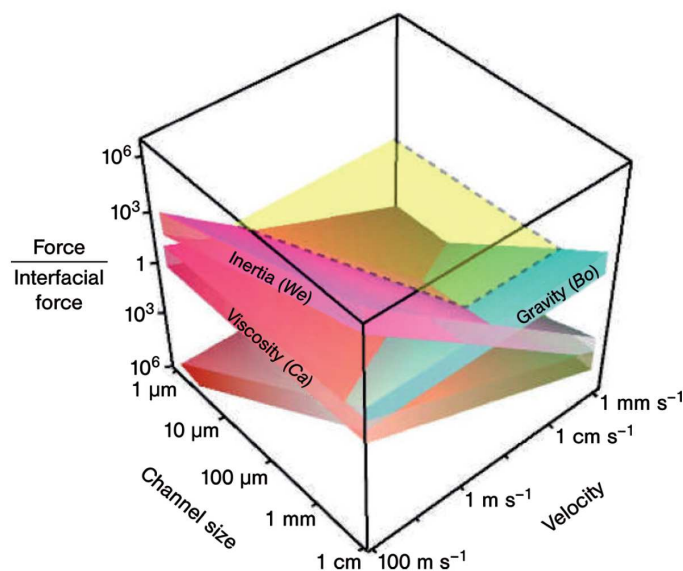
**Figure 2.14.** A microchannel-based reactor used for ATRP (a), SEC traces of poly(HPMA) produced from different flow rates and monomer to initiator concentration ratios (b).<sup>93</sup>

Block copolymers of poly(ethylene oxide-2-hydroxypropyl methacrylate) (PEO-*b*-PHPMA) have also been synthesized by Wu *et al.*, using the same strategy.<sup>94</sup> A three-input-one-output chip was used for the mixing area and two other one-input-one-output microchannels were connected to increase the reactor length. A macromolecular PEO initiated the polymerization and a wide range of well-defined second blocks have been obtained by varying the total flow rate; similar material variations were achieved by changing polymerization time or initiator concentration.

### 2.2.2.2 Micromixers

Due to their small dimensions, microdevices are characterized by a small hydraulic diameter which is defined as four times the cross-section divided by the wetted perimeter. Thus friction along the walls of the device is important and viscous forces become the first and foremost important parameter of consideration (Figure 2.15).<sup>95</sup> Therefore, as the internal dimensions of microreactor and flow rate decrease the influence of viscosity becomes prominent; Reynolds

numbers are thus usually quite low and the flow remains laminar or in the transition regime when the flow velocity is set high (Re can then be a few times 100). In the true laminar regime, the two fluids entering a microdevice flow parallel to each other and mixing takes place at the interface by mass diffusion. If the Re number is higher and even in the intermediate regime, a so-called intertwining regime sets in with strong mutual exchange of fluid segments via recirculation, i.e. the mixing mechanism becomes convective. This is quite difficult to achieve, however, for viscous flows such as polymeric solutions. To speed up the pure diffusional mixing, the length of diffusion must be as short as possible. This was the starting point in the design of different types of micromixers. They can operate either by multilamination of the fluids streams to be mixed into lamellae of low thicknesses (few tens of microns), by splitting and recombining the main flow or by impacting jet streams at high velocity on a spot of small dimension (less than one square millimeter).



**Figure 2.15.** Relation between gravitational, inertial, viscous forces to interfacial forces as a function of channel size and velocity.<sup>95</sup>

It is usually required that a homogeneous mixture resulting from the mixing of multiple main streams enters the microreactor, otherwise local zones of highly concentrated reactants are generated which might lead to the formation of hot spots. In polymer synthesis, one can experience an additional phenomenon: the production of high molecular weight macromolecules.<sup>96</sup> A very interesting observation was made by Bayer and co-workers,<sup>97</sup> they found severe fouling of a 5 mm static mixer (Figure 2.16a) in the continuous-flow polymerization of acrylates in a tubular reactor. Investigation confirmed that, polymers with extremely high molecular weights in the range of  $10^5$  to  $10^6$  g/mol was the cause of fouling.



Being very reactive, acrylic monomers react fast and poor mixing of monomer and initiator solutions leads to uneven propagation of polymerization. Thus very high molecular weight compounds are generated which can make them at some point insoluble in the mixture or solvent and unreacted monomer leading to their precipitation. To avoid such fouling, a multilamination type micromixer (IMM, Mainz, Germany) was used prior to the static mixer. This micromixer laminates both inlet solutions into 36 lamellae of 25  $\mu\text{m}$  thickness. The generation of such thin lamellae and the subsequent rapid and efficient mixing prevented the precipitation of the polymer as seen in Figure 2.16b. Thus the polymer synthesized had a number-average molecular weight of  $10^4$  g/mol.

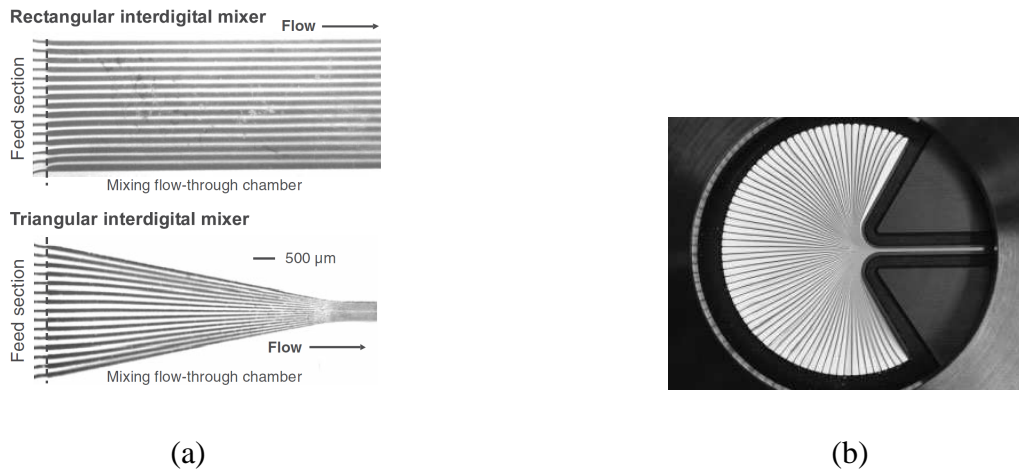


**Figure 2.16.** Fouled static mixer due to precipitation of high molecular weight acrylic polymer (a), clean static mixer after premixing of the reactant by a micromixer (b).<sup>97</sup>

Looking at such examples it becomes clear that micromixers are important components of any polymerization microreaction set up. Therefore, it appears essential to briefly discuss some of the most widely used micromixer principles (for more detailed description see also ref.<sup>98</sup>). Many micromixers have been ingeniously designed accordingly to the required application with the common goal to increase the contact surface area per volume unit of fluid to improve mixing as already discussed above.<sup>71,78,99</sup> These micrometric devices can broadly be classified into two groups as active and passive. Micromixers which need external energy to generate mixing are known as active micromixers. They rely for instance on thermal, electrical or mechanical energy to mix fluids. On the other hand geometrical features play a key role for passive micromixers in order to transform flow energy into mixing action. The basic geometries are the Y or T-junction. While being efficient at high flow velocities due to convection, mixing is not efficient in the laminar flow regime.<sup>102,103</sup> In such cases, multilamination, split and recombine or impact jet micromixers are preferred.

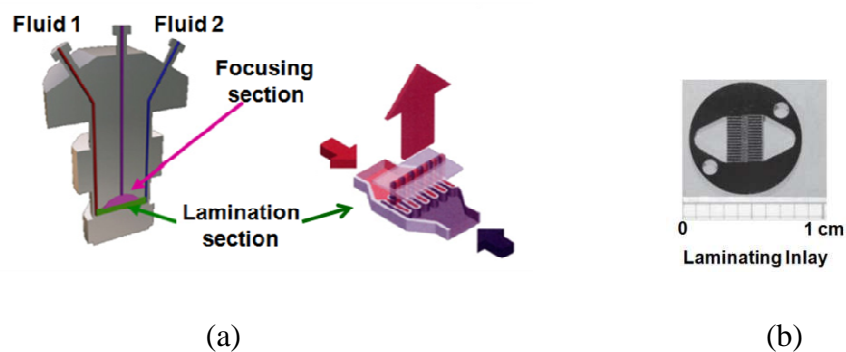
### 2.2.2.2.1 Multilamination

As the name implies, in multilamination micromixers incoming fluid streams are divided into multiple lamellae as shown in Figure 2.17a.<sup>104,105</sup> Then the lamellae are alternatively arranged by means of a specific designed microstructure (Figure 2.17a). This process brings down the mixing time from tenths to few seconds by enhancing diffusion. If combined with flow compressing (geometric focussing) millisecond mixing can be achieved. The High Pressure Interdigital Multilamination Micromixer (HPIMM, IMM, Mainz, Germany) is suitable for operation up to 200 bars and suits therefore well to the needs of some polymerization reactions (Figure 2.18a). Mixing efficiency depends upon the number and width of microchannels present in the laminating element known as inlay (Figure 2.18b) which is housed in the lamination section, and on the focusing ratio in the so-called slit located in the top micromixer part and on top of the inlay.



**Figure 2.17.** Comparison of multilamination and flow focusing adapted to multilamination.

Unfocused and focused (a), Focused with large focussing ratio–SuperFocus micromixer (b).<sup>105,106</sup>



**Figure 2.18.** Schematic of the HPIMM (a) and optical micrograph of a laminating inlay (b).<sup>105</sup>

A remarkable improvement for this kind of micromixers was made possible by systematic variation and investigation of the so-called flow-focusing technology (Figure 2.17a).<sup>106</sup> This technique allows generating lamellae of nearly 1  $\mu\text{m}$  thickness by forcing them to flow through a converging chamber. In this way, thinner lamellae can be achieved which is difficult to obtain by simple microstructuring. Generation of such thin lamellae allows reducing the mixing time down to few milliseconds, as said above. Such modifications not only enhance the mixing but also increase the throughput up to 8-10 L/h (since the large entry cross-section of the focussing chamber needs to be fed by a very large number of parallel lamellae/feeds).<sup>106</sup>

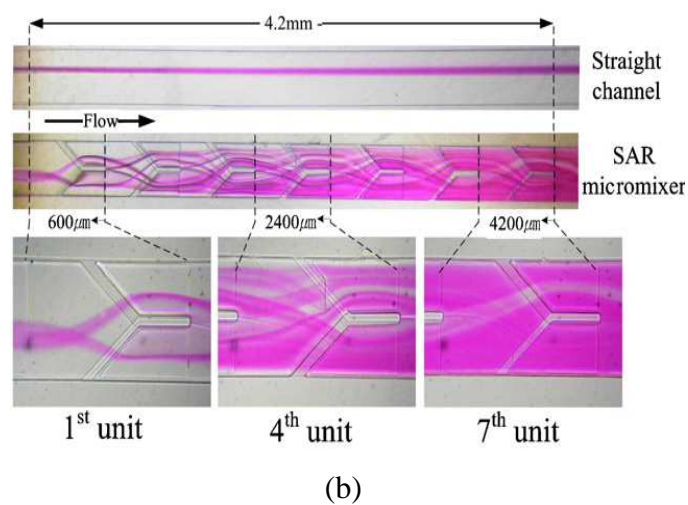
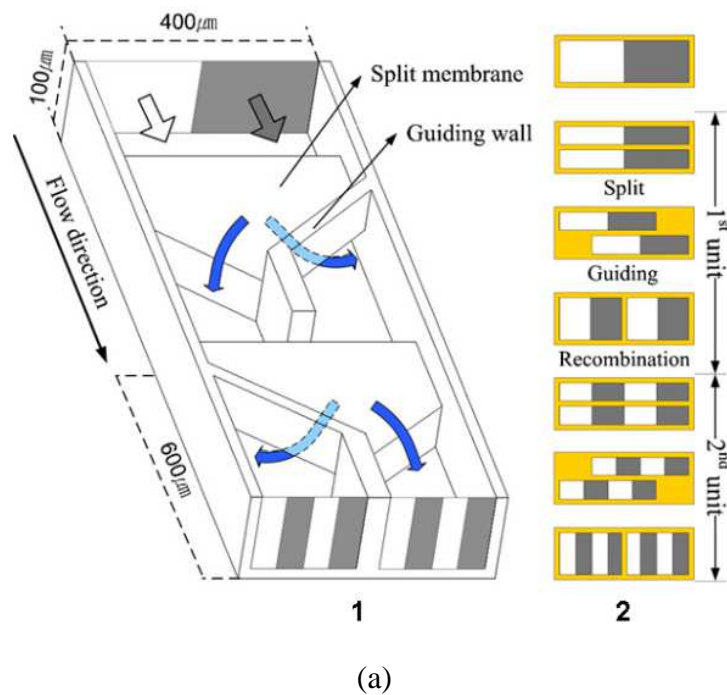
#### 2.2.2.2.2 Split and recombine

This kind of micromixers relies on the splitting of the incoming streams into multiple substreams and thereafter on their recombination.<sup>99</sup> This operation of splitting and recombination can be divided into different steps as shown in Figure 2.19. Starting from splitting of multilayered streams perpendicular to the lamellae orientation into substreams, followed by the re-alignment of substream lamellae and finally by the recombination of these lamellae. It should be kept in mind, however, that the splitting in Figure 2.19 is ideal and may be – more or less – different from reality. Even under laminar conditions, it is known that lamellae deform due to shear forces, giving rise, e.g. to convex and concave-shaped lamellae with varying local thickness (at one cross-section) and along the flow axis varying average thickness. Moreover, for flows at higher Re number, the inseting recirculation finally will disrupt the lamellae causing actually finer dispersed cross-sections as given in Figure 2.19, which means much improved mixing as compared to simple serial lamination.

Figure 2.20a shows a schematic view of a mixer working on this principle. The overall mixing efficiency of such mixer compared to that of a straight tube is shown in Figure 2.20b.<sup>108</sup> The pink color, representing one of the two components being mixed, progressively tends to propagate through the whole micromixer cross-section for each additional split and recombine unit demonstrating an efficient and fast mixing. When compared to same length straight tube, the fluids clearly do not mix as the pink color remains in the central line of the tube. For such kind of micromixers, the minimum channel width is usually well above the channel width of multilamination type micromixers, which reduces the pressure loss and increases its resistance to fouling. Thus these micromixers are quite efficient in handling mixing operations where precipitation may occur while meeting high throughput requirements.



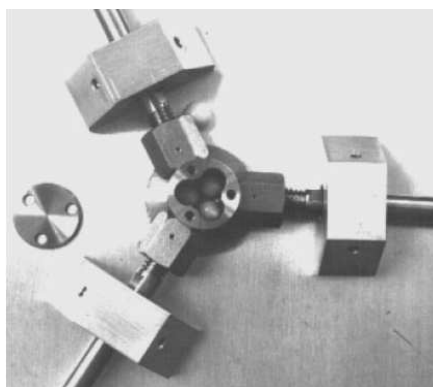
**Figure 2.19.** Schematic of split and recombine principle.<sup>99</sup>



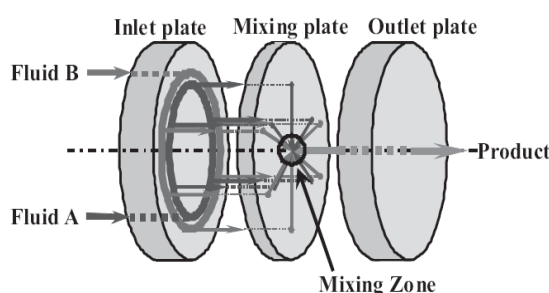
**Figure 2.20.** Schematic view and cross-sectional view of the SAR micromixer (a), comparison between straight channel and channel with mixer (b).<sup>108</sup>

### 2.2.2.2.3 Impact jet

The working principle of such kind of micromixers is based on both providing high kinetic energy which after jet collision enables turbulence in a much confined mixing chamber ('atomization'). Inlet fluid streams are first divided into several multiple micro jets by using nozzles; then these jets are allowed to collide at the mixing chamber and finally guided to a microchannel.<sup>72,109</sup> Micromixers developed by Synthese Chemie (Lebach, Germany) and KM mixer (Fujifilm Corporation, Kyoto, Japan) are based on this principle (Figures 2.21 & 2.22). Besides for mixing leading to a mixed single-phase such as given in homogeneous polymerisations, these micromixers can be advantageously used for dispersion making essential for heterogeneous (emulsion) polymerisations and even for particle making.<sup>72</sup>



**Figure 2.21.** Micromixer developed by Synthesechemie (Lebach, Germany).<sup>72</sup>



**Figure 2.22.** Schematic drawing of the flow inside a KM mixer.<sup>109</sup>

## 2.2.3 Benefits of microdevices for polymers and copolymers synthesis

Among all polymerization techniques available, polycondensation has been rarely investigated in microreactors. Indeed this type of polymerization reaction requires the removal of a byproduct to shift the equilibrium towards high molecular weights. Till date no phase separation microdevice for viscous fluids has been yet developed successfully. However, ionic and free or controlled radical polymerizations are devoid of such kind of

constraint, which makes them suitable candidates for microreactors. Some beneficial features of microreactors compared to macrodevices are discussed in the following sections.

### 2.2.3.1 Polymers with controlled macromolecular characteristics

Free Radical Polymerization (FRP) is a polymerization technique that enables production of polymers on an industrial scale due to favourable operating conditions and reaction time. However, the polydispersity of the final product is often high because of poor control over the polymerization course. This is mainly due to inefficient temperature control within the whole volume of batch reactor, leading to undesired hot spots. In order to improve the heat transfer, microreactors with a surface to volume ratio much larger than conventional heat exchangers have been developed. The AIBN (2,2-Azobis(isobutyronitrile)) initiated FRP of 5 different monomers was investigated by Iwasaki *et al.*<sup>110</sup> The micro-chemical plant (Figure 2.23) was composed of a T-shape micromixer (M1: 800  $\mu\text{m}$  I.D.), a primary microtube for achieving complete mixing (R1 250  $\mu\text{m}$  I.D., 2 m length), a microtubular reactor immersed in a 100°C oil bath (R2: 500  $\mu\text{m}$  I.D., 9 m length) and a microtube immersed in a water bath at 0°C for polymerization quenching (R3: 500  $\mu\text{m}$  I.D., 1 m length). The results were compared with those obtained in a conventional macroscale batch reactor. For butyl acrylate (BA), the molecular weight distribution was found much narrower than for the batch reactor as seen in Figure 2.24. The difference was smaller but still noticeable for benzyl methacrylate (BMA) and methyl methacrylate (MMA) and almost null for vinyl benzoate (VBz) and styrene (St). Authors claimed that the observed results are directly related to the superior heat transfer ability of the microtubular reactor. The more exothermic the polymerization reaction, the more effective is the microdevice to control the molecular weight distribution. Similar results conducted on the polymerization of styrene were also obtained by Leveson *et al.*<sup>111</sup> with a microtubular reactor of 500  $\mu\text{m}$  I.D. and a tubular reactor of 4.2 mm I.D.

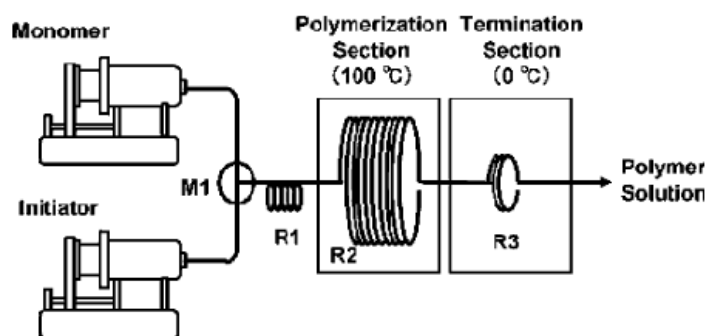
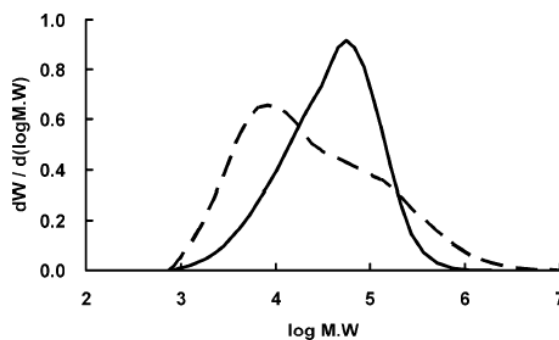


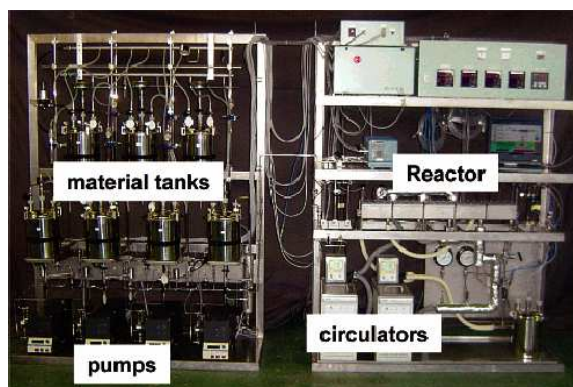
Figure 2.23. Micro-chemical plant for the FRP of 5 different monomers.<sup>110</sup>



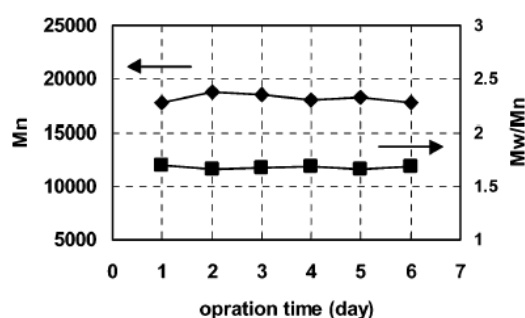
**Figure 2.24.** Molecular weight distribution of poly(butyl acrylate) produced in the microreactor (plain line) and in the macroscale batch reactor (dashed line). Residence time was 4 min.<sup>110</sup>

Since the control of the molecular weight distribution in microtubular reactors was demonstrated, Iwasaki *et al* investigated the large-scale production of polymers by numbering-up microreactors.<sup>112</sup> AIBN-initiated FRPs of butyl acrylate (BA) and methyl methacrylate (MMA) were conducted in a Type-1 numbering-up reactor under various residence times. Type-1 numbering-up reactor was composed of 94 microtubular reactors (510  $\mu\text{m}$  I.D., 600 mm length) in a shell (60 mm I.D., 600 mm length). The shell had two different sections. The first section (500 mm length) was traversed by hot oil while the second was in contact with a cooling fluid. The results were then compared with those obtained with the previously single tube microreactor (Figure 2.23). For MMA, polydispersity indices, number-average molecular weights and monomer conversions were in good agreement for the two systems. However, for BA, a lower monomer conversion was obtained with the Type-1 numbering-up reactor within a large range of experimental conditions. Conversely to MMA for which the monomer conversion was less than 26%, BA conversion was higher than 65%. Thus, the viscosity of the reactive medium has significantly increased along the microtubular reactors. According to the authors, this high viscosity might have induced clogging of some microtubular reactors. Therefore, the overall volume was reduced which implied a decrease in the residence time. From the use of the Type-1 numbering-up reactor, it was learnt that flow uniformity is probably the most important parameter to consider when numbering-up reactors. Iwasaki *et al.* have then developed a Type-2 numbering-up reactor with special attention to flow uniformity.<sup>112</sup> This Type-2 numbering-up reactor consisted of 5 shells (178 mm length each) coupled with tube connectors. In the first shell, a single microtube was branched to 8 other microtubes in a low temperature environment. The next three sections were heated with hot oil to promote the polymerization reaction. These sections contained 8 coiled microtubular

reactors of 1950 mm length with successively increasing internal diameter: 250, 500 and 1000  $\mu\text{m}$ . Finally, the fifth section allowed merging all 8 microtubular reactors into one microtube at low temperature to quench the polymerization. AIBN-initiated FRP of BA performed in a single tube of varied inner diameters (250  $\mu\text{m}$ , + 500  $\mu\text{m}$ , + 1000  $\mu\text{m}$ ) gave similar results to those obtained with this Type-2 numbering-up reactor demonstrating that a good flow uniformity was achieved in this latter system. Finally, as depicted in Figure 2.25, a pilot plant was constructed based on the Type-2 numbering-up reactor. This pilot has been operated continuously for 6 days producing up to 4 kg of PMMA without any increase in the pressure or reactor temperature. The quality of the polymer was constant over one week of operation as seen in Figure 2.26. This pilot plant operation demonstrates that microdevices can be applied to production of polymers at comparatively large scale.



**Figure 2.25.** Photograph of the microchemical pilot plant.<sup>112</sup>



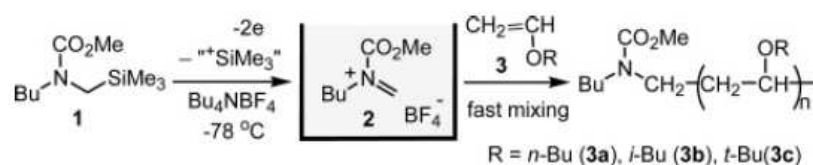
**Figure 2.26.** Variation of the number-average molecular weight and polydispersity index of poly(MMA) against days of operation.<sup>112</sup>

Mixing is an ongoing challenge for ionic polymerization processes since they are characterized by very fast initiation and propagation rates in batch systems. High concentration gradients can therefore be generated during anionic or cationic polymerizations. Consequently, the molecular weight distribution of the resulting polymer is usually large and

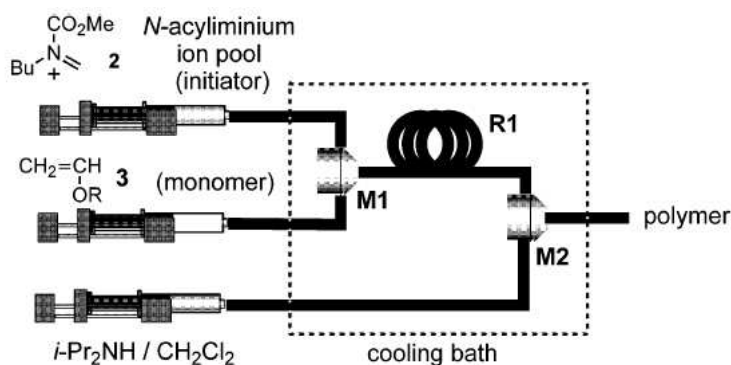


this is more pronounced in the case of high reactants concentration. To avoid these gradients and to ensure an improved control of polymerization kinetics, micromixing of the reactants before or during polymerization is advantageous.

In this field, Yoshida and coworkers have studied the carbocationic polymerization of vinyl ethers in microflow devices.<sup>113</sup> Objective was to develop a controlled/living cationic polymerization that could be run with very high propagation rate. The usual strategy to control the course of polymerizations is the establishment of an equilibrium between active (growing) and dormant species, this drastically slows down the propagation rate as the concentration of active species is very low. On the contrary, Yoshida and coworkers<sup>114</sup> used a highly reactive initiator, preventing propagation deceleration, but considered it with the combination of an extremely fast mixing device to maintain the control of macromolecular characteristics. They successfully prepared vinyl ether homopolymers by a so-called “cation pool” initiated polymerization described in Figure 2.27. An efficient and very rapid mixing of the solution of N-acyliminium (initiator) with several vinyl ethers was achieved by a multilamination-type micromixer (IMM, Mainz, Germany) having microchannels of 40  $\mu\text{m}$  width. The polymerization then took place in a 1 mm I.D. and 10 cm length microtube reactor, kept at a constant temperature of  $-78^\circ\text{C}$ . At the exit of the reactor, a solution of  $i\text{-Pr}_2\text{NH}/\text{CH}_2\text{Cl}_2$  was mixed with the reactive solution thanks to a split and recombine-type micromixer (YM-1, Yamatake Corp, Fujisawa, Japan) for quenching the polymerization (see Figure 2.28). Compared with a batchwise system, polymers with a significant narrower size distribution (PDI lower by 1 to 3 units) were quantitatively obtained within 0.5 s showing that a better control of the molecular weight was achieved. In an additional study, Nagaki *et al.* looked at the influence of the M1 micromixer characteristics (Figure 2.27) on the control of the polymerization, mainly through the PDI.<sup>115</sup> They compared the results obtained with the IMM micromixer and two Yamatake micromixers of different microchannel sizes (400 or 200  $\mu\text{m}$ ). They found that large microchannels led to higher PDIs which were attributed to the lower efficiency of mixing when the microchannel width was increased.

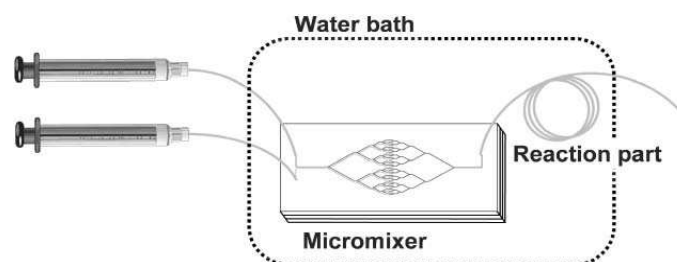


**Figure 2.27.** Schematic drawing of the cationic polymerization of different vinyl ethers and N-acyliminium generated from N-methoxycarbonyl-N-(trimethylsilylmethyl)-butylamine.<sup>114</sup>

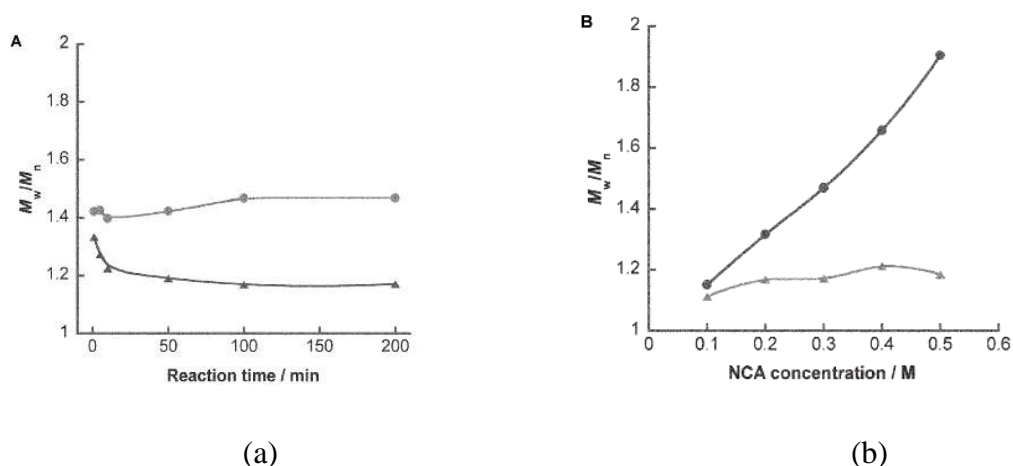


**Figure 2.28.** Schematic drawing of the continuous micromixer-assisted process for the production of polymer through the cation pool technique; M1&M2: micromixer, R1: microtube reactor.<sup>114</sup>

The benefit of a micromixer prior to the polymerization has also been demonstrated with anionic polymerizations. The work of Honda and coworkers<sup>116</sup>, who have studied the anion ring opening polymerization of N-carboxyanhydride in a microtube reactor of 250  $\mu\text{m}$  I.D, showed that the presence of a custom-made PDMS-based split and recombine-type micromixer prior to the polymerization (Figure 2.29) greatly decreased the polydispersity index as shown in Figure 2.30a. Moreover, an increase in the initial monomer concentration led to almost unchanged polydispersity indices in the microtube reactor while a sharp increase was observed in the batchwise system (Figure. 2.30b) because of local concentration gradients of reactants. The importance of efficient micromixing has also been confirmed by repeating an experiment using a T-shaped micromixer instead of the split and recombine-type micromixer: the polydispersity increased from 1.20 to 1.75. In a further study, a silicon glass-based split and recombine-type micromixer was developed<sup>117</sup> and the feed was given through gear pumps instead of syringe pumps; this together allowed for longer-term operation (more than 2 months). This new continuous micromixer-assisted reactor was tested both for homo and copolymerizations of different amino acids.

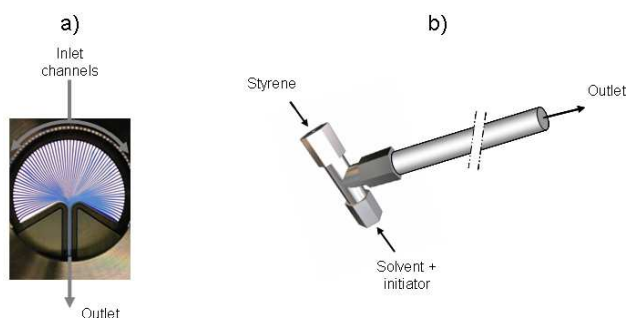


**Figure 2.29.** Schematic drawing of the continuous micromixer-assisted reactor for the production of poly(amino acid).<sup>116</sup>



**Figure 2.30.** Polydispersity index ( $M_w/M_n$ ) for the polymerization of Z-Lys-NCA by the batch(circle)and the continuous micromixer-assisted(triangle) process against reaction time (a) and concentration of the monomer (b).<sup>116</sup>

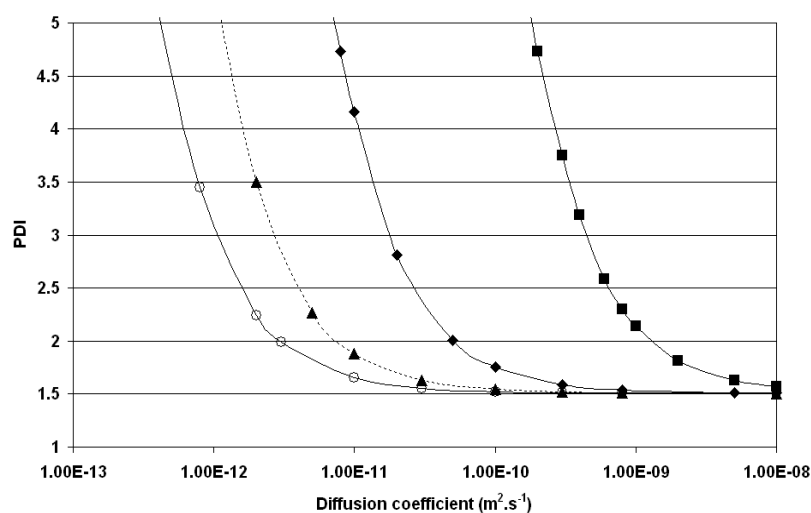
To better understand the influence of microdimension on polymerization and macromolecular characteristics, Serra and coworkers performed numerical studies<sup>118,119</sup> on the free radical polymerization of styrene with the help of micromixers. The two micromixers studied were considered not only as microdevices for the mixing of the reactants but also as the place for polymerization. Both microreactors had the same total volume. The first micromixer studied was the SFIMM (IMM, Mainz, Germany), a multilamination micromixer (Figure 2.31a). This micromixer uses the principle of interdigital multilamination and geometrical focusing. The two inlet flows (pure styrene and solvent + initiator) were delaminated into 69 streams of 250  $\mu\text{m}$  thickness and distributed in staggered rows along an arc. Then, the fluids were focused in a delta shaped section and exited from the microdevice through a 500  $\mu\text{m}$  wide straight channel, the fluid lamellae had an average thickness of 4  $\mu\text{m}$ . The second micromixer considered in this work was a bilamination micromixer, simply consisting in a T-shape inlet manifold supplied with a tubular reactor of different radii (Figure 2.31b).



**Figure 2.31.** Multilamination (a) and bilamination (b) micromixers.<sup>119</sup>

The numerical simulations were performed with the help of a multiphysics CFD software package (Femlab™). The finite elements method allowed solving the set of partial differential equations resulting from the hydrodynamics, thermal and mass transfer (convection, diffusion and chemical reaction). The monomer conversion ( $X_M$ ), number-average chain length ( $DP_n$ ) and polydispersity index (PDI) were analyzed as a function of the chemical species diffusion coefficient, assuming that a decrease in this coefficient will mimic an increase in the medium viscosity.

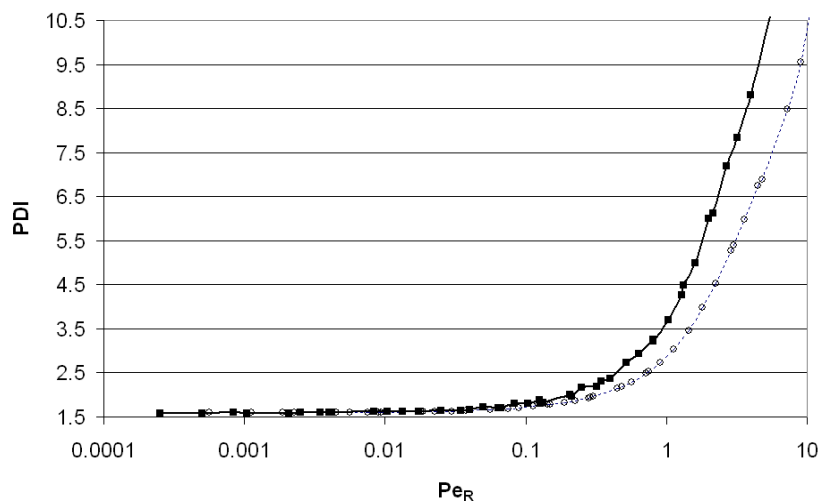
As shown in Figure 2.32, it was found that the range of diffusion coefficients over which the polydispersity index can be maintained close to the theoretical value of 1.5, for ideal conditions increases as the tube reactor radius decreases.



**Figure 2.32.** Variation of the polydispersity index with respect to the diffusion coefficient; multilamination microreactor(-▲-), bilamination microreactor with tube radius of 0.24mm (-○-), 1mm (-◆-) and 5mm (-■-).<sup>119</sup>

This result can be explained relatively to the radial Peclet number which is defined as the ratio of the characteristic time of diffusion in the direction perpendicular to the main flow to the characteristic time of convection in the flow direction, i.e. the mean residence time. As the perpendicular to flow characteristic length of the reactor increases (tube radius or microchannel width), i.e. for high radial Peclet number, the reactive medium cannot be fully homogenized by the diffusion transport before leaving the system resulting in a high polydispersity index and a loss in the control of the polymerization (Figure 2.33). Figure 2.32 shows that the multilamination microreactor exhibits behaviour similar to a tubular reactor, which length and radius would be respectively equal to 8.23 m and 0.39 mm. However due to

its shorter length (15 mm), the multilamination microreactor induces less pressure drop and thus requires less input energy. Furthermore it can be cleaned up in case of fouling more easily as compared to other bilamination microdevices due to its more enlarged dimensions.

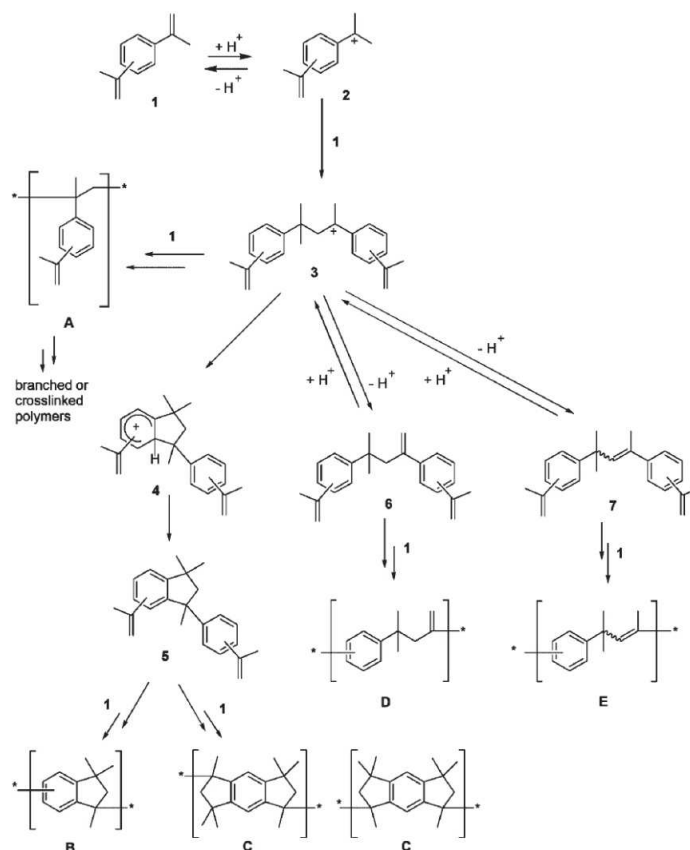


**Figure 2.33.** Comparison of the polydispersity index obtained in a multilamination microreactor (filled symbol) and in a tubular reactor (open symbols) as a function of the radial Peclet number.<sup>118</sup>

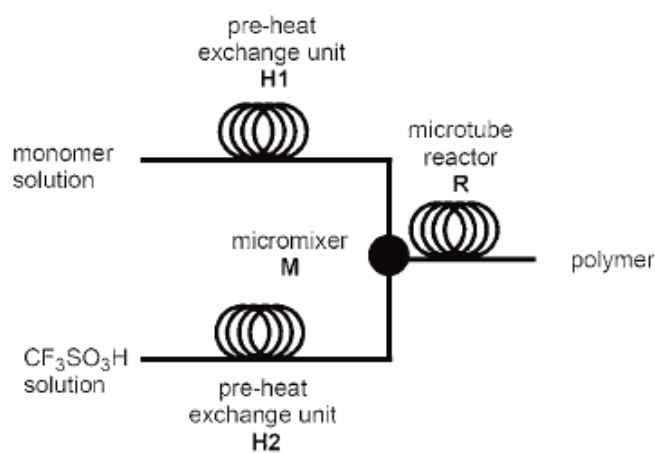
Apart from free radical and ionic polymerizations different controlled radical polymerizations were also investigated. Haddleton and coworkers<sup>120</sup> were among the first to demonstrate that ATRP could be carried out in a small scale continuous-flow reactor, although the dimension of the tubular reactor (1.6 mm I.D.) classifies it more as millireactor. However by varying the temperature they found that the enthalpy of reaction (56.9 kJ/mol) was quite close to that usually reported for batch reactors. Hornung *et al.*<sup>82</sup> who have studied Reversible Addition-Fragmentation Chain Transfer (RAFT) polymerization in a stainless steel microreactor (1 mm I.D.) observed a significant increase of ~2,000g/mol in molecular weight compared to batch reactor while maintaining the same controlled feature of RAFT polymerization. Fukuyama *et al.*<sup>121</sup> studied polymerization of styrene by Nitroxide Mediated Polymerization (NMP) in a stainless steel tubular microreactor (1 mm I.D.). Like for RAFT and ATRP they observed an increase in molecular weight and conversion (48% compared to 39% in batch mode). Moreover, the PDI was found to be quite lower (1.09) in the microreactor compared to 1.16 in the batch reactor, indicating a better control over the polymerization in continuous-microflow.

### 2.2.3.2 *Polymers with controlled chemical composition*

Chemical reactions are usually achieved by putting in contact several reactants. When the reaction is sufficiently fast, mixing is of prior interest as it is the key to obtain the desired distribution of the reactants within the reactive medium. Whether it is to generate composition gradients in a copolymeric chain or to favour kinetic selectivity, the fast and efficient mixing of micromixers make them ideal tools to control the chemical composition of polymers. Thanks to micromixers, fluid segments can all have the same chemical composition. Therefore, if these segments are small enough to minimize the diffusion path of the reactants, the reaction pathway is only governed by kinetics and not masked by transport phenomena. Micromixers thus affect product selectivity for the case of competitive parallel or competitive consecutive reactions.<sup>122</sup> The group of Yoshida investigated this enhancement of chemical selectivity by use of a micromixer for the cationic polymerization of diisopropenylbenzenes. As depicted in Figure 2.34, cationic polymerization of diisopropenylbenzenes can lead to several reaction pathways. High B-type indane unit content (Figure 2.34) greatly improves thermal properties of the polymer. To that extent, Yoshida and coworkers tried to improve polyindane content through kinetic selectivity.<sup>123</sup> They performed cationic polymerization of diisopropenylbenzenes initiated by a Brønsted acid (trifluoromethane-sulfonic acid, TfOH) instead of conventional slower acids (such as sulfuric acid) in microflow systems. As can be seen in Figure 2.35, the micromixer-assisted process consisted in a 250  $\mu\text{m}$  I.D. T-junction (M), where monomer and initiator solutions were mixed after a pre-heat exchange units (H1 and H2, 1000  $\mu\text{m}$  I.D., 200 cm length), followed by a microtube tube reactor R (1000  $\mu\text{m}$  I.D., 215 cm length). The polymer solution was finally quenched in methanol saturated with potassium carbonate. In spite of a slight increase in the PDI, the micromixer-assisted process led to polymers with a higher B-type indane unit content in comparison to the batchwise process (from an average of 80 indane % to an average of 95%). This result is very promising as it reflects the selective pathway promoted by the microprocess in the overall chemical scheme of the cationic polymerization of diisopropenylbenzenes, leading to higher thermal resistance of the final poly(indane). The synthesis of dendritic and hyperbranched polymers can also benefit from the rapid mixing achieved in micromixers, in terms of reaction selectivity. The first work was reported by Liu and Chang and concerned the production of dendritic poly(amino amine) by the convergent method (Figure 2.36).<sup>124</sup>



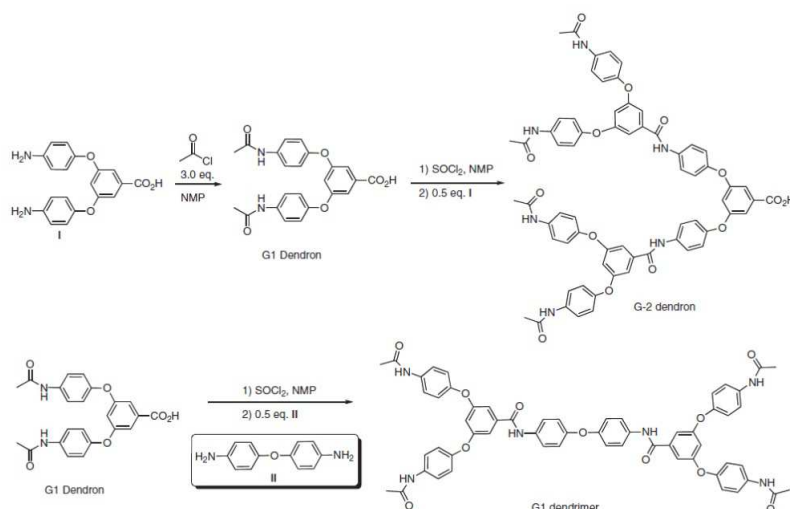
**Figure 2.34.** Reactions pathways for the cationic polymerization of diisopropenyl enzenes.<sup>123</sup>



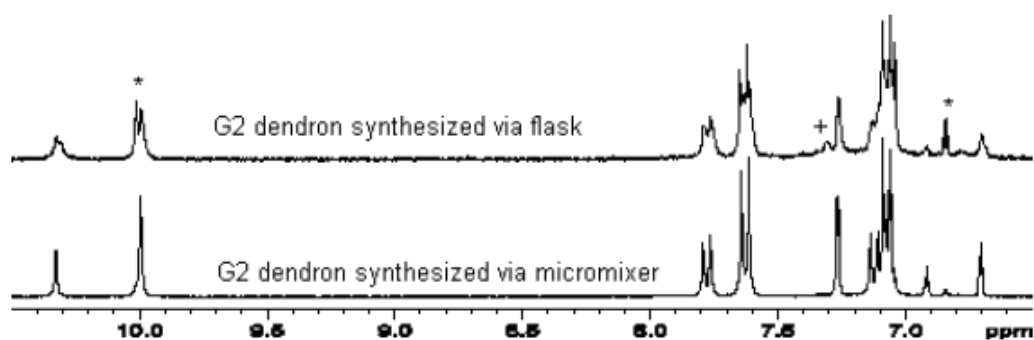
**Figure 2.35.** Schematic drawing of microflow system for  $\text{CF}_3\text{SO}_3\text{H}$  initiated polymerization of diisopropenyl benzenes.<sup>123</sup>

An interdigital-type micromixer (IMM, Mainz, Germany) was used to mix the reactants and to promote the reaction for the production of G1&G2 dendrons as well as G1 dendrimer. Compared to batchwise reactors, the analysis of the product showed a better conversion of G1 to G2 dendron (disappearance of the  $^1\text{H}$  NMR peaks marked with \*) and no measurable side

products (distinguished by +) which are known to be a severe drawback of conventional batch processes (see Figure 2.37).



**Figure 2.36.** Schematic representation of the multi-steps convergent syntheses of dendrons and dendrimers.<sup>124</sup>

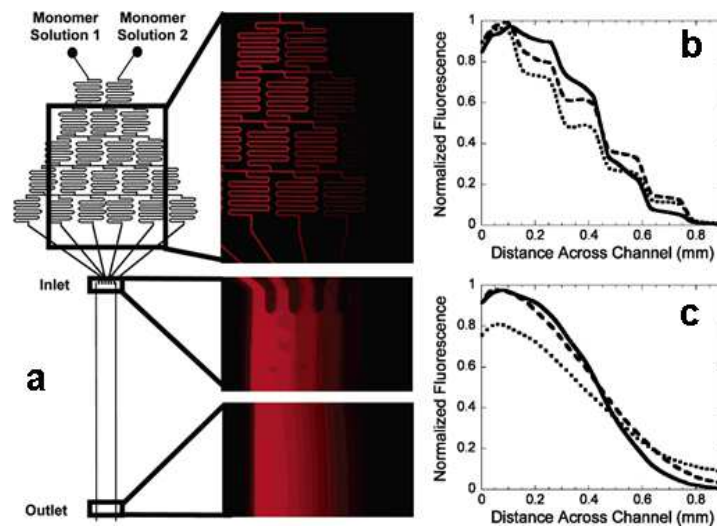


**Figure 2.37.** Comparison of  $^1\text{H}$  NMR spectra of G2 dendron synthesized in batch reactors and in micro-flow systems.<sup>124</sup>

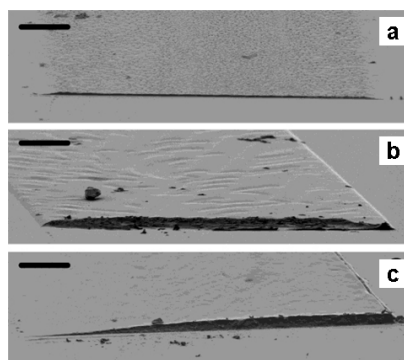
Micromixers are not only dedicated to the homogeneous mixing of two fluids but can also be designed in such a way that they will induce a gradient of mixing between two fluids; in this way virtually performing innumerable reactions with different reactant compositions in parallel. This elegant method was applied by Burdick and coworkers to establish hydrogels with gradients of immobilized molecules and cross-linking densities.<sup>125</sup> As depicted in Figure 2.38a, the gradient maker, made out of PDMS, consists in a network of microchannels where injected solution streams are repeatedly combined, mixed and split to yield distinct compositions in each of the branch channel. After creating the composition gradient, the monomer solution passes along a larger viewing channel, where the gradient is made more



linear before UV-initiated polymerization of the hydrogel through the PDMS mould occurs. The optimization of the inlet flow rate has shown that the best (most linear) gradient at the outlet has been achieved for an inlet flow rate of  $0.3 \mu\text{L}/\text{min}$  (Figure 2.38c). In these conditions, a first hydrogel has been synthesized by mixing poly(ethylene glycol)-4000 diacrylate (PEG4000DA) with a solution of acryloyl-poly(ethylene glycol) linked with adhesive ligands (RGDS) for endothelial cells (HUVEC) (Acr-PEG-RGDS). Authors thus obtained hydrogels presenting a gradient of tethered HUVEC. The mixing of a solution containing 10 wt.% PEG4000DA (low macromer concentration, high macromer molecular weight) with a solution containing 50 wt.% of poly(ethylene glycol)-1000 diacrylate (PEG1000DA) (high macromer concentration, low macromer molecular weight) turned into a hydrogel presenting a linear gradient of cross-linking across the large outlet channel (Figure 2.39). These two examples are very promising to produce unique tissue engineering scaffolds by encapsulating cells and molecules in these gradient hydrogels.

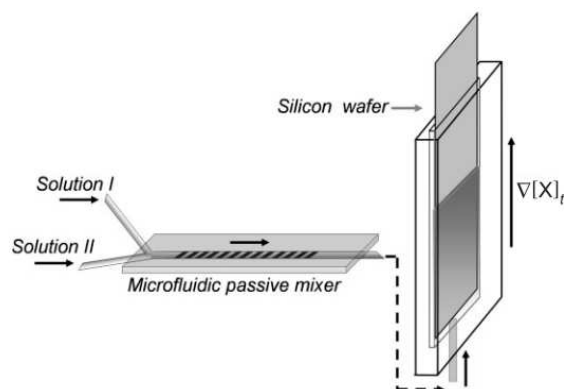


**Figure 2.38.** Schematic of the channel network used in the photopolymerization microfluidic process (a) along with fluorescent images of the gradient maker and channel gradients at the inlet and outlet ( $\sim 20$  mm downstream of the inlet), where rhodamine is incorporated into monomer solution 1 and the monomer solutions are flowed at a rate of  $0.3 \mu\text{L}/\text{min}$ . Gradient quantification at the inlet (b) and outlet (c) for monomer solution flow rates of  $1.0 \mu\text{L}/\text{min}$  (solid line),  $0.3 \mu\text{L}/\text{min}$  (dashed line), and  $0.05 \mu\text{L}/\text{min}$  (dotted line).<sup>125</sup>



**Figure 2.39.** SEM micrographs of cross sections of dried hydrogels fabricated from 10 wt.% PEG4000DA (a), 50 wt.% PEG1000DA (b), and a gradient of 10 wt.% PEG4000DA (left) to 50 wt.% PEG1000DA (right; c); bar ) 100 $\mu$ m.<sup>125</sup>

Microdevices have also been used as tools to assist the fabrication of statistical-copolymer-brush composition gradients. Beers and coworkers have developed a nice microfluidic process using confined surface-initiated polymerization.<sup>126</sup> The aim was to transfer the solution gradient of two monomers (n-butyl methacrylate BMA and 2-(dimethylamino)ethyl methacrylate (DMAEMA)) onto a surface layered with an ATRP initiator. The obstacle was to generate this gradient in a microchannel by mixing very intimately the two (co)monomer solutions. To that extent, they have used a microfluidic passive mixer since this device enabled a transversally mixing.<sup>127</sup> This micromixer improved the mixing by generating transverse components of flow that stretched and folded volumes of fluid over the cross section of the microchannel leading to chaotic, convection-driven mixing. Experimentally, each (co)monomer solution was individually pumped with syringe pumps in the micromixer. The composition gradient has been generated by continuously varying the relative flow rate of the input solutions. Then, the mixed solution entered the microchannel (0.5 mm x 15 mm x 68 mm) and was stopped when the channel, containing the ATRP initiator layered surface, was filled (Figure 2.40). The channel was quickly filled (less than 2 minutes) to minimize polymerization during this infusion step and to consider that polymerization only occurred during the following 40 minutes. It has been demonstrated that the continuous relative flow rate variation and the fast chaotic mixing provided a microreactor with regions having various compositions. This microfluidic device also had the ability to preserve the solution gradient profile over a long period of time because of very slow liquid diffusion once the flow was stopped. Finally, the statistical-copolymer-brush gradient has been transferred to the silicon wafer, forming gradual variable properties across the length of the substrate, with a very well-defined composition.



**Figure 2.40.** Experimental setup for the formation of solution gradients inside a microchannel.<sup>124</sup>

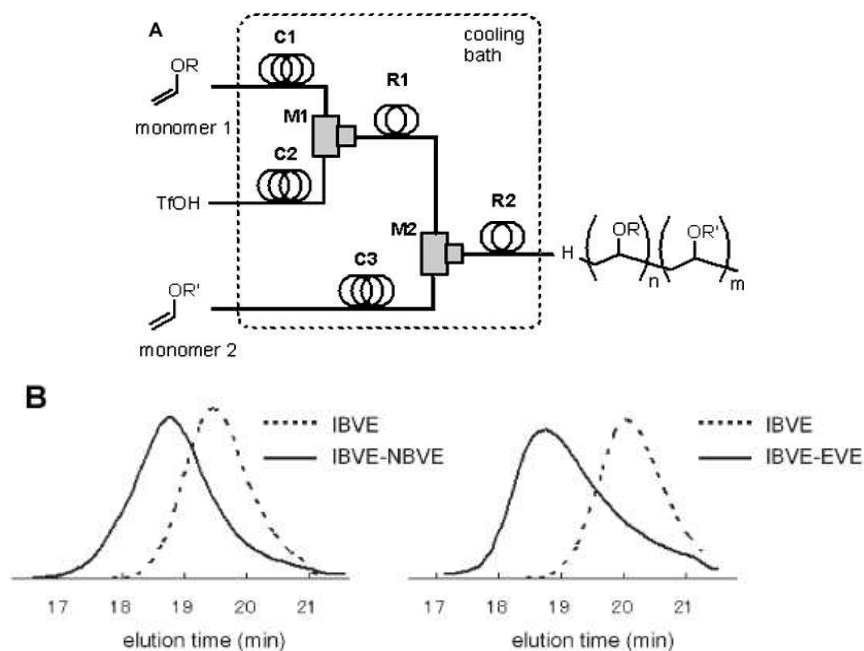
### 2.2.3.3 Polymers with controlled architecture

In addition to the unique properties of micromixers to favour intimate mixing of the initial reactants, micromixers can also assist continuous-flow copolymerization to control the macromolecular architecture, for instance in order to synthesize block copolymers.

Ionic polymerizations are living type reactions, i.e. the end of the polymer chains remains active throughout the whole reaction and does not fate deactivation by coupling or disproportionation. This enables the synthesis of well defined block copolymer architectures. Taking advantage of the modularity of micromixer-assisted microreactor, block copolymers can thus be easily synthesized through continuous-microflow ionic polymerization. By adding another micromixer and tube microreactor (Figure 2.41a) to their initial set-up, Yoshida and co-workers have completed their work on the cationic polymerization of vinyl ethers by making block copolymers from iso-butyl vinyl ether (IBVE), n-butyl vinyl ether (NBVE) and ethyl vinyl ether (EVE).<sup>128</sup> Effective higher molecular weights were observed (Figure. 2.41b) along with a slight broadening of the copolymer molecular weight distribution. The cation pool techniques, as well as the anionic polymerization, have also been successfully extended to the synthesis of block copolymers.<sup>113,129</sup>

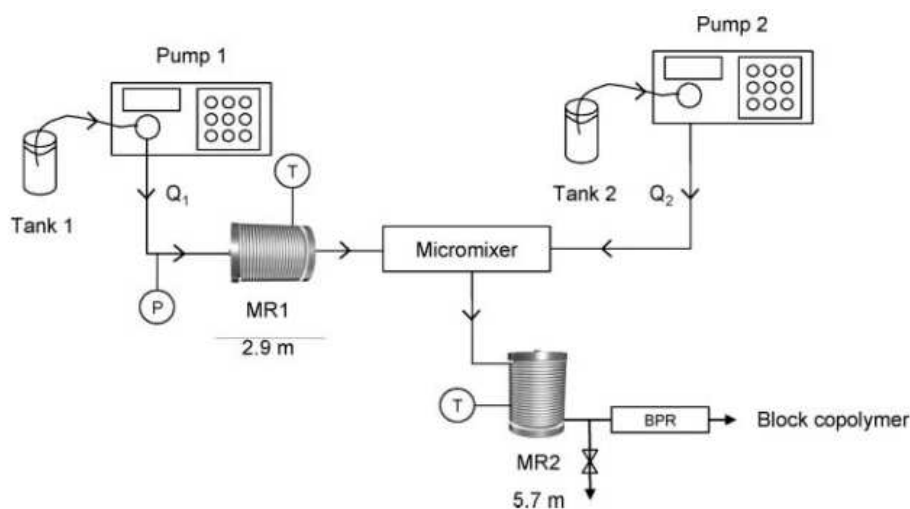
The same approach has also been adopted for the synthesis of high molecular weight block copolymers via NMRP in two serial microtube reactors (Figure 2.42). A big challenge actually consists in putting in contact the first viscous homopolymer ( $M_n \sim 27000$  g/mol) and the second liquid comonomer. Serra and co-workers have investigated the use of different micromixers (Figure 2.43) to synthesize poly(n-butyl acrylate-b-styrene) in microtubes reactors (900  $\mu\text{m}$  I.D.) to improve the control of the final molecular weight distribution

compared to macroscale batch reactions.<sup>130</sup> The first block of poly(*n*-butyl acrylate), synthesized in the first microtube reactor, was mixed with the liquid second (co)monomer (styrene) inside micromixers having various geometries (characteristic length and number of microchannels).

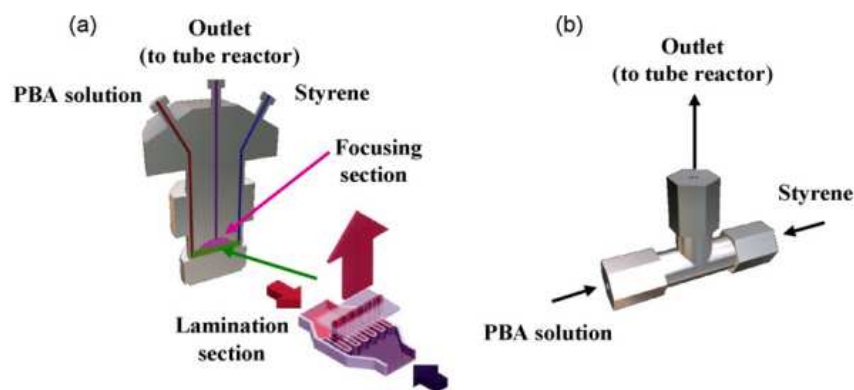


**Figure 2.41.** Schematic drawing of the microdevice used in the block copolymerization of different vinyl ethers; C: pre-cooling units, M: T-shaped micromixers, R: tube microreactors

(a). GPC traces homo and copolymers of vinyl ethers (b).<sup>128</sup>

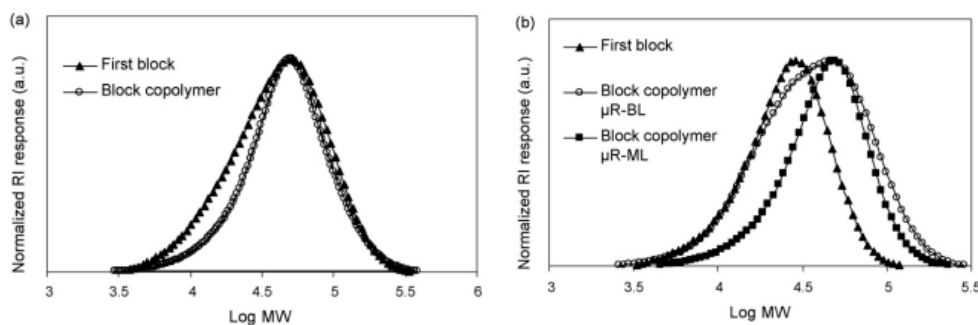


**Figure 2.42.** Continuous microtubes setup for block copolymerization via NMRP.<sup>107</sup>



**Figure 2.43.** Microfluidic devices considered: high pressure interdigital multilamination micromixer (a) and T-junction(b).<sup>130</sup>

A first study revealed that the use of micromixers enabled a significant growth of the second block, unlike the experiment run in batch reactors (Figure 2.44a).<sup>107</sup> In addition, the molecular weight distribution of the polymer was narrower when the lamination provided by the micromixer increased, as can be seen in Figure 2.44b. With a T-junction, the bilamination was not enough to mix intimately both fluids. On the contrary, multilamination enabled a good mixing through diffusional transport across thin lamellae and maintained narrow molecular mass distribution even when copolymerization was run at high temperature.



**Figure 2.44.** Evolution of the molecular weight distribution of the first block and the block copolymer in batch (a) and in microreactors (b).<sup>107</sup>

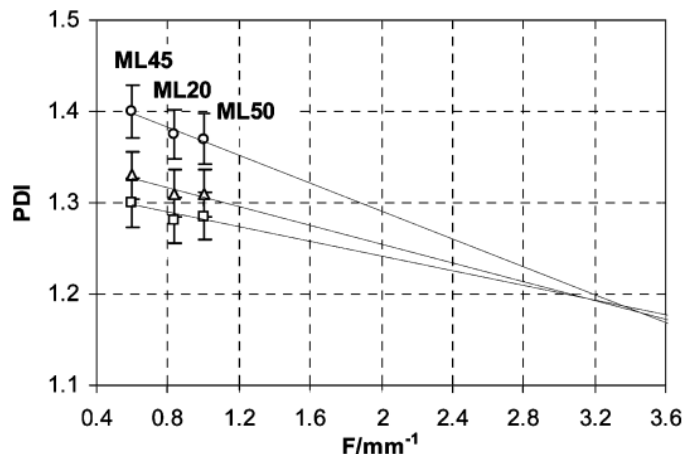
By investigating the characteristics of micromixers (Table 2.1), authors defined, by Eq. 1, a form factor  $F$ , that depicts the geometry of the micromixer and allows to predict the polydispersity indexes of block copolymers (Figure 2.45).<sup>130</sup> This study on multilamination micromixers is promising to optimize the efficiency of mixing just by designing the appropriate micromixer geometry.

$$F = \frac{1}{N(W_C + W_L)} \quad (1)$$

Where, N is the number of microchannels per inlet fluids,  $W_c$  and  $W_L$  the microchannel and slit widths respectively.

**Table 2.1.** Characteristics of the micromixers tested in the NMP synthesis of poly(n-butyl acrylate-b-styrene) in microreactor.<sup>130</sup>

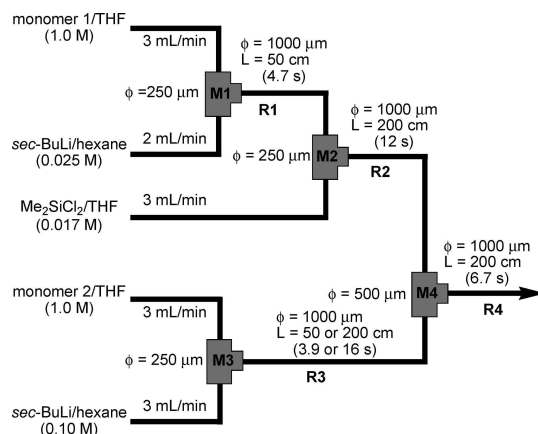
Micromixer	HPIMM	LH2	
Abbreviation	ML45	ML20	ML50
Number of channels per inlet	16	15	10
N			
Channel width $W_C/\mu\text{m}$	45	20	50
Microstructure thickness/ $\mu\text{m}$	250	100	300
Slit or aperture width $W_L/\mu\text{m}$	60	60	50
Form factor $F/\text{mm}^{-1}$	0.59	0.83	1.0



**Figure 2.45.** Polydispersity indexes of final block copolymer depending on the feed flow rate ( $Q_2$ ) of the second comonomer ( $-\circ-$ ,  $Q_2=6.8 \mu\text{l min}^{-1}$ ;  $-\triangle-$ ,  $Q_2=11.8 \mu\text{l min}^{-1}$ ;  $-\square-$ ,  $Q_2=23.9 \mu\text{l min}^{-1}$ ).<sup>130</sup>

Yoshida and coworkers<sup>115</sup> also performed parallel ionic polymerization and coupling reactions to get end functionalized polymers and block copolymers having two different polymer chains on a silicon core. As shown in Figure 2.46, the reaction of dichloromethylsilane on the active polymer chain is performed in R2, after

homopolymerization of monomer 1 in R1. Functionalization yields of 95% were achieved during this first step. At the same time, homopolymerization of a second monomer was carried out in R3. Final coupling, in R4, of the second active polymer chain with the chlorosilane having a single polymer chain allows obtaining structurally well-defined block copolymers on a silicone core.



**Figure 2.46.** Schematic diagram of the continuous-microflow process for the synthesis of block copolymers having two different polymer chains on a silicon core (M1, M2, M3, M4: T-shaped micromixers; R1, R2, R3, R4: microtube reactors).<sup>115</sup>

As stressed out in the above paragraphs, microdevices are suitable for sequential synthesis and allow the production of block copolymers with better controlled macromolecular characteristics than in macroscale batch reactors. There are also evidences that improved mixing in microreactor helps in controlling the architecture of branched polymers. Serra and coworkers<sup>131</sup> observed a significant increase in the branching efficiency in microreaction compared to batch reaction for the synthesis of poly(MMA) by self-condensing vinyl copolymerization (SCVCP) adapted to ATRP. The branching efficiency, defined as the ratio of branches really present within the polymer architecture over the amount of inimer units (2-(2-bromoisobutyryloxy)-ethyl methacrylate, BIEM) introduced in the feeding solution, was found to be 14 to 47% higher in microreaction for BIEM to MMA molar ratios of 2 and 5% respectively.

### 2.2.3.4 New operating windows

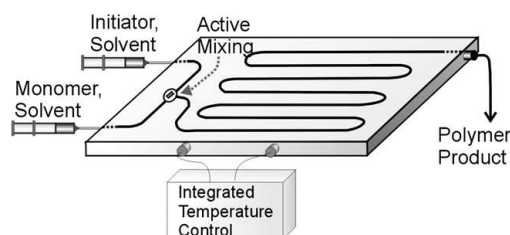
An efficient mixing and thermal management can allow the synthesis of polymers under conditions that were not conceivable in batch processes. Yoshida and co-workers investigated ionic polymerizations in continuous-flow microdevices in order to achieve well-controlled

polymer synthesis under much more favourable ambient temperature conditions instead being cryogenic.<sup>115,123,132,133</sup> Ionic polymerization actually suffers from drastic temperature operating conditions as reaction intermediates are very unstable. Therefore, polymerization is usually performed at  $-78^{\circ}\text{C}$ , which severely limits industrial applications. Controlled/living polymerization has then been developed as an alternative polymerization technique in order to facilitate operating conditions. However, this strategy is based on equilibrium between active and dormant species, which highly decelerates the polymerization rate. Micromixer-assisted ionic polymerization has thus been suggested as a solution that combines feasible operating temperature and reasonable reaction time. Cationic polymerization of vinyl ethers initiated by  $\text{CF}_3\text{SO}_3\text{H}$  has been achieved at  $-25^{\circ}\text{C}$  with high control on polydispersity index instead of usual  $-78^{\circ}\text{C}$  just by implementing a  $250\ \mu\text{m}$  I.D.<sup>128</sup> T-junction in the microflow system. Controlled anionic polymerization of styrene has also been performed at  $0^{\circ}\text{C}$  and even at room temperature.<sup>115</sup> Very narrow molecular weight distributions ( $M_w/M_n = 1.08$  at  $0^{\circ}\text{C}$  and  $1.10$  at  $24^{\circ}\text{C}$ ) have been obtained with a residence time of 16 sec instead of the  $-78^{\circ}\text{C}$  required for conventional batch macroreactors. In this paper, authors also looked specifically at the effect of the T-junction micromixer internal diameter (I.D.) on molecular weight control. By varying I.D. from  $250\ \mu\text{m}$  up to  $800\ \mu\text{m}$  they found a lower controllability of the molecular weight distribution at low flow rates, yet still superior to that obtained in batch mode, and no appreciable PDI variations at high flow rates. This result could be explained by the increase in the diffusion path when the internal diameter is increased and by the high mixing caused by higher flow rates. The same tendency has been observed for anionic polymerization of methyl methacrylate and n-butyl methacrylate. Microflow polymerizations from  $-48^{\circ}\text{C}$  to  $0^{\circ}\text{C}$  gave lower polydispersity indices than conventional macrobatch polymerizations run at  $-78^{\circ}\text{C}$ .<sup>132</sup>

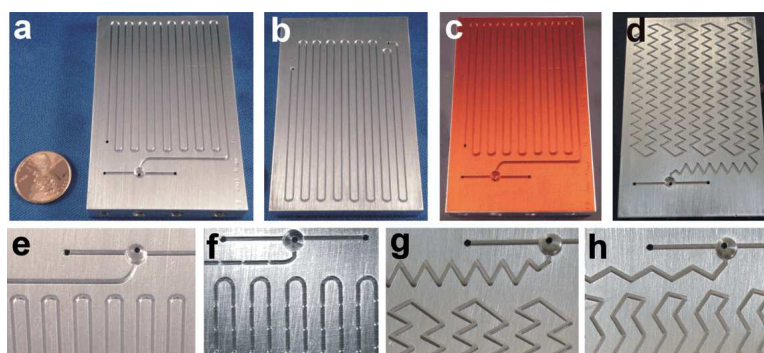
Beers and coworkers also evaluated the performance of patterned microchannels on living anionic polymerization of styrene in cyclohexane at elevated temperature ( $60^{\circ}\text{C}$  instead of usual  $<40^{\circ}\text{C}$ ) and high monomer concentration (42 vol.% instead of  $<20$  vol.%).<sup>134</sup> After active mixing of the initiator and the monomer solutions (Figure 2.47), polymerization occurred within microchannels ( $790\ \mu\text{m}$  width,  $500\ \mu\text{m}$  depth, 2 m length), presenting four different designs (Figure 2.48). These specific microchannel designs aimed at enhancing the micromixing along the length of the channel when mass diffusion is insufficient to obtain narrow molecular mass distributions. Straight, pinched, obtuse zigzag and acute zigzag microchannels (Figure 2.48) have been designed and PDIs have been decreased from 1.31 (for



the first) to 1.18 (for the last). Zigzag microchannels act as mixers by inducing convection recirculation in eddies of the corners. Furthermore, efficient micromixer along the reaction enables synthesizing polystyrene at high temperature while limiting the risk of solvent ebullition and thus any dangerous rise in pressure. Strict requirement of polymerization conditions like dryness and impurity tolerance can be improved in microreactors by simply flushing the reactor before the reaction.<sup>135</sup>



**Figure 2.47.** Schematic drawing of the experimental setup for continuous living polymerization of styrene in patterned microchannels.<sup>134</sup>



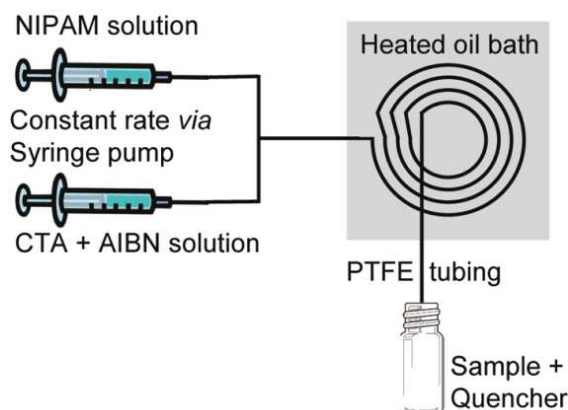
**Figure 2.48.** Pictures of (a) machined aluminum plate, top side, (b) back side of microfluidic device, (c) microreactor sealed with polyimide film, (d) microfluidic reactor with zigzag pattern and also views of (e) straight channel, (f) straight channel with periodic pinches, (g) channel periodically bent at acute angles and (h) channel periodically bent at obtuse angles.<sup>134</sup>

Frey and coworkers used a commercial multilamination-type micromixer (SIMM-V2, IMM, Mainz, Germany) for the carbanionic polymerization of styrene.<sup>135</sup> Monomer and solvent (THF or cyclohexane) on one hand, initiator (*sec*-BuLi) and solvent on the other hand, were fed separately to the micromixer. The resulting reactive mixture was then thermally polymerized in a downstream tubular reactor consisting in a 1 mm I.D. and 250 cm length tube for experiments with cyclohexane and a 500  $\mu\text{m}$  I.D. and 30 cm length tube for experiments with THF. Upon reaction, the solution was continuously quenched with methanol

or dimethylchlorosilane to recover the polymer. For a polar solvent (THF), the polymerization was estimated to take place within several seconds which required usually to carry out this reaction in batch system at low temperature (c.a.  $-78^{\circ}\text{C}$ ) in order to control the heat released by the reaction. Due to the efficient mixing achieved in few milliseconds by the micromixer, polymers with very narrow size distributions (PDI as low as 1.09) were obtained at room temperature ( $25^{\circ}\text{C}$ ) within 10 seconds. For a nonpolar solvent (cyclohexane), polymers could not be obtained at room temperature as expected but full monomer conversion was observed at  $80^{\circ}\text{C}$  for which low polydispersity polymers were obtained within few hours. Authors claimed that their continuous-flow microprocess allowed a rapid synthesis of well defined polymer giving an interesting alternative to the time-consuming and laborious conventional methods involving batch reactors. With the same approach, Yoshida and coworkers reported the cationic polymerization of vinyl ethers at high monomer concentrations using halogen free solvent in order to improve the productivity of their laboratory scale system.<sup>115</sup>

The role of thermal management in microreactor-based polymerization is clearly visible as it lowers down the reaction time in several studies. For instance, Liu and Chang reported the fast synthesis of polyamide dendrons and dendrimers.<sup>124</sup> In this work, an interdigital-type micromixer (IMM, Mainz, Germany) was used to mix the reactants and to promote the reaction for the production of G1&G2 dendrons as well as for G1 dendrimer. Compared to batch reactors, authors obtained a tremendous reduction in the reaction time for the synthesis of G1 dendrimer, from several hours (typically 20 h) down to few seconds or minutes. The reason is a compression and partial elimination of a multitude of sequential batch processing steps into a more continuous, kinetically determined flow processing. This impressive reduction in reaction time was also observed more recently by Frey and co-workers for the production of hyperbranched polyglycerol with a continuous micromixer-assisted process similar to that of Liu and Chang.<sup>124</sup> As emphasized by the two previous examples, microreactors can significantly intensify the production of polymers by reducing significantly the reaction time. Similarly, Seeberger and coworkers<sup>137</sup> studied RAFT polymerization of N-Isopropylacrylamide (NIPAM) in two PTFE microreactors as shown in Figure 2.49. PTFE tube having an internal diameter of  $750\ \mu\text{m}$  and  $1550\ \mu\text{m}$  were used for the study. Polymerization in a  $750\ \mu\text{m}$  microreactor gave 88% conversion compared to 40% in batch reactor with similar PDI. However, with increase in diameter from  $750\ \mu\text{m}$  to  $1550\ \mu\text{m}$ , an

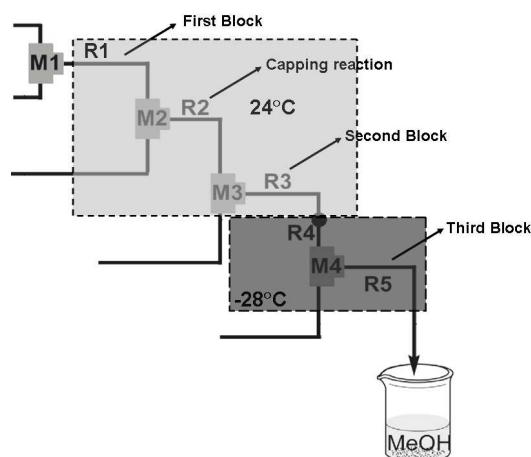
increase in throughput was achieved but the conversion was reduced from 88% to 78% with increase in PDI from 1.15 to 1.31.



**Figure 2.49.** Experimental setup for continuous-flow RAFT polymerization.<sup>137</sup>

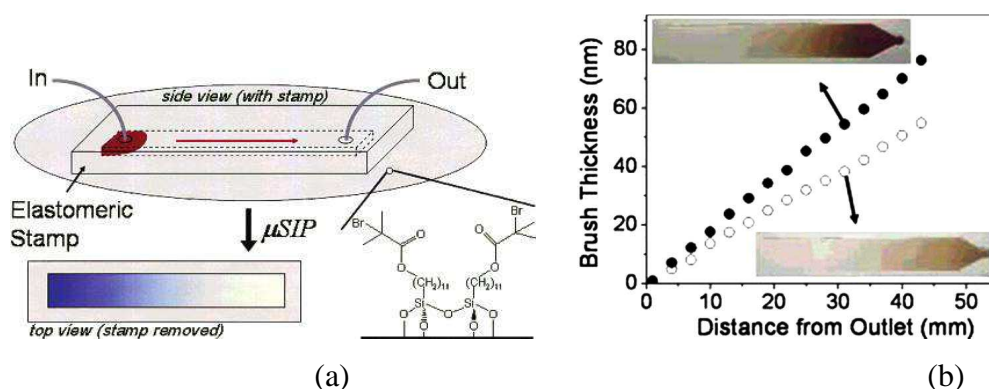
Apart from all these beneficial features, the modularity of microdevices allows to control the temperature of the reaction independently at different sections along the process line to accommodate reactants kinetics which is not readily possible in a batch process. This was demonstrated by Nagaki *et al* during the synthesis of multiblock copolymers in microreactor using anionic polymerization (Figure 2.50).<sup>138</sup> Due to strong differences in their respective reactivity, quantitative anionic polymerization within a few seconds of styrene, tert-butyl methacrylate (Bu<sup>t</sup>MA) and methyl methacrylate (MMA) in THF are usually conducted at different temperatures respectively 0–24°C, 24°C and –28°C. Therefore the synthesis of block copolymers of poly(styrene-*b*- Bu<sup>t</sup>MA-*b*-MMA) in a single batch reactor becomes quite tedious but could be easily achieved in continuous-microflow process. As depicted in Figure 39, polymerization of styrene block was carried out in the first microreactor (R1) at 24°C. In the next stage a capping/trapping reaction with 1,1-diphenylethylene was carried out in the second microreactor (R2) by supplying the required reagents via a micromixer (M2) place upstream to R2. Then Bu<sup>t</sup>MA for a second block was introduced by micromixer M3 and polymerization took place in microreactor R3 at 24°C. Downstream the main stream was cooled down to –28°C by passing through the microreactor R4 and mixed with MMA by the micromixer M4. Last block polymerization was then finally performed in the microreactor R5 which was also maintained at –28 °C. Thus triblock copolymers of poly(styrene-*b*- Bu<sup>t</sup>MA-*b*-MMA) were successfully synthesized with low PDI (<1.25) and controlled molecular weights (8,800 g/mol). Another alkyl methacrylate, namely butyl methacrylate (BuMA), was successfully tested for the third block and polymerized at –4°C demonstrating the versatility

of the developed continuous-microflow process for the production of different poly(styrene-*b*-alkyl methacrylate -*b*- alkyl methacrylate) block copolymers.



**Figure 2.4850.** Microreactor setup for the synthesis of triblock copolymers in which polymerization of different blocks was carried out at different temperatures. Micromixers consisted in T-junctions of 250  $\mu\text{m}$  I.D. (M1, M3, M4) or 500  $\mu\text{m}$  I.D. (M2) while 1 mm I.D. stainless steel tubing of 100, 50, 100, 100, 400 cm length composed microreactors R1, R2, R3, R4 and R5 respectively.<sup>138</sup>

The use of microdevices also allows new opportunities to produce polymer films with gradient properties. To that extend Xu *et al.* have also developed a microchannel technique to generate surface-initiated polymerization.<sup>140</sup> A microchannel (300  $\mu\text{m}$  deep, 8 mm wide, 4.5 cm long) was designed on a silicon wafer and functionalized with initiator-functionalized self-assembled monolayer (Figure 2.51a). The polymerization solution was introduced into the reactor at a controlled flow rate. 2-hydroxyethyl methacrylate (HEMA) has been chosen as monomer to perform fast ATRP. The conversion of HEMA decreased with the length of the channel as the surface exposure to the monomer was directly proportional to the distance from the outlet of the channel. A polymer gradient has therefore been created along the microchannel and the thickness of the polymer brush increased linearly from the outlet to the inlet of the channel. It has also been demonstrated that the slope of the polymer brush thickness along the channel could be adjusted by changing the flow rate in the channel (Figure 2.51b) and that multilayered copolymer brushes could be achieved with consecutive microchannel confined surface-initiated polymerization ( $\mu\text{SIP}$ ) steps. Polymerization reinitiation was immediate and did not require multi-step patterning of different initiator segments, which is very interesting for large scale production.



**Figure 2.51.** Microchannel confined surface-initiated polymerization (a), thickness profile along the microchannel (b).<sup>139</sup>

### 2.2.4 Online monitoring

Exploratory and high throughput application of microfluidics in the field of chemical reaction demands for monitoring of ongoing reaction to optimise operating parameters and reaction yield or selectivity.<sup>140</sup> Optimization is always a time consuming and tedious task. It requires ample amount of data usually obtained by repeated experiments. Sometimes this process can introduce experimental errors. Robotic technologies are quite effective in this respect but, they remain complex, expensive and time consuming as they rely on batch reaction. In contrast, online monitoring in microreaction seems to be simpler. Recent advances in analytical techniques, especially in the direction of miniaturization of instruments made the integration of microreactors with characterization equipments possible. Thus considerable development has taken place in recent years in the field of online or inline analytical methods which includes NMR, IR, Visible and Raman spectroscopy, pH probes and size exclusion chromatography (SEC).<sup>142-146</sup> Some potential applications of these techniques for online monitoring of polymerization microprocesses are discussed in the following. For clarity it is worth mentioning that many of these techniques are still in the developing stage. This part won't be detailed further as this is not the primary focus of the thesis, however more details can be found in the chapter published considering such aspects.

### 2.2.5 Summary

As evident from the many examples reported above, continuous-microflow processes for polymer synthesis have some tremendous advantages in comparison with macroscale

processes and, in addition, open new opportunities. On top of these, the large surface to volume ratio allows for a rapid removal of the heat released by the polymerization. Thus highly exothermic polymerizations can be carried out in controlled manner resulting in a high degree of control over molecular weight distribution. Moreover the polymer chain length can be conveniently and fastly adjusted by varying the flow rates of the reactants. Hence in combination with the minute sample consumption and high operational reliability, libraries of macromolecules can be rapidly generated and with improved chance to provide meaningful information. Microdevices also allow for the rapid mixing of reactants, typically within few milliseconds up to a few tens of milliseconds. As a consequence specific reaction pathways can be favoured without the generation of side products. Finally the modularity of these continuous-microflow processes combined with living polymerization techniques permits the synthesis of structurally controlled block and branched copolymers. Thus microdevices appear as elements of choice when intensifying polymerization processes.

### **2.3 Conclusion**

It has been seen that the production of polymers with well controlled characteristics can be achieved through the use of appropriate polymerization methods (i.e. controlled radical polymerization) and microprocesses. Although microreaction technology has been widely considered in combination with free radical and ionic polymerization methods, few examples are reported in the literature for controlled radical polymerization. In the following chapters, we will continue our group effort to implement CRP, and more precisely ATRP, in microfluidic processes with the aim to intensify the synthetic route by using micromixers and a new tubular microreactor geometry (chapter 3) for the production of linear (co)polymers (chapter 4) and branched polymers (chapter 5). Moreover effect of operating parameters and scale-up considerations will be addressed in chapter 4 and 5 respectively.

---

## References

- (1) Odian, G. *Principles of Polymerization, 4th Edition; 4 ed.*; John Wiley & Sons, **2004**.
- (2) Hawker, C. J.; Bosman, A. W.; Harth, E. *Chemical Reviews* **2001**, *101*, 3661.
- (3) Sciannamea, V.; Jerome, R.; Detrembleur, C. *Chemical Reviews* **2008**, *108*, 1104.
- (4) Tebben, L.; Studer, A. *Angewandte Chemie International Edition* **2011**, *50*, 5034.
- (5) Chiefari, J.; Chong, Y. K.; Ercole, F.; Krstina, J.; Jeffery, J.; Le, T. P. T.; Mayadunne, R. T. A.; Meijs, G. F.; Moad, C. L.; Moad, G.; Rizzardo, E.; Thang, S. H. *Macromolecules* **1998**, *31*, 5559.
- (6) Mayadunne, R. T. A.; Rizzardo, E.; Chiefari, J.; Chong, Y. K.; Moad, G.; Thang, S. H. *Macromolecules* **1999**, *32*, 6977.
- (7) Destarac, M.; Charmot, D.; Franck, X.; Zard, S. Z. *Macromolecular Rapid Communications* **2000**, *21*, 1035.
- (8) Wang, J.-S.; Matyjaszewski, K. *Journal of the American Chemical Society* **1995**, *117*, 5614.
- (9) Kato, M.; Kamigaito, M.; Sawamoto, M.; Higashimura, T. *Macromolecules* **1995**, *28*, 1721.
- (10) Matyjaszewski, K.; Spanswick, J. *Materials Today* **2005**, *8*, 26.
- (11) Braunecker, W. A.; Matyjaszewski, K. *Progress in Polymer Science* **2007**, *32*, 93.
- (12) Qiu, J.; Charleux, B.; Matyjaszewski, K. *Progress in Polymer Science* **2001**, *26*, 2083.
- (13) Matyjaszewski, K. In *Encyclopedia of Radicals in Chemistry, Biology and Materials*; John Wiley & Sons, Ltd: **2012**.
- (14) Matyjaszewski, K.; Ziegler, M. J.; Arehart, S. V.; Greszta, D.; Pakula, T. *Journal of Physical Organic Chemistry* **2000**, *13*, 775.
- (15) Matyjaszewski, K. *Polymer International* **2003**, *52*, 1559.
- (16) Shinoda, H.; Matyjaszewski, K. *Macromolecular Rapid Communications* **2001**, *22*, 1176.

- 
- (17) Sarbu, T.; Matyjaszewski, K. *Macromolecular Chemistry and Physics* **2001**, *202*, 3379.
- (18) Xia, J.; Johnson, T.; Gaynor, S. G.; Matyjaszewski, K.; DeSimone, J. *Macromolecules* **1999**, *32*, 4802.
- (19) Löwe A, B.; Sumerlin B, S.; Donovan M, S.; Thomas D, B.; Hennaux, P.; McCormick C, L. *American Chemical Society* **2003**, *854*, 586.
- (20) Wang, X. S.; F. Lascelles, S.; A. Jackson, R.; P. Armes, S. *Chemical Communications* **1999**, 1817.
- (21) Sumerlin, B. S.; Donovan, M. S.; Mitsukami, Y.; Löwe, A. B.; McCormick, C. L. *Macromolecules* **2001**, *34*, 6561.
- (22) Sumerlin, B. S.; Löwe, A. B.; Thomas, D. B.; Convertine, A. J.; Donovan, M. S.; McCormick, C. L. *Journal of Polymer Science Part A: Polymer Chemistry* **2004**, *42*, 1724.
- (23) Tsarevsky, N. V.; Braunecker, W. A.; Matyjaszewski, K. *Journal of Organometallic Chemistry* **2007**, *692*, 3212.
- (24) Matyjaszewski, K.; Xia, J. *Chemical Reviews* **2001**, *101*, 2921.
- (25) Yin, Z.; Koulic, C.; Pagnouille, C.; Jérôme, R. *Macromolecular Chemistry and Physics* **2002**, *203*, 2021.
- (26) Schön, F.; Hartenstein, M.; Müller, A. H. E. *Macromolecules* **2001**, *34*, 5394.
- (27) Davis, K. A.; Charleux, B.; Matyjaszewski, K. *Journal of Polymer Science Part A: Polymer Chemistry* **2000**, *38*, 2274.
- (28) Sarbu, T.; Lin, K.-Y.; Spanswick, J.; Gil, R. R.; Siegwart, D. J.; Matyjaszewski, K. *Macromolecules* **2004**, *37*, 9694.
- (29) Rigolini, J.; Grassl, B.; Billon, L.; Reynaud, S.; Donard, O. F. X. *Journal of Polymer Science Part A: Polymer Chemistry* **2009**, *47*, 6919.
- (30) Hoogenboom, R.; Schubert, U. S. *Macromolecular Rapid Communications* **2007**, *28*, 368.
-



- 
- (31) Li, J.; Zhu, X.; Zhu, J.; Cheng, Z. *Radiation Physics and Chemistry* **2006**, *75*, 253.
- (32) Yoshida, E. *Open Journal of Polymer Chemistry* **2013**, *3*, 7.
- (33) Zhu, J.; Zhu, X.; Zhang, Z.; Cheng, Z. *Journal of Polymer Science Part A: Polymer Chemistry* **2006**, *44*, 6810.
- (34) Brown, S. L.; Rayner, C. M.; Perrier, S. *Macromolecular Rapid Communications* **2007**, *28*, 478.
- (35) Brown, S. L.; Rayner, C. M.; Graham, S.; Cooper, A.; Rannard, S.; Perrier, S. *Chemical Communications* **2007**, 2145.
- (36) Paulus, R. M.; Becer, C. R.; Hoogenboom, R.; Schubert, U. S. *Australian Journal of Chemistry* **2009**, *62*, 254.
- (37) Hernández-Ortiz, J. C.; Jaramillo-Soto, G.; Palacios-Alquisira, J.; Vivaldo-Lima, E. *Macromolecular Reaction Engineering* **2010**, *4*, 210.
- (38) Roy, D.; Ullah, A.; Sumerlin, B. S. *Macromolecules* **2009**, *42*, 7701.
- (39) Arita, T.; Buback, M.; Janssen, O.; Vana, P. *Macromolecular Rapid Communications* **2004**, *25*, 1376.
- (40) Rzayev, J.; Penelle, J. *Angewandte Chemie International Edition* **2004**, *43*, 1691.
- (41) Rzayev, J.; Penelle, J. *Macromolecules* **2002**, *35*, 1489.
- (42) Abreu, C. M. R.; Mendonça, P. V.; Serra, A. C.; Coelho, J. F. J.; Popov, A. V.; Guliashvili, T. *Macromolecular Chemistry and Physics* **2012**, *213*, 1677.
- (43) Liu, C.-H.; Pan, C.-Y. *Polymer Chemistry* **2011**, *2*, 563.
- (44) Arita, T.; Kayama, Y.; Ohno, K.; Tsujii, Y.; Fukuda, T. *Polymer* **2008**, *49*, 2426.
- (45) Mueller L.; Jakubowski W.; Pietrasik J.; Kwiatkowski P.; Jurczak, J.; Matyjaszewski, K. *Polymer Preprints* **2008**, *49*, 2.
- (46) Buback, M.; Morick, J. *Macromolecular Chemistry and Physics* **2010**, *211*, 2154.
- (47) Mueller, L.; Jakubowski, W.; Matyjaszewski, K.; Pietrasik, J.; Kwiatkowski, P.; Chaladaj, W.; Jurczak, J. *European Polymer Journal* **2011**, *47*, 730.
-

- 
- (48) Morick, J.; Buback, M.; Matyjaszewski, K. *Macromolecular Chemistry and Physics* **2012**, *213*, 2287.
- (49) Wang, Y.; Schroeder, H.; Morick, J.; Buback, M.; Matyjaszewski, K. *Macromolecular Rapid Communications* **2013**, *34*, 604.
- (50) Terry, S. C.; Jerman, J. H.; Angell, J. B. *IEEE Transactions on Electron Devices* **1979**, *26*, 1880.
- (51) Manz, A.; Graber, N.; Widmer, H. M. *Sensors and Actuators: B. Chemical* **1990**, *1*, 244.
- (52) Ehrfeld, W.; Löwe, H.; Hessel, V.; Richter, T. *Chemie Ingenieur Technik* **1996**, *68*, 1091.
- (53) Löwe, H.; Ehrfeld, W. *Electrochimica Acta* **1999**, *44*, 3679.
- (54) Hoffman, J. M.; Ebara, M.; Lai, J. J.; Hoffman, A. S.; Folch, A.; Stayton, P. S. *Lab on a Chip* **2010**, *10*, 3130.
- (55) Urban, P. L.; Goodall, D. M.; Bruce, N. C. *Biotechnology Advances* **2006**, *24*, 42.
- (56) Kundu, S.; Bhangale, A. S.; Wallace, W. E.; Flynn, K. M.; Guttman, C. M.; Gross, R. A.; Beers, K. L. *Journal of the American Chemical Society* **2011**, *133*, 6006.
- (57) Biesenberger, J. A. S., Donald H. *Principles of Polymerization Engineering* Malabar, USA., **1993**.
- (58) T. Meyer, J. K. *Handbook of Polymer Reaction Engineering*; Wiley-VCH: Weinheim, **2005**; Vol.1 and 2.
- (59) Wirth, T. *Microreactors in Organic Synthesis and Catalysis*; Wiley-VCH Verlag GmbH & Co. KGaA: Weinheim, **2008**.
- (60) Wiles, C.; Watts, P. *European Journal of Organic Chemistry* **2008**, 1655.
- (61) Watts, P.; Wiles, C. *Organic & Biomolecular Chemistry* **2007**, *5*, 727.
- (62) Watts, P.; Haswell, S. J. *Chemical Society Reviews* **2005**, *34*, 235.
-

- 
- (63) Snyder, D. A.; Noti, C.; Seeberger, P. H.; Schael, F.; Bieber, T.; Rimmel, G.; Ehrfeld, W. *Helvetica Chimica Acta* **2005**, 88, 1.
- (64) Pennemann, H.; Watts, P.; Haswell, S. J.; Hessel, V.; Löwe, H. *Organic Process Research and Development* **2004**, 8, 422.
- (65) Pennemann, H.; Kessel, V.; Löwe, H. *Chemical Engineering Science* **2004**, 59, 4789.
- (66) Ehrfeld, W.; Hessel, V.; Löwe, H. *Microrreactors*; Wiley-VCH: Weinheim, **2000**.
- (67) Fletcher, P. D. I.; Haswell, S. J.; Pombo-Villar, E.; Warrington, B. H.; Watts, P.; Wong, S. Y. F.; Zhang, X. *Tetrahedron* **2002**, 58, 4735.
- (68) Gavriilidis, A.; Angeli, P.; Cao, E.; Yeong, K. K.; Wan, Y. S. S. *Chemical Engineering Research and Design* **2002**, 80, 3.
- (69) Geyer, K.; Codée, J. D. C.; Seeberger, P. H. *Chemistry – A European Journal* **2006**, 12, 8434.
- (70) Geyer, K.; Wippo, H.; Seeberger, P. H. *Chimica Oggi* **2007**, 25, 38.
- (71) Hessel, V.; Löwe, H.; Müller, A.; Kolb, G. *Chemical Microprocess Engineering—Processing and Plants.*; Wiley-VCH: Weinheim., **2005a**.
- (72) Hessel, V.; Löwe, H. *Chemical Engineering & Technology* **2003**, 26, 13.
- (73) Hessel, V.; Löwe, H. *Chemical Engineering and Technology* **2003**, 26, 391.
- (74) Hessel, V.; Löwe, H. *Chemical Engineering and Technology* **2003**, 26, 531.
- (75) Hessel, V., Serra, C. A., Löwe, H., Hadziioannou, G. *Chemie Ingenieur Technik* **2005**, 11, 22.
- (76) Kiwi-Minsker, L.; Renken, A. *Catalysis Today* **2005**, 110, 2.
- (77) Kolb, G.; Hessel, V. *Chemical Engineering Journal* **2004**, 98, 1.
- (78) Nguyen, N. T.; Wu, Z. *Journal of Micromechanics and Microengineering* **2005**, 15, R1.
- (79) Bally, F.; Serra, C. A.; Hessel, V.; Hadziioannou, G. *Macromolecular Reaction Engineering* **2010**, 4, 543.
-

- 
- (80) Wilms, D.; Klos, J.; Frey, H. *Macromolecular Chemistry and Physics* **2008**, *209*, 343.
- (81) Yoon, T.-H.; Park, S.-H.; Min, K.-I.; Zhang, X.; Haswell, S. J.; Kim, D.-P. *Lab on a Chip* **2008**, *8*, 1454.
- (82) Hornung, C. H.; Guerrero-Sanchez, C.; Brasholz, M.; Saubern, S.; Chiefari, J.; Moad, G.; Rizzardo, E.; Thang, S. H. *Organic Process Research & Development* **2011**, *15*, 593.
- (83) Chen, J.-F.; Chen, G.-Z.; Wang, J.-X.; Shao, L.; Li, P.-F. *AIChE Journal* **2011**, *57*, 239.
- (84) Jähnisch, K.; Hessel, V.; Löwe, H.; Baerns, M. *Angewandte Chemie International Edition* **2004**, *43*, 406.
- (85) Ajmera, S. K.; Delattre, C.; Schmidt, M. A.; Jensen, K. F. *Sensors and Actuators B: Chemical* **2002**, *82*, 297.
- (86) Cui, T.; Fang, J.; Zheng, A.; Jones, F.; Reppond, A. *Sensors and Actuators B: Chemical* **2000**, *71*, 228.
- (87) Besser, R. S.; Ouyang, X.; Surangalikal, H. *Chemical Engineering Science* **2003**, *58*, 19.
- (88) Rebrov, E. V.; de Croon, M. H. J. M.; Schouten, J. C. *Catalysis Today* **2001**, *69*, 183.
- (89) Schwalbe, T.; Autze, V.; Hohmann, M.; Stirner, W. *Organic Process Research and Development* **2004**, *8*, 440.
- (90) Jovanovic J. *Eindhoven University of Technology*, Ph.D **2011**, 151.
- (91) Nagaki A.; Yoshida, J.-i. *Advanced polymer science*; Springer-Verlag Berlin: Heidelberg, **2012**.
- (92) Yamashita, K.; Yamaguchi, Y.; Miyazaki, M.; Nakamura, H.; Shimizu, H.; Maeda, H. *Analytical Biochemistry* **2004**, *332*, 274.
- (93) Wu, T.; Mei, Y.; Cabral, J. T.; Xu, C.; Beers, K. L. *Journal of the American Chemical Society* **2004**, *126*, 9880.
-

- 
- (94) Wu, T.; Mei, Y.; Xu, C.; Byrd, H. C. M.; Beers, K. L. *Macromolecular Rapid Communications* **2005**, *26*, 1037.
- (95) Günther, A.; Jensen, K. F. *Lab on a Chip - Miniaturisation for Chemistry and Biology* **2006**, *6*, 1487.
- (96) Bunichiro Yamada, P. B. Z. *Handbook of Radical Polymerization; John Wiley & Sons, Inc.: Hoboken, 2002.*
- (97) Bayer, T.; Pysall, D.; Wachsen, O. In *Microreaction Technology: Industrial Prospects; Ehrfeld, W., Ed.; Springer Berlin Heidelberg: 2000.*
- (98) Capretto, L.; Cheng, W.; Hill, M.; Zhang, X. In *Microfluidics; Lin, B., Ed.; Springer Berlin Heidelberg: 2011, 304, 27.*
- (99) Hardt, S.; Drese, K. S.; Hessel, V.; Schönfeld, F. *Microfluid Nanofluid* **2005**, *1*, 108.
- (100) Hessel, V.; Löwe, H.; Schönfeld, F. *Chemical Engineering Science* **2005**, *60*, 2479.
- (101) Kakuta, M.; Bessoth, F. G.; Manz, A. *The Chemical Record* **2001**, *1*, 395.
- (102) Engler, M.; Kockmann, N.; Kiefer, T.; Woias, P. *Chemical Engineering Journal* **2004**, *101*, 315.
- (103) Gobby, D.; Angeli, P.; Gavriilidis, A. J. *Micromech. Microeng.* **2001**, *11*, 126.
- (104) Ehrfeld, W.; Golbig, K.; Hessel, V.; Löwe, H.; Richter, T. *Industrial & Engineering Chemistry Research* **1999**, *38*, 1075.
- (105) Hessel, V.; Hardt, S.; Löwe, H.; Schönfeld, F. *AIChE Journal* **2003**, *49*, 566.
- (106) Löb, P.; Drese, K. S.; Hessel, V.; Hardt, S.; Hofmann, C.; Löwe, H.; Schenk, R.; Schönfeld, F.; Werner, B. *Chemical Engineering & Technology* **2004**, *27*, 340.
- (107) Rosenfeld, C.; Serra, C. A.; Brochon, C.; Hessel, V.; Hadziioannou, G. *Chemical Engineering Journal* **2008**, *135*, Supplement 1, S242.
- (108) Lee, S. W.; Kim, D. S.; Lee, S. S.; Kwon, T. H. *Journal of Micromechanics and Microengineering* **2006**, *16*, 1067.
- (109) Nagasawa, H.; Aoki, N.; Mae, K. *Chemical Engineering & Technology* **2005**, *28*, 324.
-

- (110) Iwasaki, T.; Yoshida, J.-i. *Macromolecules* **2005**, *38*, 1159.
- (111) Leveson, P.; Dunk, W. A. E.; Jachuck, R. J. *Journal of Applied Polymer Science* **2004**, *94*, 1365.
- (112) Iwasaki, T.; Kawano, N.; Yoshida, J.-i. *Organic Process Research & Development* **2006**, *10*, 1126.
- (113) Nagaki, A.; Iwasaki, T.; Kawamura, K.; Yamada, D.; Suga, S.; Ando, T.; Sawamoto, M.; Yoshida, J.-i. *Chemistry – An Asian Journal* **2008**, *3*, 1558.
- (114) Nagaki, A.; Kawamura, K.; Suga, S.; Ando, T.; Sawamoto, M.; Yoshida, J.-i. *Journal of the American Chemical Society* **2004**, *126*, 14702.
- (115) Nagaki, A.; Tomida, Y.; Yoshida, J.-i. *Macromolecules* **2008**, *41*, 6322.
- (116) Honda, T.; Miyazaki, M.; Nakamura, H.; Maeda, H. *Lab on a Chip* **2005**, *5*, 812.
- (117) Miyazaki, M.; Honda, T.; Nakamura, H.; Maeda, H. *Chemical Engineering & Technology* **2007**, *30*, 300.
- (118) Serra, C. A.; Sary, N.; Schlatter, G.; Hadziioannou, G.; Hessel, V. *Lab on a Chip - Miniaturisation for Chemistry and Biology* **2005**, *5*, 966.
- (119) Serra, C. A.; Schlatter, G.; Sary, N.; Schönfeld, F.; Hadziioannou, G. *Microfluid Nanofluid* **2007**, *3*, 451.
- (120) Noda, T.; Grice, A. J.; Levere, M. E.; Haddleton, D. M. *European Polymer Journal* **2007**, *43*, 2321.
- (121) Fukuyama, T.; Kajihara, Y.; Ryu, I.; Studer, A. *Synthesis (Germany)* **2012**, *44*, 2555.
- (122) Yoshida, J.-i; Nagaki, A.; Iwasaki, T.; Suga, S. *Chemical Engineering & Technology* **2005**, *28*, 259.
- (123) Iwasaki, T.; Yoshida, J.-i. *Macromolecular Rapid Communications* **2007**, *28*, 1219.
- (124) Liu, S.; Chang, C. H. *Chemical Engineering & Technology* **2007**, *30*, 334.
- (125) Burdick, J. A.; Khademhosseini, A.; Langer, R. *Langmuir* **2004**, *20*, 5153.
-

- 
- (126) Xu, C.; Barnes, S. E.; Wu, T.; Fischer, D. A.; DeLongchamp, D. M.; Batteas, J. D.; Beers, K. L. *Advanced Materials* **2006**, *18*, 1427.
- (127) Stroock, A. D.; Dertinger, S. K. W.; Ajdari, A.; Mezić, I.; Stone, H. A.; Whitesides, G. M. *Science* **2002**, *295*, 647.
- (128) Iwasaki, T.; Nagaki, A.; Yoshida, J.-i. *Chemical Communications* **2007**, *30*, 1263.
- (129) Aiichiro, N.; Yutaka, T.; Atsuo, M.; Yoshida, J. -i. *Macromolecules* **2009**, *42*, 4384.
- (130) Rosenfeld, C.; Serra, C. A.; Brochon, C.; Hadziioannou, G. *Lab on a Chip* **2008**, *8*, 1682.
- (131) Bally, F.; Serra, C. A.; Brochon, C.; Hadziioannou, G. *Macromolecular Rapid Communications* **2011**, *32*, 1820.
- (132) Nagaki, A.; Tomida, Y.; Miyazaki, A.; Yoshida, J.-i. *Macromolecules* **2009**, *42*, 4384.
- (133) Nagaki, A.; Miyazaki, A.; Tomida, Y.; Yoshida, J.-i. *Chemical Engineering Journal* **2011**, *167*, 548.
- (134) Iida, K.; Chastek, T. Q.; Beers, K. L.; Cavicchi, K. A.; Chun, J.; Fasolka, M. J. *Lab on a Chip* **2009**, *9*, 339.
- (135) Wurm, F.; Wilms, D.; Klos, J.; Löwe, H.; Frey, H. *Macromolecular Chemistry and Physics* **2008**, *209*, 1106.
- (136) Wilms, D.; Nieberle, J.; Klos, J.; Löwe, H.; Frey, H. *Chemical Engineering & Technology* **2007**, *30*, 1519.
- (137) Diehl, C.; Laurino, P.; Azzouz, N.; Seeberger, P. H. *Macromolecules* **2010**, *43*, 10311.
- (138) Nagaki, A.; Miyazaki, A.; Yoshida, J.-i. *Macromolecules* **2010**, *43*, 8424.
- (139) Nagaki, A.; Miyazaki, A.; Tomida, Y.; Yoshida, J. -i. *Chemical Engineering Journal* **2011**, *167*, 548.
- (140) Xu, C.; Wu, T.; Drain, C. M.; Batteas, J. D.; Beers, K. L. *Macromolecules* **2004**, *38*, 6.
- (141) Ferstl, W.; Klahn, T.; Schweikert, W.; Billeb, G.; Schwarzer, M.; Loebbecke, S. *Chemical Engineering and Technology* **2007**, *30*, 370.
-

- (142) Jacobs, T.; Kutzner, C.; Kropp, M.; Brokmann G.; Lang, W.; Steinke, A.; Kienle, A.; Hauptmann, P. *Measurement Science and Technology* **2010**, *21*.
- (143) Dietrich, T.; Freitag, A.; Schlecht, U. *Chemical Engineering Journal* **2010**, *160*, 823.
- (144) Qian, Z.; Baxendale, I. R.; Ley, S. V. *Chemistry – A European Journal* **2010**, *16*, 12342.
- (145) Leung, S. A.; Winkle, R. F.; Wootton, R. C. R.; deMello, A. J. *Analyst* **2005**, *130*, 46.
- (146) Rosenfeld, C.; Serra, C. A.; O'Donohue, S.; Hadziioannou, G. *Macromolecular Reaction Engineering* **2007**, *1*, 547.



---

# CHAPTER 3

## MATERIALS AND METHODS

<i>Preface</i>	68
<b>3.1 Materials</b>	69
3.1.1 Main reagents and chemicals	69
3.1.2 Synthesis of 2-(2-bromoisobutyryloxy)ethyl methacrylate	69
<b>3.2 ATRP in batch reactor</b>	70
3.2.1 Linear homo polymerization	70
3.2.2 Linear statistical copolymer synthesis	70
3.2.3 Branched PDMAEMA synthesis	71
<b>3.3 ATRP in microreactor</b>	72
3.3.1 Microreactor setup and instrumentation	72
3.3.2 Primary components	73
3.3.3 Secondary components	76
3.3.4 Auxiliary components	78
3.3.5 General procedure of microreaction	79
3.3.6 High pressure reaction	81
3.3.7 Reaction under high shear rate	82
<b>3.4 Characterizations</b>	83
3.4.1 Precipitation of polymer	83
3.4.2 <sup>1</sup> H NMR analysis	83
3.4.3 Gel permeation chromatography	87
3.4.4 Rheological behavior of polymerizing solution	90
3.4.5 Pressure drop determination	91
<b>References</b>	92

## ***Preface***

To reach the objective certain sub-plans are necessary and are achieved through experiments which are based on reproducible conditions and measurable quantities. Complete description of experiments with fine details is imperative not only for reproducibility but also from future direction point of view. Therefore, in this chapter details of polymerization procedures in batch and microreactors are described. Characterization techniques used to determine polymer characteristics and reactor parameters are also explained in detail. Initially synthesis of homopolymer, statistical copolymer and branched polymer in batch reactor is explained. Then, instrumentation of microreactor setup and procedure of polymerization with details of reagent composition in different reservoirs are given. Characterization section highlights different techniques and methods used to characterize reactor and polymers.

## 3.1 Materials

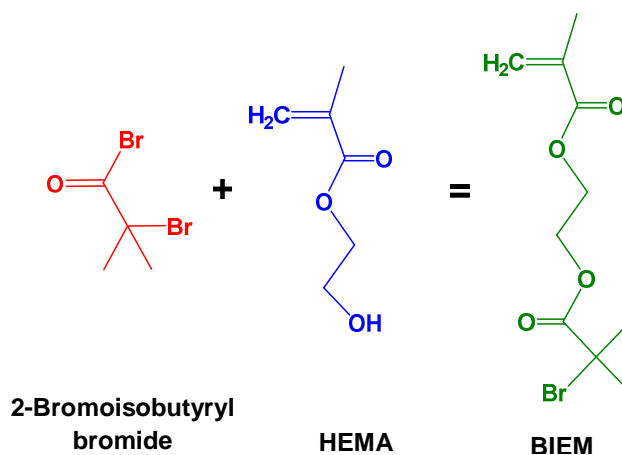
### 3.1.1 Main reagents and chemicals

2-(dimethylamino)ethyl methacrylate (DMAEMA), benzyl methacrylate (BzMA) and 2-hydroxyethyl methacrylate (HEMA) were purchased from Sigma Aldrich, Germany. These monomers were destabilised by passing through basic and neutral alumina column. Copper (I) bromide (CuBr) (Sigma Aldrich, USA) was purified by washing with glacial acetic acid and then with methanol repeatedly. Washed CuBr was then dried overnight under vacuum before use. 1,1,4,7,10,10-hexamethyltriethylenetetramine (HMTETA 97%) (Sigma Aldrich USA) and isopropanol (Sigma Aldrich, France) were used as received. Ethyl 2-bromoisobutyrate (EBIB 98%) was purchased from Sigma Aldrich (USA) and was distilled then stored under argon before use. Triethylamine, dichloromethane, cyclohexane and isopropanol were purchased from Sigma Aldrich (France). Distilled triethylamine and dichloromethane were used as solvent for synthesis purpose. For other uses, they were used as received.

### 3.1.2 Synthesis of 2-(2-bromoisobutyryloxy)ethyl methacrylate

2-(2-bromoisobutyryloxy)ethyl methacrylate (BIEM) is known as an inimer. It has the characteristics of a monomer and an initiator. Inimer was used to synthesize branched polymer as presence of inimer acts like a branching point. It was synthesized from 2-Hydroxyethyl methacrylate (HEMA) and 2-Bromoisobutyryl bromide as shown in the scheme 1.<sup>1,2</sup> Solution of HEMA (18.6 ml, 0.154 mol), distilled triethylamine (TEA, 100 ml) and dichloromethane (DCM, 100 ml) was stirred in a dry three neck round bottom flask under argon kept in an ice bath. 2-bromoisobutyryl bromide (20.89 ml, 0.169 mol) was added drop wise over a period of 45 min. After addition of 2-bromoisobutyryl bromide was completed, mixture was stirred for further 30 minute at 0 °C. Then, the ice bath was removed and the flask was warm up to room temperature and kept at this temperature for 2 hours under constant stirring. Then, reaction was terminated by adding 10 ml of water to the flask. Unreacted HEMA was removed by washing the product with 200 ml water in a separating funnel. Washing was repeated 3 times to ensure complete removal of HEMA. Trace of water in the collected product was removed by addition of MgSO<sub>4</sub> under constant stirring. Final purification was carried out by passing the product through silica column. Dichloromethane (80 vol.%) and cyclohexane (20 vol.%) was used as solvent composition for effective separation and collection of desired product. Thin layer chromatography was used

intermittently to ensure purity of BIEM. Finally, excess solvent was evaporated and recovered BIEM was stored under argon.



**Scheme 3.1.** Reaction scheme showing synthesis of 2-(2-bromoisobutyryloxy)ethyl methacrylate from  $\alpha$ -bromoisobutyryl bromide and 2-hydroxyethyl methacrylate.

## 3.2 ATRP in batch reactor

### 3.2.1 Linear homo polymerization

Linear poly(DMAEMA) for a targeted chain length (DP) of 200 was synthesized by Atom Transfer Radical Polymerization (ATRP) at 75 °C in a round bottom flask. Initially 6.5 ml of isopropanol along with 0.0228 g of CuBr and 77.6  $\mu$ l of HMTETA were poured in the flask. Then the solution was purged with argon for 15 min under constant stirring and 5.36 ml of DMAEMA (degassed prior by argon purging for 15 min) was added to the flask by syringe. Argon purging was continued for further 5 minutes. 28.5  $\mu$ l of initiator was injected into the flask by using a micro syringe and the flask was immersed in an oil bath maintained at 75 °C. At defined interval, 0.5 ml reacting solution was withdrawn from the flask for NMR and GPC analysis. Reagents composition is listed in Table 3.1.

### 3.2.2 Linear statistical copolymer synthesis

Linear statistical copolymer was synthesized using DMAEMA and BzMA as monomers. Procedure followed was very similar to the procedure described in section 3.2.1 Both (co)monomers were added simultaneously to the flask. Different molar ratios of DMAEMA/BzMA (80/20, 60/40) were used to synthesize statistical copolymer. Temperature

of polymerization was maintained at 60 °C. Details of reactants composition are given in Table 3.2.

### 3.2.3 Branched PDMAEMA synthesis

Procedure for branched polymer synthesis is very much similar to that of linear copolymer synthesis. However, inimer replaces BzMA. Inimer acts both as a monomer and an initiator. Dual nature of inimer introduces branching points in a growing polymer chain. 5 and 10% mol.% of inimer compositions were used to synthesize branched polymers. Details of Reagent composition is given in Table 3.1. DMF was used as a solvent for branched polymer synthesis as the polymer becomes insoluble after 1 hour of polymerization time when isopropanol was used as the solvent. Enough quantity of sample was withdrawn at given time intervals for analysis and collection of purified samples for determination of branching efficiency (see chapter 5 for definition). Detailed procedure for purification of polymer by precipitation is discussed in coming section.

**Table 3.1.** Recipe for linear and branched PDMAEMA synthesis in batch reactor.

Reagents	Linear	Branched (5 mol.%)	Branched (10 mol.%)
<b>CuBr</b>	0.0274 g	0.048 g	0.0507 g
<b>Isopropanol</b>	6.40 ml	6.00 ml	6.50 ml
<b>HMTETA</b>	57.10 $\mu$ l	100.20 $\mu$ l	105.70 $\mu$ l
<b>DMAEMA</b>	6.43 ml	5.36 ml	5.36 ml
<b>BIEM</b>	0	0.39 ml	0.82 ml
<b>EBIB</b>	28.50 $\mu$ l	50 $\mu$ l	52.8 $\mu$ l
<b>DP</b>	200	100	100
<b>Temperature</b>	75 °C	75 °C	75 °C

Note: isopropanol and N, N-Dimethylformamide (DMF) were used as solvent for synthesis of linear and branched polymer respectively.

**Table 3.2.** Recipe for linear Poly(DMAEMA-co-BzMA) synthesis.

<b>BzMA (mol.%)</b>	<b>20%</b>	<b>40%</b>	<b>60%</b>
<b>CuBr</b>	0.0228 g	0.0228 g	0.0228 g
<b>Isopropanol</b>	6.60 ml	6.80 ml	6.90 ml
<b>HMTETA</b>	47.60 $\mu$ l	47.60 $\mu$ l	47.60 $\mu$ l
<b>DMAEMA</b>	4.28 ml	3.215 ml	2.143 ml
<b>BzMa</b>	1.08 ml	2.16 ml	3.23 ml
<b>EBIB</b>	23.7 $\mu$ l	23.70 $\mu$ l	23.70 $\mu$ l
<b>DP</b>	200	200	200
<b>Temperature</b>	60 °C	60 °C	60 °C

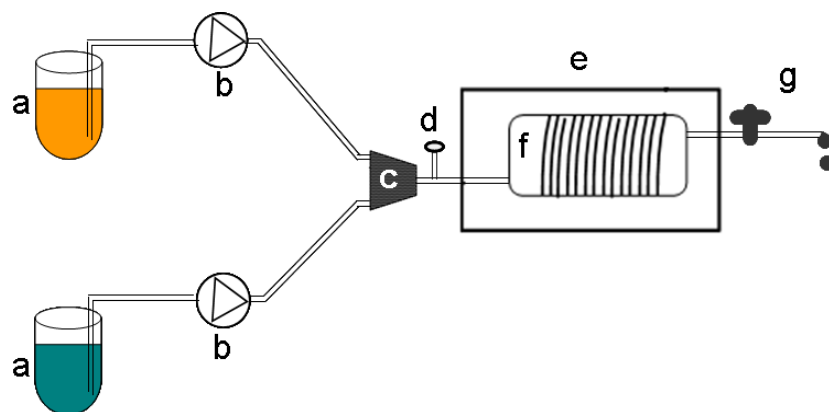
It is important to mention here that during polymerization of 60% BzMA composition, precipitation of the polymer was observed. Therefore, the study was limited to 20 and 40 mol.% BzMA composition.

### 3.3 ATRP in microreactor

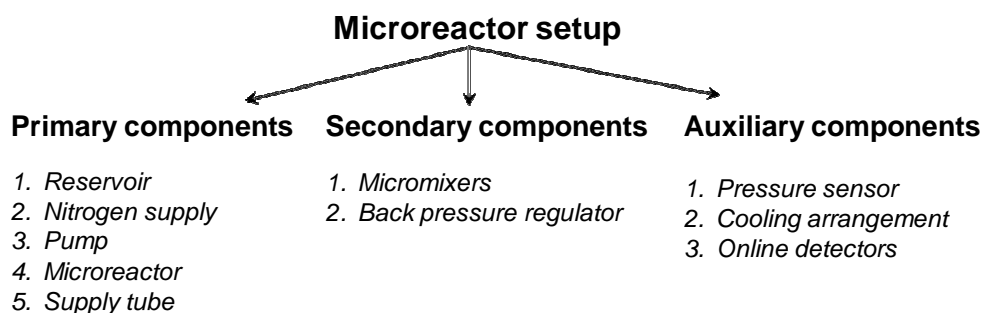
#### 3.3.1 Microreactor setup and instrumentation

Schematic diagram of microreactor setup used for ATRP process is shown in Figure 3.1. Reagents are kept in two different reservoirs to avoid any kind of instability during storage. Moreover cooling arrangements were placed at necessary locations to ensure long-term stability of reagents.

It is worthy to note that some components are of prime importance for a microreactor setup and can be considered as primary components. Components which improve the performance of the setup are grouped under secondary components. For smooth and long-term operation, additional components are necessary which are called auxiliary components. Classification of the different components is given in Scheme 3.2 and components description and their functions discussed in coming sections.



**Figure 3.1.** Schematic representation of a typical microreaction setup used for polymerization showing reservoirs (a), HPLC pumps (b), HPIMM micromixer (c), pressure sensor (d), oven (e), stainless steel microreactor (f) and back pressure regulator (g).



**Scheme 3.2.** Classification of different components used in microreaction setup.

### 3.3.2 Primary components

#### 3.3.2.1 Reservoirs and nitrogen supply

50 ml polypropylene tubes were used as standard reservoirs. Depending on flow rates larger reservoirs like glass balloons were used. Septum was used to seal the reservoir during experiments. Teflon tubings were used as supply tubes, which passed through the septum, in such a way that, the reservoir remains airtight. Inside the reservoir, a filter was attached to the supply tube to prevent tube clogging and damage to the pump due to presence of solid particles. Parker Balston nitrogen generator (Model, N2-04, USA) was used to supply nitrogen at a constant pressure for degassing of reagents and to maintain inert atmosphere during reaction. A minimum of 2 reservoirs are required to feed the microreactor as it is

advisable not to mix all the component of reactants long before the entrance of microreactor to avoid unexpected polymerization triggering.

### **3.3.2.2 Pumps**

Pumps are one of the primary components of any microreaction setup. Gilson 5 SC piston pumps (Model 307) were used to supply reagents to the microreactor. Accuracy of flow rate is prime importance to get a targeted residence time and for reproducibility of results. Therefore, routine verification of pump accuracy was conducted to ensure correct flow rate. Enough heat is generated during working of pumps which may cause premature reaction before microreactor. To avoid such unwanted situation, pump heads were cooled by circulating water.

### **3.3.3.3 Oven**

Accurate and uniform temperature is a prerequisite for any reaction. To address such issue a Binder FD series oven was used to house the microreactor. Access ports (10 mm diameter) provided on two sides of the oven allows easy passage of inlet and outlet microreactor tubings. Access ports provide enough space to insert an external thermometer for more precise control of temperature. Silicon stoppers supplied with the instrument were used to close access ports once tubings were fixed. It avoids any variation of inside temperature. Access window on the front of the oven enables visual inspection.

### **3.3.2.4 Feed tubes**

1/16" teflon tubings were used as inlet tubes for pumps. For the outlet, 1/16" stainless steel tubings were preferred as they can withstand higher pressure compared to teflon tubings. Length of supply tubings was optimized to avoid unnecessary bends and to limit dead volumes. To avoid unexpected polymerization in supply tubings, inlet tubes were kept in an ice bath. Optimized tube length also helps to reduce unexpected polymerization before microreactor.








### **3.3.2.5 Microreactor**

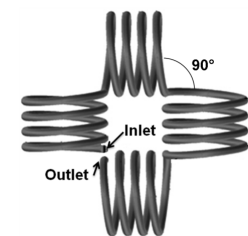

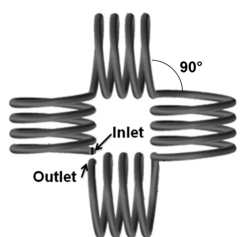

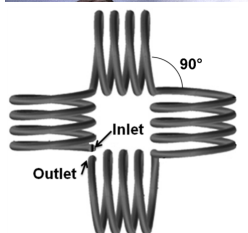
It is the prime component of a microreactor setup. Stainless steel tubular microreactors were used for polymerization because of their high pressure and temperature operability. Stainless steel tubes were coiled around a steel barrel of 5 cm diameter to reduce the space requirement and these microreactors are referred as coiled tube microreactors (CT). For all experiments diameter of coil were maintained to 5 cm. Coiled tube reactors of different diameters and



lengths were used for different experiments which are mentioned in Table 3.3 for easy reference. As a modification of CT, flow inversion was introduced in coiled microreactor and it was called as coil flow inversion microreactor (CFI). Flow inversion was achieved by introducing 90° bends at equal length interval. Bends were made in one direction so as to make the streamlines rotate 360° or more during its passage through the reactor. CFIs of different diameters and lengths investigated and are given in Table 3.3. Since number of coils were maintained in between two consecutive bends total number of bends increased proportionately with reactor length. Characteristics of different microreactors are given in Table 3.3.

**Table 3.3.** List of microreactors and their characteristics used in the different studies.

Entry	Reactor type	Dia. (μm)	Length (m)	Volume (ml)	Image	Number of Bends
1	CT	576	3	0.78		0
2	CT	876	3	1.81		0
3	CT	876	6	3.62		0
4	CT	876	9	5.42		0
5	CT	876	18	10.85		0
6	CT	1753	3	7.24		0
7	CT	4083	3	39.28		0

8	CFI	876	3	1.81		3
9	CFI	876	6	3.62		7
10	CFI	1753	3	7.24		3
11	CFI	1753	6	14.48		7
12	CFI	4083	3	39.28		3

### 3.3.3 Secondary components

#### 3.3.3.1 Micromixers

Concerning the reaction, the main issue is to have, before entering the microreactor, sub-streams from the different reservoirs pass through a micromixer which ensures an intimate mixing between all reagents. In case of poorly mixed situation, the reaction takes place at sub-streams interface and can generate large concentration gradients. This situation can also lead to different reaction pathways. To avoid such kind of inconvenience, micromixers play a vital role which makes them an integral part of any microreactor setup. Therefore micromixers can be called as secondary components as their presence or absence can significantly affect the

polymerization. Micromixer was kept inside ice bath to avoid polymerization before microreactor. Micromixers based on different principles were studied and their effect on polymerization and polymer characteristics are discussed in coming chapters. Micromixers like T-Junction, High pressure interdigital multilamination micromixer (HPIMM) and KM mixer were selected for investigation (Figure 3.2).<sup>3,4</sup> Working principle and their characteristic dimensions are given in Table 3.4.

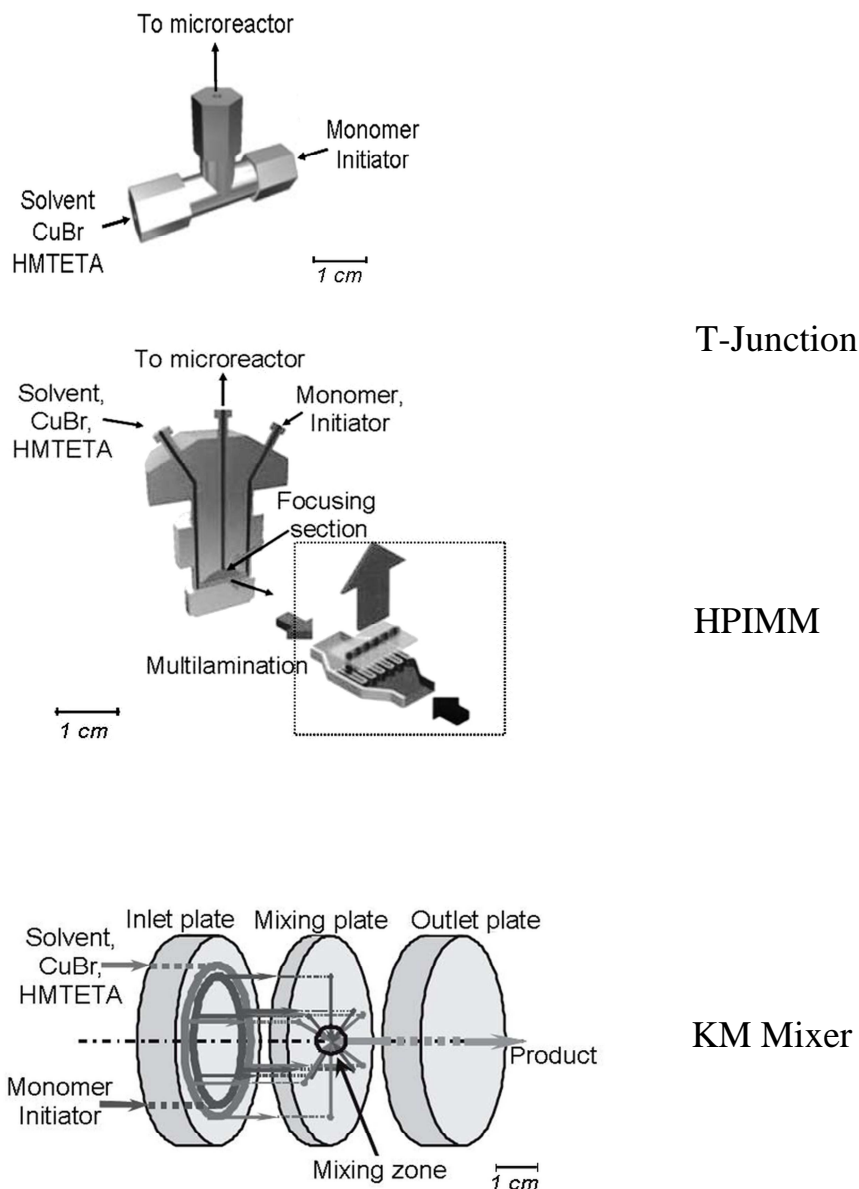
**Table 3.4.** Working principles and characteristics of different micromixers.

Type of micromixer	HPIMM	KM	T-Junction
Working principle	Multilamination	Impact mixing	Kinetic energy and long diffusion distance
Number of channels per inlet stream	15	5	1
Channel width	45 $\mu\text{m}$	100 $\mu\text{m}$	Variable, typically half of T-junction inner diameter (800 $\mu\text{m}$ )*

\* for equal flow rates and fluids viscosities

### 3.3.3 2 Back pressure regulator (BPR)

BPR is a component present at the exit of the reactor as shown in Figure 3.1. S-Series back pressure regulator was used for the experiments. BPR is very helpful to maintain uniform pressure and thus uniform reaction conditions during polymerization. Therefore this is an important component for reproducible results. However, because of narrow built-in orifice it is a point of potential clogging. Therefore, thorough cleaning of BPR and routine check of BPR seal are essential to avoid problem of clogging during polymerization. It is the most important component during high pressure polymerization in microreactor. Desired pressure inside microreactor can be achieved by closing the BPR knob to required extent. During atmospheric pressure polymerization BPR made up of polymeric materials can be used. However, in case of high pressure polymerization, it is advisable to use metallic BPR with proper seals to avoid pressure fluctuation and leakage at BPR.



**Figure 3.2.** Different micromixers used for study.

### 3.3.4 Auxiliary components

Auxiliary components of microreactor setup help to monitor and control the polymerization. Components like pressure sensors, online gel permeation chromatography falls under this category. Pressure sensor helps to monitor pressure during polymerization and control it with the help of BPR. A Swagelok pressure sensor equipped with PTU series UHP transducer (0.1 to 400 bars) was used for this purpose. Feedback and auto stop mechanism attached with the pressure sensor help to avoid damage to the pumps and other accessories. Pressure monitoring during polymerization helps to detect fouling and clogging of microreactor at the initial stage.

### 3.3.5 General procedure of microreaction

For all the experiments solvent, CuBr and HMTETA were mixed in one reservoir. In the second reservoir monomer and initiator were mixed degassed and kept in a ice bath. Both reservoirs were degassed and kept under inert atmosphere using nitrogen. To remove any traces of oxygen inside microreactor, reagents from both reservoirs were pumped into the microreactor at a flow rate of 1 to 1.5 ml per minute. Purging time depends on the volume of the reactor as the quantity of reagent purged is nearly 1.5 times the volume of the reactor. Enough care was taken to avoid premature reaction before the microreactor as discussed in previous sections. During polymerization, pressure was maintained at 1 to 1.5 bars to avoid any kind drainage due to capillary action or due to expansion of liquid inside microreactor. It is worth mentioning that a microreactor setup is a modular device. Thus another microreactor can be attached downstream to the first one such as the inlet stream of the first microreactor serves as one feed line of the second. Residence time was controlled by changing flow rates of pumps.

**Table 3.5.** Composition of different reservoirs for DMAEMA-BzMa copolymer synthesis.

	BzMA (mol.%)	→	20%	40%
<b>Reservoir 1</b>	DP		200	200
	Temperature		60 °C	60 °C
	CuBr		0.1364 g	0.1333 g
	Isopropanol		39.66 ml	39.66 ml
	HMTETA		284.5 µl	278.1 µl
<b>Reservoir 2</b>	DMAEMA		31.82 ml	23.84 ml
	BzMa		8 ml	15.98 ml
	EBIB		173.3 µl	173.1 µl

**Table 3.6.** Flow rate of reagents from reservoir 1 (R1) and reservoir 2 (R2) to get desired residence time in a 6 meter long coiled tube reactor of 876  $\mu$  internal diameter.

BzMA (mol.%)	20%		40%	
	R 1	R 2	R 1	R 2
Residence Time (min)				
5	423	340.6	426.9	336.6
15	141.0	113.6	142.3	112.14
30	70.5	56.8	71.2	56.1
60	35.2	28.4	35.6	28.0
120	17.6	14.2	17.8	14.0
240	8.8	7.1	8.9	7.0

All flow rates reported are in  $\mu$ l/min.

Composition of reservoirs and flow rate of pumps for different residence times are mentioned in Table 3.5 to Table 3.9. Sample was collected at the exit of the microreactor and cooled in ice after reaching the steady state of the reactor. Steady state of the reactor depends on its length and diameter. Steady state was determined by gel permeation chromatography and detailed procedure is given in analysis section. After completion of the study, microreactor was cleaned by flushing with acetone at a flow rate of 1 ml/min for 15 min and then with tetrahydrofuran at a similar flow rate for 15 min. It keeps the reactor reusable and avoid contamination.

**Table 3.7.** Reservoir composition for linear and branched PDMAEMA synthesis.

Reagents	Linear	Branched (5 mol.%)	Branched (10mol.%)
<b>Reservoir 1</b>	CuBr	0.1396 g	0.1976g
	Isopropanol	39.70 ml	24.60 ml
	HMTETA	291.2 $\mu$ l	412.1 $\mu$ l
<b>Reservoir 2</b>	DMAEMA	37.16 g	17.41 g
	Inimer	0	1.16 ml
	Initiator	173.4 $\mu$ l	171.1 $\mu$ l

Targeted degree of polymerization of linear PDMAEMA= 200, branched = 100

Temperature of polymerization 75 °C

**Table 3.8.** Flow rates for different residence time in a 3 meter microreactor (876  $\mu\text{m}$ ).

Time (min.)	Linear		Branched (5 mol.%)		Branched (10 mol.%)	
	<i>R 1</i>	<i>R 2</i>	<i>R 1</i>	<i>R 2</i>	<i>R 1</i>	<i>R 2</i>
5	198.6	163.2	200.4	161.4	201	160.8
15	66.1	54.4	66.8	53.8	67.0	53.6
30	33.1	27.2	33.4	26.9	33.5	26.8
60	16.5	13.6	16.7	13.7	16.7	13.4
120	8.3	6.8	8.4	6.9	8.4	6.7

All flow rates reported are in  $\mu\text{l}/\text{min}$ .

R1 and R2 are reservoir 1 and reservoir 2 respectively.

Note: flow rate was increased proportionately with increase in reactor length.

**Table 3.9.** Flow rates for desired residence time in microreactor of different diameters.

Time (min.)	572 $\mu\text{m}$ (6 meters)		1753 $\mu\text{m}$ (3 meters)		4083 $\mu\text{m}$ (3 meters)	
	<i>R 1</i>	<i>R 2</i>	<i>R 1</i>	<i>R 2</i>	<i>R 1</i>	<i>R 2</i>
5	169.2	139.2				
15	56.4	46.4				
30	28.2	23.2	132.4	109		
60	14.1	11.6	66.2	54.5		
120	7.0	5.8	33.1	27.2	179.5	147.8

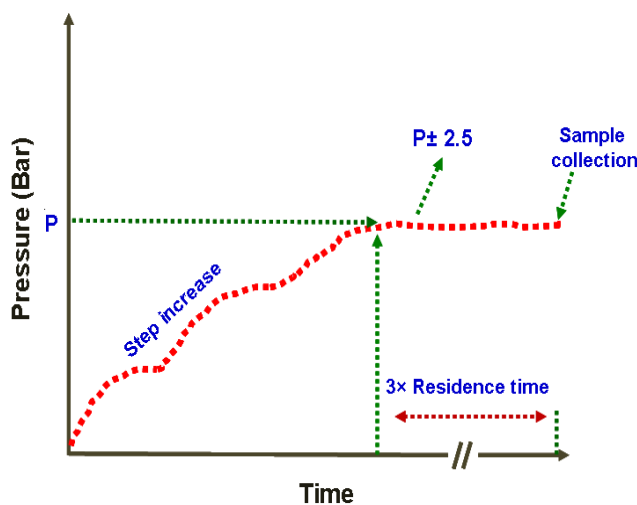
All flow rates reported are in  $\mu\text{l}/\text{min}$ .

R1 and R2 are reservoir 1 and reservoir 2 respectively.

### 3.3.6 High pressure reaction

Back Pressure Regulator (BPR) is the vital element of microreactor setup for high pressure polymerization. It was used to achieve desired pressure inside microreactor by closing or opening the knob of the regulator. Desired pressure inside the microreactor was achieved by stepwise pressure increase as shown in Figure 3.3 as it was difficult to reach the desired pressure in one single step. In between each step of increase, the pressure was allowed to stabilize. It may take 30 min to 2.5 hours to reach the desired pressure depending on residence time. For longer residence times, longer time was needed to reach the targeted pressure as viscosity of the reactants evolves during a long period of time. Once the desired pressure was reached, polymerization was continued till the steady state (approx.  $2.5 \times$  residence times) of the reactor was reached. During polymerization the pressure varied within  $\pm 2$  bars for low pressures (50 bars) and  $\pm 2.5$  bars for high pressures (100 bars). Polymerizations were carried

out at 1 bar, 50 bars, 75 bars and 100 bars. Three different microreactor diameters (576  $\mu\text{m}$ , 876  $\mu\text{m}$ , 1753  $\mu\text{m}$ ) of 3 meters length each were used to study the effect of pressure on polymerization while keeping the residence time the same for all reactors.



**Figure 3.3.** General strategy followed to achieve desired pressure in microreactor.

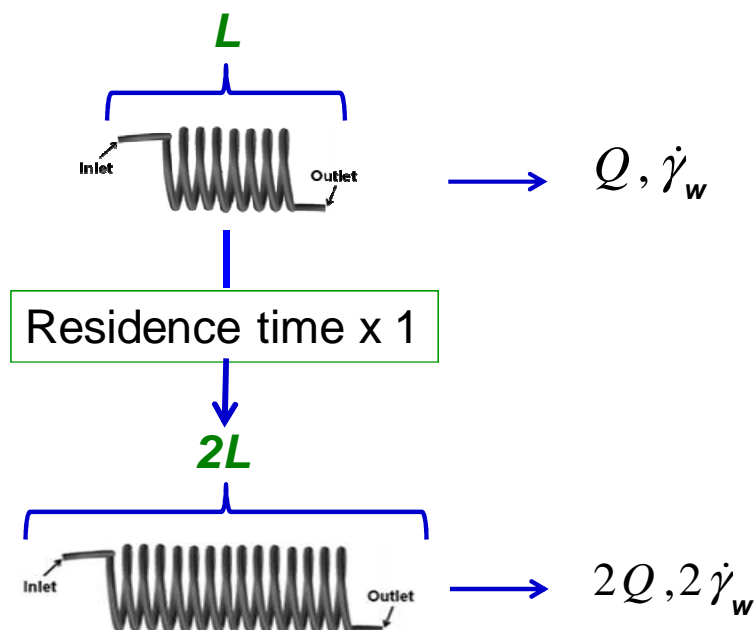
### 3.3.7 Reaction under high shear rate

Shear rate depends upon flow rate/velocity of the fluid inside microreactor. In order to increase the shear rate without changing the residence time, length of the reactor was changed proportionately as shown in Figure 3.4. Shear rate at the wall for a power-law fluid was calculated by using the formula given in equation 3.1. For Newtonian fluids (flow index  $n$  being equal to one as emphasized in §4.2.5) equation 3.2 is considered where  $\dot{\gamma}_w$  is the shear rate at the wall,  $Q$  is the flow rate and  $R$  is the radius of the microtube reactor. Four different microreactor lengths of 876  $\mu\text{m}$  internal diameter were used for these experiments. Maximum length of reactor received from supplier was 6 meters, therefore reactors were connected in series to get the desired length. For example, three CT microreactors of 6 meters length were connected to make a 18 meters length CT microreactor.

$$\dot{\gamma}_w = \frac{4Q}{\pi R^3} \frac{3n+1}{4n} \quad \text{For power law fluids} \quad (3.1)$$

$$\dot{\gamma}_w = \frac{4Q}{\pi R^3} \quad \text{For Newtonian fluids} \quad (3.2)$$





**Figure 3.4.** Strategy to achieve higher shear rate ( $\dot{\gamma}_w$ ) at a given residence time ( $L$  is the length and  $Q$  the flow rate).

## 3.4 Characterizations

### 3.4.1 Precipitation of polymer

Purification of crude polymer solution is necessary prior to any characterization aiming at determining some essential polymer characteristics like polymer composition in case of copolymers and branching efficiency for branched polymers. Polymer solutions were cooled in ice during collection at the exit of the microreactor or after withdrawing from batch reactor. Then the solution was passed through neutral alumina column to remove copper and charged in a rotary evaporator to concentrate the polymer. Cold heptane was used to precipitate this concentrated solution. Finally, polymer was recovered by centrifugation (Eppendorf Centrifuge 5804, 5000 rpm) and dried overnight under vacuum at 35 °C.

### 3.4.2 $^1\text{H}$ NMR analysis

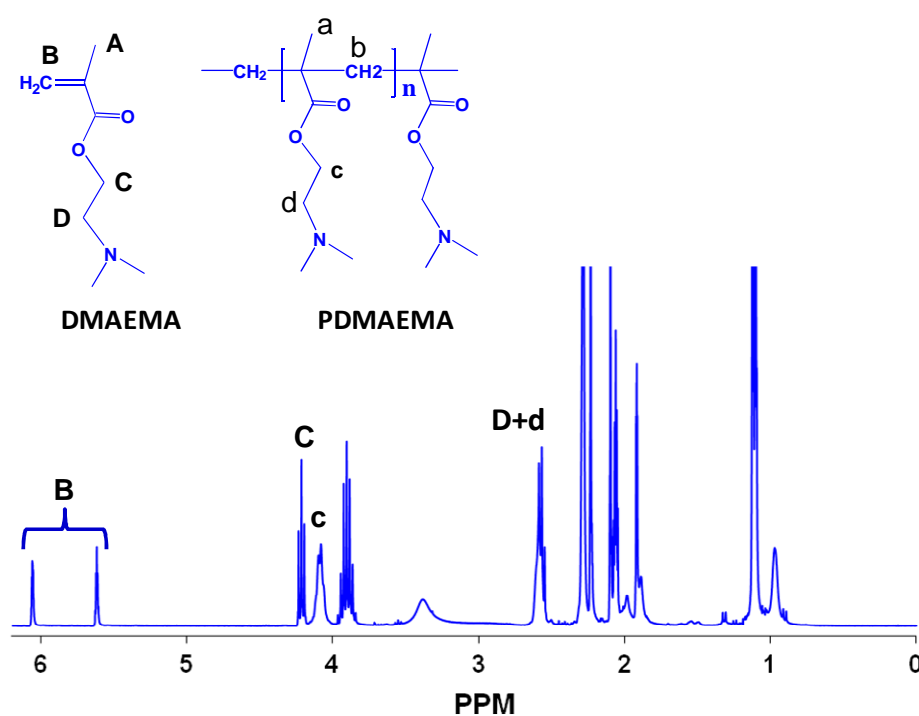
NMR analysis was carried out to find conversion of monomer during polymerization and final composition of polymer after polymerization. Proton NMR spectra of solution collected at different interval of polymerization were used to determine conversion of monomer at the particular time. Deuterated acetone or chloroform was used as solvent for NMR analysis. Bruker 300 equipped with Topspin software was used to record and analyse the spectra. Representative spectra and calculations followed to determine conversion and composition

are given below. However, in case of specific NMR analysis, relevant calculations are described in the respective chapter.

### 3.4.1.1 Conversion calculation during homopolymerization

Figure 3.5 shows the  $^1\text{H}$  NMR spectra of DMAEMA polymerizing solution using isopropanol as the solvent. Conversion of DMAEMA was calculated using the integration of protons corresponding to monomer and polymer as per equation 3.3.<sup>5-7</sup>

$$\text{Conversion of DMAEMA} = \frac{c}{B+c} \text{ or } \frac{(D+d)-B}{D+d} \quad (3.3)$$



**Figure 3.5.** Representative proton NMR spectra of DMAEMA polymerizing solution

### 3.4.1.2 Conversion calculation during copolymerization of DMAEMA and BzMA

Figure 3.6 (1) represents  $^1\text{H}$  NMR spectra of DMEAMA and BzMA copolymerizing solution in isopropanol. Protons used to calculate conversion are indicated in the spectra and formulas used are given in equation (3.4) and (3.5).

$$\text{Conversion of DMAEMA} = \frac{C}{2b1+C} \text{ or } \frac{(D+d)-2b1}{2b1+d} \quad (3.4)$$

$$\text{Conversion of BzMA} = \frac{F}{F+f} \quad (3.5)$$

To calculate the composition of synthesized polymer, first the polymerizing solution was precipitated and dried as described in section 3.4.1 and then  $^1\text{H}$  NMR spectra was recorded.  $^1\text{H}$  NMR spectra in Figure 3.6 (2) shows protons of DMAEMA-BzMA statistical copolymer used to calculate polymer composition using equation 3.6.

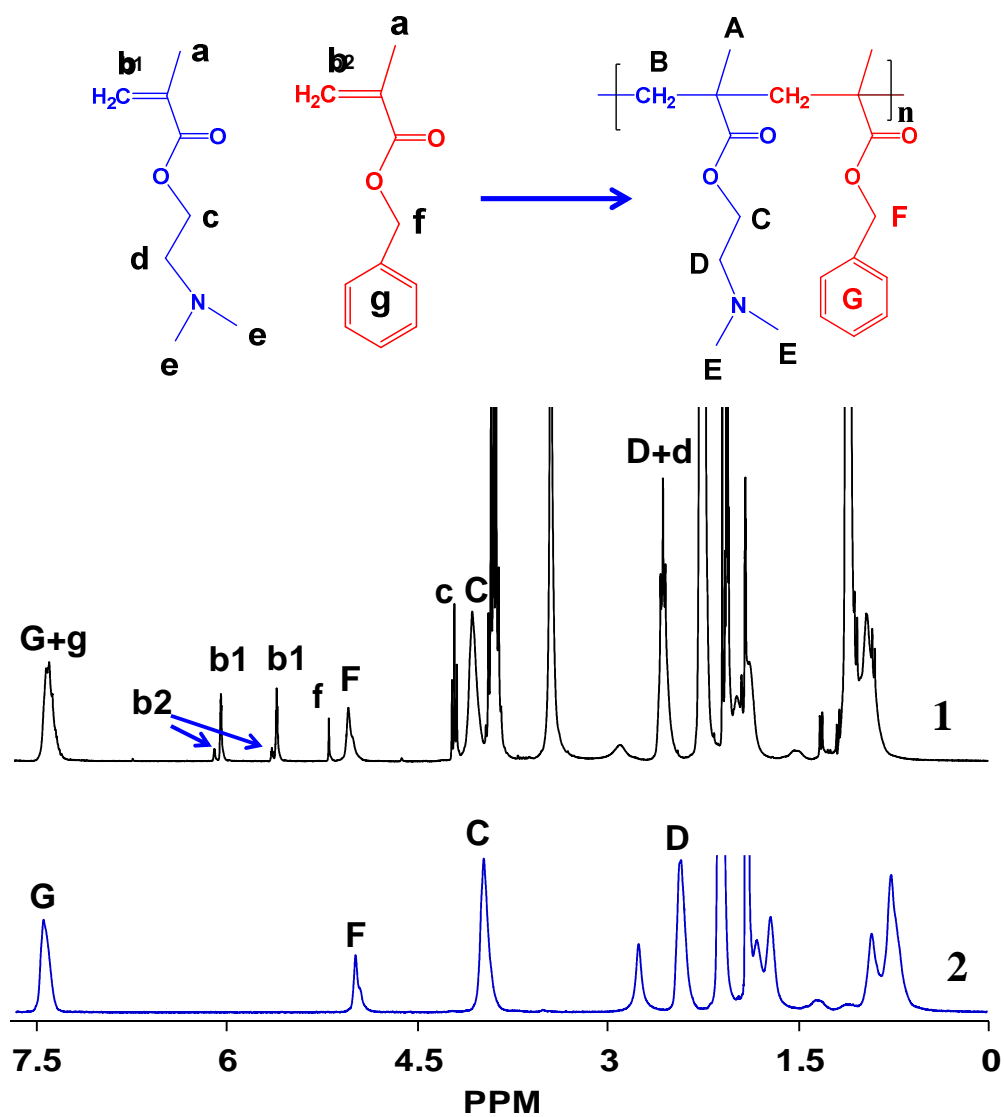
$$\text{Composition of BzMA} = \frac{F}{C + F} \quad (3.6)$$

### 3.4.1.3 Conversion calculation during branched polymerization

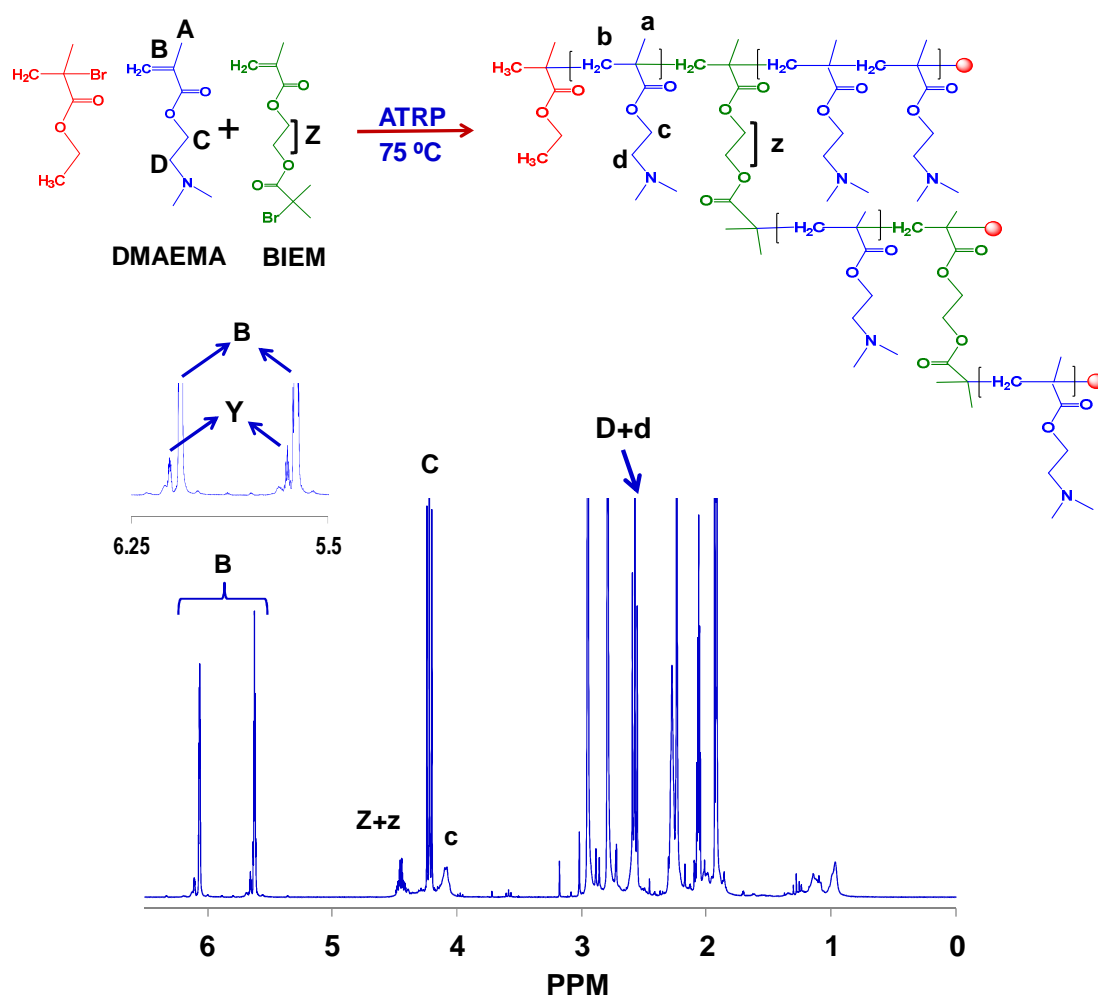
Conversion of DMAEMA and BIEM during polymerization of branched polymer was calculated using eq. (3.7) and (3.8) respectively.<sup>10-11</sup> The representative  $^1\text{H}$  NMR spectra is shown in Figure 3.7 indicating protons used for conversion calculation.

$$\text{Conversion of DMAEMA} = \frac{c}{B + c} \text{ or } \frac{(D + d) - B}{D + d} \quad (3.7)$$

$$\text{Conversion of BIEM} = \frac{(Z + z) - 2Y}{Z + z} \quad (3.8)$$



**Figure 3.6.** Representative <sup>1</sup>H NMR spectra of DMAEMA and BzMA (80/20) copolymerizing solution (1) and purified copolymer (2).



**Figure 3.7.** Representative <sup>1</sup>H NMR spectra of DMAEMA-BIEM polymerizing solution.

### 3.4.3 Gel permeation chromatography

Gel permeation chromatography (GPC) technique was used to determine the molecular weight and molecular weight distribution of crude and purified polymer. GPC was an important tool to determine the steady state of the microreactor. Branching efficiency, an important parameter to determine the architecture of branched polymer was also determined by GPC. An online PL-GPC 120 platform (CORSEMP)<sup>12-13</sup> equipped with a Shimadzu LC-10AD pump, a column (PL-gel 5 μm MIXED-C, Polymer Laboratories, 300 mm) and four online detectors was used for the above mentioned task: Series of detectors includes a Knauer K-2501 UV detector (at 254 nm), a single capillary viscometer (length 20 cm; inner diameter 0.5 mm), a dual angle-light scattering detector (MALS) and a PL-Refractive Index detector. Tetrahydrofuran (THF) was used as an eluent at a flow rate of 1 ml/min at 35 °C). Narrow

linear poly(methyl methacrylate) (PMMA) standards were used for calibration of the apparatus. Determination of steady state and branching efficiency are explained in detail in following sections.

### 3.4.3.1 Determination of steady state of continuous polymerization microreactor.

A condition at which the composition of the output is uniform with respect to time is known as steady state. Accurate determination of steady state is not only essential to collect product of uniform quality but also to reduce waste. During polymerization in a tubular microreactor, conversion and molecular weight changes along reactor length. Therefore, after the required flow rate was set for a desired residence time, sufficient time was allowed to ensure a uniform reaction condition for incoming stream. Uniform reaction conditions ensure uniform product characteristics. In case of polymerization in microreactors, polymer characteristics like number-average molecular weight ( $M_n$ ) and polydispersity index (PDI) were chosen as indicators of steady state and GPC was used to determine these parameters. Crude polymer solution was collected at equal interval (typically 15 minutes) and passed through GPC after required dilution. This procedure was continued till further increase in  $M_n$  and change in PDI was observed. It is worth to mention that, steady state of reactor changes with change in length and diameter. Therefore, steady state was determined for each length and diameter of reactor. Figure 3.8 shows series of overlaid GPC traces of polymer collected at different interval and steady state was determined as the overlapping of elution traces started.

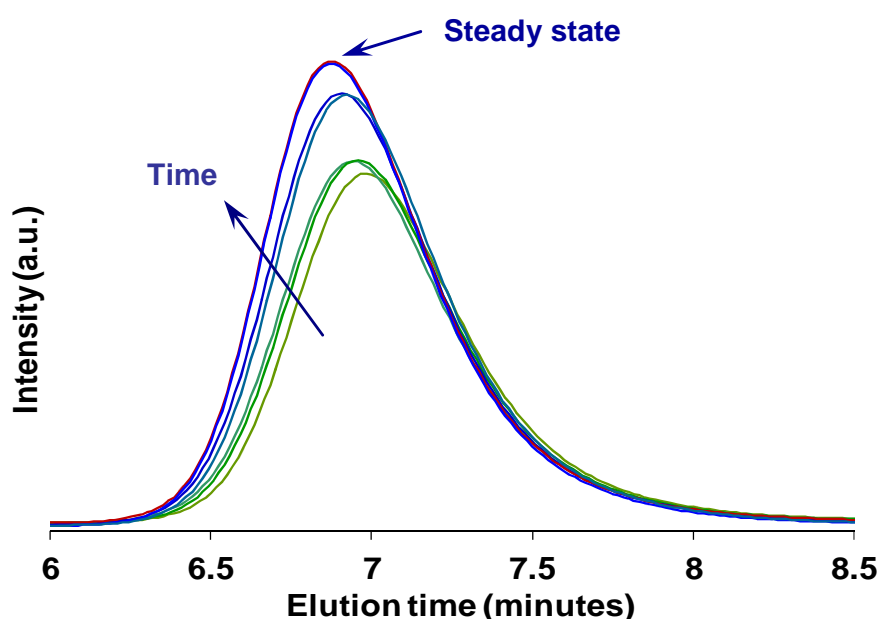
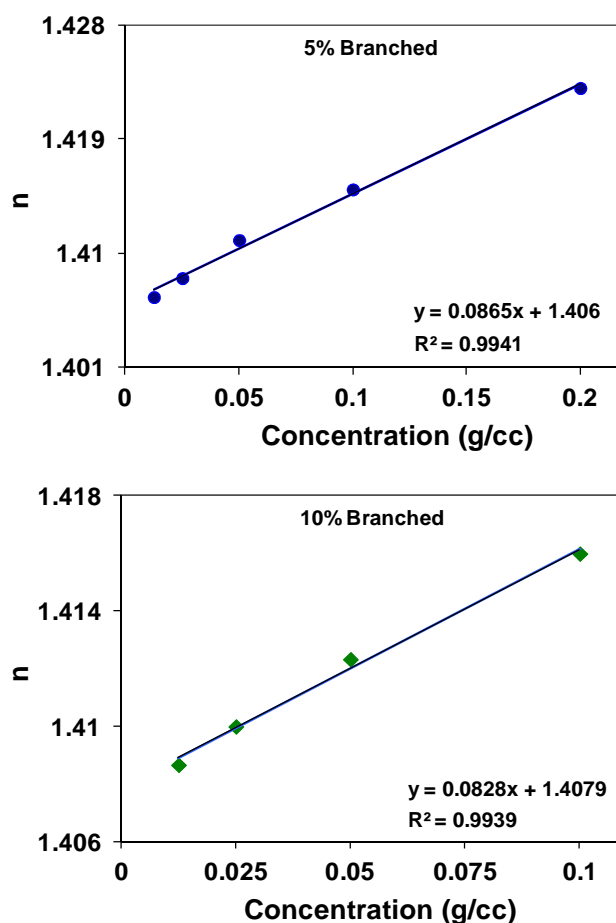


Figure 3.8. Elution traces showing steady state with time.

### 3.4.3.2 Branching efficiency

Branching efficiency of branched polymers was determined by GPC. Refractive index detection (RI) and Multiangle light scattering (MALS) was used to calculate the branching efficiency qualitatively. Ratio between the size exclusion molecular weight ( $M_w$  by RI) and absolute molecular weight ( $M_{w \text{ MALS}}$ ) of the polymer determined by MALS ( $M_{w \text{ RI}}/M_{w \text{ MALS}}$ ) gives branching efficiency.<sup>14-16</sup> Lower the value of ratio better is the branching efficiency. However, determination of  $M_w$  by light scattering detector requires refractive index ( $dn/dc$ ) of the polymer. Therefore,  $dn/dc$  of different branched polymers was determined using THF as the solvent. Solutions of purified polymer of different concentration were prepared. THF was considered as the solvent because it is used as the eluent in GPC analysis. Refractive index of branched polymer was determined by Abbe (Atago 302) refractometer. Then, refractive index of polymer solution at different concentration was plotted and gave a straight line. Slope of the line gives the  $dn/dc$  value of the polymer.  $dn/dc$  was determined for each inimer feed ratio.  $dn/dc$  of 5 mol.% BIEM branched polymer is given as an example in Figure 3.9.



**Figure 3.9.**  $dn/dc$  of 5 and 10 mol.% branched PDMAEMA indicated as the slope of the line.

### 3.4.4 Rheological behavior of polymerizing solution

#### 3.4.4.1 General procedure

Steady state shear viscosity of polymerizing solution at different polymerization times was determined by Anton Paar Physica MCR 301 rheometer (Paris, France). Concentric cylinder geometry with a conical end bob was used for this study. First the polymer solution was poured into the cup then the bob was lowered down to measuring position and temperature was raised till 75 °C. After reaching the set temperature, solution was allowed to stay at the set temperature for further 2 minutes. It allows getting uniform temperature throughout the solution before the beginning of test. Steady state shear was applied with a range from 0.1 to 200 s<sup>-1</sup> and viscosity of the solution was recorded. Values below the limiting torque value for the geometry were excluded from the analysis.

#### 3.4.4.2 Intrinsic viscosity and different rheological parameters

Intrinsic viscosities of polymerizing solutions at 75 °C for 4 different residence times were determined. Viscosities of these 4 polymerizing solutions after successive dilutions (down to 25%) were determined as described in general procedure for rheological measurements. Solvent used for dilution was prepared by mixing isopropanol and DMAEMA. Composition of diluting solvent was determined considering the conversion of DMAEMA at the particular polymerization time. Intrinsic viscosities for each solution were determined as described below in equations 3.9 to 3.11. Where,  $\eta$  is the polymer solution viscosity,  $\eta_0$  is the solvent viscosity and  $\eta_{sp}$  is the specific viscosity.

$$\text{Specific viscosity } (\eta_{sp}) = \frac{\eta - \eta_0}{\eta_0} \quad (3.9)$$

$$\text{Intrinsic viscosity } [\eta] = \lim_{c \rightarrow 0} \frac{\eta_{sp}}{c} \quad (3.10)$$

$$\text{Overlap concentration } (C^*) = \frac{1}{[\eta]} \quad (3.11)$$

From the above calculations concentration limits of the polymerizing solution was determined from  $C/C^*$  or when  $C \times [\eta]$  reaches 1. It gives indication about the transition of polymerizing

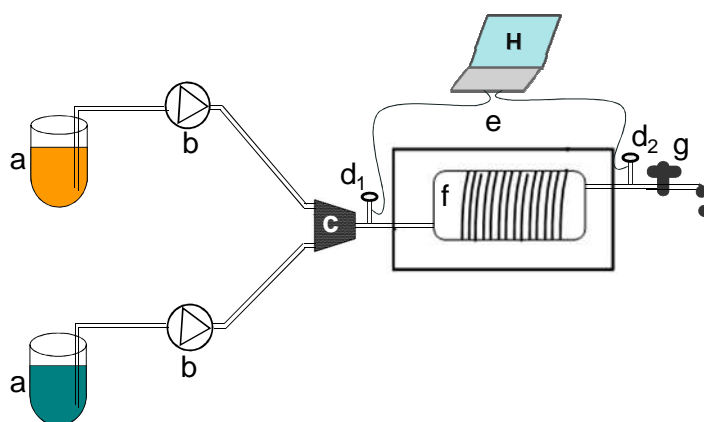


solution from dilute to semi dilute regime. Its implication and impact on polymerization is discussed in chapter 4.

### 3.4.5 Pressure drop determination

Pressure drop indicates energy consumption in the reactor. Pressure drop depends upon various factors like length of reactor, presence of joints, bends, flow rate, fluid viscosity and nature of process. In this work, polymerizations in different kind of microreactors were studied to enhance the polymerization rate and improve overall polymer quality. Therefore it becomes essential to have a clear idea about the energy consumption in different microreactors reactors.

ATRP process of DMAEMA was followed during investigation of pressure drop. A slight modification was done to the microreactor setup shown in Figure 3.1. An additional pressure sensor was attached to the microreactor just before the BPR as shown in Figure 3.10. Both sensors were connected to a computer to monitor the change in pressure during polymerization. Difference between the readings of two pressure sensors ( $d_1-d_2$ ) at idle condition was zero. Then reagents were pumped through the microreactor to achieve a residence time of 15 min. Pressure of downstream sensor was maintained within 1 to 1.5 bars with the help of BPR. Once the steady state was reached the sensor readings were noted three times after 15 minutes interval. Then flow rates of pumps were reduced to get 2 hours residence time and pressure at upstream and downstream sensors were noted after the steady state of the reactor was reached. Then pressure drop was calculated by subtracting pressure at  $d_2$  from pressure at  $d_1$ . Similar experiments were repeated for CT and CFIs of 6 meters length and different diameters.



**Figure 3.10.** Microreaction setup to determine pressure drop during polymerization, showing: reservoirs (a), HPLC Pumps (b), micromixer (c), pressure sensors (d1 and d2), oven (e), tubular microreactor (f), back pressure regulator (g) and computer (H).

---

## References

- (1) Matyjaszewski, K.; Gaynor, S. G.; Kulfan, A.; Podwika, M. *Macromolecules* **1997**, *30*, 5192.
- (2) Mori, H.; Böker, A.; Krausch, G.; Müller, A. H. E. *Macromolecules* **2001**, *34*, 6871.
- (3) Rosenfeld, C.; Serra, C.; Brochon, C.; Hessel, V.; Hadziioannou, G. *Chemical Engineering Journal* **2008**, *135*, Supplement 1, S242.
- (4) Nagasawa, H.; Aoki, N.; Mae, K. *Chemical Engineering & Technology* **2005**, *28*, 324.
- (5) Xiong, Q.; Ni, P.; Zhang, F.; Yu, Z. *Polym. Bull.* **2004**, *53*, 1.
- (6) Hu, H.; Fan, X.-D.; Cao, Z.-L.; Cheng, W.-X.; Liu, Y.-Y. *Journal of Applied Polymer Science* **2006**, *101*, 311.
- (7) You, Y.-Z.; Zhou, Q.-H.; Manickam, D. S.; Wan, L.; Mao, G.-Z.; Oupický, D. *Macromolecules* **2007**, *40*, 8617.
- (8) Mykytiuk, J.; Armes, S.; Billingham, N. *Polymer. Bulletin.* **1992**, *29*, 139.
- (9) Demirelli, K.; Coskun, M.; Kaya, E. *Journal of Polymer Science Part A: Polymer Chemistry* **2004**, *42*, 5964.
- (10) Bally, F.; Ismailova, E.; Brochon, C.; Serra, C. A.; Hadziioannou, G. *Macromolecules* **2011**, *44*, 7124.
- (11) Muthukrishnan, S.; Mori, H.; Müller, A. H. E. *Macromolecules* **2005**, *38*, 3108.
- (12) Rosenfeld, C.; Serra, C.; O'Donohue, S.; Hadziioannou, G. *Macromolecular Reaction Engineering* **2007**, *1*, 547.
- (13) Bally, F.; Serra, C. A.; Brochon, C.; Hadziioannou, G. *Macromolecular Rapid Communications* **2011**, *32*, 1820.
- (14) Podzimek, S.; Vlcek, T. *Journal of Applied Polymer Science* **2001**, *82*, 454.
- (15) Podzimek, S. *Journal of Applied Polymer Science* **1994**, *54*, 91.
- (16) Qiang, R.; Fanghong, G.; Bibiao, J.; Dongliang, Z.; Jianbo, F.; Fudi, G. *Polymer* **2006**, *47*, 3382.

---

# CHAPTER 4

## EFFECT OF PREMIXING AND OPERATING PARAMETERS ON REACTION RATE

<i>Preface</i>	94
<b>4.1 Intensifying the ATRP synthesis of statistical copolymers by continuous micromixing flow techniques</b>	
4.1.1 Introduction	96
4.1.2 Materials and methods	97
4.1.3 Results and discussion	97
4.1.4 Summary	103
4.1.5 Supporting Information	104
<b>References</b>	106
<b>4.2 Atom Transfer Radical Polymerization in continuous-microflow: effect of process parameters</b>	
4.2.1 Introduction	109
4.2.2 Materials and methods	110
4.2.3 Results and discussion	110
4.2.3.1 <i>Effect of temperature on polymerization in microreactor</i>	110
4.2.3.2 <i>Effect of pressure</i>	111
4.2.3.3 <i>Effect of shear rate on polymerization</i>	114
4.2.4 Summary	117
4.2.5 Supporting Information	119
<b>References</b>	123

## **Preface**

From the literature review, it is evident that there is a strong need to accelerate ATRP processes. To achieve such objective different chemical and process alternatives were employed. However the use of microreaction technology was scarcely reported though microreactors are well admitted by now as efficient tools for the intensification of fine chemical synthesis.

In tubular microreactors, mixing is solely operating by diffusion. Therefore a straightforward strategy to intensify the reaction is to promote the most intimately mixing of the reactive solution prior entering to the microreactor. In case of polymerization, premixing becomes crucial as a poor mixing leads to concentration gradient with subsequent low monomer conversion and broadening of the molecular weight distribution. Thus the first section of this chapter addresses this issue. It gives an idea about the effect of different micromixer principles and their impact on final polymer characteristics synthesized in a tubular microreactor.

In the next section, different operating parameters-based strategies were investigated to accelerate ATRP in tubular microreactors. It describes the polymerization at elevated temperatures and pressures to increase rate of ATRP. Effect of the shear rate through the reactor length was also investigated.

*This chapter is partially adapted from the two following articles:*

(1) D. Parida, C.A. Serra, F. Bally, D.K. Garg and Y. Hoarau, *Intensifying the ATRP synthesis of statistical copolymers by continuous micromixing flow techniques*, *Green. Proc. Synt.*, 6 (1) (2012) 525-532.

(2) D. Parida, C.A. Serra, R. Ibarra Gómez, D.K. Garg, Y. Hoarau, M. Bouquey and R. Muller, *Atom Transfer Radical Polymerization in continuous-microflow: effect of process parameters*, *J. Flow Chem.*, submitted.

## *4.1. Intensifying the ATRP synthesis of statistical copolymers by continuous micromixing flow techniques*

### *Abstract*

*The impact of micromixers on copolymer's characteristics in a continuous-flow microprocess was studied. A stainless steel coiled tube was used as the microreactor. Several micromixers with different working principles like bilamination, multilamination and impact jet, were used to mix the reactant's streams before entering the reactor. (Co)polymers of 2-dimethyl amino ethyl methacrylate (DMAEMA) and benzyl methacrylate (BzMA) were synthesized by the atom transfer radical polymerization (ATRP) technique, with two different compositions of BzMA (20% and 40%). A faster polymerization rate was observed in case of microprocess, as compared to batch process, highlighting the inherent intensification nature of microfluidic-assisted processes. Despite equal conversion for the three micromixers, a remarkable difference in molecular weight was observed. The highest molecular weights with lowest polydispersity indices (PDIs) were obtained when the multilamination micromixer was used, while the bilamination gave polymers with high PDIs and low molecular weights. Diffusion constraints arising from the increase in viscosity was clearly visible for highest residence times in the microreactor, resulting in a deviation of molecular weight from the theoretical value.*

### **KEYWORDS**

ATRP, continuous-flow, microreactor; micromixer, copolymer.

### 4.1.1 Introduction

Functional polymers have interesting properties and find numerous applications in different fields. Linear polymers find applications, like dispersants and surfactants<sup>1,2</sup> and complex counter parts like branched and crosslinked, find uses, e.g., in drug delivery, enzyme support and biomolecular transport.<sup>3-5</sup> Controlled radical polymerization techniques are widely used to synthesize architecture-controlled polymers. However, their properties strongly rely on the control of the polymerization reaction to get targeted composition and architecture. The benefits of controlled radical polymerization are not fully exploited in present conventional reactors, because of a large mixing time and broad temperature profile.

In order to maximize the benefits of controlled radical polymerization, microreaction technology is considered as an alternative. Efficient heat and mass transfers give microreaction technology an edge over conventional processes, and opened a new dimension in the field of fine chemical synthesis, pharmaceuticals and polymer chemistry. Efficient heat and mass transfers allow controlled handling of exothermic and endothermic reactions. However, polymer synthesis in microfluidic devices is still in its infancy and faces some challenges, like continuously changing reaction conditions with time and a high viscosity, which limit the equal flow distribution inside the microreactor.<sup>6</sup> This inhomogeneity can significantly neutralize the benefits of a microreactor. In spite of these challenging conditions, research is still going on to exploit the benefits of microsystems.<sup>7-9</sup> It is observed that microsystems have a pronounced impact on polymerization processes and polymer characteristics.<sup>10-12</sup> Different polymerization techniques have been recently investigated in microreactors, including controlled radical polymerizations to synthesize polymers starting from the simplest architecture as linear, to complex architectures such as hyperbranched.<sup>13-18</sup> In chemical reactions, mixing of reactants is an important step and is usually achieved by diffusion in microreactors. However, fast reactions require fast mixing to operate at their kinetic limit, instead of being diffusion controlled. This led to the development of micromixers having mixing capabilities ranging from seconds to milliseconds. Faster mixing leads to reduced reaction times, and thereby cleaner chemistry, since unwanted side reactions and terminations are suppressed. A variety of micromixers working on different principles are available.<sup>19-21</sup> Being an integral part of a microreaction setup, they can have a significant impact on reaction and polymer properties. To the best of our knowledge, the synthesis of statistical (co)polymers and the impact of different micromixers on polymerization have not been reported in the literature, especially polymerization reactions considered as “slow”, like

---

atom transfer radical polymerization (ATRP), in comparison with free radical or ionic polymerization reactions. In an attempt to fill this space, we investigated the effect of different micromixers, namely a T-Junction, an interdigital multilamination (HPIMM) and an impact jet (KM) micromixers, on the ATRP synthesis and properties of copolymers. 2-(dimethylamino) ethyl methacrylate (DMAEMA) and benzyl methacrylate (BzMA) were used in this study. DMAEMA and its (co)polymers are well known for thermal and pH response behavior,<sup>22-25</sup> while BzMA can undergo hydrogenolysis after polymerization to give desired acidic residue.<sup>25</sup> The functional behavior of these polymers makes them suitable for different biomedical applications, like drug / gene transfer or protein transport.<sup>5,26,27</sup>

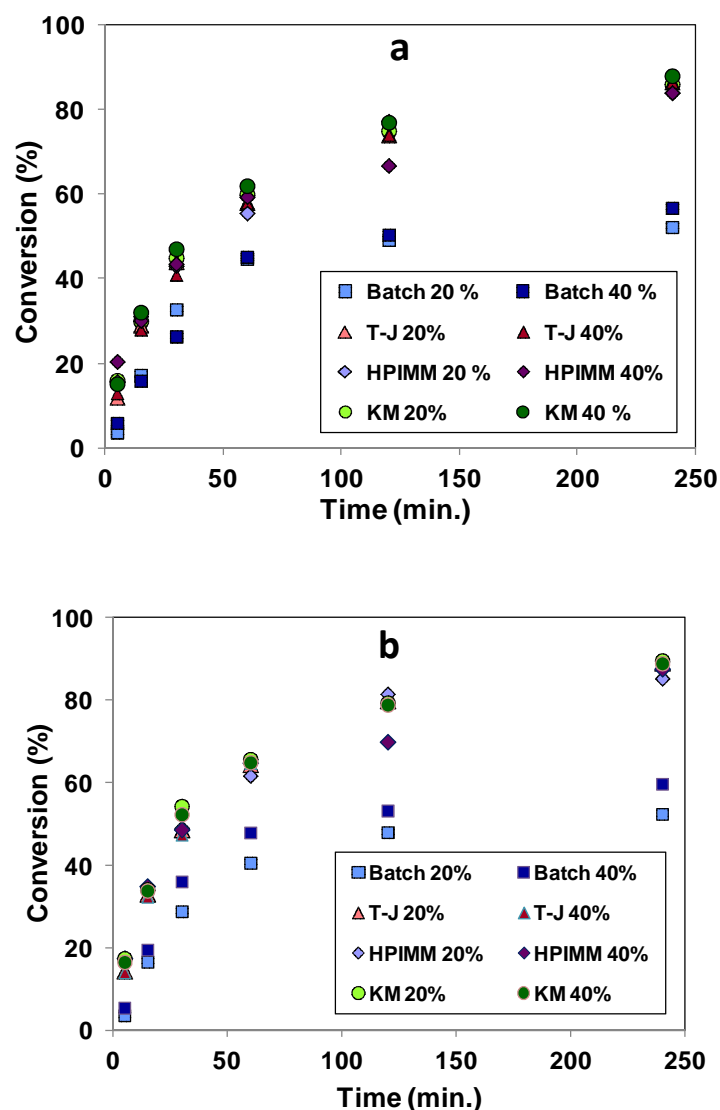
#### 4.1.2 Materials and methods

- I. List of materials is given in Chapter 3 section 3.1.1.
- II. Description of setup is provided in Chapter 3 section 3.3.
- III. Polymerization in batch reactor is given in Chapter 3 section 3.2.2 while reservoir compositions are presented in Table 3.2.
- IV. Continuous-flow reactor detailed procedure is given in Chapter 3 section 3.3.5 while reservoir compositions and flow rates are presented Table 3.5 and Table 3.6 respectively.
- V. Purification of the samples is detailed in Chapter 3 section 3.4.1.
- VI. Characterization methods include <sup>1</sup>H NMR (Chapter 3 section 3.4.1.2.), GPC (Chapter 3 section 3.4.2.) and rheological measurements (Chapter 3 section 3.4.3.)

#### 4.1.3 Results and discussion

Statistical copolymers of DMAEMA and BzMA, with 20% and 40% BzMA composition, were synthesized in batch and continuous-microflow reactors. Polymerization conditions in microreactors were maintained the same. The flow rates were varied to get the required molar ratios and residence time. It was observed that whatever the micromixer employed, the polymerization rate in the case of the microreactor is higher than for the batch reactor (Figure 4.1). Synergy of efficient heat transfer and enhanced diffusion in microscale, even at high viscosity, can be seen as a remarkable increase in conversion. Indeed the conversion of both comonomers was higher by 31 to 35 points at a residence time of 4 h. One can notice that, for the longest residence time investigated, there is not much difference in the final conversion of

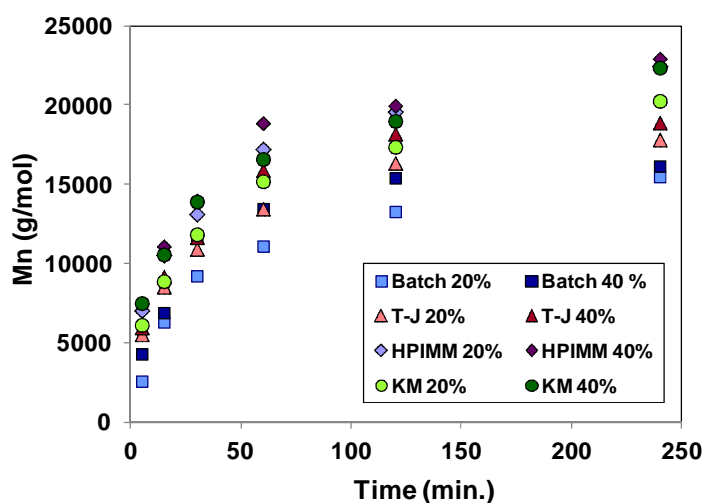
the comonomers, whatever the micromixer employed. This suggests that the final conversion is independent of the initial quality of the mixing at the entrance of the microreactor, but depends rather on the time available for diffusion. However, the copolymer characteristics will be quite different, as seen in the following section. A change in composition of BzMA in the inlet stream has no significant impact on conversion of DMAEMA and BzMA in the continuous-microflow process. However, in batch polymerization, an increase in the conversion of both comonomers is observed, with an increase in the composition of BzMA (Figure 4.1). Since the composition of the copolymers follows the initial composition of the comonomers in the polymerizing solution (Tables 4.SI1 and 4.SI2), indicating reactivity ratios close to one, the observed increase in conversion of the comonomers might result from concentration gradients in the batch reactor.



**Figure 4.1.** Conversion of monomers (%) with time for DMAEMA (a) and BzMA (b).

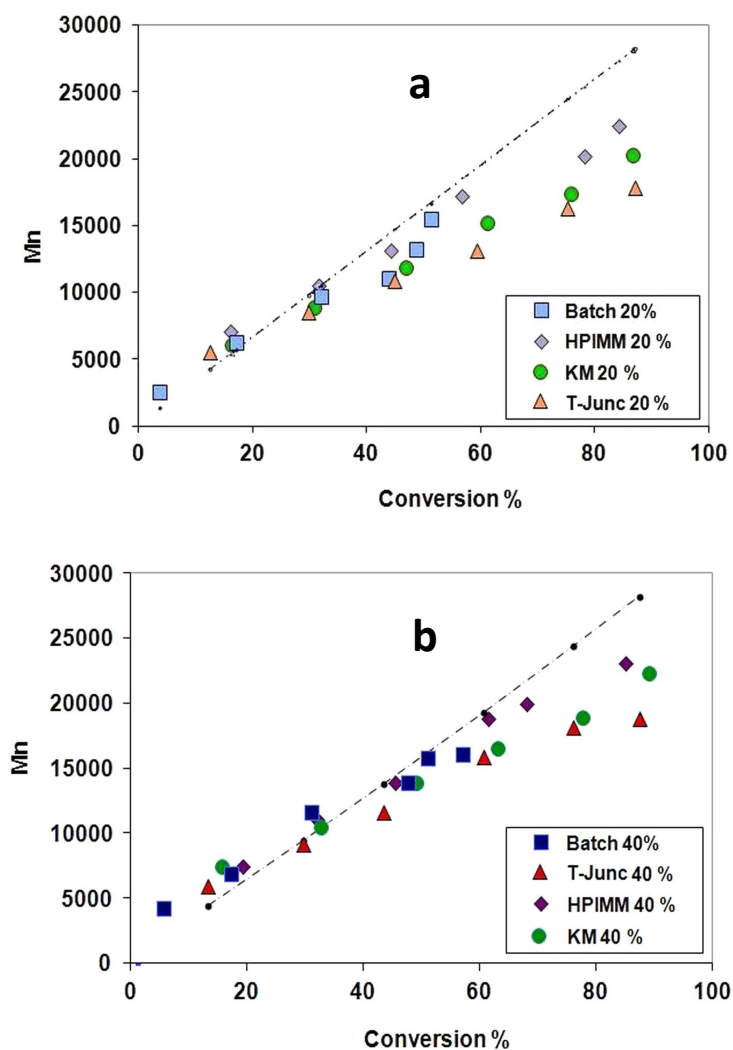


To have a better understanding of the effect of micromixers on macromolecular characteristics, molecular weights were determined. Interestingly, it was found that, even at 5 min of residence time, the molecular weights obtained by different micromixers and batch processes were different, and that they were arranged in a distinctive order (Figure 4.2); batch process gave the lowest molecular weight while the HPIMM micromixer gave the highest. Among the micromixers, the lowest molecular weight was obtained when T-junction was used as a micromixer. This may be attributed to poor initial mixing achieved by bilamination, which is also highlighted by the highest PDI (Figure 4.2).

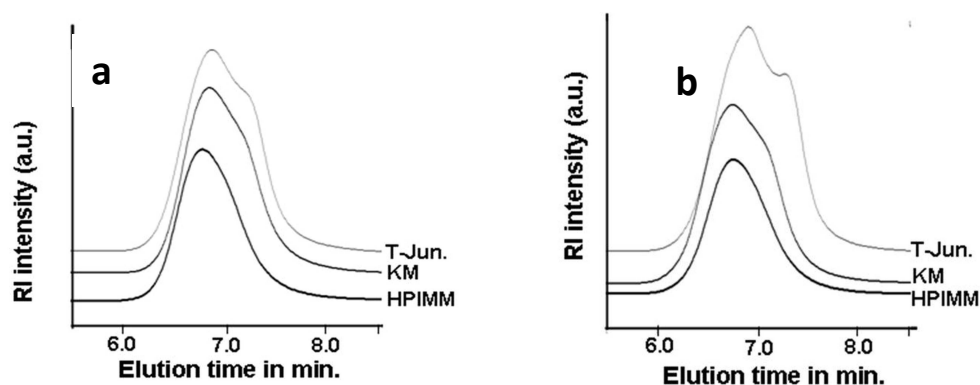


**Figure 4.2.** Evolution of molecular weight ( $M_n$ ) with time.

The effect of initial inhomogeneity becomes more prominent as the polymerization time increases. The slow increase in molecular weight can be attributed to poor mixing, whereas better mixing results in a faster increase of molecular weight, as in the case of HPIMM. More insight into polymerization and the behavior of polymerizing solutions inside a microreactor can be seen from Figure 4.3.

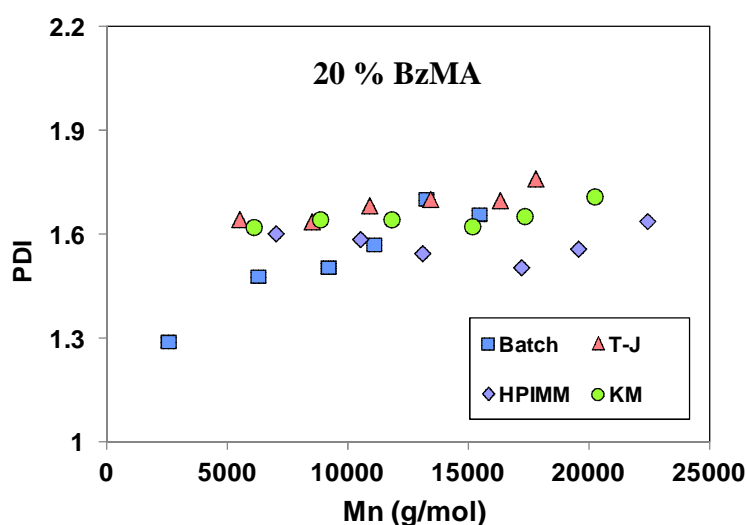


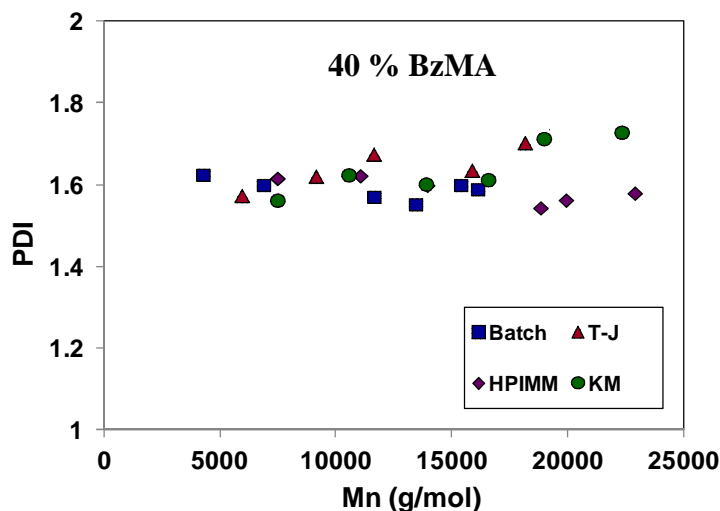
**Figure 4.3.** Comparison of theoretical and experimental molecular weights for 20% BzMA (a) and 40% BzMA (b) composition.



**Figure 4.4.** GPC traces of DMAEMA-BzMA statistical copolymers synthesized in the continuous-microflow reactor at 4 h residence time, 20 (a) and 40 mol.% BzMA (b) composition.

It can be observed that for both BzMA compositions (20% and 40%) and for low overall comonomer conversion (< 50%), evolution of molecular weight for batch and continuous-microflow reactors follows the predictable theoretical behavior. However after 1 h of residence time, corresponding to comonomer conversion > 50% (Figure 4.3), the difference between theoretical and experimental molecular weight (evaluated on non purified samples) starts to increase for both processes. It is also the time after which PDIs of copolymers start to increase (Figure 4.5). It is worth noting that after a residence time of 1 h, the availability of monomer diminishes and the viscosity of the solution increases significantly, which may lead to poor growth of macromolecular chains and unwanted termination. Therefore, a deviation in growth from the theoretical molecular weight towards lower values is observed. Amplification of inhomogeneity was also clearly visible in GPC traces. For both compositions (20% and 40% BzMA), a shoulder starts to appear in GPC traces at a residence time of 2 h for the continuous-microflow reactor equipped with the T-junction mixer (Figure 4.SI1) and becomes more pronounced at 4 h residence time. For the KM mixer, a similar shoulder also appears, but seems to be delayed in comparison with the T-junction, i.e., at 4 h residence time (Figure 4.4). This shoulder indicates the presence of copolymers with a bimodal molecular weight distribution, which may arise from polymerization in two different phases; presumably the copolymer viscous solution and the less viscous comonomers phase. However, a smooth GPC trace for the HPIMM mixer indicates an efficient homogenization during polymerization.





**Figure 4.5.** Plot for PDI vs. Mn of P(DMAEMA-co-BzMA) statistical copolymers.

PDI is an important characteristic parameter to follow the course of the polymerization reaction, and also gives an indication of the degree of control over the process. Initial PDIs, in the case of continuous-microflow polymerization, were almost the same whatever the BzMA composition (Figure 4.5). As a general trend, PDIs increase with molecular weight (i.e., polymerization time) for the 20% BzMA composition, except for the continuous-microflow reactor equipped with the HPIMM mixer (Figure 4.5a). For the latter, one can observe a decrease in the PDI, followed by an increase past 15,000 g/mol. Moreover, this micromixer induces the smallest PDIs, especially at high molecular weights. An initial higher PDI may arise from the higher flow rate, which reduces the time availability for diffusion of molecules. As a result, the residence time distribution (RTD) reflects the laminar flow profile and induces a broadening of the molecular weight distribution. With an increase in the residence time (the microreactor length was kept constant), the time available for diffusion was increased, and therefore, better homogenization is expected. This can be seen as a decrease in the PDI with an increase in polymerization time (Figure 4.5). However, after 1 h of residence time, larger macromolecular sizes and an increased viscosity induce a more pronounced resistance for diffusion. Indeed, rheological measurements (Figure 4.SI2) showed a 100-fold increase in the viscosity of the reactive solution between 5 min and 1 h residence time. Reduced diffusion results in an unequal growth of macromolecular chains, leading to an increase in PDIs of copolymers. Such phenomenon is not very distinct in the case of mixers, like T-Junction and KM. Improper mixing obtained by these last two mixers at initial stage results in an uneven initiation of polymer chain, which remains dominant over mixing inside the microreactor, by pure mass diffusion.

#### 4.1.4 Summary

The synthesis of statistical copolymers of DMAEMA and BzMA was investigated in batch and continuous-microflow reactors. Process intensification is a feature of microreaction technology, which is clearly demonstrated in terms of higher overall conversion of monomers (+ 35 %), higher molecular weights (+8000 g/mol) and lower PDIs. The effect of different micromixer working principles on polymerization was investigated and it was found that polymerization in a microreactor is better controlled when a multilamination mixer (HPIMM) is used to mix reactants streams prior to entering the reactor. The HPIMM was found to impart better mixing as compared to an impact jet (KM) or bilamination (T-Junction) mixer. It was also observed that initial inhomogeneity gets amplified with increase in the polymerization time, which is more pronounced in T-Junction, as seen by the presence of a shoulder in the GPC traces. For the batch reactor and the continuous-flow reactor, whatever micromixer was used, deviation in molecular weight from the theoretical molecular weight towards the lower side, and an increase in PDI after 1 h of residence time, indicates that the viscosity of the reactive medium inside the reactor significantly affected the polymerization. However, the microreactor equipped with the HPIMM allowed adhering more closely to ideal conditions (theoretical values). Thus it was demonstrated that even a “slow” reaction like an ATRP polymerization reaction can be accelerated significantly by means of micromixing, since a given comonomer conversion is obtained in approximately half the time required for a batch process, leading to an overall productivity twice as great. Moreover polymer characteristics can be improved in terms of higher molecular weights and lower PDIs.

*This section highlights the influence of tubular coiled microreactors on reaction rate of ATRP compared to conventional lab-scale batch reactor at low pressure (1-1.5 bars) and mild temperature (60°C). It indicates that a poor premixing can neutralize the benefit of microscale by affecting the macromolecular characteristics negatively while an intimate mixing (HPIMM) leads to a significant acceleration of the reaction. Considering the superiority of microreactors in terms of short diffusion pathways and heat management, some harsh reaction conditions like high temperatures and high pressures were investigated in the following section to enhance further the reaction rate of ATRP.*

## 4.1.5 Supporting Information

### 4.1.5.1 Polymer characteristics

**Table 4.SI 1.** Polymer characteristics at 1 hour polymerization time.

Sample		Conversion (%)		Mn (Theo.)	Mn <sup>c</sup> (g/mol.)	PDI <sup>d</sup> (Mw/Mn)	Composition <sup>e</sup> (BzMA mol. %)
		DMAEMA <sup>a</sup>	BzMA <sup>b</sup>				
Batch	20%	44.75	41	14315	11095	1.62	19.8
	40%	45.2	48	15208	13457	1.55	41.5
HPIM M	20%	55.55	61.8	18523	17210	1.50	19.5
	40%	59.5	64.9	19705	18847	1.54	40.6
KM	20%	60	65.7	19923	15181	1.62	21.2
	40%	62	65	20170	16584	1.61	41.0
T-J	20%	58.5	64.5	19135	13442	1.7	18.7
	40%	58	64.9	19160	15882	1.64	39.5

<sup>a, b, e</sup> Determined by <sup>1</sup>H NMR

<sup>c, d</sup> Determined by GPC

**Table 4.SI 2.** Polymer characteristics at 4 hours polymerization time.

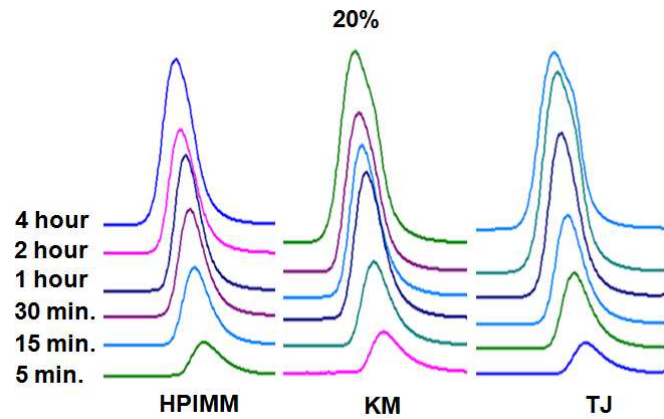
Micro mixer	Feed BZMA composition (mol.%)	Conversion (%)		Mn (Theo.)	Mn <sup>c</sup> (g/mol.)	PDI <sup>d</sup> (Mw/Mn)	Composition <sup>e</sup> (BzMA mol. %)
		DMAEMA <sup>a</sup>	BzMA <sup>b</sup>				
Batch	20	53	53.5	16664	15465	1.65	19.8
	40	57	59	18697	16134	1.59	42.5
HPIM M	20	84	85.3	27315	22438	1.64	20.5
	40	85	87.5	27456	22913	1.58	40.8
KM	20	86	89	28149	20235	1.67	19.0
	40	88	89	28744	22348	1.72	40.0
T-J	20	86.5	87	28235	17806	1.76	18.5
	40	86.5	87	28228	18880	1.75	38.5

<sup>a, b, e</sup> Determined by <sup>1</sup>H NMR

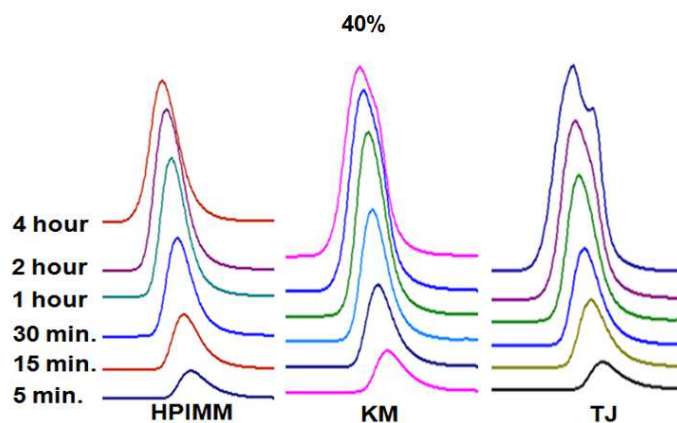
<sup>c, d</sup> Determined by GPC

#### 4.1.5.2 Monitoring of polymerization by GPC

Polymer samples were collected at different polymerization time and analysed by Gel Permeation Chromatography (GPC). When GPC traces of different polymerization times and different micromixers are compared, effect of micromixing is clearly visible. Negative impact of poor mixing on polymerization in microreactor is observed in case of T-Junction and KM mixers where a bimodal distribution in molecular weight is to be seen.



(a)



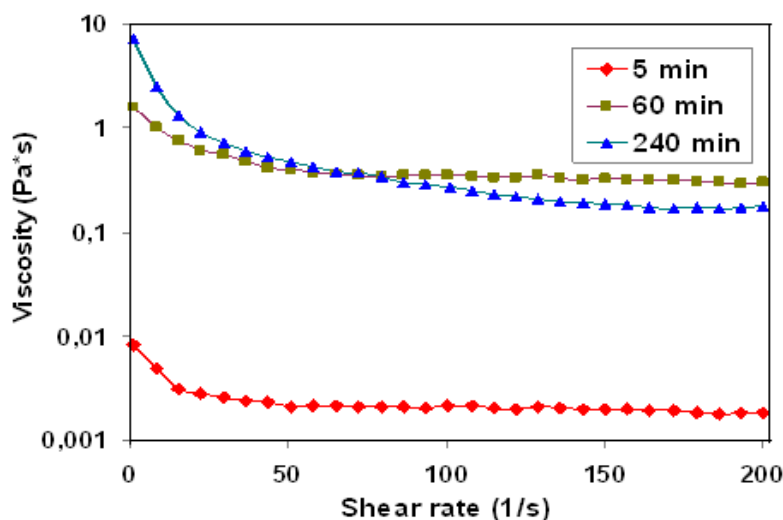
(b)

**Figure 4.SI 1.** GPC traces for 20% (a) and 40% (b) BzMA composition at different residence times and for the three micromixers employed.

#### 4.1.5.3 Rheological characterization

Unpurified samples of polymer solutions obtained from the continuous-flow microprocess equipped with HPIMM after 5 min, 1 hr and 4 hrs residence times were analyzed by dynamical mechanical analysis in a cone and plate rheometer. It is observed a shear thinning for all three samples tested as the viscosity is decreasing with an increase in the shear rate.

However, the shear thinning seems to be more pronounced when the residence time increases, i.e. when the molecular weight is higher. Thus the samples clearly exhibit a non-newtonian behaviour. Since among the three micromixers investigated, HPIMM gave the highest molecular weights, it is expected that the shear thinning will be less pronounced for the T-junction and KM mixer.



**Figure 4.SI 2.** Viscosity of crude polymer solution under shear shear rate.

Note: increase in viscosity with decreasing shear towards zero (0) is an experimental artefact.

## References

- (1) Nashy, E. L. S. H. A.; Essa, M. M.; Hussain, A. I. *Journal of Applied Polymer Science* **2012**, *124*, 3293.
- (2) Kyriacou, M. S.; Hadjiyannakou, S. C.; Vamvakaki, M.; Patrickios, C. S. *Macromolecules* **2004**, *37*, 7181.
- (3) Zhu, C.; Hard, C.; Lin, C.; Gitsov, I. *Journal of Polymer Science Part A: Polymer Chemistry* **2005**, *43*, 4017.
- (4) Bruns, N.; Tiller, J. C. *Nano Letters* **2004**, *5*, 45.
- (5) Achilleos, D. S.; Georgiou, T. K.; Patrickios, C. S. *Biomacromolecules* **2006**, *7*, 3396.
- (6) Hessel, V.; Löwe, H.; Serra, C.; Hadziioannou, G. *Chemie Ingenieur Technik* **2005**, *77*, 1693.
- (7) Wu, T.; Mei, Y.; Cabral, J. T.; Xu, C.; Beers, K. L. *Journal of the American Chemical Society* **2004**, *126*, 9880.



- 
- (8) Iwasaki, T.; Kawano, N.; Yoshida, J.-i. *Organic Process Research & Development* **2006**, *10*, 1126.
  - (9) Honda, T.; Miyazaki, M.; Nakamura, H.; Maeda, H. *Lab on a Chip* **2005**, *5*, 812.
  - (10) Iwasaki, T.; Yoshida, J.-i. *Macromolecules* **2005**, *38*, 1159.
  - (11) Nagaki, A.; Miyazaki, A.; Yoshida, J.-i. *Macromolecules* **2010**, *43*, 8424.
  - (12) Iida, K.; Chastek, T. Q.; Beers, K. L.; Cavicchi, K. A.; Chun, J.; Fasolka, M. J. *Lab on a Chip* **2009**, *9*, 339.
  - (13) Rosenfeld, C.; Serra, C. A.; Brochon, C.; Hadziioannou, G. *Lab on a Chip* **2008**, *8*, 1682.
  - (14) Hornung, C. H.; Guerrero-Sanchez, C.; Brasholz, M.; Saubern, S.; Chiefari, J.; Moad, G.; Rizzardo, E.; Thang, S. H. *Organic Process Research & Development* **2011**, *15*, 593.
  - (15) Müller, M.; Cunningham, M. F.; Hutchinson, R. A. *Macromolecular Reaction Engineering* **2008**, *2*, 31.
  - (16) Noda, T.; Grice, A. J.; Levere, M. E.; Haddleton, D. M. *European Polymer Journal* **2007**, *43*, 2321.
  - (17) Bally, F.; Serra, C. A.; Brochon, C.; Hadziioannou, G. *Macromolecular Rapid Communications* **2011**, *32*, 1820.
  - (18) Wilms, D.; Nieberle, J.; Klos, J.; Löwe, H.; Frey, H. *Chemical Engineering & Technology* **2007**, *30*, 1519.
  - (19) Hessel, V.; Hardt, S.; Löwe, H.; Schönfeld, F. *AIChE Journal* **2003**, *49*, 566.
  - (20) Nagasawa, H.; Aoki, N.; Mae, K. *Chemical Engineering & Technology* **2005**, *28*, 324.
  - (21) Liu, G.; Wu, D.; Ma, C.; Zhang, G.; Wang, H.; Yang, S. *ChemPhysChem* **2007**, *8*, 2254.
  - (22) Yanfeng, C.; Min, Y. *Radiation Physics and Chemistry* **2001**, *61*, 65.
  - (23) Zhang, C.; Maric, M. *Polymers* **2011**, *3*, 1398.
  - (24) Schmaljohann, D. *Advanced Drug Delivery Reviews* **2006**, *58*, 1655.
  - (25) Vamvakaki, M.; Billingham, N. C.; Armes, S. P. *Polymer* **1998**, *39*, 2331.
  - (26) Georgiou, T. K.; Vamvakaki, M.; Phylactou, L. A.; Patrickios, C. S. *Biomacromolecules* **2005**, *6*, 2990.
  - (27) Lin, S.; Du, F.; Wang, Y.; Ji, S.; Liang, D.; Yu, L.; Li, Z. *Biomacromolecules* **2007**, *9*, 109.
-

## *4.2. Atom Transfer Radical Polymerization in continuous-microflow: effect of process parameters*

### *Abstract*

*We report on the synthesis of 2-(dimethylamino)ethyl methacrylate by Atom Transfer Radical Polymerization in tubular microreactors. Different process parameters, temperature, pressure and shear rate, were considered to accelerate the reaction. Increase in temperature induced a faster reaction but controlled nature of ATRP decreased past a threshold value that can be increased up to 95°C by reducing the residence time. Positive effect of pressure was observed since significant increases in monomer conversion (+12.5%) and molecular weight (+5,000 g/mol) were obtained. Moreover polydispersity index was found to decrease from 1.52 at normal pressure to 1.44 at 100 bars. Benefit of pressure was more visible in smaller reaction space (smaller tube diameter). Finally shear rate has quite an influence on the early stage of the polymerization and is expressed by an increase in the reaction rate. However effect was dimed for long residence times.*

### **KEYWORDS**

ATRP, microreactors, high pressure polymerization

### 4.2.1 Introduction

Demand for narrow molecular weight distributions along with controlled architectures (e.g. block, branched) in free radical polymerizations triggered the development of different controlled radical polymerization techniques like nitroxide mediated polymerization (NMP), atom transfer radical polymerization (ATRP) and reversible addition fragmentation technique (RAFT). These techniques of polymerization rely on the dynamic equilibrium between propagating radicals and dormant species thereby increasing the life of a growing chain from seconds to hours and making the reaction slower because of intermittent activation and deactivation processes.<sup>1</sup> However, fast controlled radical polymerizations are still highly desirable not only for throughput concerns but also for energy consumption and reduction of equipment size.

Recent findings show potentials of microreactors to carry out polymerization in a controlled way.<sup>2,3</sup> High interface and heat exchange surface per volume unit are the key factors for fast mixing and efficient heat transfers respectively. These features of microreactors, in contrast to lab-scale or large scale reactors provide a better control from the beginning of reaction to achieve controlled macromolecular characteristics.<sup>4-9</sup> Efficient heat management and short diffusion pathways in microreactors unleash the possibility to carry out the reaction at new operating windows. Thus it was found that anionic polymerization can be operated at room or even moderate temperatures compared to conventional cryogenic temperatures in macroscale.<sup>10-13</sup> Controlled radical polymerization techniques in microreactors are not new and were reported by many authors.<sup>8,14-20</sup> However, accelerating these polymerization processes in microreactor without sacrificing their controlled characteristics was surprisingly less studied. Recent findings suggest controlled radical polymerizations (RAFT and ATRP) can be accelerated significantly by microreactors.<sup>21</sup> These findings rely purely on the primary characteristic of microreactor (i.e. high surface to volume ratio). On the other hand, when a batch polymerization is transferred to a continuous polymerization in microreactor, some additional process parameters like pressure, shear rate comes into picture, which can significantly influence polymerization and polymer characteristics. In the short history of polymerization in microreactors, effects of these parameters on polymerization were never studied thoroughly. Though, effect of pressure was studied extensively in macro/batch reactors<sup>21</sup> and significant acceleration of controlled radical polymerizations was observed. However, these studies were performed under a very high pressure of 2000-6000 bars.<sup>23-26</sup> Need of specialised equipments and limited reaction volume limits the applicability of such

high pressure reaction of controlled radical polymerization other than research and academic purpose. Following the intuition and to bridge this gap, effect of temperature, pressure (range of 100 bars) and shear rate on ATRP of DMAEMA in microreactor are reported in this article. To the best of our knowledge, such studies concerning ATRP in microreactor have never been reported before.

## 4.2.2 Materials and methods

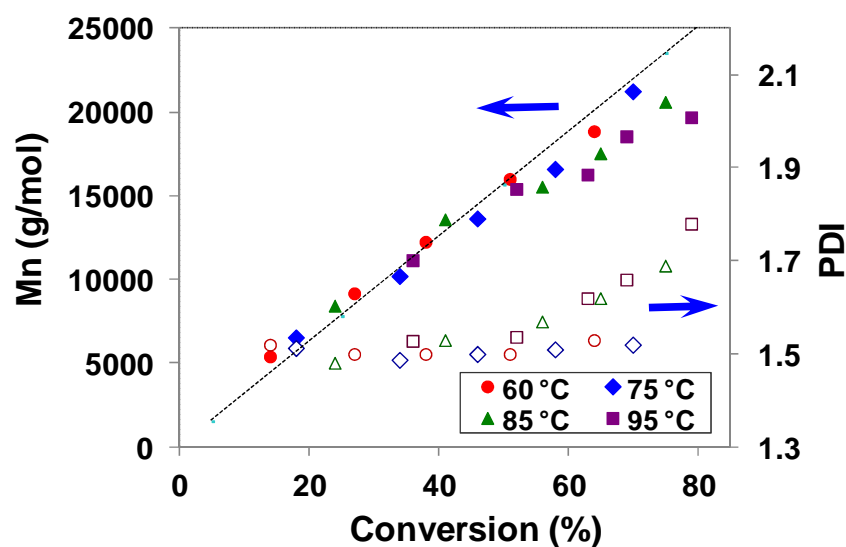
- I. List of materials is given in Chapter 3 section 3.1.1.
- II. Description of setup is provided in Chapter 3 section 3.3.
  - I. Continuous-flow polymerization detailed procedure is given in Chapter 3 section 3.3.5 while reservoir compositions and flow rates are presented Table 3.7 and Tables 3.8 & 3.9 respectively.
  - III. Procedures for high pressure reaction and reaction with high shear rate are given in Chapter 3 section 3.3.6 and 3.3.7 respectively.
  - IV. Characterization methods include  $^1\text{H}$  NMR (Chapter 3 section 3.4.1.2) and GPC (Chapter 3 section 3.4.2).

## 4.2.3 Results and discussion

### 4.2.3.1 Effect of temperature on polymerization in microreactor

It is well known that temperature has an accelerating effect on polymerization. On the other hand termination rate also increases with temperature resulting polymer with broader molecular weight distribution. If the diffusion of monomer towards the growing chain can be facilitated to decrease termination, then significant acceleration can be achieved with a controlled way. Known for diffusion driven mixing capability, microreactors have potentials for such requirements. Microreactors allow broader reaction temperature selection as they can operate at higher temperatures owing to the large surface to volume ratio which guarantee nearly isothermal conditions. Considering these features, kinetics of ATRP of DMAEMA was studied in a microreactor at different temperatures. Polymerization rate increased significantly with temperature as shown in Figure 4.6 and Figure 4.SI 6. Molecular weight of polymer obtained are very close to the theoretical values for 60 °C and 75 °C indicating controlled characteristics of polymerization. However, difference between theoretical and experimental  $M_n$  starts to appear at polymerization temperature 85 °C and 95 °C after 30 minute residence time. More insight about the polymerization was seen when PDIs (Figure 4.6) obtained for

different polymerization temperatures were compared. Significant increase in PDI was observed after 30 minutes of residence time, at high polymerization temperatures (i.e. 85 °C and 95 °C) indicating uncontrolled reaction. Dominating transfer reactions and auto initiation may be responsible for such uncontrolled behaviour of ATRP. Considering the controlled characteristic and faster polymerization, 75 °C was chosen as the polymerization temperature for further investigations. However, for molecular weights around 15000 g/mol, higher temperature seems to be a good alternative as it reduces the polymerization time significantly (Figure 4.6 and Figure 4.SI 6), without sacrificing the controlled nature of ATRP.

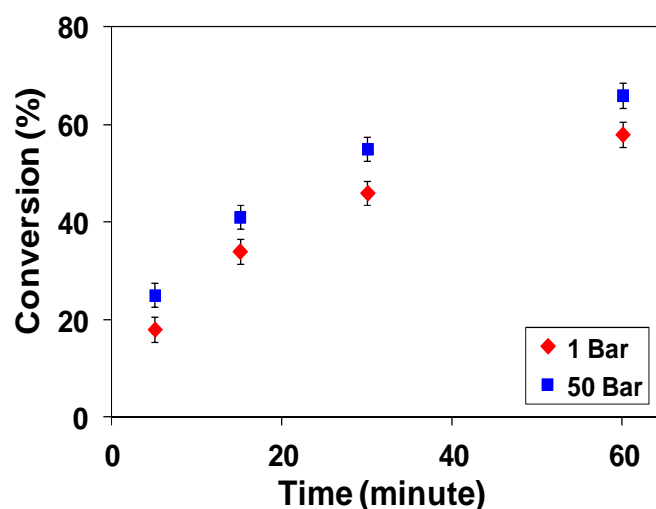


**Figure 4.6.** Evolution of molecular weight (Mn, filled symbols) and PDI (empty symbols) with conversion at different temperatures.

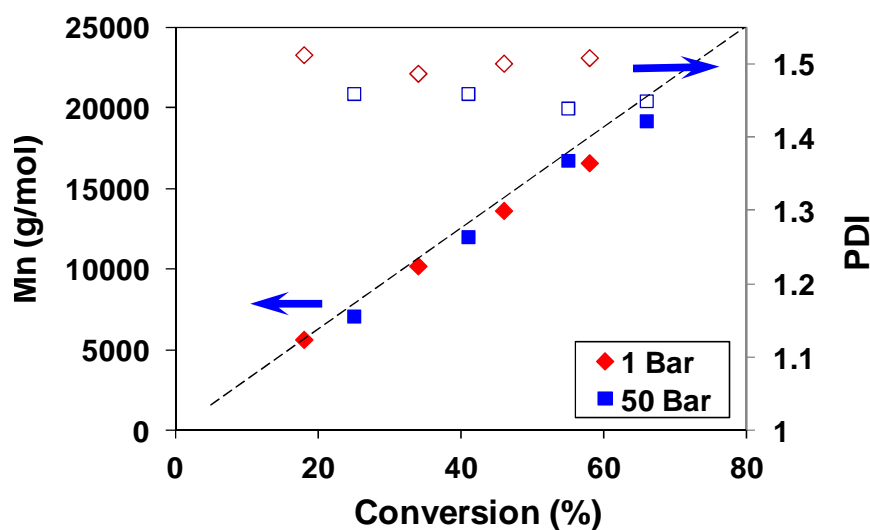
#### 4.2.3.2 Effect of pressure

Increase in conversion and molecular weight was observed with increase in pressure from 1 bar to 50 bars at different residence times as shown in Figure 4.7 and 4.8. Mn/Conversion plot shown in Figure 4.8 indicates a controlled polymerization as the Mn obtained by GPC lies close to theoretical values. A significant increase in conversion can be attributed partially to increased propagation rate constant with pressure.<sup>27</sup> Increased density of polymerizing solution with application of pressure can be another factor for increased conversion in microreactor. In literature enough evidences are available indicating increased density of liquid and polymer solution with pressure.<sup>28-30</sup> As the polymerization was carried out in a continuous-flow microreactor, increased density under pressure leads to reduced volumetric flow rate which results in higher residence times than the set ones. Therefore increased polymerization rate cannot be only due to one of these two factors solely but rather is due to the synergistic effect of both. Furthermore unexpected PDI reduction was observed as shown

in Figure 4.8 and table 1 (entry 2 and 9 respectively) and may be explained by a decrease in the termination rate under higher pressures.<sup>31</sup>



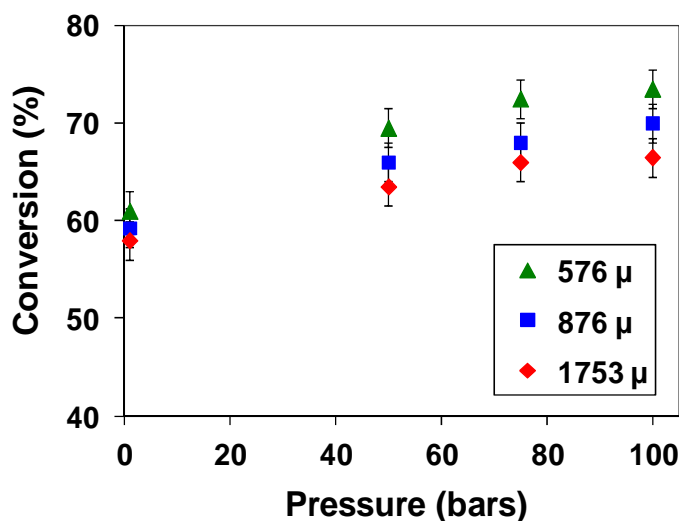
**Figure 4.7.** Conversion of DMAEMA under different polymerization pressures in a microreactor of 810  $\mu\text{m}$  internal diameter and 3 meters length.



**Figure 4.8.** Effect of pressure on molecular weight ( $M_n$ , filled symbols) and PDI.

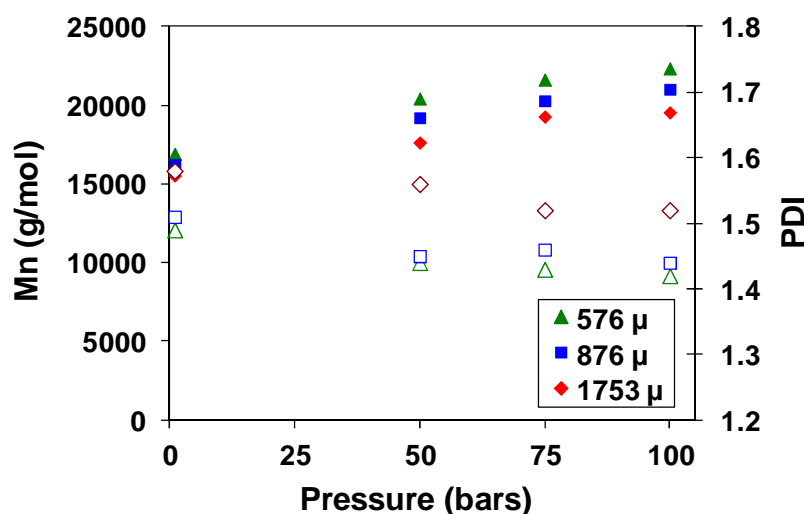
In order to have a clear idea about impact of pressure on polymerization in micro dimension, polymerization was carried out in microreactors of 576, 876 and 1753  $\mu\text{m}$  internal diameter. As shown in Figure 4.9, conversions obtained at 1 bar were nearly same for all three diameters. Interestingly, an increase in conversion with pressure was observed for all 3 reactors but followed distinct paths. Moreover, a plateau at high pressure indicates a non linear relationship between pressure and conversion (in the studied range). This means that a significant increase in pressure is required to increase the conversion further. Evolution in

molecular weight ( $M_n$ ) with pressure (Figure 4.10) followed the same trend as conversion. Higher propagation rates at higher pressures in conjunction with favourable diffusion of monomer in smaller diameter microreactor resulted in a faster kinetics.



**Figure 4.9.** Plot showing the effect of pressure on monomer conversion for different microreactor diameters at a polymerization time of 1 hour.

In contrast, under similar conditions, longer diffusion times in larger diameter microreactors reduce conversion while PDI decreases with pressure in all micro reactors. However, higher PDI was obtained in larger diameter reactors probably due to longer diffusion paths as diameter increases. These observations suggest that polymerization can be significantly accelerated, + 12.5% increase in conversion within 1 hour with moderate increase in pressure from 1 bar to 100 bars.



**Figure 4.10.** Plot showing effect of pressure on molecular weight ( $M_n$ , filled symbols) and PDI (empty symbols) for different microreactor diameters and for 1 hour residence time.

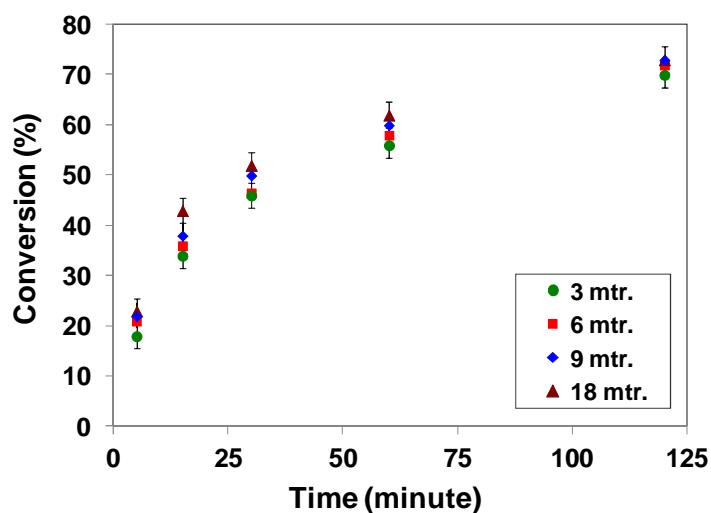
### 4.2.3.3 Effect of shear rate on polymerization

In a tubular geometry, the inner wall surface to volume ratio is inversely proportional to the inner tube radius. Thus tubular microreactors are characterized by a much higher wall surface per volume unit than their macroscale counterparts (e.g. there is a factor of 8 between 1/16" and 1/2" tubes). Therefore a good portion of the fluid flowing in a tubular microreactor experiences the shear at the wall which may, unlike in bigger tubes, affect significantly the overall polymer characteristics (molecular weight, PDI). Indeed wall shear inside a microreactor can not only alter mixing but may also change the conformation of macromolecules.<sup>32</sup> Elongated conformation of a growing polymer chain can make the reacting site more accessible for reaction than a coiled conformation. This condition can enhance the reaction rate as well as the control over the polymerization. Shear rate was changed by increasing the length of reactor while keeping the residence time constant and was varied from 3.81 to 547.7 s<sup>-1</sup> for 3 m length / 2 hours residence time and 18 m length / 5 minutes residence time respectively (Table 4.1 and supporting information for detailed calculations). Increase in conversion was observed (Figure 4.11) with an increase in reactor length (i.e. an increase in shear rate). However, when the residence time increases, the relative gain in conversion for the longest reactor length diminishes. Rheological measurements were conducted to determine the intrinsic viscosity of the reactive solution for the following residence times 5 min, 15 min, 30 min and 2 hrs (see supporting information for detail). From the obtained values, the product of concentration times intrinsic viscosity was found superior to 1 for residence times above 5 min. It can be concluded that the polymerization operates in the dilute regime up to 5 minutes and then in the semi-diluted regime.<sup>33, 34</sup> This last regime is characterized by an overlapping of the hydrodynamic spheres of individual macromolecules while in the dilute regime there are no interactions in-between polymer chains. Therefore the following explanation can be drawn and is qualitatively summarized in Figure 4.12. This figure shows the conformation of polymer chains when the residence time increases (i.e. for different monomer conversions) and when the length of the reactor is increased (i.e. for higher shear rates).

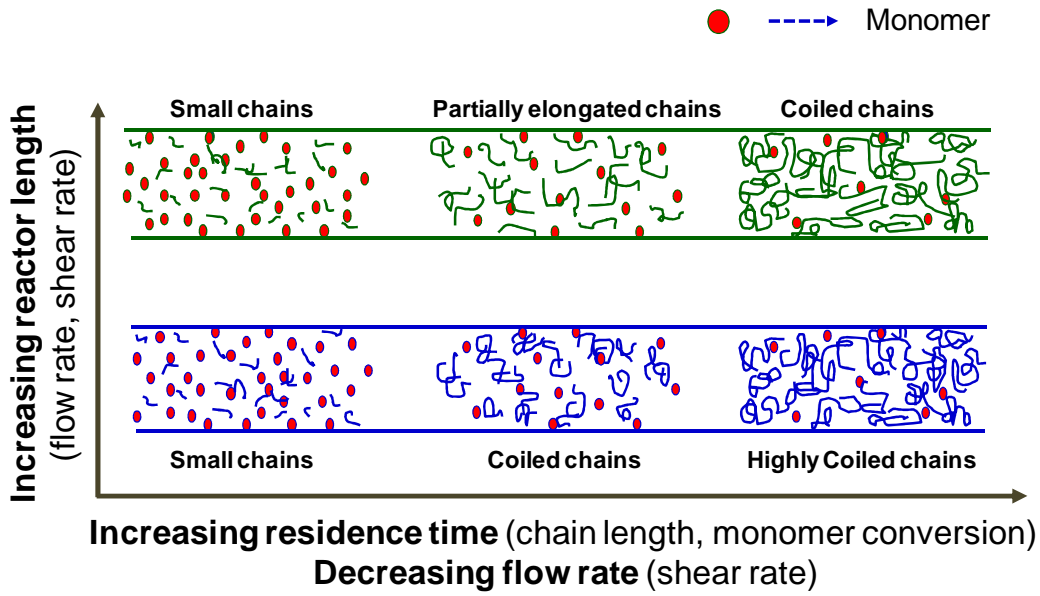
At the beginning, the polymerization solution contained a large amount of monomer (low conversion) and thus polymer chains were quite short, the mean number-average chain length (DP<sub>n</sub>) for all 4 reactors was equal to 43 for 5 min. Therefore shear rate had little effect on the polymerization kinetics and a marginal increase in conversion (+4 points) was observed at the lowest residence time (5 min). For 15 min residence time, molecular weight was increased



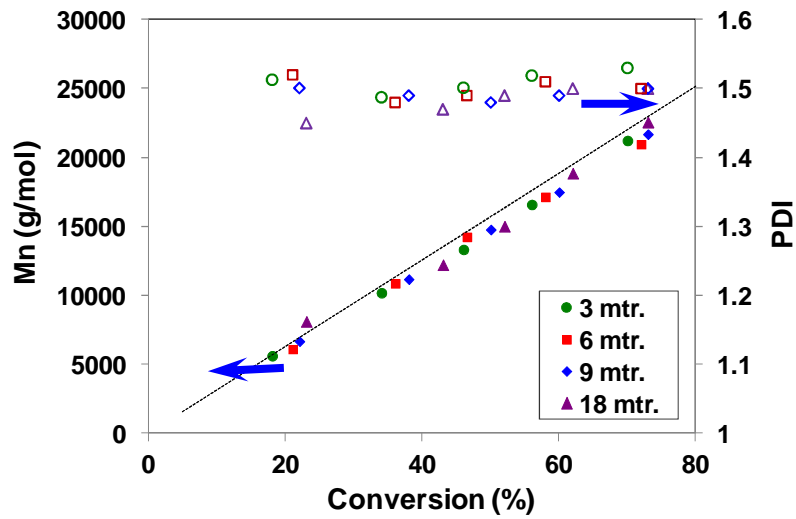
(average  $DP_n = 71$ ) and chains adopted a coiled conformation which under shear tend to be elongated as reported by numerical studies.<sup>35-37</sup> Following our aforementioned discussion, it resulted in an increase in conversion, +10 % for the longest reactor in comparison with the shortest one. This result is in agreement with the findings of Agarwal *et al.* during polymerization of (poly (*p*-phenylene terephthalamide)).<sup>38</sup> When the residence time was further increased, the gain in conversion for the longest reactor decreased and ultimately no significant effect of shear rate was observed for the highest residence time (2 hours) which complies with similar observations made by Leveson *et al.*<sup>39</sup> It is worthy to note that since the flow rate was reduced to accommodate higher residence times, the shear rate also reduced accordingly, thus explaining the observed behavior. As shown in Figure 4.13, molecular weight ( $M_n$ ) evolution followed the same behavior as monomer conversion for different shear rates. However it is worthy to note that no significant difference in PDI was observed between samples polymerized at different shear rates.



**Figure 4.9.** Conversion of DMAEMA with respect to the residence time for different reactor lengths.



**Figure 4.10.** Schematic drawings of the polymer chains conformation as a function of residence time and reactor length.



**Figure 4.11.** Evolution of molecular weight ( $M_n$ , filled symbols) and PDI (Empty symbols) with respect to residence time for different reactor lengths.

**Table 4.1.** Summary of monomer conversion and macromolecular characteristics obtained at different polymerization conditions and for different microreactor dimensions.

Entry	Reactor length (meter)	Reactor diameter ( $\mu\text{m}$ )	Temp. ( $^{\circ}\text{C}$ )	Pressure (bar)	Shear rate* ( $\text{s}^{-1}$ )	Residence time (min.)	Conv. (%)	Mn (g/mol)	PDI
1	3	876	60	0.5-1	-	120	64	18860	1.53
2	3	876	75	0.5-1	15.2	30	46	13852	1.51
3	3	876	75	0.5-1	3.8	120	70	21242	1.52
4	3	876	85	0.5-1	-	30	56	15549	1.56
5	3	876	85	0.5-1	-	120	76	20610	1.69
6	3	876	95	0.5-1	-	15	52	15410	1.53
7	3	876	95	0.5-1	-	120	80	19685	1.77
8	3	876	75	50	-	60	66	19743	1.46
9	3	876	75	100	-	60	70	21300	1.44
10	3	576	75	0.5-1	-	60	61	16912	1.49
11	3	576	75	100	-	60	73.5	22348	1.42
12	3	1753	75	0.5-1	-	60	58	15350	1.58
13	3	1753	75	100	69.80	60	67	19557	1.51
14	6	876	75	0.5-1	30.44	30	46.5	14260	1.49
15	6	876	75	0.5-1	7.62	120	72	20975	1.50
16	9	876	75	0.5-1	45.66	30	50	14789	1.48
17	9	876	75	0.5-1	11.43	120	72	21700	1.51
18	18	876	75	0.5-1	91.32	30	52	15030	1.49
19	18	876	75	0.5-1	22.86	120	73	22578	1.50

\*: at wall

#### 4.2.4 Summary

Continuous–microflow ATRP of 2–(dimethylamino)ethyl methacrylate was carried out in tubular microreactor and variations of temperature, pressure and reactor length were investigated to accelerate the reaction. Higher temperatures increase polymerization rate but at the same time lead to a broadening of the molecular weight distribution because termination reactions are also favoured. A trade off can be found considering the desired molecular weight. For low molecular weights (up to 17000 g/mol), temperatures of 95 $^{\circ}\text{C}$  was beneficial to reduce the polymerization time by a quarter in comparison with 75 $^{\circ}\text{C}$  while still keeping a low PDI value (1.53 compared to 1.51). However, increase in PDI (from 1.51 to 1.76) was observed when molecular weights are above 17000 g/mol.

High pressure (100 bars) in microreactor was found to accelerate the polymerization significantly (+12.5% in monomer conversion compared to 1 bar) with an additional benefit of an improved control of the molecular weight distribution (PDI reduced from 1.52 to 1.44). However pressure affects the polymerization kinetics quite differently upon reactor diameter; smaller diameters supporting a higher polymerisation rate.

Finally effect of shear rate was visible at low conversion and molecular weights due to an effective elongation of the polymer chains under the shear. However, past the critical entanglement molecular weight, which depends upon the polymer concentration (i.e. residence time), shear rate has less effect on the monomer conversion. Thus, it was demonstrated that under given constraints, an ATRP microprocess can be significantly intensified by increasing the temperature and shear rate but above all by increasing the pressure.

## 4.2.5 Supporting Information

### 4.2.5.1 Rheological behaviour of polymerizing solution

#### 4.2.5.1.1 Viscosity evolution as a function of shear rate (5 min & 2 hours)

Steady state viscosity of polymerizing solution at different polymerization time was determined. It was observed that, solution remains Newtonian irrespective of polymerization time as shown in Figure 4.SI3.

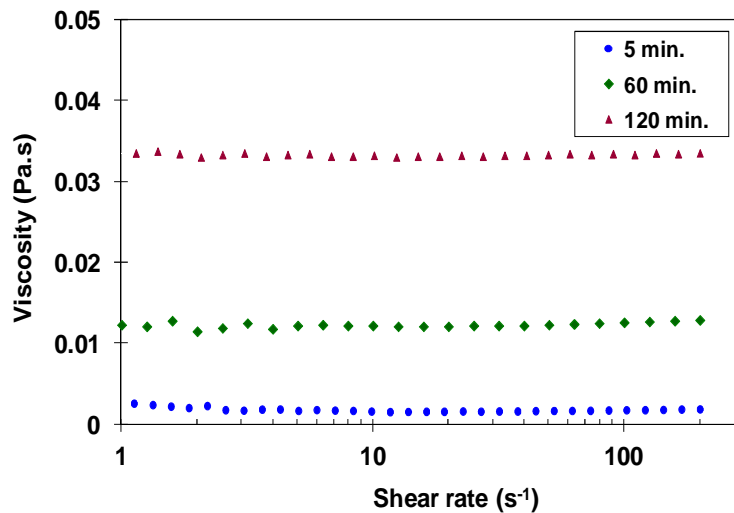


Figure 4.SI 3. Steady state shear viscosity of DMAEMA polymerizing solution at different residence time.

#### 4.2.5.1.2 Intrinsic viscosity

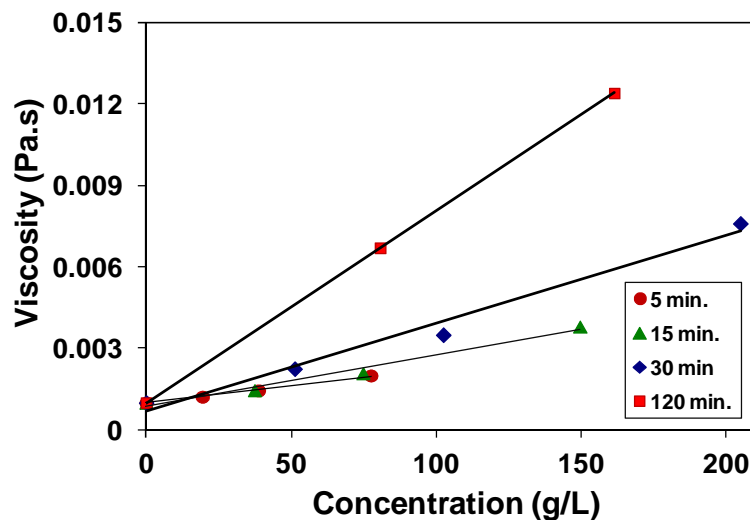
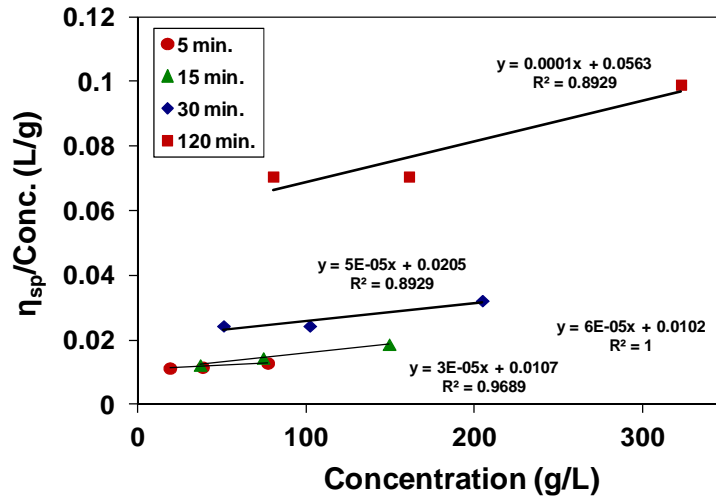


Figure 4.SI 4. Plot showing viscosity of polymerizing solutions at different dilutions.



**Figure 4.SI 5.** Plot used to determine intrinsic viscosity of polymerizing DMAEMA at different polymerization time.

**Table 4.SI 3.** Detailed calculation to determine concentration limits of polymerizing DMAEMA in isopropanol at different polymerization time.

Residence time (min.)	Dilution factor	C (g/L)	$\eta$ (Pa.s)	$\eta_{sp}$ (-)	$\eta_{sp}/C$ (L/g)	$[\eta]$ (L/g)	$[C \times \eta]$
5	100%	77.51	0.00200	1.00	0.0129		
	50%	38.755	0.00145	0.45	0.0116		
	25%	19.377	0.00122	0.22	0.0114		
	0%					<u>0.01070</u>	0.8
15	100%	149.62	0.00380	2.80	0.0187		
	50%	74.81	0.00208	1.08	0.0144		
	25%	37.4	0.00146	0.46	0.0123		
	0%					<u>0.01020</u>	1.5
30	100%	205	0.00760	6.60	0.0322		
	50%	102.5	0.00350	2.50	0.0244		
	25%	51.25	0.00225	1.25	0.0244		
	0%					<u>0.0205</u>	4.2
120	100%	323	0.03300	32.00	0.0991		
	50%	161.5	0.01240	11.40	0.0706		
	25%	80.75	0.00670	5.70	0.0706		
	0					<u>0.0563</u>	18.2

## 4.2.5.2 Effect temperature, reactor length and diameter on polymerization

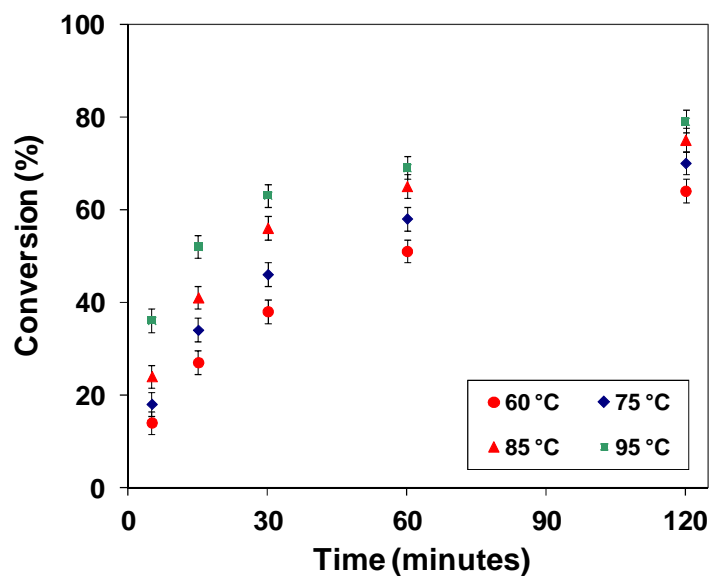


Figure 4.SI 6. Conversion of DMAEMA in 3 m length microreactor at different polymerization temperatures and 1-1.5 bars.

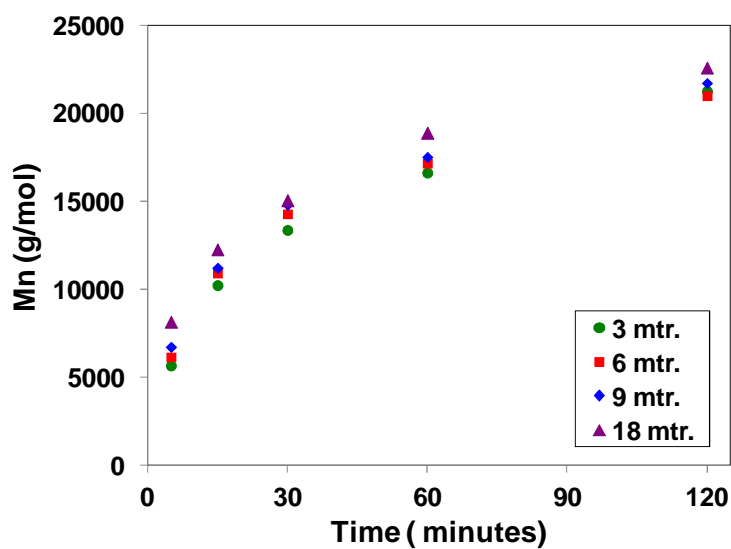


Figure 4.SI 7. Evolution of molecular weight (Mn) with residence time in different length of microreactors.

**Table 4.SI 4.** Summary of monomer conversion and macromolecular characteristics obtained at different polymerization conditions and for different microreactor dimensions.

Entry	Reactor length (meter)	Reactor diameter ( $\mu\text{m}$ )	Temp. ( $^{\circ}\text{C}$ )	Pressure (bars)	Shear rate* ( $\text{s}^{-1}$ )	Residence Time (min.)	Conv. (%)	Mn (g/mol)	PDI
1	3	876	60	1-1.5	7.62	120	64	18860	1.53
2	3	876	75	1-1.5	91.2	5	18	5646	1.51
3	3	876	75	1-1.5	30.4	15	34	10210	1.48
4	3	876	75	1-1.5	15.2	30	46	13852	1.51
5	3	876	75	1-1.5	3.8	120	70	21242	1.52
6	3	876	85	1-1.5	30.44	30	56	15549	1.56
7	3	876	85	1-1.5	7.62	120	76	20610	1.69
8	3	876	95	1-1.5	60.88	15	52	15410	1.53
9	3	876	95	1-1.5	7.62	120	80	19685	1.77
10	3	876	75	50	15.22	60	66	19743	1.46
11	3	876	75	100	15.22	60	70	21300	1.44
12	3	576	75	0.5-1	15.22	60	61	16912	1.49
13	3	576	75	100	15.22	60	73.5	22348	1.42
14	3	1753	75	0.5-1	15.22	60	58	15350	1.58
15	3	1753	75	100	15.22	60	67	19557	1.51
16	6	876	75	1-1.5	182.64	5	21	6130	1.52
17	6	876	75	1-1.5	60.88	15	36	10897	1.48
18	6	876	75	1-1.5	30.44	30	46.5	14260	1.49
19	6	876	75	1-1.5	7.62	120	72	20975	1.50
20	9	876	75	1-1.5	273.93	5	22	6700	1.48
21	9	876	75	1-1.5	91.32	15	38	10897	1.49
22	9	876	75	1-1.5	45.66	30	50	14789	1.48
23	9	876	75	1-1.5	11.43	120	72	21700	1.51
24	18	876	75	1-1.5	547.9	5	23	8130	1.45
25	18	876	75	1-1.5	182.64	15	43	12240	1.47
26	18	876	75	1-1.5	91.32	30	52	15030	1.49
27	18	876	75	1-1.5	22.86	120	73	22578	1.50



## References

- (1) Braunecker, W. A.; Matyjaszewski, K. *Progress in Polymer Science* **2007**, *32*, 93.
- (2) Wu, T.; Mei, Y.; Cabral, J. T.; Xu, C.; Beers, K. L. *Journal of the American Chemical Society* **2004**, *126*, 9880.
- (3) Nagaki, A.; Kawamura, K.; Suga, S.; Ando, T.; Sawamoto, M.; Yoshida, J.-i. *Journal of the American Chemical Society* **2004**, *126*, 14702.
- (4) Becker, H.; Gärtner, C. *Reviews in Molecular Biotechnology* **2001**, *82*, 89.
- (5) Schwalbe, T.; Autze, V.; Hohmann, M.; Stirner, W. *Organic Process Research & Development* **2004**, *8*, 440.
- (6) Iwasaki, T.; Yoshida, J.-i. *Macromolecules* **2005**, *38*, 1159.
- (7) Miyazaki, M.; Honda, T.; Nakamura, H.; Maeda, H. *Chemical Engineering & Technology* **2007**, *30*, 300.
- (8) Rosenfeld, C.; Serra, C.; Brochon, C.; Hessel, V.; Hadziioannou, G. *Chemical Engineering Journal* **2008**, *135*, Supplement 1, S242.
- (9) Wilms, D.; Nieberle, J.; Klos, J.; Löwe, H.; Frey, H. *Chemical Engineering and Technology* **2007**, *30*, 1519.
- (10) Nagaki, A.; Tomida, Y.; Yoshida, J.-i. *Macromolecules* **2008**, *41*, 6322.
- (11) Nagaki, A.; Tomida, Y.; Miyazaki, A.; Yoshida, J.-i. *Macromolecules* **2009**, *42*, 4384.
- (12) Nagaki, A.; Miyazaki, A.; Tomida, Y.; Yoshida, J.-i. *Chemical Engineering Journal* **2011**, *167*, 548.
- (13) Iida, K.; Chastek, T. Q.; Beers, K. L.; Cavicchi, K. A.; Chun, J.; Fasolka, M. J. *Lab on a Chip* **2009**, *9*, 339.
- (14) Fukuyama, T.; Kajihara, Y.; Ryu, I.; Studer, A. *Synthesis (Germany)* **2012**, *44*, 2555.
- (15) Rosenfeld, C.; Serra, C. A.; Brochon, C.; Hadziioannou, G. *Lab on a Chip* **2008**, *8*, 1682.

- (16) Bally, F.; Serra, C. A.; Hessel, V.; Hadziioannou, G. *Macromolecular Reaction Engineering* **2010**, *4*, 543.
- (17) Bally, F.; Serra, C. A.; Brochon, C.; Hadziioannou, G. *Macromolecular Rapid Communications* **2011**, *32*, 1820.
- (18) Hornung, C. H.; Guerrero-Sanchez, C.; Brasholz, M.; Saubern, S.; Chiefari, J.; Moad, G.; Rizzardo, E.; Thang, S. H. *Organic Process Research & Development* **2011**, *15*, 593.
- (19) Voicu, D.; Scholl, C.; Li, W.; Jagadeesan, D.; Nasimova, I.; Greener, J.; Kumacheva, E. *Macromolecules* **2012**, *45*, 4469.
- (20) Noda, T.; Grice, A. J.; Levere, M. E.; Haddleton, D. M. *European Polymer Journal* **2007**, *43*, 2321.
- (21) Diehl, C.; Laurino, P.; Azzouz, N.; Seeberger, P. H. *Macromolecules* **2010**, *43*, 10311.
- (22) Wang, Y.; Schroeder, H.; Morick, J.; Buback, M.; Matyjaszewski, K. *Macromolecular Rapid Communications* **2013**, *34*, 604.
- (23) Xia, J.; Johnson, T.; Gaynor, S. G.; Matyjaszewski, K.; DeSimone, J. *Macromolecules* **1999**, *32*, 4802.
- (24) Rzayev, J.; Penelle, J. *Angewandte Chemie International Edition* **2004**, *43*, 1691.
- (25) Morick, J.; Buback, M.; Matyjaszewski, K. *Macromolecular Chemistry and Physics* **2011**, *212*, 2423.
- (26) Mueller, L.; Jakubowski, W.; Matyjaszewski, K.; Pietrasik, J.; Kwiatkowski, P.; Chaladaj, W.; Jurczak, J. *European Polymer Journal* **2011**, *47*, 730.
- (27) Ogo, Y.; Yokawa, M. *Die Makromolekulare Chemie* **1977**, *178*, 453.
- (28) Vieira dos Santos, F. J.; Castro, C. A. N. *Int J Thermophys* **1997**, *18*, 367.
- (29) Et-Tahir, A.; Boned, C.; Lagourette, B.; Xans, P. *Int J Thermophys* **1995**, *16*, 1309.

- (30) Yeo, S. D.; Kiran, E. *The Journal of Supercritical Fluids* **1999**, *15*, 261.
- (31) Morick, J.; Buback, M.; Matyjaszewski, K. *Macromolecular Chemistry and Physics* **2011**, *212*, 2423.
- (32) Yamashita, K.; Yamaguchi, Y.; Miyazaki, M.; Nakamura, H.; Shimizu, H.; Maeda, H. *Analytical Biochemistry* **2004**, *332*, 274.
- (33) Brown, W.; Nicolai, T. *Colloid and Polymer Science* **1990**, *268*, 977.
- (34) Omari, A.; Moan, M.; Chauveteau, G. *Rheol Acta* **1989**, *28*, 520.
- (35) Ripoll, M.; Winkler, R. G.; Gompper, G. *Physical Review Letters* **2006**, *96*, 188302.
- (36) Huang, C. C.; Winkler, R. G.; Sutmann, G.; Gompper, G. *Macromolecules* **2010**, *43*, 10107.
- (37) Chen, W.; Chen, J.; Liu, L.; Xu, X.; An, L. *Macromolecules* **2013**, *46*, 7542.
- (38) Agarwal U. S.; Khakhar, D. V. *Nature* **1992**, *360*, 53.
- (39) Leveson, P.; Dunk, W. A. E.; Jachuck, R. J. *Journal of Applied Polymer Science* **2004**, *94*, 1365.

---

# CHAPTER 5

## COIL FLOW INVERSION AS A ROUTE TO CONTROL POLYMERIZATION IN MICROREACTORS

<i>Preface</i>	127
<b>5.1 Effect of coil flow inversion on macromolecular characteristics</b>	
5.1.1 Introduction	129
5.1.2 Materials and methods	130
5.1.3 Results and discussions	130
5.1.3.1 <i>Linear polymer synthesis</i>	130
5.1.3.2 <i>Branched polymer synthesis</i>	131
5.1.4 Summary	137
5.1.5 Supporting Information	138
<b>References</b>	141
<b>5.2. Flow inversion: an effective means to scale-up controlled radical polymerization in tubular microreactors</b>	
5.2.1 Introduction	144
5.2.2 Materials and methods	145
5.2.3 Results and discussion	146
5.2.3.1 <i>Effect of reactor geometry</i>	146
5.2.3.2 <i>Effect of reactor diameter</i>	147
5.2.3.3 <i>Effect of reactor length</i>	149
5.2.3.4 <i>Process parameters</i>	151
5.2.4 Summary	152
5.2.5 Supporting Information	153
<b>References</b>	158

## ***Preface***

In the previous chapter, impact of micromixers and operating parameters on polymerization rate was evaluated. However in a normal coiled tube reactor there is no provision of mixing other than by diffusion. Thus the reaction tends to be diffusion-controlled when the viscosity increases which is mostly the case for long residence times even for moderate concentrated solutions. As a consequence the PDI is generally increasing and the development of more compact structure like branched architectures by convergent methods should be highly impeded.

In the first section of this chapter, additional mixing arrangements inside the reactor were introduced in the form of flow inversion as an attempt to alleviate this detrimental effect of viscosity increase. Thus branched polymers were synthesized by SCVCP adapted to ATRP in a coil flow inverter (CFI) microreactor and their characteristics compared to those obtained in the normal coiled tube (CT) microreactor.

Due to their small dimensions, the throughput of microreactors is quite low. Therefore in the second section of this chapter, their scale-up was considered by increasing their diameter up to 4 mm. Special attention was paid to the trade-off between increase in throughput and control over macromolecular characteristics.

*This chapter is partially adapted from the two following articles:*

*(1) D. Parida, C.A. Serra, F. Bally, D.K. Garg, Y. Hoarau, M. Bouquey and R. Muller, Coil flow inversion as a route to control polymerization in microreactors, Macromolecules, submitted.*

*(2) D. Parida, C.A. Serra, D.K. Garg, Y. Hoarau, M. Bouquey and R. Muller, Flow inversion: an effective means to scale-up controlled radical polymerization in tubular microreactors, Macromol. React. Eng., submitted.*

## *5.1. Effect of coil flow inversion on macromolecular characteristics*

### *Abstract*

*Linear and branched polymers of 2-(dimethylamino)ethyl methacrylate (PDMAEMA) were synthesised in flow, by atom transfer radical polymerization (ATRP) and self-condensing vinyl copolymerization adapted to ATRP respectively, in capillary type stainless steel coiled tube (CT) microreactors. Coil flow inversion (CFI) was introduced to achieve better mixing and narrower residence time distributions during polymerization. This strategy was adopted to improve control over macromolecular characteristics and polymer architecture. Polydispersity index (PDI), as an overall indicator of control over polymerization, was significantly lower for CFI in case of linear PDMAEMA. For branched polymers containing up to 10 mol. % of inimer, a reduced PDI was also obtained for this microreactor. As for the branching efficiency, it was found to follow the following trend CFI > CT > batch reactor.*

### **KEYWORDS**

Intensification, polymerization, process, microreactor, ATRP

### 5.1.1 Introduction

Application of microreaction technology in polymer synthesis dates back roughly to one decade.<sup>1</sup> However, it has showed enormous potentials to produce polymers with well defined characteristics. Microdevices derive these potentials from their high surface to volume ratio, small diffusion pathways and large interfacial areas which give them the ability to overcome heat transfer and mixing limitations often encountered in their macroscale counterparts. Thus microreactors and micromixers were found to be elements of choice when comes the need to increase the control of macromolecular characteristics.<sup>2</sup> Polymerization reactions carried out in microreactors showed improved control over architecture and chemical composition.<sup>3-8</sup> Their high surface to volume ratio allowed considering new operating windows like higher temperatures, which permitted for instance to carry out extremely exothermic reactions (ionic polymerizations) at much more convenient conditions (non-cryogenic).<sup>9-12</sup> Slower polymerization reactions like Nitroxide Mediated polymerization (NMP), Atom Transfer Radical Polymerization (ATRP) or reversible addition-fragmentation chain transfer (RAFT) were also investigated in microreactors and under certain conditions found to be significantly accelerated.<sup>7,13-15</sup>

In spite of all these benefits and since mixing in continuous-flow microchannel- or capillary-based microreactors is mainly governed by mass diffusion, increased viscosity and diminished monomer concentration at higher conversion can trigger for (controlled) radical polymerizations unwanted termination reactions resulting in increased PDIs as discussed in last chapter. Increasing solvent content is one of the possible strategies to overcome diffusion limitations as the increase in viscosity could be maintained low. However, such strategy will affect the throughput of microreactor negatively. Another strategy suggested in literature was the use of patterned microreactors to enhance mixing inside microreactor during polymerization. However, fabrication of such patterned microreactors are not only difficult but also expensive.<sup>16</sup> Therefore, a simpler and robust alternative needs to be explored in order to expand the applicability of microreactors as well as to improve polymer quality. As a part of this effort to achieve a better control over polymerization in microreactor when the reactive medium viscosity is increasing, flow inversion technique in capillary-based microreactor was considered in this study and its effect on polymerization kinetics and polymer characteristics of both linear and branched polymers investigated. Although the concept of flow inversion is not new in chemical engineering, it has been only investigated as heat exchanger in macroscale devices.<sup>17-19</sup> Thus, effect of flow inversion has never been experimentally

investigated in micro geometry for homogeneous polymerization reactions, although numerical studies have emphasized their benefit over straight tubular reactor.<sup>20</sup>

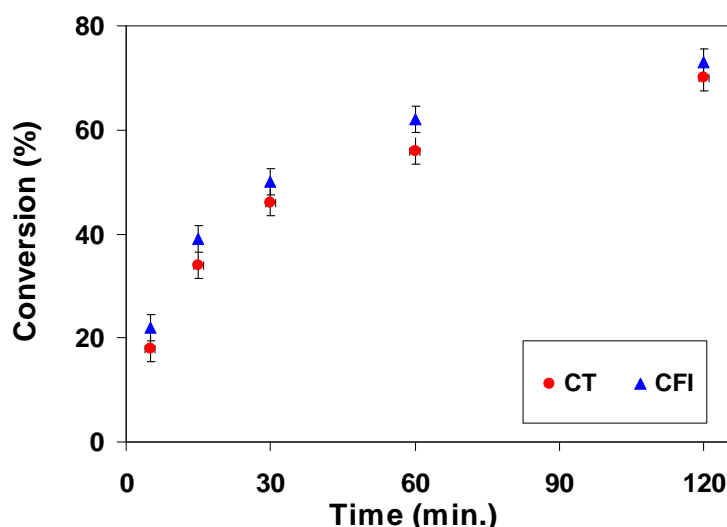
### 5.1.2 Materials and methods

- I. List of materials is given in Chapter 3 section 3.1.1.
- II. Description of setup is provided in Chapter 3 section 3.3.
- III. Polymerization in batch reactor is given in Chapter 3 section 3.2.3 while reservoir compositions are presented in Table 3.1
- IV. Continuous-flow reactor detailed procedure is given in Chapter 3 section 3.3.5 while reservoir compositions and flow rates are presented Table 3.7 and Table 3.8 respectively.
- V. Purification of the samples is detailed in Chapter 3 section 3.4.1.
- VI. Characterization methods include  $^1\text{H}$  NMR (Chapter 3 section 3.4.1.2), GPC (Chapter 3 section 3.4.2).

### 5.1.3 Results and discussions

#### 5.1.3.1 Linear polymer synthesis

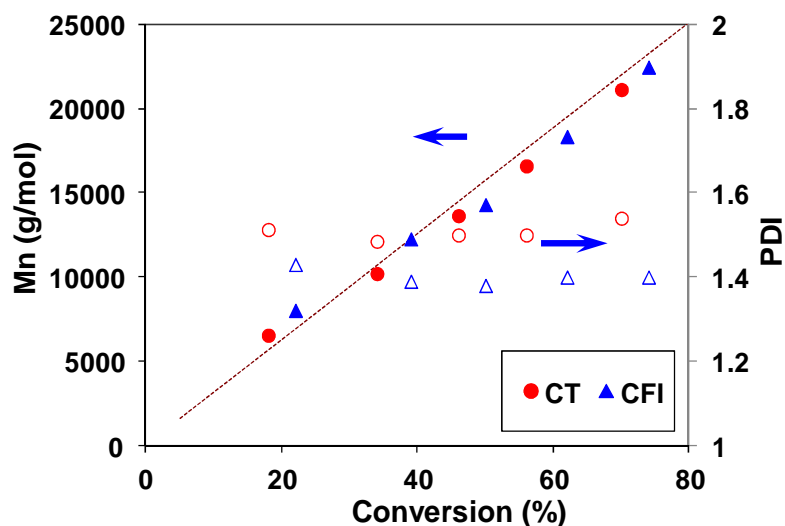
Increase in viscosity during polymerization in microreactor limits the diffusion of reacting species, resulting in a poor control over polymerization especially at high monomer conversions. To overcome such limitation and reduce residence time distribution inside microreactor, alternative like flow inversion was considered. A marginal increase (~3-5 %) in monomer conversion was observed in case of CFI microreactor compared to CT (Figure 5.1).



**Figure 5.1.** Plot showing the effect of microreactor geometry on conversion of DMAEMA.



Due to presence of  $90^\circ$  bends in microreactor, direction of flow changes after given interval, which brings the growing chains near the wall to the centre and vice versa.<sup>18</sup> A reactor having such characteristics will not only improve mixing during flow but also will reduce residence time distribution (RTD) in the reactor. Improved mixing reduces concentration gradients and allows polymer chains growing equally throughout the length of microreactor. On the other hand, reduced RTD ensures equal residence time of molecules inside the reactor which is a prerequisite in controlled radical polymerizations for producing macromolecules with narrow chain length distributions. Polymers synthesized in CFI were found to have higher molecular weights ( $M_n$ ), up to +2,000 g/mol compared to CT (Figure 5.2). Gain in  $M_n$  was observed at each residence time (Figure 5.SI 2). Effect of improved mixing and narrow RTD was evident from reduced polydispersity index (PDI) as shown in Figure 3 and entry 1, 2 of Table 5.1.

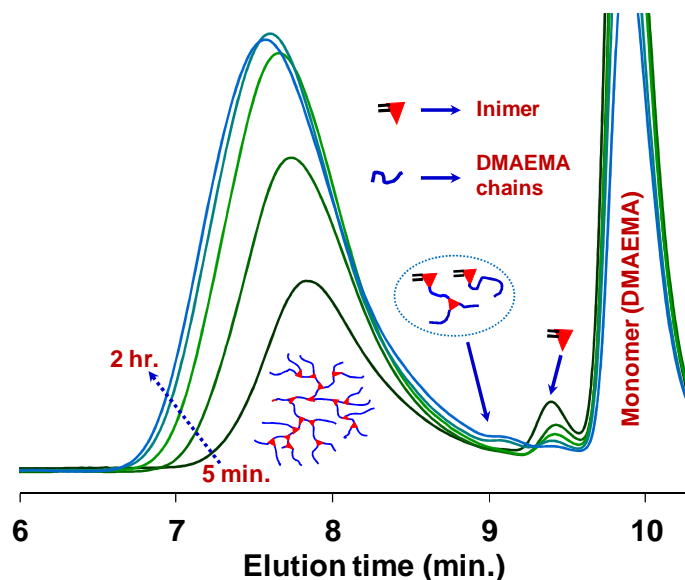


**Figure 5.1.** Evolution of molecular weight ( $M_n$ , filled symbols) and PDI (empty symbols) with respect to monomer conversion for different microreactor geometries.

### 5.1.3.2 Branched polymer synthesis

More clear evidences about mixing and its effect on branched polymerization were obtained during polymerization in different reactors, i.e. batch, CT and CFI. Elution traces (Figure 5.3) of batch branched polymerization with 5 mol. % inimer indicates a rapid disappearance of the peak corresponding to inimer for 1 hr polymerization time. This suggests major portion of BIEM (inimer) molecules has reacted, either as a monomer or as an initiator. From  $^1\text{H}$  NMR analysis, it was found that 56% (Figure 5.4) of BIEM molecules had their double bond reacted meaning that inimer was incorporated into a growing chain as a monomer. Thus, it can be concluded with the support of NMR spectra (see supporting information) that a significant proportion of the inimer (44%) has acted like an initiator. This explains the appearance of a

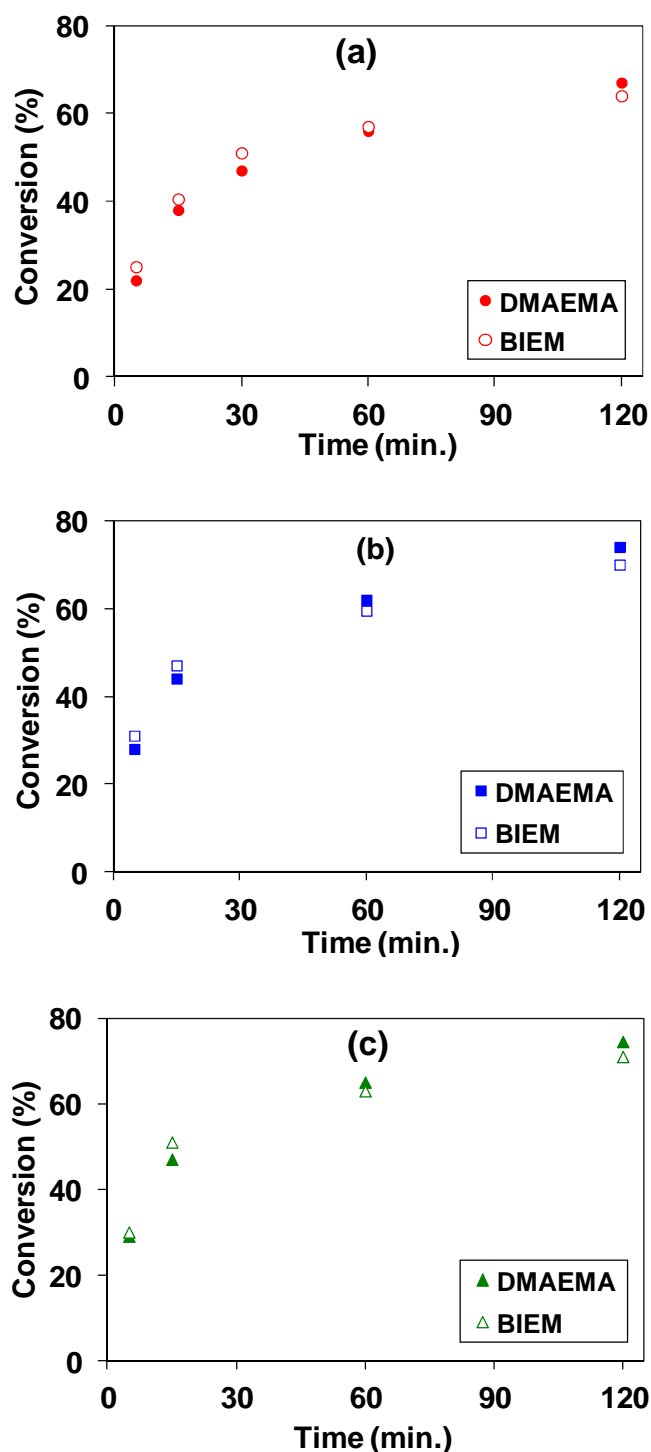
broad peak at low molecular weights region of elution traces at 1 hr polymerization time corresponding to the formation of oligomers initiated by BIEM molecules and having a double bond at one chain ends. These oligomers can be considered as a macromonomer but their incorporation in the main branched structure will be impeded by steric hindrance and slow diffusion coefficient.



**Figure 5.2.** GPC elution traces of branched polymers obtained after 5 minutes to 2 hours in a batch reactor.

It is worthy to note that the initial consumption rate of BIEM double bond (as determined by  $^1\text{H}$  NMR) is higher than that of DMAEMA irrespective of reactor type (Figure 5.4) and that for long polymerization times (after 30 min) this rate somehow diminishes and become lower than for DMAEMA. Thus this decrease in rate may be ascribed for the formation of these macromonomers. In such condition, mixing can affect the polymerization and architecture of the branched polymer. Easy and faster diffusion increases the probability of macromonomers to react with a growing branched chain. On the opposite, slow diffusion will make oligomers growing as a separate chain and results in lower average molecular weight polymers and higher polydispersity. This argument was supported by Figure 5.SI 1 where conversion of inimer at any time in CFI was higher than the conversion achieved in batch reactor. As a result, the molecular weight of branched polymers synthesized in microreactors is higher at a given polymerization time as shown in Figure 5.5. Another consequence is the lower proportion of macromonomer/oligomers for CT and CTI as seen in the GPC traces of Figure 5.6a where the peak at low molecular weights is barely visible. The overall consequence is a

reduced PDI for these two microreactors (Figure 5.5). It is worthy to mention that this observation remains valid for higher BIEM composition (i.e. 10 mol.% inimer, Figure 5.6b and Table 5.1). Note that higher molecular weights observed in microreactors result also from higher DMAEMA conversions (Figure 5.4 and Table 5.SI 1).



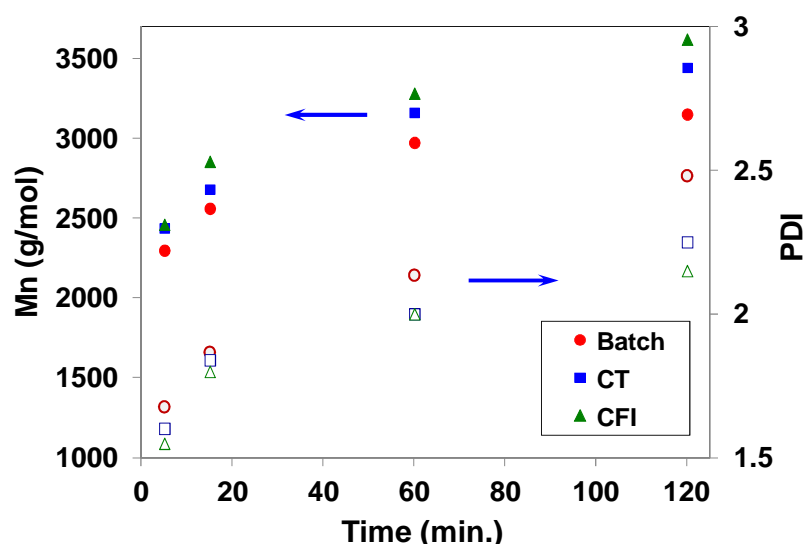
**Figure 5.3.** Conversions of DMAEMA and BIEM in batch (a), CT (b) and CFI (c) at different polymerization times.

**Table 5.1.** Summary of linear and branched PDMAEMA characteristics synthesised after 2 hours in different reactors.

Entry	Mol.% BIEM	Reactor type	Mn (g/mol)	PDI	Mw <sub>RI</sub> (g/mole)	Mw <sub>MALS</sub> (g/mole)	$\frac{Mw_{RI}^*}{Mw_{MALS}}$	Unreacted C=C (%) <sup>#</sup>
1	0	CT	21042	1.54	32404	--	--	--
2	0	CFI	22574	1.40	31603	--	--	--
3	5	Batch	3156	2.48	8172	9150	0.86	27.4
4	5	CT	3477	2.35	8170	10770	0.75	23.4
5	5	CFI	3618	2.20	8140	11770	0.69	20.6
6	10	Batch	1814	2.8	5124	8836	0.58	18.1
7	10	CT	2100	2.56	5220	10004	0.52	15.4
8	10	CFI	2218	2.50	5567	12160	0.46	14.1

\*Mw<sub>RI</sub> and Mw<sub>MALS</sub> are the weight-average molecular weights obtained by refractive index (RI) or by multi angle light scattering (MALS) detectors

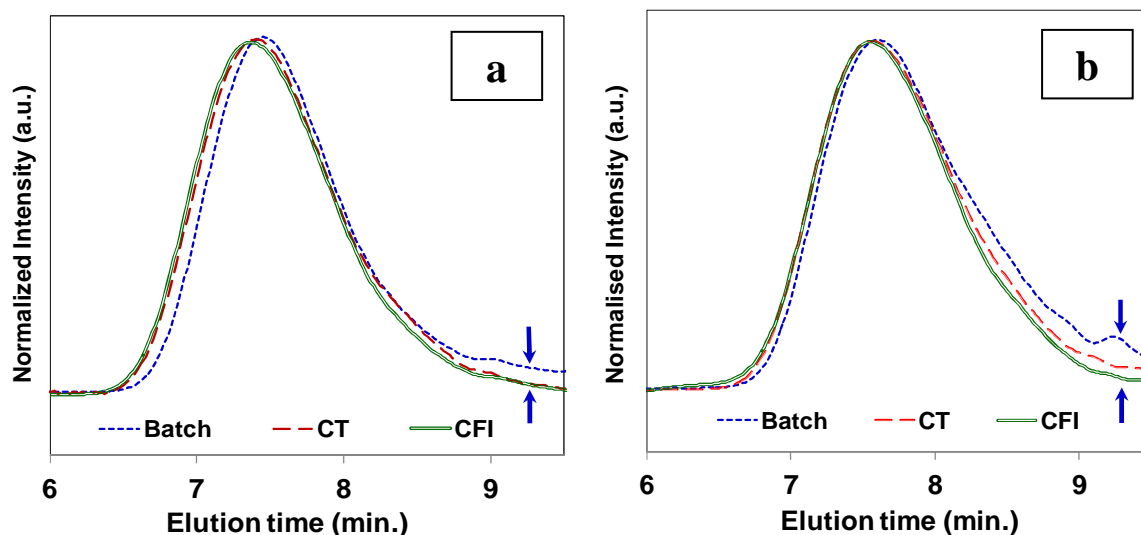
<sup>#</sup>determined by <sup>1</sup>H NMR (Figure 5.SI 3)



**Figure 5.4.** Evolution of molecular weight (Mn, filled symbols) and PDI (empty symbols) with time in different reactors.

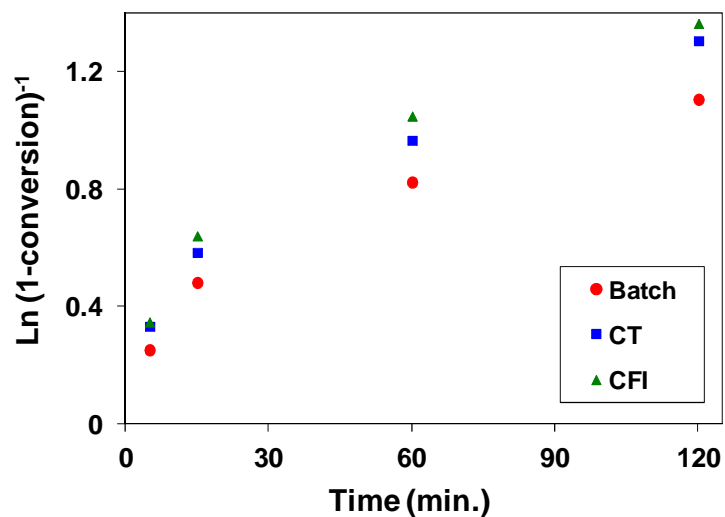
Additional information is provided by the first-order plot of polymerization (Figure 5.7). At the early stage of the polymerization (5 min), the continuous-flow mode (irrespective of the geometry of the tubular microreactor, CFI or CT), promotes an efficient initiation though the concentration of initiating species  $[I]_0$  is same for all reactors. Later on (after 5 min) and for each reactor, the downward curvature indicates a decrease in the propagating species concentration. However a clear trend is to be seen in between the three reactors; CFI leading always to the highest conversion index while the batch reactor exhibits the lowest.

Furthermore the discrepancy between batch and microscale reactors is getting higher as the polymerization time increases. This discrepancy originates from a slower diffusion of chemical species in batch reactor while a shorter diffusion pathway (small diameter) and effect of 90° bends for the CFI enhanced diffusion of species as discussed in section relative to linear polymers.

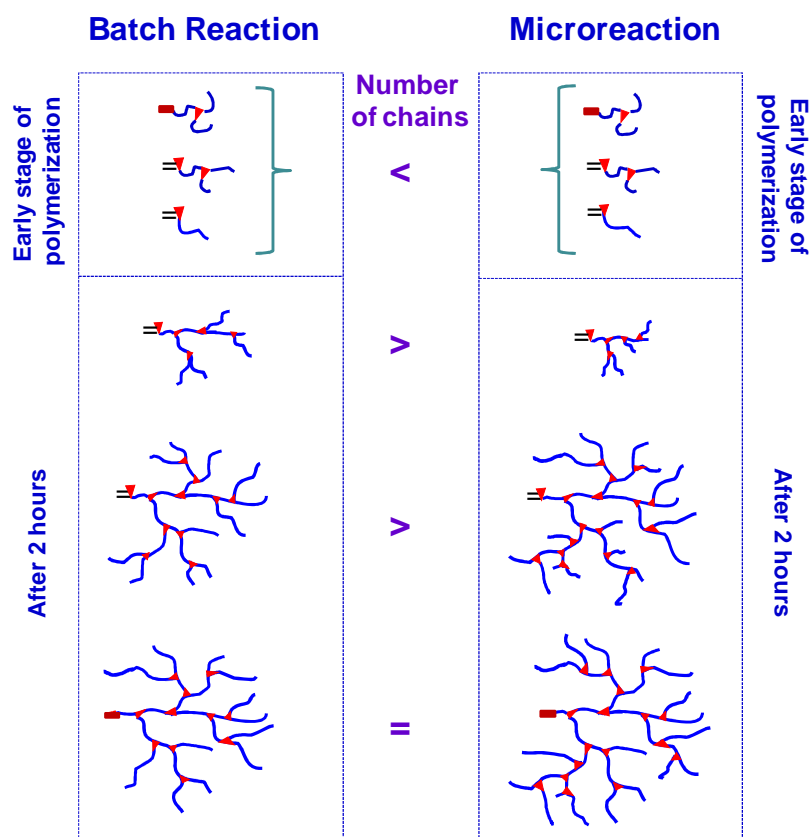


**Figure 5.5.** GPC traces of branched polymers synthesized in different reactor at 5 mol. % (a) and 10 mol. % (b) of BIEM composition, after 2 hours of polymerization time.

Moreover incorporation of inimer into a growing chain may result in a branching point. One can define an apparent branching efficiency defined as the percentage of BIEM incorporated in the branched structure. Thus this parameter is simply calculated from the complement of the percentage of unreacted BIEM C=C bonds as seen by NMR analysis (Table 5.1). Unfortunately NMR analysis on purified polymer cannot discriminate among the incorporated inimers which has led to a branching point. Ratio between  $M_w$  as determined by refractive index detector (RI) and  $M_w$  determined by multi angle light scattering detector (MALS) ( $M_{w,RI}/M_{w,MALS}$ ) was used as a qualitative indicator of branching efficiency<sup>22</sup> and is listed in Table 1 for investigated conditions. Interestingly whatever the BIEM composition, a better branched structure was obtained in CFI compared to other two reactors. Considering the above observations from GPC and <sup>1</sup>H NMR analysis a simple schematic drawing is proposed in scheme 3 to explain the main difference between the mechanisms of branched polymer synthesis in batch and continuous-microflow reactors.



**Figure 5.6.** Overall monomer conversion (DMAEMA+BIEM) with respect to the polymerization time for different reactors.



**Scheme 5.3.** Schematic comparison of branched polymer synthesis in batch and microreactors after 2 hours polymerization time.

### 5.1.4 Summary

This work aimed at comparing different geometries of capillary-type microreactors to highlight the effect of mixing on ATRP linear and branched synthesis. Compared to the standard coiled tube geometry (CT), a simpler alternative like flow inversion (CFI) was used for the first time in microreaction to reduce the mass diffusion limitation arising from the increased viscosity at high conversion. Thus improved mixing condition in CFI was found to be quite effective to reduce PDI of synthesised linear PDMAEMA. Diffusion driven mixing and its impact on branched polymer characteristics was clearly visible when polymerization in the different microreactors were compared. Improvement in branching efficiency from batch to CFI microreactor showed more controlled incorporation of branching points in polymer chain evidencing that flow inversion can be an effective tool to improve control over polymer characteristics.

*In this section it was demonstrated that flow inversion adapted to tubular microreactors is quite an effective method to intensify the production of polymers by ATRP. However the low productivity of microreactors is still an issue to be addressed. Throughput can be increased either by parallelizing several microreactors (known as the numbering-up approach) or by increasing the dimension of the microreactor (i.e. to move towards milliscale geometry). In the first alternative, the cost of multiple microreactors and the multiplexing of their feed lines may increase the investment cost significantly. In the second alternative, negative effect of viscosity will be amplified as the diffusion pathways will increase with the size of the reactor. Considering the demonstrated benefit of flow inversion at microscale, one may ask if this benefit still holds for milliscale geometries. Thus in the next section, the microreactor diameter will be increased till 4 mm. Macromolecular characteristics like number-average molecular weight ( $M_n$ ) and polydispersity index (PDI) as well as monomer conversion will be used as indicators to assess the benefits of such strategy. Polymerization will be carried out in both CT and CFI reactors having different internal diameters. Moreover different process parameters like steady state, pressure drop and throughput will be studied.*

## 5.1.5 Supporting Information

### 5.1.5.1 Conversion of comonomers

**Table 5.SI 1.** Summary of polymerization conditions.

Entry	Reactors	Time (minutes)	BIEM (%)	DMAEMA conv. (%)	BIEM conv. (%)
1		5	0	18	--
2		15	0	34	--
3	CT	30	0	46	--
4		60	0	56	--
5		120	0	70	--
6		5	0	22	--
7		15	0	39	--
8	CFI	30	0	50	--
9		60	0	62	--
10		120	0	73	--
11		5	5%	22	25
12	Batch	15	5%	38	40.5
13		60	5%	56	57
14		120	5%	67	64
16		5	5%	28	31
17		15	5%	44	47
18	CT	60	5%	62	59.5
19		120	5%	73	70
21		5	5%	29	33
22		15	5%	47	51
23	CFI	60	5%	66	63
24		120	5%	74.5	72
26	Batch	120	10%	71	68
27	CT	120	10%	75	72
28	CFI	120	10%	77	75



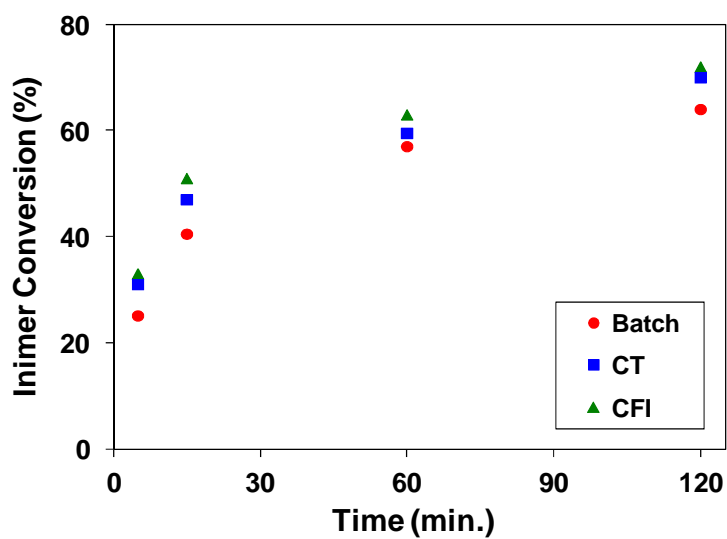


Figure 5.SI 1. Conversion of inimer in different reactors.

#### 5.1.5.2 Evolution of molecular weight ( $M_n$ ) with time during linear PDMAEMA synthesis

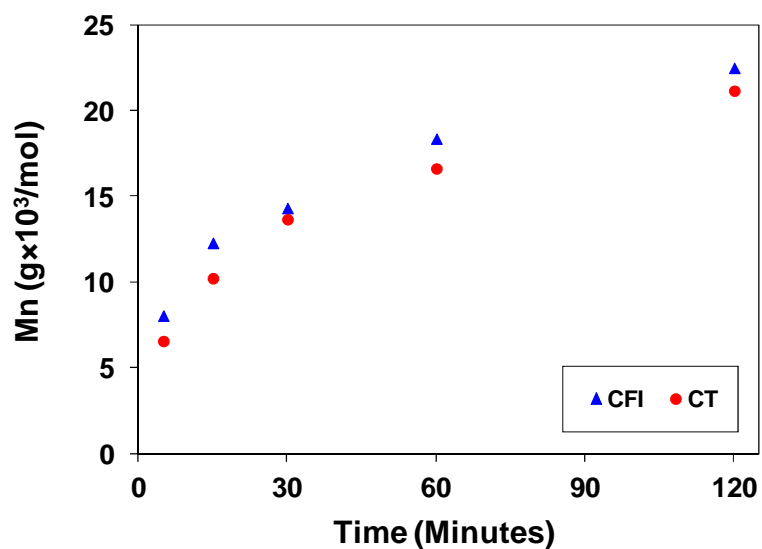
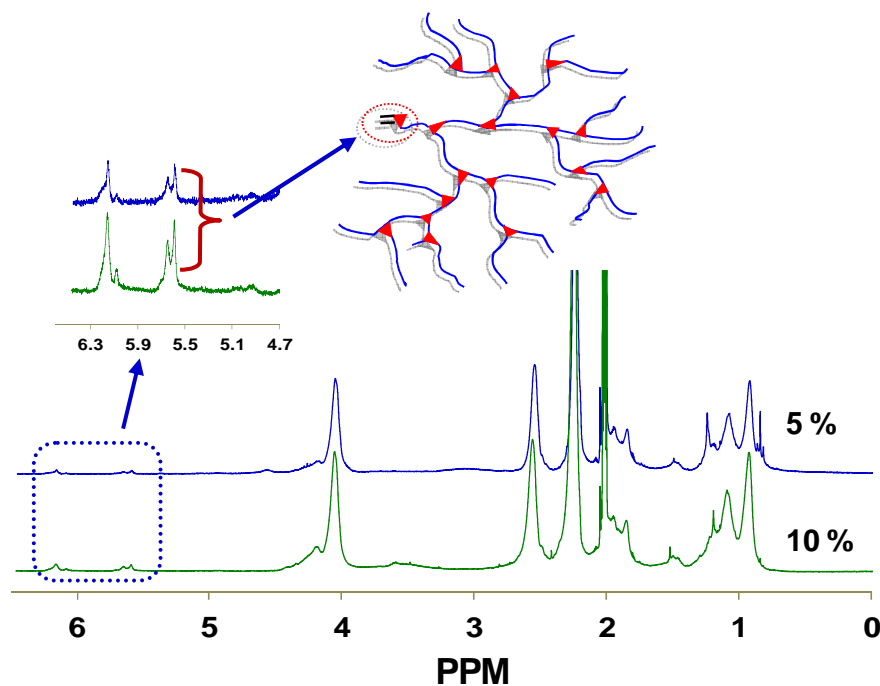


Figure 5.SI 2. Evolution of  $M_n$  with time for CT and CFI microreactors.

### 5.1.5.3 Determination of unreacted double bonds of inimer

NMR spectra of precipitated polymers provided valuable information about polymerization. Peaks in 6.2 and 5.6 regions of Figure 5.SI3 witnessed the presence of unreacted double bond of inimer in precipitated polymer. Presence of lower proportion of unreacted inimer than calculated value in batch reactor suggests loss of some fraction of polymer chains, which were difficult to precipitate due to their low molecular weight. However, in case of microreactors the observed values were in agreement with calculated values.



**Figure 5.SI 3.**  $^1\text{H}$  NMR spectra of precipitated PDMAEMA showing the presence of unreacted double bond of inimer for two different BIEM composition (5% and 10%) and for a batch reactor at a polymerization time of 2 hrs.

---

## References

- (1) Wu, T.; Mei, Y.; Cabral, J. T.; Xu, C.; Beers, K. L. *Journal of the American Chemical Society* **2004**, *126*, 9880.
- (2) Micro process engineering: *a comprehensive handbook. Devices, reactions and applications*; Wiley-VCH Verlag GmbH: Weinheim, Germany, **2009**; Vol. 2.
- (3) Leveson, P.; Dunk, W. A. E.; Jachuck, R. J. *Journal of Applied Polymer Science* **2004**, *94*, 1365.
- (4) Honda, T.; Miyazaki, M.; Nakamura, H.; Maeda, H. *Lab on a Chip* **2005**, *5*, 812.
- (5) Iwasaki, T.; Kawano, N.; Yoshida, J.-i. *Organic Process Research & Development* **2006**, *10*, 1126.
- (6) Rosenfeld, C.; Serra, C. A.; Brochon, C.; Hadziioannou, G. *Lab on a Chip* **2008**, *8*, 1682.
- (7) Bally, F.; Serra, C. A.; Brochon, C.; Hadziioannou, G. *Macromolecular Rapid Communications* **2011**, *32*, 1820.
- (8) Bally, F.; Serra, C. A.; Hessel, V.; Hadziioannou, G. *Chemical Engineering Science* **2011**, *66*, 1449.
- (9) Nagaki, A.; Tomida, Y.; Yoshida, J.-i. *Macromolecules* **2008**, *41*, 6322.
- (10) Iwasaki, T.; Yoshida, J.-i. *Macromolecular Rapid Communications* **2007**, *28*, 1219.
- (11) Nagaki, A.; Tomida, Y.; Miyazaki, A.; Yoshida, J. I. *Macromolecules* **2009**, *42*, 4384.
- (12) Nagaki, A.; Miyazaki, A.; Tomida, Y.; Yoshida, J.-i. *Chemical Engineering Journal* **2011**, *167*, 548.
- (13) Rosenfeld, C.; Serra, C. A.; Brochon, C.; Hessel, V.; Hadziioannou, G. *Chemical Engineering Journal* **2008**, *135*, Supplement 1, S242.
- (14) Bally, F.; Serra, C. A.; Hessel, V.; Hadziioannou, G. *Macromolecular Reaction Engineering* **2010**, *4*, 543.
- (15) Diehl, C.; Laurino, P.; Azzouz, N.; Seeberger, P. H. *Macromolecules* **2010**, *43*, 10311.
- (16) Iida, K.; Chastek, T. Q.; Beers, K. L.; Cavicchi, K. A.; Chun, J.; Fasolka, M. J. *Lab on a Chip* **2009**, *9*, 339.
- (17) Saxena, A. K.; Nigam, K. D. P. *AIChE J.* **1984**, *30*, 6.
- (18) Kumar, V.; Nigam, K. D. P. *International Journal of Heat and Mass Transfer* **2005**, *48*, 4811.
- (19) Mandal, M. M.; Aggarwal, P.; Nigam, K. D. P. *Industrial & Engineering Chemistry Research* **2011**, *50*, 13230.

- (20) Mandal, M.; Serra, C.; Hoarau, Y.; Nigam, K. D. P. *Microfluid Nanofluid* **2011**, *10*, 415.
- (21) Matyjaszewski, K.; Gaynor, S. G.; Kulfan, A.; Podwika, M. *Macromolecules* **1997**, *30*, 5192.
- (22) Qiang, R.; Fanghong, G.; Bibiao, J.; Dongliang, Z.; Jianbo, F.; Fudi, G. *Polymer* **2006**, *47*, 3382.

## *5.2. Flow inversion: an effective means to scale-up controlled radical polymerization in tubular microreactors*

### *Abstract*

*Continuous-flow Atom Transfer Radical Polymerization of 2-(dimethylamino)ethyl methacrylate in tubular microreactors of different diameters and geometries was studied. Scale-up of tubular reactors from micro (876  $\mu\text{m}$  ID) to miliscales (1753 and 4083  $\mu\text{m}$  IDs) was investigated. Coil Flow Inverter (CFI) reactors having 3 m and 6 m length (3 and 7 bends respectively) were also considered for this study. Positive effect of flow inversion was visible in all three types of reactors expressed by an increase in molecular weight and monomer conversion as well as a decrease in the PDI for a given residence time. Increase in diameter of reactor results in an increase in the throughput. It is worthy to mention that, from productivity point of view (PDI of polymer), CFI reactor having 1753  $\mu\text{m}$  ID and 6 m (7 bends) was found to increase throughput by ~4 times compared to the CFI of 876  $\mu\text{m}$  ID without increasing the PDI significantly. However, pressure drops were higher (+0.1 bar) in case of larger diameter tubes.*

### **KEYWORDS**

Flow inversion, ATRP, polymer, throughput, scale-up

### 5.2.1 Introduction

Since their first use in synthetic chemistry, microdevices are praised for their fast mixing and heat transfer ability over their macroscale counterparts. Mixing times as low as few milliseconds and surface to volume ratio in the range of 10 000 to 50 000  $\text{m}^2 \cdot \text{m}^{-3}$  enable them to handle a wide range of reactions from diffusion controlled to extremely fast and exothermic reactions.<sup>1,2</sup> However the most important criticism faced by microreactors is their low throughput. The classical way to address such limitation is to increase the size of the reactors. In such approach, benefits of smaller dimension will be adversely affected. Another approach to solve this problem of low throughput is the concept of numbering-up for which several identical microreactors are placed in parallel to increase the overall throughput.<sup>3-6</sup> Most of the attempts reported in the literature are focused on fine chemicals synthesis. Very few examples concern the throughput increase of polymerization microreactors. One of such work is reported by Yoshida and coworkers and aims at improving the throughput of radical polymerization in microreactor following this numbering-up approach.<sup>7</sup> They achieved a throughput of 4 Kg of an acrylate-based polymer in 6 day with 8 parallel microreactors. On the other hand, when a comparatively slower polymerization reaction, like controlled radical polymerizations (CRP), is considered the throughput will go down significantly because of the inherent slow kinetics.<sup>8</sup> However CRPs (NMP, RAFT, and ATRP) are more in demand because of their positive control over macromolecular characteristics.<sup>8-10</sup> Considering these features, CRPs were successfully carried out in microreactors to enhance the reaction rate without significant loss of control over the polymerization reaction.<sup>11, 12</sup> Polymerization rate was improved in microreactors because of fast mixing and heat exchange. This suggests that the combination of efficient controlled polymerization techniques and microdevices is an effective strategy. Despite of aforementioned increase in polymerization rate, polymerization microreactors still face challenges arising from increased viscosity and low throughput. Addressing such issues could make microreactors and CRP widely acceptable not only in laboratory but also in industries.






To overcome mixing limitations due to increased viscosity, flow inversion was introduced in simple capillary type coiled tube (CT) microreactors. Effect of flow inversion on mixing and residence time distribution was already reported in literature.<sup>12</sup> Considering such advantages of flow inversion, reactor's diameter was increased from micro to milliscale. This approach was considered to increase the throughput of an Atom Transfer Radical Polymerization microprocess while maintaining an effective control over macromolecular characteristics.

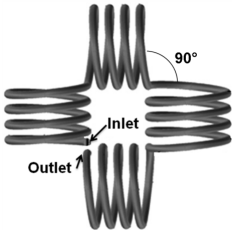

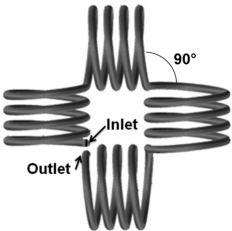

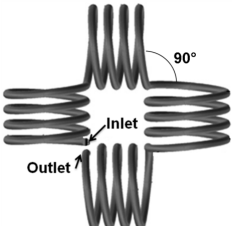
## 5.2.2 Materials and methods

- I. List of materials is given in Chapter 3 section 3.1.1.
- II. Description of setup is provided in Chapter 3 section 3.3.
- III. Polymerization continuous-flow reactor is described in Chapter 3 sections 3.3.5 while composition of reservoirs is given in Table 3.7 and flow rates in Tables 3.8 & 3.9.
- IV. Purification of the samples is detailed in Chapter 3, section 3.4.1.
- V. Characterization methods include  $^1\text{H}$  NMR (Chapter 3 section 3.4.1.2.) and GPC (Chapter 3 section 3.4.2.).

Microreactors used in this study are summarized in Table 5.1. Stainless steel coiled tube (CT) and coil flow inverter (CFI) reactors of 3 and 6 meters length were investigated. Three different diameters of reactor were also considered in both geometries. CFI is a tubular microreactor having same number of coils as in CT. However,  $90^\circ$  bends were introduced at equal interval in one direction as shown in Table 5.1. In this study CFIs having 3 and 7 bends and having same number of coils between each bend were used for polymerization.

**Table 5.1.** List and characteristics of the different microreactors considered.

Entry	Reactor type	I ( $\mu\text{m}$ )	Length (m)	Image	Volume (ml)
1	CT	876	3		01.81
2	CT	876	6		03.62
3	CT	1753	3		7.24
4	CT	1753	6		14.48
7	CT	4083	3		39.28

6	CFI	876	3		1.81
7	CFI	876	6		3.61
8	CFI	1753	3		7.24
9	CFI	1753	6		14.48
10	CFI	4083	3		39.28

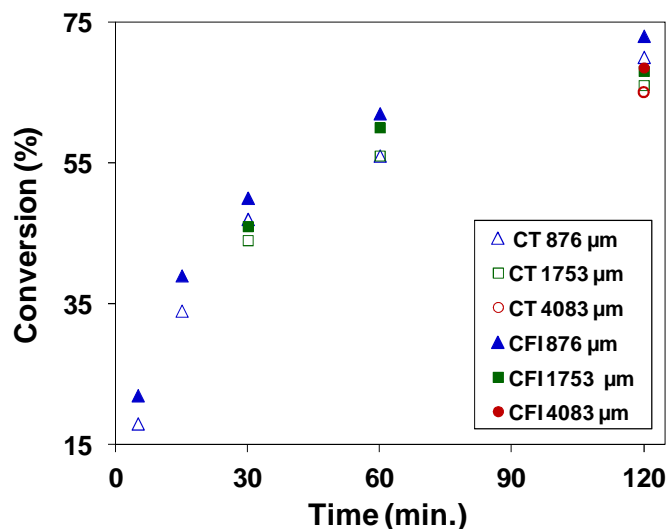
## 5.2.3 Results and discussion

### 5.2.3.1 Effect of reactor geometry

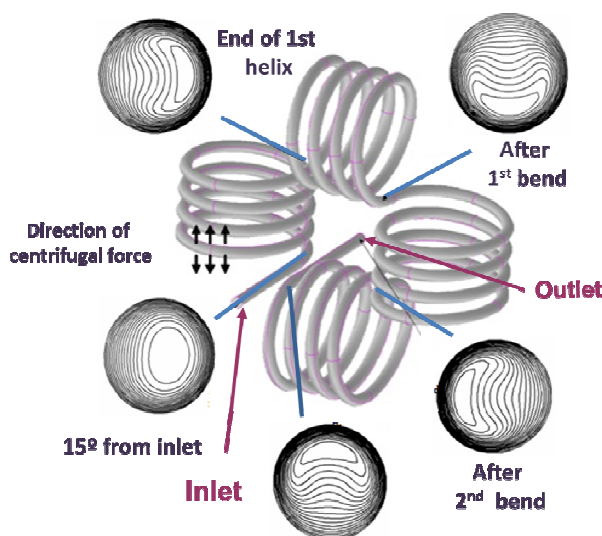
Figure 5.8 shows the variation of monomer conversion with respect to time for CT and CFI reactors of different diameters and 3 m length. It is worth noting that whatever the reactor diameter, CFI reactors always exhibit a higher conversion than their CT counterparts (+5 % in average). This can be ascribed to the bends introduced in the CFI geometry. The direction of flow changes upon each bend which induces a rotation of the streamlines as stressed out in Figure 5.9.<sup>12</sup> Thus the growing chains near the wall are brought back to the centre of the reactor and vice versa. As a consequences concentration gradients are reduced, mixing is



enhanced, homogeneity of reactive medium is improved which results in the observed conversion increase, higher  $M_n$  (Figure 5.SI 4) and significantly lower PDI (Figure 5.10).



**Figure 5.7.** Conversion of DMAEMA in continuous-flow coiled tube (CT) and coil flow inverter (CFI) reactors of 3 m length and different diameters.



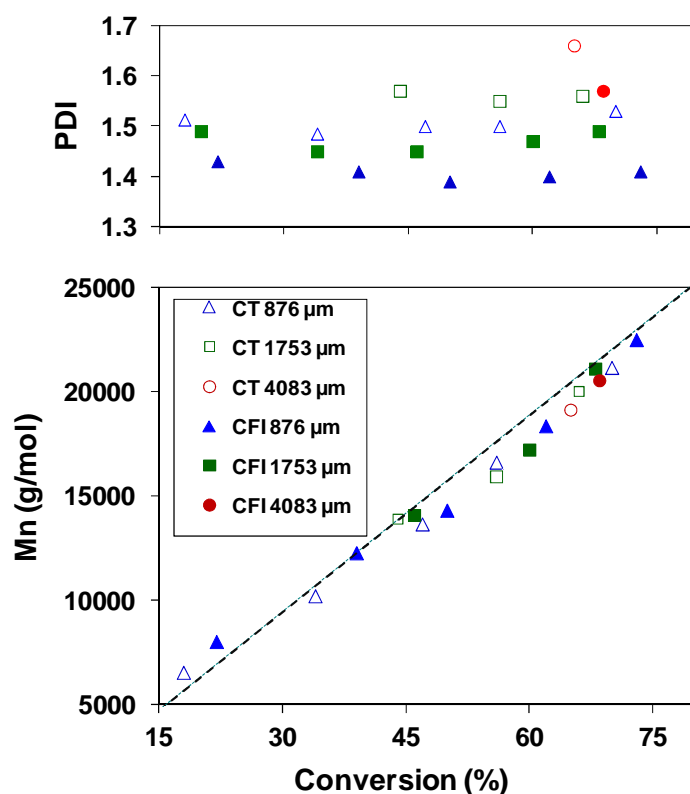
**Figure 5.8.** Streamlines along the length of a coil flow inverter reactor (adapted from ref.<sup>12</sup>).

### 5.2.3.2 Effect of reactor diameter

For a given length, any increase in reactor diameter will increase the internal volume. Thus in order to keep the residence time constant, the flow rate has to be increased which in turn induce a higher throughput. On the other hand, any increase in reactor diameter will increase the diffusion distance of chemical species and may give rise to concentration and temperature gradients along the reactor radius. Figure 5.8 shows the effect of such changes expressed as a decrease in conversion with increasing diameter of the reactor from micro to milliscale (i.e.

from 876  $\mu\text{m}$  to 4084  $\mu\text{m}$  IDs) for CT reactors. Difference in conversion is not very significant between intermediate diameters (876  $\mu\text{m}$  and 1753  $\mu\text{m}$  IDs), but considerable difference (6%) can be seen between largest (4083  $\mu\text{m}$ ) and smallest (876  $\mu\text{m}$ ) diameters. Same trends are observed in  $M_n$  decrease (Figure 5.SI 4) and PDI increase (Figure 5.10). To overcome the detrimental effect of such changes and improve the uniformity of reaction conditions inside larger diameter reactors, flow inversion was introduced. Although a mild improvement in monomer conversion was observed after introducing flow inversion (see previous section),  $M_n$  and PDI exhibit larger variations.

Figure 5.10 clearly shows that PDI increase and  $M_n$  decrease (Figure 5.SI 4) with reactor diameter are severely limited in case of CT reactors. It is noteworthy that CFI reactor of 1753  $\mu\text{m}$  in diameter produces a lower PDI than its CT counterpart of smaller diameter (876  $\mu\text{m}$ ). It suggests an improved homogenization of reagents during polymerization upon flow inversion. Moreover evolution of  $M_n$  with respect to monomer conversion (Figure 5.10) shows that the controlled nature of the polymerization is fairly well maintained in higher diameters when flow inversion is considered



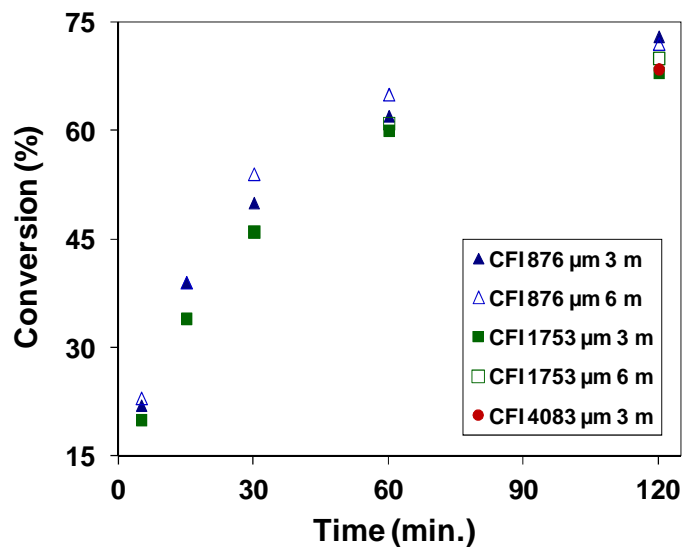
**Figure 5.9.** Effect of reactor diameter and geometry of a 3 m reactor (CT or CFI) on the evolution of molecular weight ( $M_n$ ) and PDI with monomer conversion. Dash line represents theoretical molecular weight.

### 5.2.3.3 Effect of reactor length

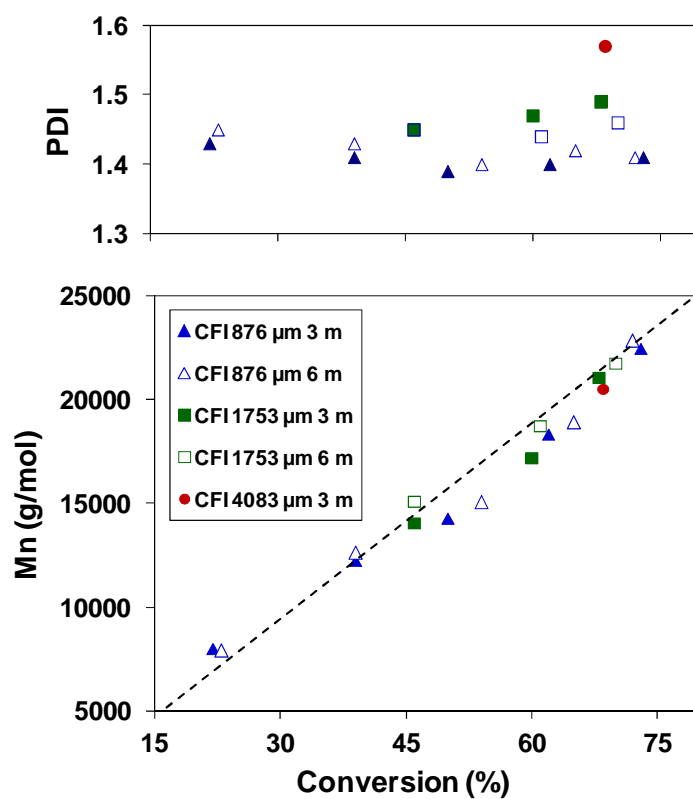
Increasing the reactor length is another option to increase reactor throughput. Longer reactors need higher flow rates to accommodate the same residence time; for a given diameter the flow rate varies proportionately to the reactor length. Flow inversion is known to be more effective when it operates at higher Reynolds numbers (i.e. higher flow rates).<sup>13</sup> Therefore, longer reactors give the opportunity to study effect of flow rate and number of bends. One has to recall that number of coils is kept constant in-between two bends. Figure 5.11 presents the variations of monomer conversion with respect to time for CFI reactors having different lengths and diameters. From previous section, we have observed the superiority of CFI over CT reactors, therefore length effect for the latter are not presented in this section but can be visualized in Figures 5.SI 5 and 5.SI 6. As mentioned in Table 5.1, 3 m length CFI reactors have only 3 bends while 6 m length have 7 bends. Note that accommodating a 4083  $\mu\text{m}$  CFI reactor of 6 m length in the oven was quite challenging and thus results for this reactor were not accessible.

It is observed that at any given residence time except 2 hours, longer reactors give rise to highest monomer conversions (+4% for 30 min). Considering that microscale reactor favor mass diffusion as mentioned in previous sections, any new bends resulting from an increase in reactor length will not play a significant role. However, when reactor diameter increases, the addition of new bends clearly helps to improve mixing with a subsequent rate acceleration of the polymerization reaction. For 2 hours residence time, there is almost no effect of reactor length. It is believed that at such residence time, high medium viscosity makes the flow inversion less effective because of the decreasing Reynolds number with viscosity.

Variations of  $M_n$  and PDI with respect to monomer conversion are presented in Figure 5.12. PDI clearly decreases with reactor length but increases with reactor diameter. Opposite trend is to be seen for variation of  $M_n$  with respect to residence time (Figure 5.SI 7). The former observation emphasizes that higher flow rates are more efficient for flow inversion internal mixing as aforementioned. The lowest PDI value (1.4) was obtained with the reactor having the lowest diameter as previously stressed out. The evolution of  $M_n$  as a function of monomer conversion (Figure 5.12) shows that the controlled nature of the polymerization is also fairly well maintained.



**Figure 5.10.** Conversion of DMAEMA during polymerization in CFI reactors having different lengths and internal diameters.



**Figure 5.11.** Evolution of molecular weight ( $M_n$ ) and PDI during polymerization in CFI reactors having different lengths and internal diameters. Dash line represents theoretical  $M_n$ .

### 5.2.3.4 Process parameters

Process parameters like time for steady state, pressure drop, and throughput of reactors were determined to compare the effectiveness of reactors listed in Table 5.1. Steady state times of reactors were found to increase with an increase in diameter and length of the reactors but seemed to be unaffected by the geometry (CT or CFI) (Table 5.2). Details of steady state of reactors can be found in supporting information.

**Table 5.2.** Summary of polymer characteristics and process parameters obtained in different reactors for a residence time of 2 hours.

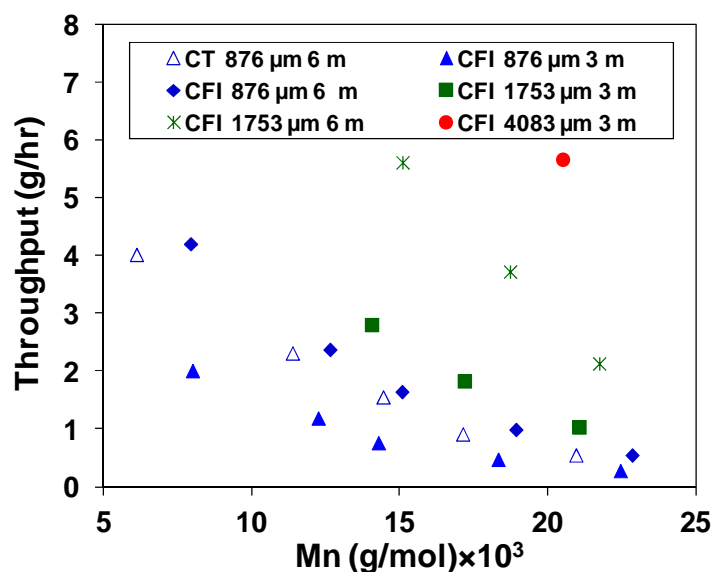
Entry	Reactor type	Dia. (μm)	Length (m)	Mn (g/mol)	PDI	Through-put (g/hr)	PD <sup>1</sup> (bar)	SST <sup>2</sup> (hrs)
1	CT	876	6	21142	1.53	0.54	0.1	2.25
2	CFI	876	3	22474	1.41	0.28	0.1	2.25
3	CFI	876	6	22874	1.43	0.55	0.1	2.5
4	CT	1753	6	20012	1.57	2.00	0.1	3
5	CFI	1753	3	21080	1.49	1.03	0.2	3
6	CFI	1753	6	21761	1.46	2.13	0.2	3.5
7	CT	4083	3	19121	1.67	5.37	0.1	3.75
8	CFI	4083	6	20525	1.59	5.66	0.2	3.75

<sup>1</sup> Pressure drop (PD), precision of the pressure sensors is 0.25%, <sup>2</sup> Steady state time (SST)

In straight tubes, pressure drop is directly related to the flow rate required to achieve a given residence time through the reactor and is an indicator of the raw energy input required by the pump. From a hydraulic point of view, 90° bends which promote flow inversion can be considered as an additional length of tube which dissipates energy by friction. Thus one may expect that higher pressure drops will be observed in case of CFI reactors. As reported in Table 5.2, at the most an additional 0.1 bar was recorded for CFI reactors in comparison to CT counterparts. Thus the introduction of flow inversion does not seem to induce excessive energy consumption. This is probably due to the relative low flow rate at which operated the CFI reactors but still high enough to affect positively macromolecular characteristics as stressed out in previous sections.

Figure 5.13 shows the throughput of reactors with different geometries, diameters and lengths with respect to the molecular weight (i.e. residence times). One can clearly see that the highest throughput is obtained for the reactor having the largest diameter (4083 μm). However loss of control over polymerization was observed as discussed before (Figure 5.12). Conversely CFI reactor with the smallest diameter and length promote the highest control on

polymerization but with the lowest throughput. When polymer quality is the priority, such reactor is a good alternative and by increasing the length of the reactor, the throughput can be increased proportionately with no polymer quality changes. When the throughput of a 3 m length reactor having 1753  $\mu\text{m}$  internal diameter was compared with other reactors an interesting observation can be placed. The throughput was significantly increased without sacrificing too much the control over polymerization significantly as observed in 4083  $\mu\text{m}$  reactor (Figure 5.12). When the length of this reactor was increased to 6 m, a further reduction in PDI was observed (slightly higher than CFI of 876  $\mu\text{m}$ , Figure 5.12).



**Figure 5.12.** Throughput of different tubular reactors with respect to molecular weight ( $M_n$ ).

## 5.2.4 Summary

Continuous–microflow ATRP of 2–(dimethylamino)ethyl methacrylate (DMAEMA) was carried out in tubular microreactor of different geometries, diameters and lengths. Increase in diameter results in a marginal decrease in conversion and adversely affect the control over polymerization as the polydispersity index (PDI) of synthesized PDMAEMA was found to increase. However higher diameter of reactors has a benefit of higher throughput.

Interestingly improvement in conversion was observed by introducing 90° bends in the above coiled tube (CT) reactors at regular interval. Such observations were consistent for all three diameters of tubular reactors investigated (876, 1753 and 4083  $\mu\text{m}$ ). Increased number-average molecular weight ( $M_n$ ) and reduced PDI indicated a better mixing in these coil flow inverter (CFI) reactors during polymerization even at high viscosity encountered during longer residence times. Increasing the length of the CFI reactors (i.e. the number of bends)

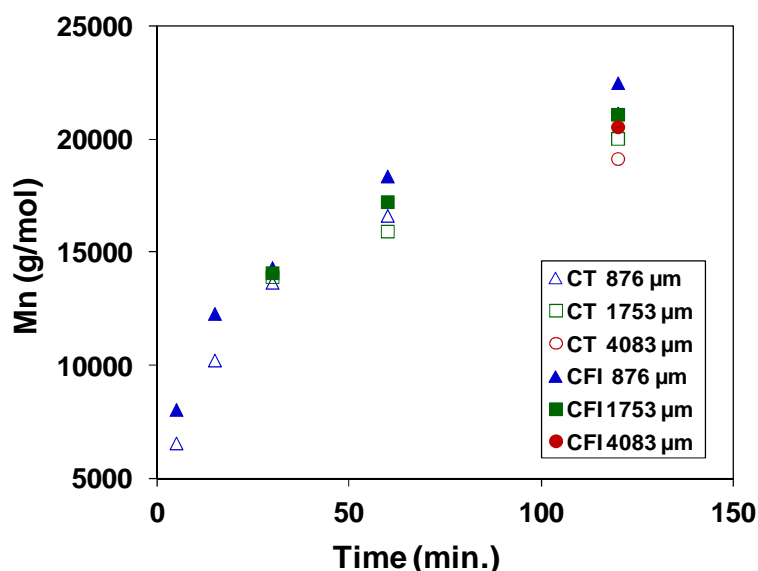
was also beneficial in terms of PDI of synthesised polymer. However, it was more pronounced in larger tube diameter (1753  $\mu\text{m}$ ).

Flow inversion allowed increasing the reactor diameter without increasing the PDI significantly. PDI of PDMAEMA synthesised in a 1753  $\mu\text{m}$  CFI reactor was found to be less than the PDI obtained in a normal CT microreactor having an internal diameter of 876  $\mu\text{m}$ . As a result throughput was increased significantly. Finally introduction of 90° bends was found not to affect significantly the pressure drop. No additional pressure drop was observed in case of CFI reactor of 876  $\mu\text{m}$  in diameter while an excess of 0.1 bar was recorded in CFIs of 1753 and 4083  $\mu\text{m}$  in diameter compared to their CT counterparts.

Thus it was demonstrated that flow inversion is a valuable technique that enable the scale-up of controlled radical polymerization tubular microreactor while severely limiting the detrimental effects observed in the scale-up of coiled tube reactors.

## 5.2.5 Supporting Information

### 5.2.5.1 Conversion, Mn and PDI for continuous-flow reactors of different diameters and lengths



**Figure 5.SI 4.** Evolution of molecular during polymerization in different tubular reactors (CT and CFI) of different diameters and having 3 m length.

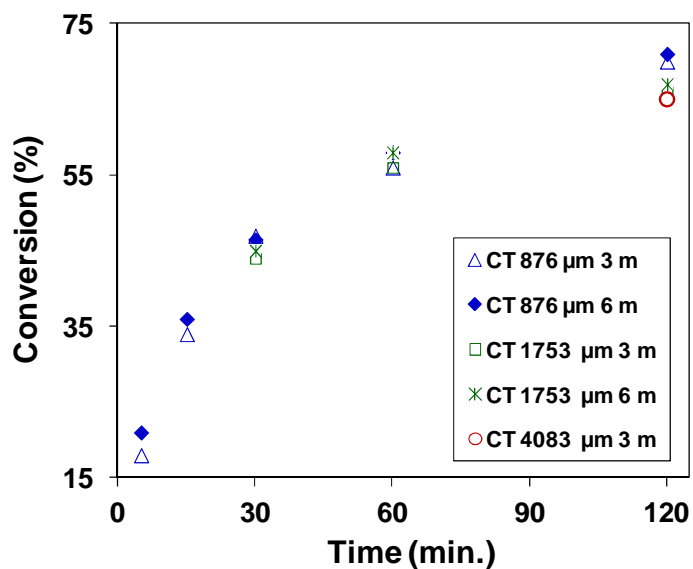


Figure 5.SI 5. Evolution of molecular weight during polymerization in coiled tube reactor of different diameters and lengths.

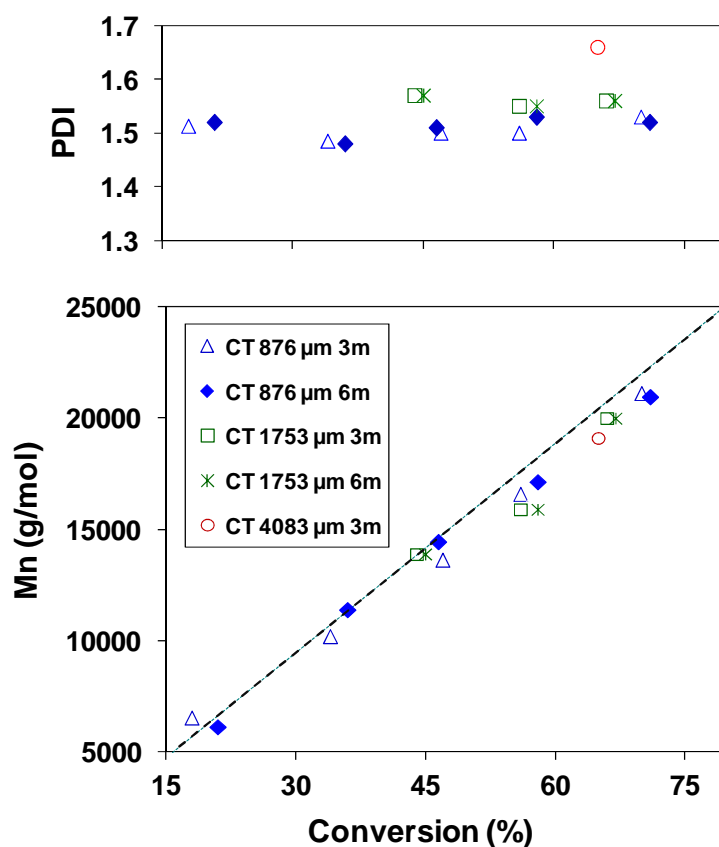
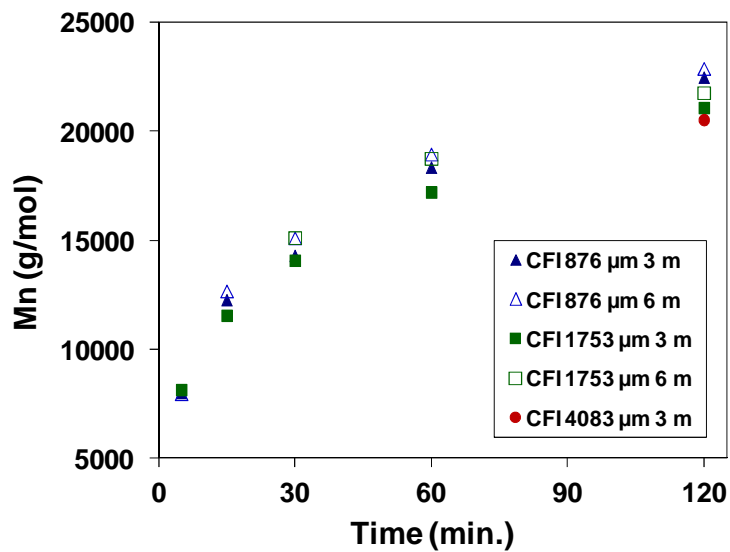


Figure 5.SI 6. Effect of coil tube (CT) reactor diameter and length on the evolution of molecular weight ( $M_n$ ) and PDI with monomer conversion.

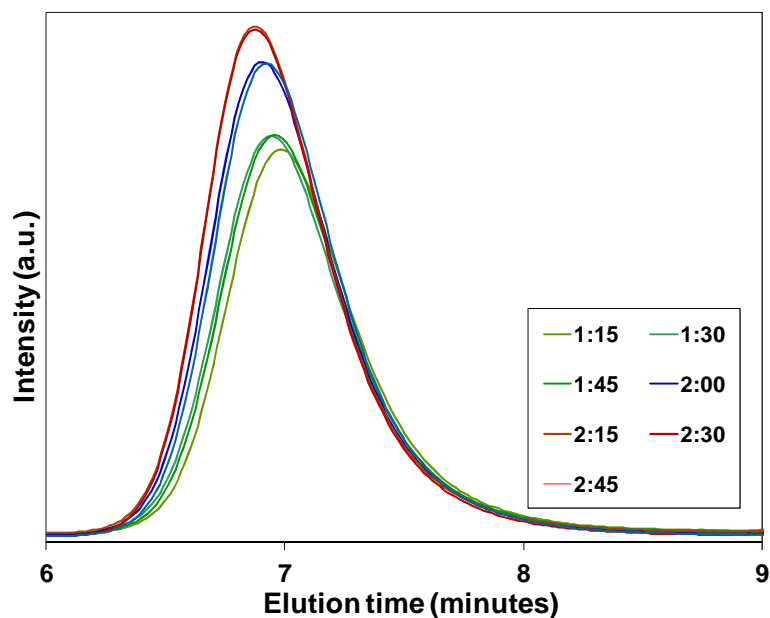




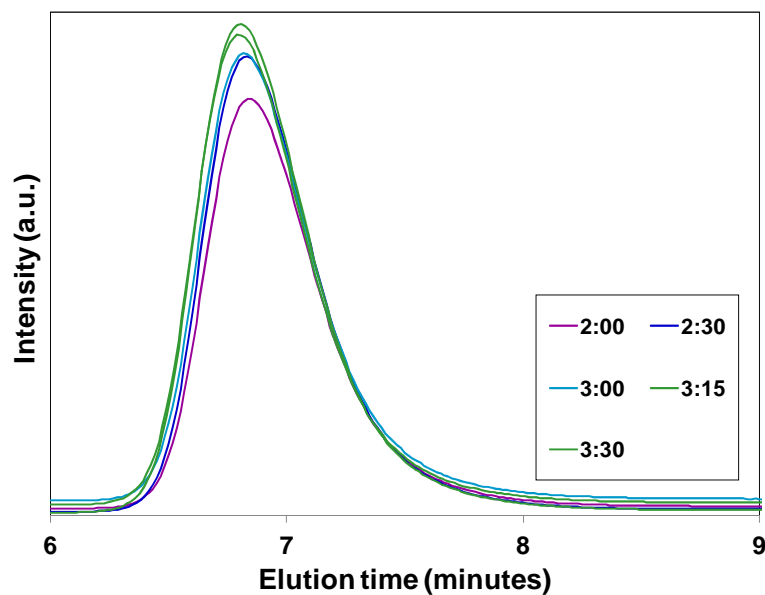
**Figure 5.SI 7.** Evolution of Mn during polymerization in CFI tubular reactor of different diameter and length.

## 5.2.5.2 Steady state of tubular reactors determined by GPC

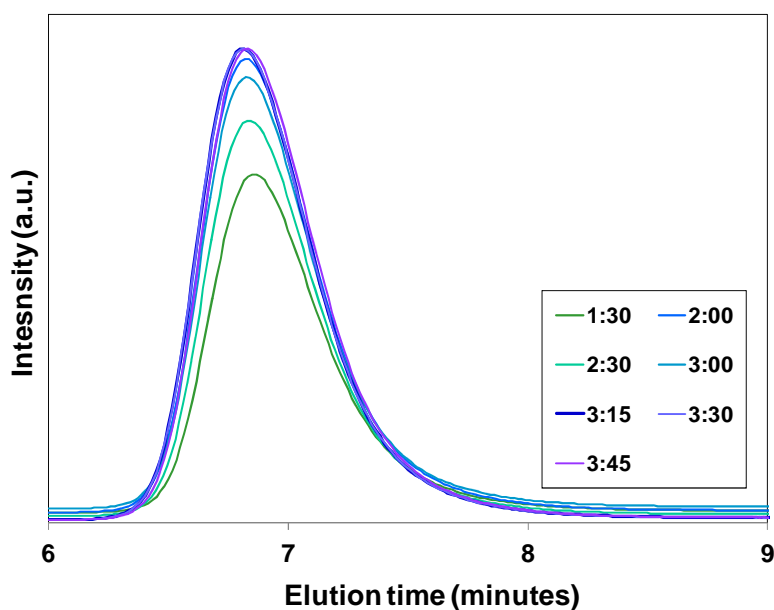
### 5.2.5.2.1. Steady state of 876 $\mu\text{m}$ reactor (CT) of 6 m length



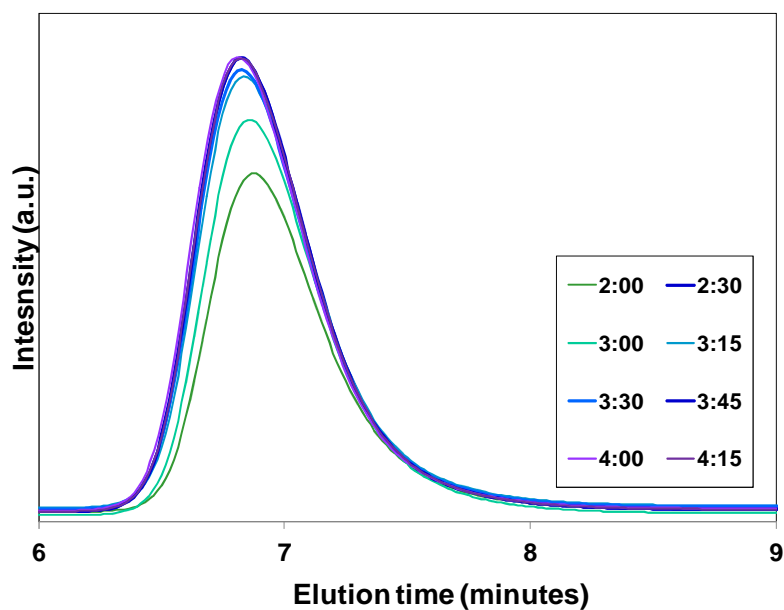
**Figure 5.SI 8.** Overlaid GPC traces indicating steady state of 876  $\mu\text{m}$  tubular reactor of 6 m length at residence time of 1 hr.

5.2.5.2.2 Steady state of 1753  $\mu\text{m}$  reactor (CT) of 3 m and 6 m length

**Figure 5.SI 9.** Overlaid GPC traces indicating steady state of 1753  $\mu\text{m}$  tubular reactor of 3 m length at residence time of 1 hr.



**Figure 5.SI 10.** Overlaid GPC traces indicating steady state of 1753  $\mu\text{m}$  tubular reactor of 6 m length at residence time of 1 hr.

5.2.5.2.3. Steady state of 4083  $\mu\text{m}$  reactor (CT) of 3 m length

**Figure 5.SI 11.** Overlaid GPC traces indicating steady state of 4083  $\mu\text{m}$  tubular reactor of 3 m length at residence time of 1 hr.

## 5.2.5.3 Summary

**Table 5.SI 3.** Complete summary of polymer characteristics and process parameters after two hours polymerization in tubular reactors of different geometries, diameters and lengths.

Entry no.	Reactor	Dia. ( $\mu\text{m}$ )	Length (m)	Volume (ml)	Mn (g/mol)	PDI	Output (g/hr)	PD (bar)	SST (hr)
1	CT	876	3	0	21142	1.53	0.54	0.1	2.25
2	CT	876	6	0	20975	1.52	0,55	0.1	2.5
3	CFI	876	3	3	22474	1.41	0.28	0.1	2.25
4	CFI	876	6	7	22874	1.43	0.55	0.1	2.5
5	CT	1753	3	0	20012	1.57	1.00	0.1	3
6	CT	1753	6	0	20410	1.56	2.09	0.2	3.5
7	CFI	1753	3	3	21080	1.49	1.03	0.2	3
8	CFI	1753	6	7	21761	1.46	2.13	0.2	3.5
9	CT	4083	3	0	19121	1.67	5.37	0.1	3.75
10	CFI	4083	3	3	20525	1.59	5.66	0.2	3.75

Note: Throughput of polymer reported here for CT corresponds to CT of 6 m length except 4083  $\mu\text{m}$  which has a 3 m length

## References

- (1) Ehrfeld, W., Hessel, V., Löwe, H., *Microreactors*; Wiley-VCH: Weinheim, **2000**.
- (2) Serra, C. A.; Parida, D.; Bally, F.; Garg, D. K.; Hoarau, Y.; Hessel, V. In *Encyclopedia of Polymer Science and Technology*; John Wiley & Sons, Inc.: 2013.
- (3) Gavriilidis, A.; Angeli, P.; Cao, E.; Yeong, K. K.; Wan, Y. S. S. *Chemical Engineering Research and Design* **2002**, *80*, 3.
- (4) Tonkovich, A.; Kuhlmann, D.; Rogers, A.; McDaniel, J.; Fitzgerald, S.; Arora, R.; Yuschak, T. *Chemical Engineering Research and Design* **2005**, *83*, 634.
- (5) Togashi, S.; Miyamoto, T.; Sano, T.; Suzuki, M. In *New Trends in Fluid Mechanics Research*; Zhuang, F. G., Li, J. C., Eds.; Springer Berlin Heidelberg: **2009**, 678.
- (6) Kockmann, N.; Gottsponer, M.; Roberge, D. M. *Chemical Engineering Journal* **2011**, *167*, 718.
- (7) Iwasaki, T.; Kawano, N.; Yoshida, J.-i. *Organic Process Research & Development* **2006**, *10*, 1126.
- (8) Braunecker, W. A.; Matyjaszewski, K. *Progress in Polymer Science* **2007**, *32*, 93.
- (9) Patten, T. E.; Matyjaszewski, K. *Advanced Materials* **1998**, *10*, 901.
- (10) Matyjaszewski, K. *Encyclopedia of Radicals in Chemistry, Biology and Materials*; John Wiley & Sons, Ltd: **2012**.
- (11) Diehl, C.; Laurino, P.; Azzouz, N.; Seeberger, P. H. *Macromolecules* **2010**, *43*, 10311.
- (12) Kumar, V.; Nigam, K. D. P. *International Journal of Heat and Mass Transfer* **2005**, *48*, 4811.
- (13) Saxena, A. K.; Nigam, K. D. P. *AIChE Journal* **1984**, *30*, 363.

---

*CHAPTER 6*  
*CONCLUSION AND PERSPECTIVES*

---

## Conclusion

Atom Transfer Radical Polymerization (ATRP) finds increasing wide acceptance due to its positive control over polymer characteristics. However slow polymerization rate is a concern from commercial perspective. In this work, efforts were made to accelerate the ATRP synthesis of DMAEMA-based (2-(N,N-dimethylamino)ethyl methacrylate) polymers using microreaction technologies. Different process conditions and microreactor geometries were considered for the intensification of ATRP. Finally, scale-up of microreactor was carried out to increase the throughput. Most important findings of this work are summarized bellow.

Micromixer is one of the key elements of any microreaction system. Careful selection of micromixer is essential to avoid any kind of uncontrolled reaction conditions inside microreactor arising from improper upstream mixing of reagents. Therefore at the early stage of this work, impact of different micromixing principles on polymer characteristics was studied. HPIMM (interdigital multilamination), KM (impact jet) and T-Junction (bilamination) micromixers were used to premix the reactive streams prior the coiled tube (CT) microreactor during the synthesis of P(DMAEMA-co-BzMA) (20 and 40 mol.% BzMA). Impact of different premixing conditions was quite evident as a clear difference between polymer characteristics was observed. HPIMM gave highest conversion (+ 35 points) and molecular weight (+ 8000 g/mole) as well as the lowest PDI. Whereas T-Junction gave the lowest conversion along with bimodal GPC elution traces, indicating a poor control over polymerization due to improper mixing.

In an attempt to intensify ATRP of DMAEMA in microreactors, elevated temperatures were investigated. Polymerization rate increased significantly with temperature. However control over polymerization was reduced for  $M_n$  higher than 15000 g/mol (i.e. for long residence times). High pressures were used as another alternative to accelerate polymerization. Effect of pressure was found to have a profound impact on reaction rate in microreactor. Increase in conversion (+15%) and molecular weight (+5000 g/mol) was observed with an increase in pressure from 1.5 to 100 bars. Interestingly, this study indicated that moderate pressure can accelerate polymerization significantly in microreactor. To get more knowledge about the effect of pressure, polymerization was carried out in microreactors of different internal diameters. Positive effect of higher pressure was more pronounced for small tube diameters. In another strategy of intensification, shear rate was increased to make the growing chain end more accessible for reaction. It was observed that shear rate has a noticeable effect on

polymerization when macromolecular weight is comparatively small and polymerizing solution in dilute regime. When chain length increases effect of shear rate is dimed.

To overcome the diffusion limitation encountered during polymerization in microreactor towards longer residence times, coiled flow inverter (CFI) reactors were considered in which 90° bends were introduced at equal interval. Due to the change in direction of flow, growing chains near the wall were brought back to the centre and vice versa. A reactor having such characteristics can not only improve mixing during flow but also can reduce residence time distribution (RTD). When polymer characteristics synthesized in CT and CFI reactors were compared, higher molecular weights were observed in CFI reactors conversely to its CT counterparts. Gain of ~2000 g/mol in molecular weight along with a significant reduction in PDI (from 1.53 down 1.39) was observed. More clear evidence of flow inversion and its effect were obtained during synthesis of branched polymers (5 and 10 mol.% inimer) in different microreactors. Formation and accumulation of oligomeric units were found to be low in CFI reactor compared to batch and CT reactors. Higher branching efficiency and lower PDI (- 0.3) in CFI reactor indicated a controlled and dense branched structure. Considering the consumption of inimer, monomer and the generation of oligomers, a general scheme of branched polymerization in batch, CT and CFI reactor was proposed.

In order to increase the throughput of tubular microreactors, tube diameter was increased from 876 μm to 1753 μm and 4083 μm and length from 3 to 6 m. Moreover to counter balance the detrimental effect of longer diffusion distance in large diameter tubular reactors, flow inversion was considered. With an increase in diameter, control over polymerization was found to decrease both in CT and CFI reactors. However in case of CFI the loss of control was less. Moreover it was observed that any increase in length (i.e. higher number of bends) seems to compensate the negative effect of increased diameter. Interestingly PDI obtained in a 1753 μm CFI reactor of 6 m length was close to the PDI obtained in a 3 m length 876 μm CT microreactor while throughput was increased by a factor close to 4. However, in case of tube diameter of 4083 μm, diffusion limitations due to long radial distance was predominant over mixing achieved by flow inversion as PDI was much higher compared to CFIs of smaller diameters.

The work accomplished during this thesis has clearly demonstrated that a “slow” reaction like ATRP can be readily accelerated if appropriate microreaction technologies are employed. Thus micromixers and microreactors made the intensification of continuous-flow ATRP

processes possible. To some extent, microreactor throughput was significantly increased without any compromise on the control over macromolecular characteristics if flow inversion technique is implemented.

However the various experiments carried out have raised unanswered questions that would be definitely worth to address in the future.

## ***Perspectives***

### ***Intensification by combination of high temperature and pressure***

In chapter 4 effect of temperature and pressure were explained independently. Elevated temperatures showed faster kinetics. However loss of control over polymerization was an issue for long residence times. On the other hand, high pressure demonstrated faster kinetics and improved control. Therefore it will be interesting to investigate the possible control of high pressure along with high temperature for further intensification of ATRP.

### ***Optimization of CFI geometric parameters***

Presence of bends in a CFI reactor may be designed in various permutations and combinations. With each possibility mixing may vary, which in turn might affect the result of the polymerization. Examples of such designs include different number of bends at a fixed length or fixed number of bends at different length, curvature and pitch of the coils. Therefore a specific investigation is necessary to optimize the CFI geometry. Along with experimental techniques, mathematical modeling and simulations will be definitely very useful for this optimization task.

### ***CFI as micromixer***

Chapter 4 revealed the importance of premixing and the efficiency of micromixers to intensify ATRP. Flow inversion was found an effective technique for internal mixing during polymerization. Thus given the high price of commercially available micromixers and the relative cheap manufacturing cost of CFI, one may wonder if a CFI could not act as a pretty decent micromixer.

### ***Synthesis of more complex architectures***

In chapter 5, it was demonstrated that microreaction technology allowed increasing the branching efficiency of SCVCP to get in a one pot recipe branched polymers. There is



probably some room here for investigations directed to the synthesis of more complex architecture; like core-shell structure resulting from the two-stage copolymerization of a branched core with a linear shell for drug delivery applications for instance. Another example would be the continuous-flow synthesis of dendrimers from a convergent strategy for which micromixing would be probably a key step.

# Thesis Resume

**Thesis title** Intensification of ATRP polymer syntheses by microreaction technologies

**Candidate Name** Dambarudhar Parida

**Thesis Advisor** Christophe A. Serra

**Organization** ICPEES, University de Strasbourg

---

## Publications

---

1. D. Parida, C.A. Serra, D.K. Garg, Y. Hoarau, M. Bouquey, R. Muller, Flow inversion: an effective means to scale-up controlled radical polymerization in tubular microreactors, Submitted to *Macromolecular reaction engineering*.
2. D. Parida, C.A Serra, F. Bally, D. K. Garg and Y. Hoarau, Effect of coil flow inversion on macromolecular characteristics, Submitted to *Macromolecules*
3. D. Parida, C.A Serra, D. K. Garg and Y. Hoarau, Atom Transfer Radical Polymerization in continuous-microflow: effect of process parameters, Submitted to *Journal of Flow Chemistry*.
4. C. A. Serra, D. Parida, D. K. Garg and Y. Hoarau, V. Hessel 2013, *Encyclopedia of Polymer Science and Technology* » ; Wiley-VCH, Weinheim (Germany), DOI: 10.1002/0471440264.pst612.
5. D. Prida, C.A. Serra, F. Bally, D.K. Garg and Y. Hoarau, Intensifying the ATRP synthesis of statistical copolymers by continuous micromixing flow techniques, *Green. Proc. Synt.*, 6 (1) (2012) 525-532.

---

## Conference presentations

---

### Oral Presentations

- 1 Effect of microreactor geometry and operating parameters on ATRP processes, D. Parida, C. A. Serra, D. K. Garg and Y. Hoarau at *EFCE WPPRE 2*, May 24-26, 2012, Hamburg, Germany.
- 2 Effect of microreactor geometry and reaction parameters on polymerization, D. Parida, C. A. Serra, D. K. Garg and Y. Hoarau at *PRE Workshop 11*, 2013, May 21-24, Hamburg, Germany.
- 3 Intensifying the ATRP synthesis of (co)polymers by continuous-microflow techniques, D. Parida, C. A. Serra, D. K. Garg and Y. Hoarau at *EFCE WPPRE 1*, 2012, October 12-13, Lyon, France.
- 4 Polymerization microreactors for control of macromolecular characteristics, D. Parida, C. A. Serra, D. K. Garg and Y. Hoarau at *CHISA 20*, August 25-29, 2012, Prague, Czech Republic.
- 5 Coil flow inverter: novel intensified reactor for the synthesis of architecture-controlled polymers, D. Parida, F. Bally, C. A. Serra at *IMRET 12*, February 20-22, 2012, Lyon, France.

### Poster Presentations

1. Effect of microreactor geometry and reaction parameters on polymerization, D. Parida, C. A. Serra, D. K. Garg and Y. Hoarau at *PRE Workshop 11*, 2013, May 21-24, Hamburg, Germany.
2. Microreaction Technology: A tool for the intensification of Atom transfer radical polymerization process, D. Parida, C. A. Serra, D. K. Garg and Y. Hoarau at *ERC Grantees Conference, 2012*, November 22-24, Strasbourg, France.

3. Intensifying the ATRP synthesis of (co)polymers by continuous-microflow techniques, D. Parida, C. A. Serra, D. K. Garg and Y. Hoarau at *EFCE WPPRE 1*, 2012, October 12-13, Lyon, France.
  
4. Improvement of the control of polymer architecture by means of a coil flow inverter microreactor, D. Parida, C. A. Serra, D. K. Garg and Y. Hoarau at *ISCRE 22*, 2012, September 2-5, Maastricht, The Netherlands (**Best Poster Award**).